



da Silva Costa, Ana Filipa (2019) *Investigation into the mechanisms determining spontaneous activity in human-induced pluripotent stem cell-derived cardiomyocytes*. PhD thesis.

<https://theses.gla.ac.uk/41143/>

Copyright and moral rights for this work are retained by the author

A copy can be downloaded for personal non-commercial research or study, without prior permission or charge

This work cannot be reproduced or quoted extensively from without first obtaining permission from the author

The content must not be changed in any way or sold commercially in any format or medium without the formal permission of the author

When referring to this work, full bibliographic details including the author, title, awarding institution and date of the thesis must be given

Enlighten: Theses

<https://theses.gla.ac.uk/>  
[research-enlighten@glasgow.ac.uk](mailto:research-enlighten@glasgow.ac.uk)

**Investigation into the mechanisms  
determining spontaneous activity in human-  
induced pluripotent stem cell-derived  
cardiomyocytes**

**Ana Filipa da Silva Costa, BSc. (Hons), MRes**

**Submitted in fulfilment of the degree of**

**Doctor of Philosophy**

**To**

**University of Glasgow**

**School of Medical, Veterinary and Life Sciences**

**Institute of Cardiovascular and Medical Sciences**

**April 2019**

## Abstract

**Background:** Human induced-pluripotent stem cell-derived cardiomyocytes (hiPSC-CMs) provide an alternative to adult primary cells for scientific and commercial research, but they have an embryonic rather than adult electrophysiological phenotype. In particular: low expression of inward rectifying channel ( $I_{K1}$ ) contributes towards the unstable resting membrane potential and results in spontaneous electrical activity.

**Purpose:** This study examines contribution of  $I_{K1}$  and other ionic currents to the spontaneous electrical activity of hiPSC-CMs and tests the concept that additional external  $I_{K1}$  activity can be added via co-culture with  $I_{K1}$ -expressing HEK293 cells.

**Methods:** hiPSC-CM's ionic currents and channels were investigated using different ion channel blockers.  $I_{K1}$  was externally added to hiPSC-CM culture via co-culture with  $I_{K1}$ -overexpressing HEK at different densities and ratios. The effects on contractility and voltage (action potentials) were investigated using two in-house platforms: CelloPTIQ and MUSCLEMOTION.

**Results:** Based on the sensitivity to the  $I_f$  blocker, the pacemaker current ( $I_f$ ) is either absent or not a dominant contributor to pacemaking in hiPSC-CMs. Blockade of  $I_{K1}$  with  $BaCl_2$  and PA-6 did not affect interval time, thus showing that there is low availability of  $I_{K1}$ . Co-culture with  $I_{K1}$ -HEK at 1:1 HEK:hiPSC led to a prolongation of mean interval (from  $963.5 \pm 24.5$ ms to  $1516.0 \pm 79.3$ ms,  $n=15$ ,  $p < 0.05$ ). The cause of this is unknown. Co-culture using fibroblasts and hiPSC-CMs was done to study the effects of a different cell type in co-culture. These indicated that the amplitude of the contraction signals might be affected by different cell types and their elasticity, rather than effects within the hiPSC-CMs. To improve cell-to-cell coupling,  $I_{K1}$ -HEK were transfected with Cx43 and introduced into co-culture. Under these conditions, the electrophysiological behaviour was similar to co-culture with  $I_{K1}$ -HEK cells. The signal to noise ratio (SNR) of membrane dye (FluoVolt) was used to estimate the degree of coupling of iPSC-CMs to  $I_{K1}$ -HEK.

**Conclusions:** hiPSC-CMs have low contribution from  $I_{K1}$ , but the spontaneous activity was not dominated by  $I_f$ . Co-culture with  $I_{K1}$ -HEK rather than wild-type HEK led to prolongation of interval between APs, suggesting that hiPSC-CMs were successfully coupled to  $I_{K1}$ -expressing HEK cells. Increased expression of Cx43 to potentially further develop this effect - by improving electrical linkage - did not enhance  $I_{K1}$  effects further. In summary, enhancing  $I_{K1}$  pharmacologically was not possible, but co-culture with specific

ion channel cell lines appeared to successfully add to the channels contributing to the AP in hiPSC-CMs.

# Table of Contents

<b>Abstract .....</b>	<b>2</b>
<b>List of Tables .....</b>	<b>8</b>
<b>List of Figures .....</b>	<b>9</b>
<b>Acknowledgements .....</b>	<b>11</b>
<b>Author's Declaration .....</b>	<b>12</b>
<b>Publications and abstracts .....</b>	<b>13</b>
<b>Definitions/Abbreviations .....</b>	<b>14</b>
<b>1 Introduction .....</b>	<b>17</b>
<b>1.1 Introduction .....</b>	<b>18</b>
<b>1.2 Creation of human-induced pluripotent stem cells .....</b>	<b>19</b>
<b>1.3 Methods for maturation .....</b>	<b>22</b>
1.3.1 T3 .....	22
1.3.2 Ascorbic acid .....	23
1.3.3 Extracellular matrix maturation .....	23
<b>1.4 Nonadult-like behaviour of hiPSC-CMs .....</b>	<b>23</b>
1.4.1 Electrical activity in the adult heart .....	23
1.4.2 Excitation-contraction coupling .....	24
1.4.3 Electrophysiology in hiPSC-CMs .....	25
<b>1.5 Candidate channels for maturation .....</b>	<b>29</b>
1.5.1 $I_{K1}$ .....	29
1.5.2 The presence of $I_f$ .....	32
1.5.3 Other pacemaker currents (NCX/Ca) .....	34
<b>1.6 Gap junctional channels .....</b>	<b>34</b>
<b>1.7 Alternative approach to changing electrical phenotype .....</b>	<b>35</b>
<b>1.8 Conclusion and aims .....</b>	<b>36</b>
1.8.1 Aims .....	36
<b>2 General Methods .....</b>	<b>38</b>

<b>2.1</b>	<b>Health and Safety .....</b>	<b>39</b>
<b>2.2</b>	<b>Cell culture .....</b>	<b>39</b>
2.2.1	Pre-plating protocol.....	39
2.2.2	Pluricytes® hiPSC-CMs handling and plating.....	39
2.2.3	Cor.4U® hiPSC-CMs (Axiogenesis, Germany) handling and plating .....	40
2.2.4	General HEK293 handling .....	40
<b>2.3</b>	<b>Solutions used .....</b>	<b>41</b>
<b>2.4</b>	<b>Measuring voltage with dyes.....</b>	<b>42</b>
2.4.1	Cell culture loading with different dyes .....	42
2.4.2	Di-4-ANEPPS .....	43
2.4.3	FluoVolt.....	44
<b>2.5</b>	<b>Measuring calcium signals .....</b>	<b>45</b>
2.5.1	Fura-4F/AM .....	45
<b>2.6</b>	<b>Measuring movement/contraction .....</b>	<b>47</b>
2.6.1	MUSCLEMOTION.....	47
<b>2.7</b>	<b>Integration of voltage, contractility and calcium measurements on CelloPTIQ.....</b>	<b>49</b>
2.7.1	Analysis using CelloPTIQ .....	50
2.7.2	Signal-to-noise calculations.....	53
<b>2.8</b>	<b>Statistical analysis .....</b>	<b>55</b>
<b>3</b>	<b><i>Characterisation of human induced pluripotent stem cell-derived cardiomyocytes</i></b>	<b>56</b>
<b>3.1</b>	<b>Introduction .....</b>	<b>57</b>
3.1.1	Pacemaker current blockade.....	57
3.1.2	Inward rectifying current blockade.....	58
3.1.3	Potassium availability and uptake.....	59
3.1.4	SERCA blockade .....	59
3.1.5	Ryanodine-receptor calcium release.....	59
3.1.6	Other potential mechanisms for spontaneous activity .....	60
3.1.7	Aims of this chapter .....	60
<b>3.2</b>	<b>Methods .....</b>	<b>60</b>
3.2.1	Ivabradine – I <sub>f</sub> block .....	60
3.2.2	Barium Chloride – non-specific I <sub>k1</sub> block.....	61
3.2.3	PA-6 - I <sub>k1</sub> block.....	61
3.2.4	Potassium Chloride – K <sup>+</sup> depletion and re-introduction.....	62
3.2.5	Thapsigargin .....	62
3.2.6	Ryanodine.....	63

<b>3.3</b>	<b>Results</b> .....	<b>63</b>
3.3.1	Ivabradine – I <sub>f</sub> block .....	63
3.3.2	Barium Chloride – non-specific I <sub>k1</sub> block.....	65
3.3.3	PA-6.....	68
3.3.4	Potassium depletion and re-introduction .....	70
3.3.5	Thapsigargin .....	74
3.3.6	Ryanodine.....	77
<b>3.4</b>	<b>Discussion</b> .....	<b>79</b>
3.4.1	I <sub>f</sub> and its contribution towards spontaneous activity .....	79
3.4.2	I <sub>k1</sub> presence in hiPSC-CMs.....	80
3.4.3	SERCA and other potential contributions towards spontaneous activity.....	81
3.4.4	Conclusion .....	82
<b>4</b>	<b><i>Co-culture of hiPSC-CMs and HEK293</i></b> .....	<b>83</b>
<b>4.1</b>	<b>Introduction</b> .....	<b>84</b>
4.1.1	Aims .....	85
<b>4.2</b>	<b>Methods</b> .....	<b>85</b>
4.2.1	HEK293 proliferation assay.....	85
4.2.2	Co-culture of Pluricyte hiPSC-CMs and HEK293.....	86
4.2.3	Co-culture of Cor.4U hiPSC-CMs and HEK293.....	86
4.2.4	The effects of different media in cell proliferation and co-culture .....	87
4.2.5	Blocking of I <sub>k1</sub> in co-culture with HEK-I <sub>k1</sub> .....	88
4.2.6	Co-culture of hiPSC-CMs with human cardiac fibroblasts .....	89
<b>4.3</b>	<b>Results</b> .....	<b>89</b>
4.3.1	HEK293 proliferation assay.....	89
	.....	90
4.3.2	Pluricyte co-culture with HEK293.....	91
4.3.3	Cor.4U co-culture with HEK293 .....	92
4.3.4	High densities of HEK293 affect amplitude of contraction.....	107
4.3.5	I <sub>k1</sub> antagonist PA-6 has no effect on 1:1 co-culture.....	108
<b>4.4</b>	<b>Investigating the effects of co-culture using human cardiac fibroblasts</b> .....	<b>110</b>
<b>4.5</b>	<b>Discussion</b> .....	<b>117</b>
4.5.1	Conclusion .....	120
<b>5</b>	<b><i>Co-culture of hiPSC-CMs and Cx43 and I<sub>k1</sub>-overexpressing HEK293</i></b> .....	<b>121</b>
<b>5.1</b>	<b>Introduction</b> .....	<b>122</b>
5.1.1	Connexin expression in hiPSC-CMs .....	124

5.1.2	Connexin expression in HEK293.....	125
5.1.3	Aims .....	125
<b>5.2</b>	<b>Methods.....</b>	<b>125</b>
5.2.1	Transfection protocol.....	125
5.2.2	Immunocytochemistry .....	126
5.2.3	Co-culture with Cx43-transfected HEK.....	127
<b>5.3</b>	<b>Results and discussion .....</b>	<b>127</b>
5.3.1	Setting the transfection protocol.....	127
5.3.2	Co-culture overexpressing Cx43 .....	129
<b>5.4</b>	<b>Discussion and conclusion .....</b>	<b>137</b>
5.4.1	Limitations.....	139
<b>6</b>	<b><i>Discussion and Conclusion.....</i></b>	<b>140</b>
<b>6.1</b>	<b>Discussion and Conclusion.....</b>	<b>141</b>
<b>6.2</b>	<b>Ionic currents and channels in hiPSC-CMs .....</b>	<b>141</b>
<b>6.3</b>	<b>Co-culture of hiPSC-CMs with I<sub>K1</sub>-HEK .....</b>	<b>142</b>
<b>6.4</b>	<b>Connexin overexpression in HEK293 does not alter electrophysiology in co-culture</b>	<b>143</b>
<b>6.5</b>	<b>Co-culture affects Signal-to-noise ratio .....</b>	<b>144</b>
<b>6.6</b>	<b>Conclusion .....</b>	<b>145</b>
<b>6.7</b>	<b>Future directions .....</b>	<b>146</b>
6.7.1	Co-culture strategies.....	146
6.7.2	Expression strategies.....	146
6.7.3	Alternative geometries of cells in culture.....	146
6.7.4	Methods to control spontaneous rate .....	147
	<b><i>Appendix.....</i></b>	<b>148</b>
	<b><i>List of References.....</i></b>	<b>156</b>

## List of Tables

Table 4.1 – Maintenance of co-cultures of HEK:hiPSC-CMs in different media. \_\_\_\_\_97

# List of Figures

<i>Figure 1.1 - Transcription factors involved in the derivation of hiPSC-CMs from the fibroblast stage.</i>	21
<i>Figure 1.2 - Excitation-contraction coupling in the adult heart. <math>Ca^{2+}</math> enters the cell through depolarisation-activated <math>Ca^{2+}</math> channels, such as the inward <math>Ca^{2+}</math> current (<math>I_{Ca}</math>).</i>	24
<i>Figure 1.3 – Ultrastructural differences between adult myocytes (left) and hiPSC-CMs (right) in ECC.</i>	26
<i>Figure 1.4 - Adult cardiomyocyte action potential and the action of the different ionic currents on depolarisation, repolarisation and the resting membrane potential.</i>	27
<i>Figure 1.5 - I/V (current-voltage) relationships of atrial and ventricular <math>I_{K1}</math>.</i>	30
<i>Figure 1.6 - Fully activated I-V relationship for <math>I_f</math>.</i>	33
<i>Figure 2.1 - di-4-ANEPPS excitation/ emission spectrum.</i>	43
<i>Figure 2.2 – Ratiometric dye, di-4-ANEPPS, as measured by CelloOPTIQ.</i>	44
<i>Figure 2.3 – FluoVolt spectrum.</i>	45
<i>Figure 2.4 - <math>Ca^{2+}</math> transient recording principle by CelloOPTIQ.</i>	46
<i>Figure 2.5 – Contractility measurements from hiPSC-CMs using MUSCLEMOTION.</i>	48
<i>Figure 2.6 – Settings for CelloOPTIQ.</i>	49
<i>Figure 2.7 - Example traces obtained from hiPSC-CMs dyed with di-4-ANEPPS.</i>	50
<i>Figure 2.8 - FluoVolt analysis.</i>	51
<i>Figure 2.9 - Fura-4F/AM analysis.</i>	51
<i>Figure 2.10 - Correlation of the three different conditions measured using CelloOPTIQ: Voltage, calcium signalling and contractility.</i>	52
<i>Figure 2.11 – Signal-to-noise can be calculated by measuring the fluorescence amplitude collected from 470nm excitation using a voltage-sensitive dye and/or the AP amplitude.</i>	53
<i>Figure 3.1 - The effects of a pacemaker current inhibitor on hiPSC-CMs. Voltage changes as a result of the addition of ivabradine at 1, 3 and 10 <math>\mu</math>M.</i>	64
<i>Figure 3.2 - The effects of ivabradine on hiPSC-CMs at different pacing frequencies.</i>	65
<i>Figure 3.3 - Barium chloride affects electrophysiological behaviour in hiPSC-CMs.</i>	67
<i>Figure 3.4 - The effects of PA-6 at 100, 150 and 200nM on voltage in hiPSC-CMs at increasing concentrations.</i>	69
<i>Figure 3.5 – <math>K^+</math> depletion and re-introduction affects voltage in hiPSC-CMs.</i>	71
<i>Figure 3.6 – <math>K^+</math> depletion and re-introduction affects contractile behaviour.</i>	73
<i>Figure 3.7 – The effects of thapsigargin on hiPSC-CMs' electrophysiological behaviour.</i>	75
<i>Figure 3.8 - Calcium handling is affected by thapsigargin.</i>	76
<i>Figure 3.9 - Ryanodine affects electrophysiological behaviour in hiPSC-CMs.</i>	78
<i>Figure 3.10 - Calcium handling in hiPSC-CMs is affected by ryanodine.</i>	79
<i>Figure 4.1- Principle of co-culture of hiPSC-CMs and HEK293.</i>	84
<i>Figure 4.2 – HEK293 cells do not proliferate over 72h.</i>	90
<i>Figure 4.3 - Cell proliferation assay using an MTT assay.</i>	90

Figure 4.4 – Pluricyte hiPSC-CMs were cultured with Normal HEK (N) to a final density of 30,000 cells/well in a 96 well glass-bottom plate. ....	91
Figure 4.5 - Pluricytes were cultured with HEK to a final density of 40,000 cells/well in a 96 well glass-bottom plate. ....	92
Figure 4.6 - Different co-culture densities Cor.4U. ....	93
Figure 4.7 - The effects of co-culture of iPSC-CMs with an increasing density of HEK293, for both $I_{K1}$ -expressing ( $I_{K1}$ ) and untransfected (Normal) cells timeline. ....	94
Figure 4.8 – Electrophysiology of HEK:hiPSC-CM co-cultures on day 8 after maintenance in different serum-containing or serum-free media. ....	99
Figure 4.9 - Contractile behaviour is affected by the presence of HEK293 at 1:1 ratio with hiPSC-CM. ....	101
Figure 4.10 - The effects of 1:1 co-culture on contraction interval. ....	102
Figure 4.11 - Electrophysiological behaviour is affected by the presence of HEK at 1:1 HEK:hiPSC. ....	104
Figure 4.12 - The effects of 1:1 HEK:hiPSC co-culture on electrophysiological interval. ....	106
Figure 4.13 – Effects on voltage of $I_{K1}$ blockage in HEK:hiPSC-CM co-culture. ....	108
Figure 4.14 – Effects on contraction of $I_{K1}$ antagonist, PA-6. ....	109
Figure 4.15 - Co-culture of hiPSC-CMs with HCF at different ratios. ....	111
Figure 4.16 – The effects on voltage of co-culture of HCF with hiPSC-CMs. ....	112
Figure 4.17 - The effects on contractile behaviour of co-culture of fibroblasts with hiPSC-CMs. ....	113
Figure 4.18 - Contractile behaviour is affected differently in co-culture with different cell lines. ....	114
Figure 4.19 – Electrophysiology is only affected in co-culture with HEK. ....	116
Figure 4.20 - Example AP traces obtained from a plating. ....	117
Figure 5.1 - Gap junctions and the intercalated disk. ....	123
Figure 5.2 - CDI hiPSC-CMs express Cx43. ....	124
Figure 5.3 - Cx43 expression on HEK, normal and $I_{K1}$ -expressing on day 4 post-transfection with 2.5 $\mu$ g and 5 $\mu$ g of plasmid. ....	128
Figure 5.4 - Electrophysiological effects of co-culture of HEK-Cx43 with and without $I_{K1}$ expression on hiPSC-CMs. ....	130
Figure 5.5 - Voltage in the Cx43-overexpressing co-culture at spontaneous rates and increasing pacing frequencies. ....	132
Figure 5.6 - Voltage in the Cx43-overexpressing co-culture at spontaneous rates and increasing pacing frequencies. ....	134
Figure 5.7 - Voltage in the Cx43-overexpressing co-culture at spontaneous rates and increasing pacing frequencies. ....	136
Figure 5.8 – The contribution of the different cell types to the AP shape and size are unknown. ....	137
Figure 6.1 - Different ion channel blockers elicit different effects on CL and APD <sub>90</sub> . ....	141

# Acknowledgements

First, I would like to thank my supervisor, Professor Godfrey Smith, for his guidance, support and encouragement. I would also like to thank my second supervisor, Dr Francis Burton, for his support with software.

I would also like to thank Aileen Rankin and Michael Dunne for their technical support and advice as I navigated through the PhD. A huge thank to all my colleagues for all their support, both moral and technical, with a special thank you to Aline Gurgel and Craig Hamilton. We started together, and we finished our PhDs together.

I would like to thank the EPSRC for funding this PhD and for providing courses which will help develop my career.

A very big thank you to my family (Avó Eva e Goreti Silva) and friends (Lee, Calum, Teja, Jernej and Pia). A special thank you to Judi Farrel and my MCY family. Teaching yoga as a hobby and having to commit to weekly classes helped me immensely in staying grounded.

Finally, I would like to thank my parents and my brother, Danny, without whom I could never have done this. They have given me constant love, patience and support throughout the PhD and the writing of my thesis.

*This thesis is dedicated to the memory of my Grandpa, Manuel Pereira, who, unfortunately, did not live to see its completion.*

## **Author's Declaration**

The material contained within this thesis is my own work.

This material has not been submitted for the fulfilment of any other degree.

## Publications and abstracts

A. Costa; MP. Hortigon-Vinagre; M. Van Der Heyden; FL. Burton; GL. Smith (2016). Introduction of external Ik1 to human-induced pluripotent stem cell-derived cardiomyocytes via Ik1-expressing HEK293. *Cardiovascular Research Supplements* 111: S92–S116. doi:10.1093/cvr/cvw150

Saxena, P., Hortigon-Vinagre, M. P., Beyl, S., Baburin, I., Andranovits, S., Iqbal, S. M., Costa, A., IJzerman, A. P., Kügler, P., Timin, E., Smith, G. L., ... Hering, S. (2017). Correlation between human ether-a-go-go-related gene channel inhibition and action potential prolongation. *British journal of pharmacology*, 174(18), 3081-3093.

## Conferences

[Presentation] CrackIT meeting, June 2015, Leiden, Netherlands

[Poster] Ivabradine prolongs action potential duration on spontaneous rate in cardiomyocytes derived from induced pluripotent stem cells. EHRA Europace – Cardiostim 2015, Milan, Italy

[Poster] Introduction of external Ik1 to human-induced pluripotent stem cell-derived cardiomyocytes via Ik1-expressing HEK293. *Frontiers in CardioVascular Biology* 2016, Florence, Italy – Abstract published in *Cardiovascular Research supplements*

[Poster] Introduction of external Ik1-expressing HEK293 to human-induced pluripotent stem cell-derived cardiomyocytes. EHRA Europace – Cardiostim 2017, Vienna, Austria - Awarded European Working Group in Cardiac and Cellular Electrophysiology Travel Grant

## Definitions/Abbreviations

<b>1D</b>	1 Dimension
<b>2D</b>	2 dimensions
<b>3D</b>	3 dimensions
<b>AM</b>	Acetoxymethyl esters
<b>AP</b>	Action Potential
<b>APD</b>	Action Potential Duration
<b>BaCl<sub>2</sub></b>	Barium chloride
<b>bFGF</b>	Basic fibroblast growth factor
<b>BMCC</b>	Cor.4U serum-free medium
<b>Ca<sup>2+</sup>/Ca</b>	Calcium
<b>CaT</b>	Calcium transient
<b>CaTAmp</b>	Calcium transient amplitude
<b>CD<sub>50</sub></b>	Contraction duration 50%
<b>CICR</b>	Ca <sup>2+</sup> -induced Ca <sup>2+</sup> -release
<b>CL</b>	Cycle length
<b>cTnI</b>	Cardiac troponin I
<b>Cx43</b>	Connexin-43
<b>DI</b>	Diastolic Interval
<b>di-4-ANEPPS</b>	Pyridinium, 4-(2-(6-(dibutylamino)-2-naphthalenyl)ethenyl)-1-(3-sulfopropyl)-, hydroxide, inner salt 90134-00-2
<b>DMEM</b>	Dulbecco's Modified Eagle Medium
<b>DMSO</b>	Dimethylsulfoxide
<b>Dn90</b>	Time for relaxation 90%
<b>(D)PBS</b>	Dulbecco's phosphate-buffered saline
<b>FBS</b>	Foetal bovine serum
<b>FFR</b>	Force-frequency response
<b>EAD</b>	Early after depolarisation
<b>ECC</b>	Excitation-contraction coupling
<b>E<sub>m</sub></b>	Membrane potential
<b>ER</b>	Endoplasmic reticulum
<b>G</b>	Conductance
<b>GA</b>	Growth arrest
<b>GFP</b>	Green fluorescent protein
<b>GIJC</b>	GJ intercellular communication
<b>GJ</b>	Gap junction

<b>HCF</b>	Human cardiac fibroblasts
<b>HCN</b>	Hyperpolarization-activated cyclic nucleotide-gated channels
<b>HEK(293)</b>	Human embryonic kidney cell type 293
<b>hESC</b>	Human embryonic stem cell
<b>hERG</b>	Human Ether-a-go-go-related Gene
<b>hiPSC-CMs</b>	Human-induced pluripotent stem cell-derived cardiomyocytes
<b>hTERT</b>	Telomerase reverse transcriptase
<b>I</b>	Current
<b>ID</b>	Intercalated disk
<b>I<sub>f</sub></b>	Pacemaker current
<b>I<sub>kl</sub></b>	Inward rectifier current
<b>IP3R</b>	Inositol-triphosphate receptor
<b>K<sup>+</sup></b>	Potassium
<b>KCNJ</b>	Potassium voltage-gated channel subfamily J
<b>kPa</b>	Kilo Pascals
<b>LED</b>	Light-emitting diode
<b>LP</b>	Long-pass filter
<b>LTCC</b>	L-type Ca <sup>2+</sup> channel
<b>lwPMT</b>	long-wavelength PMT
<b>MTT</b>	3-(4,5-dimethylthiazol-2-yl)-2,5-diphenyltetrazolium bromide
<b>N</b>	Normal (standard) HEK293
<b>NCX</b>	Sodium-calcium exchanger
<b>PDMS</b>	Polydimethylsiloxane scaffold
<b>PFA</b>	Paraformaldehyde
<b>PLN</b>	Phospholamban
<b>PMT</b>	Photomultiplier
<b>R</b>	Resistance
<b>RyR</b>	Ryanodine receptor
<b>RT</b>	Room temperature
<b>S/N or SNR</b>	Signal-to-noise
<b>SAN</b>	Sino-atrial node
<b>SERCA</b>	Sarco/endoplasmic reticulum Ca <sup>2+</sup> -ATPase
<b>SEM</b>	Standard error mean
<b>swPMT</b>	Short-wavelength PMT
<b>T3</b>	Triiodothyronine
<b>T<sub>Peak</sub></b>	Time to peak
<b>T<sub>Rise</sub></b>	Time to rise AP
<b>Up<sub>90</sub></b>	Time for contraction 90%

<b>UV</b>	Ultra-violet
<b>V</b>	Voltage gradient
<b>vERP</b>	Ventricular effective refractory period
<b>VSDs</b>	Voltage-sensitive dyes
<b><math>\lambda_{exc}</math></b>	Wavelength of excitation

# 1 Introduction

## 1.1 Introduction

Human induced pluripotent stem cells (hiPSCs) are candidates for disease modelling, drug screening, regenerative medicine and cell therapy (Jiang et al., 2014). They have been differentiated into cardiomyocytes (hiPSC-CMs) which exhibit sarcomeres, calcium transients and spontaneous beating. They are a promising future *in vitro* cellular model to study cardiac arrhythmia-related diseases and for screening of proarrhythmic and cardiotoxic compounds during drug development (Van Den Heuvel et al., 2014, Jonsson et al., 2012, Gibson et al., 2014). The limited availability of human cardiomyocytes for research has resulted in hiPSCs being the preferred candidates for drug screening and toxicity testing. This also provides the grounds to potentially help replace animal cells, both ethically sensitive and costly, in pharmacological research and avoid the physiological and molecular differences among species (Van Den Heuvel et al., 2014, Jonsson et al., 2009, Bett et al., 2013, Himmel, 2013) which complicate the translation of findings to humans due to important physiological and molecular differences (Ivashchenko et al., 2013). The need for human cardiac models has led to the development of the Comprehensive *in vitro* Proarrhythmia Assay (CiPA) initiative (Gintant et al., 2016). CiPA's aim is to establish a new safety testing paradigm that is not exclusively focused on hERG block, but instead involves drug screening on ion channels expressed in cell lines with computer models to predict drug effects on human action potentials. These results are then tested with *in vitro* drug screens on hiPSC-CMs (Goversen et al., 2017). Despite the human source of the tissue, there is a general consensus that these cells are lacking in maturation status.

In 2000, the derivation of cardiomyocytes from human embryonic stem cells (hESCs) was first reported (Denning and Anderson, 2008, Itskovitz-Eldor et al., 2000). Most hESCs are derived from the inner cell mass of the blastocyst stage of an embryo, normally an *in vitro* fertilised egg grown for 4 to 5 days (Denning and Anderson, 2008, Jensen et al., 2009). By using differentiation factors, such as activin and basic fibroblast growth factor (bFGF), it is possible to differentiate these cells into cardiomyocytes, which show spontaneous contraction, therefore proving that functional excitation-contraction coupling occurs. These cells show “classical” indicators established in whole hearts, as they contract 50 to 60 times per minute (from a range of ~20 to ~130bpm) (Denning and Anderson, 2008, Hayakawa et al., 2014). Using the Microelectrode Array (MEA) system, it has been shown that hESC-CM clusters respond to a variety of drugs affecting different ion currents (Caspì

et al., 2009). Intracellular recordings using either patch-clamp or sharp microelectrodes do, on the other hand, provide information on arrhythmic events. Even though several studies have identified electrophysiological characteristics of hESC-CMs, standardization and quantification of arrhythmic endpoints, and comparison to contemporary models are generally lacking.

It is accepted that these cell models are not identical to differentiated adult cells *in vivo*, but despite being immature, they can still considerably improve drug screening. The use of these cells is controversial due to ethical issues, as some people regard elective termination of pregnancy as ethically unacceptable, as a foetus cannot give informed consent (McLaren, 2001, Robertson, 2001). Also, some provide the defence that these should not be viewed as an alternative to the existing *in vivo* and *in vitro* QT screening systems, but as complementary (Caspi et al., 2009). For this reason, it is important to find another cell type which can replace hESCs with fewer ethical issues.

For hiPSC-CMs to be used as screening models, these cells would have to resemble adult cardiomyocytes in structure, excitation and contraction (Van Den Heuvel et al., 2014, Himmel, 2013). The developmental profile of cardiomyocytes *in vivo* has been well characterised, but there is still a challenge in tracking and documenting stem cell-derived cardiomyocytes. Despite these cells exhibiting sarcomeres, calcium transients and spontaneous beating, a consensus has emerged that the maturity of hiPSC-CMs is important when using these cells for *in vitro* drug studies (Bedada et al., 2014). hiPSC-CMs have an immature electrophysiological and structural phenotype and maturation protocols must be developed to maximise the therapeutic application (Yang et al., 2014, Jonsson et al., 2012, Cao et al., 2012).

## **1.2 Creation of human-induced pluripotent stem cells**

Takahashi and Yamanaka (2006) were the first to show that differentiated cells can be reprogrammed to an embryonic-like state. These scientists were the pioneers of techniques that allow pluripotent stem cells to be induced from mouse embryonic or adult fibroblasts by introducing transcription factors. In 2006, Takahashi and Yamanaka induced pluripotent stem cells from human dermal fibroblasts for the first time using the same four transcription factors used to induce pluripotent stem cells from mouse fibroblasts (Takahashi et al., 2007, Khan et al., 2013, Takahashi and Yamanaka, 2006). Oct3/4 is

essential for stem cell renewal, and its amount must be regulated to maintain stem-cell phenotype (Niwa et al., 2000). Sox2 is required in early embryonic cells for pluripotency (Avilion et al., 2003). Klf4 belongs to the Krüppel-like factors family, which are characterised as zinc-finger proteins which contain amino acid sequences similar to the *Drosophila* embryonic pattern regulator Krüppel (Nakagawa et al., 2008). It promotes embryonic stem cell self-renewal (Li et al., 2005), whereas c-Myc is an amplifier of gene activation (Nie et al., 2012). Together, the last two encourage rapid proliferation of embryonic stem cells in culture and maintain the embryonic stem cell phenotype (Khan et al., 2013). After 8 days in suspension culture, iPSCs formed ball-shaped structures, embryoid body-like structures which have the potential to differentiate. Induction of differentiation using activin A and bone morphogenetic protein (BMP) leads to clumps of beating cells with cardiomyocyte markers, such as troponin T type 2, myocyte enhancer factor 2C (MEF2C), myosin light polypeptide 7, regulatory (MYL2A), myosin heavy polypeptide 7, cardiac muscle beta (MYHCB), and NK2 transcription factor-related, locus 5 (NKX2.5). Expression of NANOG, Oct3/4 and Sox 2 was decreased. This showed that hiPSCs can differentiate into cardiac myocytes *in vitro*, as they express cardiac markers. The group did not conduct electrophysiological or pharmacological studies (Takahashi et al., 2007).

Since Takahashi et al. (2007), different protocols have been created (Figure 1.1) for differentiating these cells. In the same year, on a parallel study, another group (Yu et al., 2007) reported the four transcription factors (Oct4, Sox 2, c-myc and Klf4) were sufficient to reprogram mouse fibroblasts to pluripotent, undifferentiated stem cells. It was reported that the expression of c-Myc caused differentiation of hESCs but, depending on the target genes expressed in various cell types which this can be used in, the outcome may differ and instead result in cell death (Sumi et al., 2007). The same group investigated the reprogramming of human somatic cells, where they combined Oct4, Sox2, Nanog and Lin28 and cloned them into a lentiviral vector. Oct4, an endogenous promoter, was used to drive the expression of neomycin phosphotransferase, as it is a gene highly expressed in pluripotent cells, but not in differentiated cells. Yu et al. (2007) reported that if either Oct4 or Sox2 were removed from the reprogramming mixture then the appearance of geneticin-resistant (Oct4<sup>+</sup>) reprogrammed mesenchymal clones was stopped. Nanog improves the cloning efficiency but is not necessary for the initial appearance of clones (Darr et al., 2006). The latter is highly important for pluripotency. Nanog is expressed in pluripotent embryo cells, and has been shown to facilitate molecular reprogramming and promotes the

transfer of pluripotency after ES cell fusion (Silva et al., 2009). These three transgenes were all present in the clones, and Lin28 was absent from one clone, showing that although it can influence the frequency of reprogramming, it is not necessary for the initial steps nor for the stable expansion of reprogrammed cells.

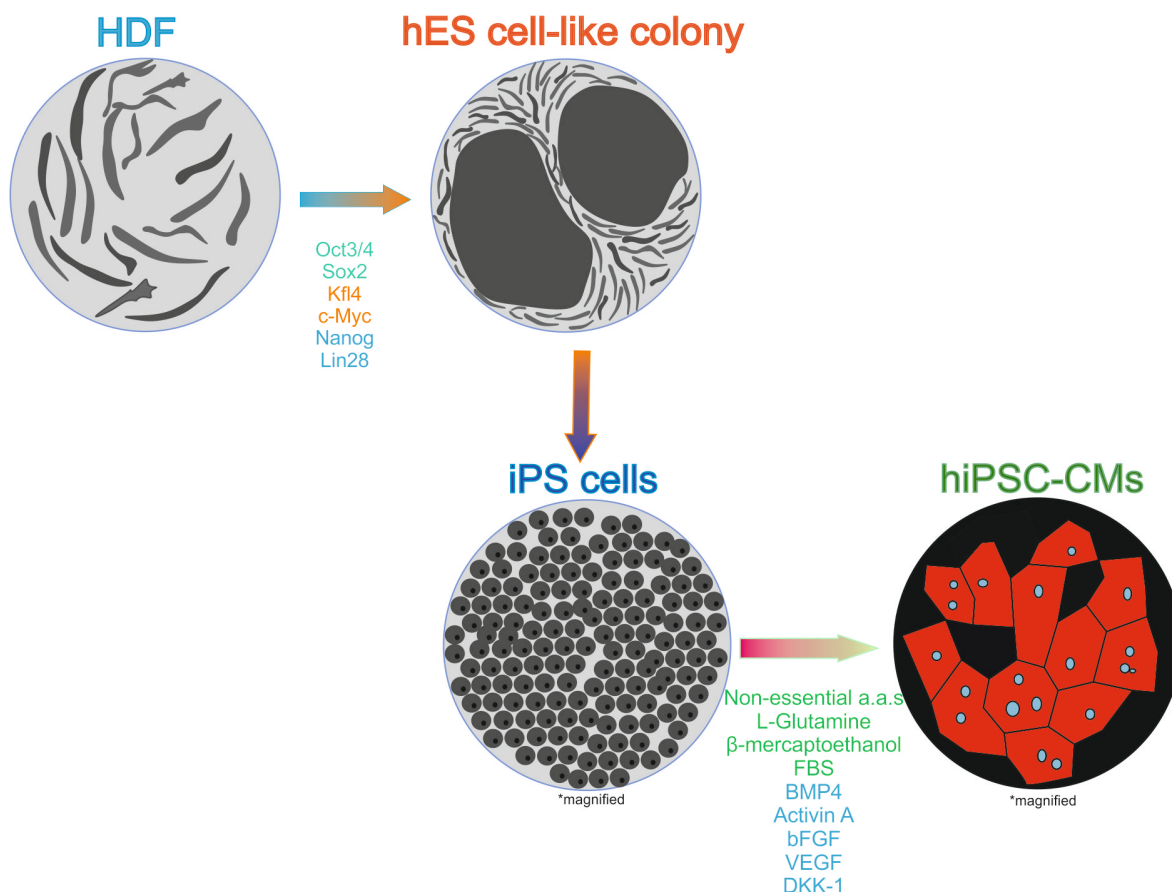


**Figure 1.1 - Transcription factors involved in the derivation of hiPSC-CMs from the fibroblast stage. Initially human dermal fibroblasts (HDF) are collected from adult donors and cultured in medium with retrovirus containing Oct3/4, Sox2 and/or either Klf4 and c-Myc, or Nanog and Lin28 (this combination varies in different laboratories). Upon adding this retrovirus, HDF cells form a colony that are visually hES cell-like. With time these cells differentiate into pluripotent stem cells. Once again, different laboratories will use different transcription factors to derive into cardiomyocytes (Green: (Takahashi et al., 2007); Blue: (Doss et al., 2012)).**

Since these studies were published, many researchers have induced/reprogrammed pluripotent stem cells from human fibroblasts using different transcription factors. The use of Oct3/4 is important as using either of two homologs (Oct1 or Oct6) leads to an inability to induce iPSCs. The same study reported that the Myc retrovirus is not necessary for the generation of hiPSCs (Nakagawa et al., 2008). There appears to be no consensus as to what the best combination of factors is. Some research groups use Takahashi's factors for the induction of pluripotent stem cells from human fibroblasts: Oct4, Sox2, Klf4 and c-myc

(Woltjen et al., 2009, Fujiwara et al., 2011, Zwi et al., 2009, Lahti et al., 2012). Other groups use Oct4, Sox2, Nanog and Lin28 (Doss et al., 2012, Zhang et al., 2009, Hoekstra et al., 2012, Yu et al., 2007).

Using the same lentiviral-transduced transcription factors as Yu et al. (2007), Zhang et al. (2009) were able to produce embryoid bodies (EBs) and subsequently derived functional beating human cardiomyocytes. These EBs were cultured in a differentiation medium containing non-essential amino acids, L-Glutamine,  $\beta$ -mercaptoethanol and foetal bovine serum (FBS). After 4 days in this medium they were plated, and spontaneously contracting areas could be observed after 8-9 days. It was reported that these derived cardiomyocytes had a well-organised sarcomeric structure, with a striated pattern for  $\alpha$ -actinin in the Z-line of the sarcomere. In the same year, another group (Zwi et al., 2009) derived cardiomyocytes from pluripotent stem cells induced using Takahashi's factors, with the addition of hTERT and SV40-large T, a catalytic transcriptase and an antigen, which have anti-apoptotic properties and allow for a faster cell culture growth (Park et al., 2008). To derive into cardiomyocytes, small clumps of pluripotent stem cells were spread on collagenase IV to form EBs. After 4 days of differentiation, cardiac markers and cardiac-associated transcription factors were present: Nkx2.5, Mef-2c, and Gata-4. Another author added five different growth factors to Yu's (2007) factors for this derivation: BMP4, Activin A, bFGF, VEGF and DKK-1 (Doss et al., 2012).

## **1.3 Methods for maturation**

### **1.3.1 T3**

Thyroid hormone T3 (Tri-iodo-L-thyronine) is important in the regulation of the switch of the isoform titin from foetal to adult type (Klein and Ojamaa, 2001, Kruger et al., 2008). Titin is involved in the maintenance of the elasticity of the sarcomere, and this shift alters the passive tension that occurs in maturing cardiomyocytes (Yang et al., 2014, Warren et al., 2004, Lahmers et al., 2004, Opitz et al., 2004). T3 is also involved in repression of the expression of foetal genes in neonatal cardiomyocytes so they can go through the maturation process (Klein and Ojamaa, 2001, Dillmann, 2002). The addition of T3 to hiPSC-CMs led to physiological hypertrophy and increased contractile force generation and mitochondrial respiratory capacity (Yang et al., 2014). Further studies have shown that T3 might be sufficient for T-tubule development, enhanced Ca-induced Ca release, and more ventricular-like excitation-contraction coupling (Parikh et al. 2012).

### 1.3.2 Ascorbic acid

Cao et al. (2012) investigated the effect of ascorbic acid (AA) in the promotion of cardiac differentiation in hiPSC-CMs. Despite its exact role being unknown, this treatment increased the expression of GATA4, Isl1, and Mef2c, known cardiac transcription factors, while reducing the expression of the pluripotency markers Oct4, Nanog and Rex1 more rapidly. This led to the suggestion that AA might be useful in overcoming cell line variation and in improving maturation.

### 1.3.3 Extracellular matrix maturation

Da Rocha et al. (2017) significantly induced the expression of mature cardiomyocyte markers including cardiac specific troponin I (cTnI), sodium channel (Nav1.5, Kir2.1 and Cx43), by plating commercially available hiPSC-CMs on Polydimethylsiloxane (PDMS) vulcanised silicone for seven days.

## 1.4 Nonadult-like behaviour of hiPSC-CMs

Despite the potential of hiPSC-CMs, there are concerns about their reliability for studying arrhythmogenic mechanisms and drug safety screening. Studies have shown that action potentials (APs) from these derived cardiomyocytes lack the classic spike and dome and hence have been named “immature” (Bett et al., 2013, Jonsson et al., 2012). Before hiPSC-CMs are designated the cells to use for high-throughput pharmacological screening, they need to have similar genomic, proteomic, pharmacological, mechanical and electrophysiological properties to human cardiomyocytes *in vivo* (Khan et al., 2013). To understand why they are defined as functionally immature, we have to look at their characteristics.

### 1.4.1 Electrical activity in the adult heart

In an adult heart impulse propagation is initiated within the sinoatrial node (SAN) by spontaneous impulse generation. This spreads to the atria, pauses briefly at the atrioventricular node (AVN) and progresses to the ventricles via Bundle of His and Purkinje fibres. The SAN is a specialised cardiac tissue consisting of pacemaker cells. The generation of cardiac rhythm is highly controlled by the funny current ( $I_f$ ) (Tse et al., 2009).

### 1.4.2 Excitation-contraction coupling

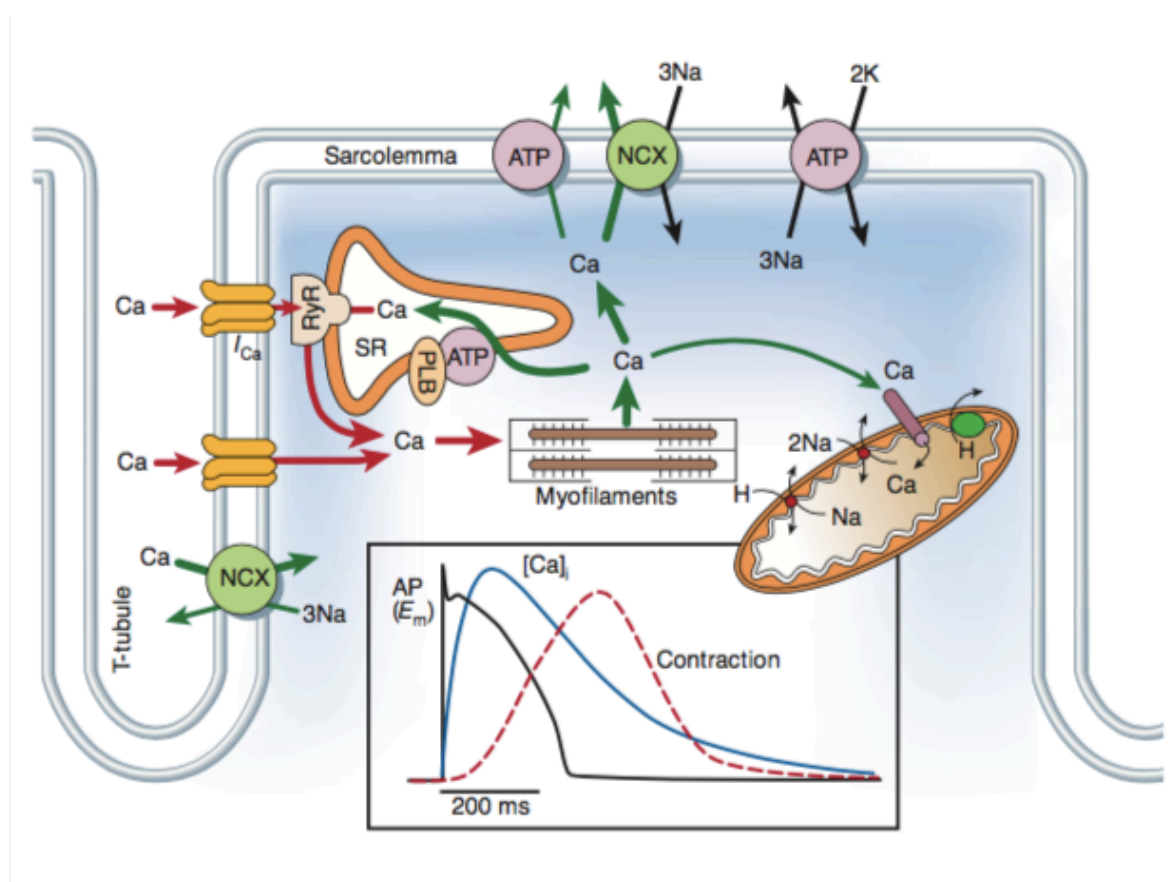


**Figure 1.2 - Excitation-contraction coupling in the adult heart.** Ca<sup>2+</sup> enters the cell through depolarisation-activated Ca<sup>2+</sup> channels, such as the inward Ca<sup>2+</sup> current (I<sub>Ca</sub>). Ca<sup>2+</sup> entry triggers Ca<sup>2+</sup> release from the SR, which raises free intracellular Ca<sup>2+</sup> concentration, allowing Ca<sup>2+</sup> to bind to the myofilament protein: troponin C, which then starts the contraction. To relax, intracellular Ca<sup>2+</sup> declines via transport out of the cytosol by SERCA, sarcolemmal Na<sup>+</sup>/Ca<sup>2+</sup> exchange, Ca<sup>2+</sup>-ATPase, or the mitochondrial Ca<sup>2+</sup> uniporter. Figure from Bers (2002).

Ca<sup>2+</sup>-induced Ca<sup>2+</sup>-release (CICR) from the sarcoplasmic reticulum (SR) is the key link between electrophysiological stimulation and the production of mechanical force as well as the feature that distinguishes cardiomyocytes from other types of muscle cells. In the adult, SR contribution to CICR in the rat myocyte is 87-92%, in the rabbit 70-74%, and in the human myocyte 63% (Bers, 2008). Depolarisation leads to Ca<sup>2+</sup> entry via L-type voltage-sensitive Ca<sup>2+</sup> channels, which in turn triggers the release of Ca<sup>2+</sup> from the SR via ryanodine receptors (RyR). This raises the intracellular Ca<sup>2+</sup> concentration and causes contraction. Relaxation occurs when Ca<sup>2+</sup> is removed from the cytosol, by re-sequestering it in the SR via the sarco-endoplasmic reticulum ATP-ase (SERCA), or extruding it into the extracellular space through the Na<sup>+</sup>-Ca<sup>2+</sup> exchanger (NCX) or Ca<sup>2+</sup> ATPase pump (Bers, 2002). The SR plays an important role in ECC in adult CMs. Low levels of

calsequestrin, phospholamban, RyR and SERCA have been reported and corroborated by relatively low amount of SR and mixed responses to caffeine, thapsigargin and ryanodine (Denning et al., 2016).

The sodium-potassium exchanger (NCX) has a key role in maintaining  $\text{Ca}^{2+}$  homeostasis, as it moves  $\text{Ca}^{2+}$  across the sarcolemma during systole in exchange for  $\text{Na}^{+}$  moving into the cell at a ratio of 3:1 (3  $\text{Na}^{+}$  move in for each  $\text{Ca}^{2+}$  out). Due to this stoichiometry, NCX generates a substantial inward current ( $I_{\text{NCX}}$ ) that contributes to cell depolarisation, pacemaker activity and action potential duration (Blaustein and Lederer, 1999).

### **1.4.3 Electrophysiology in hiPSC-CMs**

#### **1.4.3.1 Structure**

Adult ventricular cardiomyocytes show an extensive t-tubule network (Figure 1.2 and Figure 1.3), which is absent in hiPSC-CMs. In adult CMs, L-type  $\text{Ca}^{2+}$  channels ( $I_{\text{Ca-L}}$ ) are located primarily at sarcolemmal–SR junctions where the SR  $\text{Ca}^{2+}$  release channels (or ryanodine receptors) exist. During excitation–contraction coupling, SR  $\text{Ca}^{2+}$  release also contributes to  $\text{Ca}^{2+}$ -dependent inactivation of  $I_{\text{Ca}}$  (Figure 1.2) (Bers, 2002). The lack of a t-tubule network in hiPSC-CMs results in a slower excitation-contraction coupling and  $\text{Ca}^{2+}$  enters the cell primarily via the sarcolemma rather than from releasing from the sarcoplasmic reticulum (SR) (Figure 1.3) (Robertson et al., 2013).

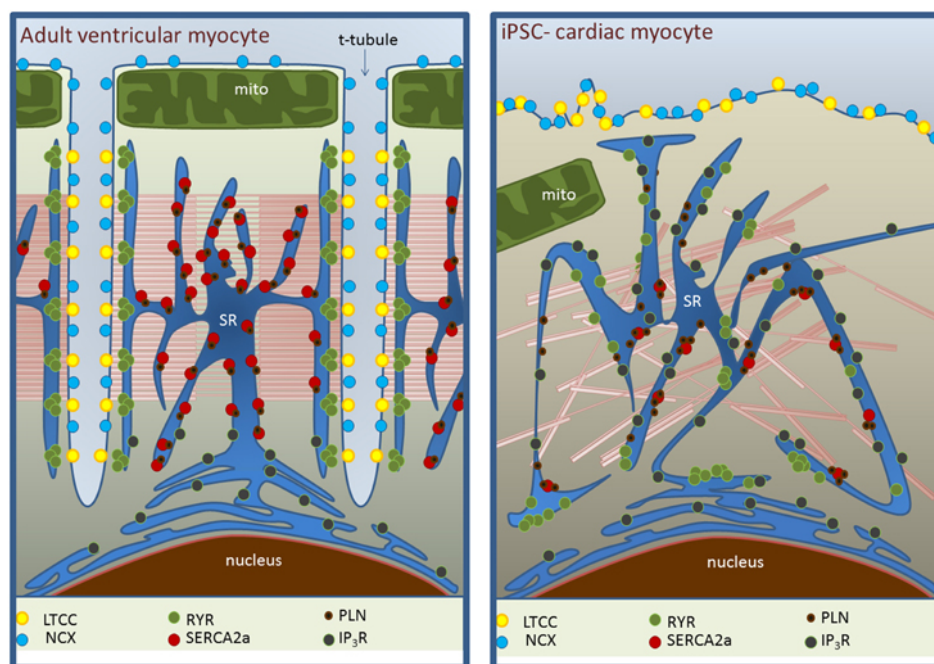


**Figure 1.3 – Ultrastructural differences between adult myocytes (left) and hiPSC-CMs (right) in ECC. T-tubules are absent in hiPSC-CMs, which is associated with a lack of regular organisation of the LTCC-RyR complexes. SERCA expression is also reduced with a maintained phospholamban (PLN) expression. Inositol-triphosphate (IP<sub>3</sub>R) activity is substantially higher (Kane et al., 2015a).**

The absence of t-tubules in hiPSC-CMs is associated with the lack of regular organisation of LTCC-RyR complexes and less homogenous distribution of RyRs. SERCA expression is reduced in hiPSC-CMs compared to adult ventricular myocytes with a maintained PLN expression. NCX expression may be maintained but its ability to extrude Ca<sup>2+</sup> in diastole is decreased. Inositol-triphosphate receptor (IP<sub>3</sub>R) activity is substantially higher (Figure 1.3) (Kane et al., 2015a). IP<sub>3</sub> activity is prominent in neonatal and failing human cardiomyocytes. There is evidence to support it plays a complex role in IP<sub>3</sub>-mediated Ca<sup>2+</sup> release in stem cells, but it is unclear how it works together with other Ca<sup>2+</sup> handling pathways (Kane et al., 2015).

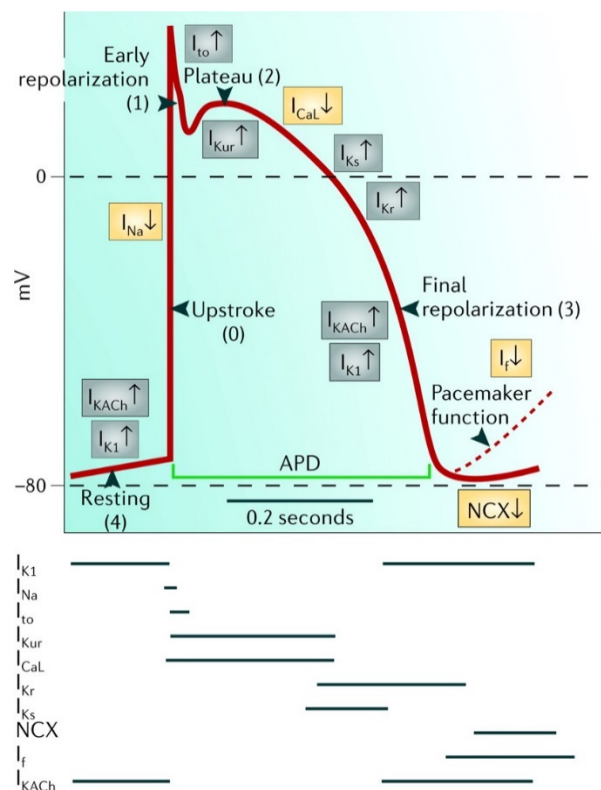
Structurally, hiPSC-CMs are round or multi-angular, small cells with a single nucleus and a chaotic alignment, also disorganised and short sarcomeres (~1.6µm) (Denning et al., 2016). Where adult CMs have Z-disks, I-, H-, M- and A-bands, hiPSC-CMs show mainly Z-disks and I-bands (Denning et al., 2016).

### 1.4.3.2 Spontaneous activity

In hiPSC-CMs, the spontaneous electrical activity is thought to occur from either low expression or absence of the inward rectifying potassium current through the expression of

the pacemaker current ( $I_f$ ), a complex interaction with the rapid delayed rectifier, or a combination of these factors (Bett et al., 2013). hiPSC-CMs resemble human CMs in many aspects, but as it was mentioned before, with a foetal-like phenotype in their ion channel profile and mechanisms of contraction.

hiPSC-CMs show spontaneous contractile activity, accompanied by the corresponding diastolic depolarisation, which results in spontaneous APs (Hoekstra et al., 2012). Jonsson et al. (2012) characterised hESC-CMs as having an immature phenotype, which could particularly be due to the lack of functional  $I_{K1}$ , resulting in smaller currents compared to those seen in adult CMs. hiPSC-CMs have a high expression of  $I_f$  (Bett et al., 2013, Ma et al., 2011b) and low expression of  $I_{K1}$  (Doss et al., 2012) (which normally stabilises  $E_m$  at around -85mV), but the value is -20 to -60mV in hiPSC-CMs (Denning et al., 2016). Although  $I_f$  has been detected in ventricular cardiomyocytes, it did not lead to automaticity. The block of  $I_{K1}$  though, has been shown to lead to automaticity, even in the presence of  $I_f$ , and genetic mutations resulting in  $I_{K1}$  loss of function are a well-established



Copyright © 2006 Nature Publishing Group  
Nature Reviews | Drug Discovery

**Figure 1.4 - Adult cardiomyocyte action potential and the action of the different ionic currents on depolarisation, repolarisation and the resting membrane potential. Picture from (Nattel & Carlsson, 2006).**

type of long QT syndrome with a propensity for increased early afterdepolarisations (EADs) (Bett et al., 2013).

Multiple studies have been conducted to compare the electrophysiology of human adult CMs and hiPSC-CMs, by recording and subsequently analysing APs from single cells or clusters. A debate exists as to whether one or more AP phenotype can be detected in hiPSC-CMs as found in the human heart. Microelectrode array and patch clamp studies have reported the existence of three different phenotypes in hiPSC-CMs: ventricular, atrial and nodal (Ivashchenko et al., 2013, Zhang et al., 2009, Cao et al., 2012, Ma et al., 2011b), and a special cell has been reported in a single study, S-type cell (Scheel et al., 2014). The latter was characterised as a cell presenting a fast typical ventricular phase 0, but completely lacking a plateau phase (Figure 1.4). This has been suggested to be a consequence of increased production or impaired scavenging of reactive oxygen species (Scheel et al., 2014). It has been reported that ventricular-like APs were distinguishable as they displayed a more negative maximum diastolic potential, a rapid action potential upstroke, and a distinct plateau phase. Atrial-like cells did not have a distinct plateau during repolarisation and had a higher frequency of spontaneous activity. Nodal-like cells were characterised as having less negative maximum diastolic potentials than ventricular-like cells, smaller AP amplitude, a slower AP upstroke, and a pronounced phase 4 of depolarisation (Scheel et al., 2014, Zhang et al., 2009, Ivashchenko et al., 2013, Ma et al., 2011b). Ivashchenko et al. (2013) reported that atrial- and ventricular-like hiPSC-CMs had no spontaneous APs but responded to stimulation with a depolarising current pulse at 0.5Hz. More recent research has started a discussion of whether there is chamber-specificity. Du et al. (2015) reported that the seeding density affects the morphology of the AP significantly, and that AP morphologies were normally distributed within a spectrum with no evidence for specific subpopulations. They concluded that there is no clear evidence of chamber-specificity and AP morphology does not predict cardiac chamber subpopulations (Du et al., 2015).

Giles and Noble (2015) proposed that  $I_{K1}$  is of critical importance, and voltage-sensitive dye recordings cannot yield any direct information concerning the resting potential and  $I_{K1}$ . This argues that to validly phenotype these cells, it is important to know the expression levels of  $I_{K1}$ . Kane et al. (2015a) added that at the current stage of development, hiPSC-CMs cannot completely mirror the highly specialised, chamber-specific, human adult cardiomyocytes. Currently it is difficult to accurately study electrophysiological

parameters as patch clamping, most commonly used, has a low throughput and is subjected to selection bias, furthermore it can only be performed on isolated cells. Also, hiPSC-CMs are morphologically heterogenous, flat, and difficult to impale. For these reasons, data obtained from isolated hiPSC-CMs should be interpreted with caution.

## 1.5 Candidate channels for maturation

### 1.5.1 $I_{K1}$

Cardiac potassium channels are proteins that exist in the sarcolemmal membrane and provide a high-conductance pathway for  $K^+$  ions. These play a critical role in the heart in maintaining normal electrical activity (Snyders, 1999, Tamargo et al., 2004, Walsh, 2014). The inwardly rectifying potassium current ( $I_{K1}$ ) is responsible for shaping the initial depolarisation by determining the excitation threshold, initiating the final repolarisation (phase 3), and the resting phases of the ventricular action potential (Dhamoon and Jalife, 2005, Tamargo et al., 2004, Vaidyanathan et al., 2010, Ma et al., 2011b). It plays an important role in maintaining the normal electrical activity and determining the shape and duration of the action potential (Walsh, 2014), and it becomes minimal at positive voltages due to its rectification properties (Ma et al., 2011b). The *KCNJ2* gene encodes the inward rectifier  $K^+$  channel 2.1 (Kir2.1), a component of the inward rectifier current  $I_{K1}$ . This current therefore provides a polarising current during the most terminal phase of repolarisation and is the primary conductance controlling the diastolic membrane potential (Tristani-Firouzi and Etheridge, 2010, Doss et al., 2012). The finding that mutations in *KCNJ2* (but not the genes encoding Kir2.2 and 2.3) cause human disease further underscores its pivotal role as a primary component of  $I_{K1}$  (Tristani-Firouzi and Etheridge, 2010). Therefore, modulation of  $I_{K1}$  would likely have a profound effect on cardiac excitability and arrhythmogenesis (Dhamoon and Jalife, 2005).

Ion channels can be conceptualised as electrical resistors in the plasma membrane, which selectively pass charges in the form of ions between the intracellular and extracellular compartments. These resistors are termed *ohmic* because they follow Ohm's law:

$$V=I.R$$

where  $V$ = voltage gradient,  $I$ = current,  $R$ = resistance. In contrast to *ohmic* channel behaviour, rectification is described as a nonlinear  $I/V$  relationship, as conductance ( $G$ ) is

the inverse of  $R$ , to describe the biophysical properties of the channel in voltage clamp experiments. A rectifying current preferentially allows current in one direction and not the other. At negative membrane potentials  $I_{k1}$  conductance is much larger than that of any other current, and so it clamps the resting membrane potential close to the  $E_k$  (Tamargo et al., 2004).

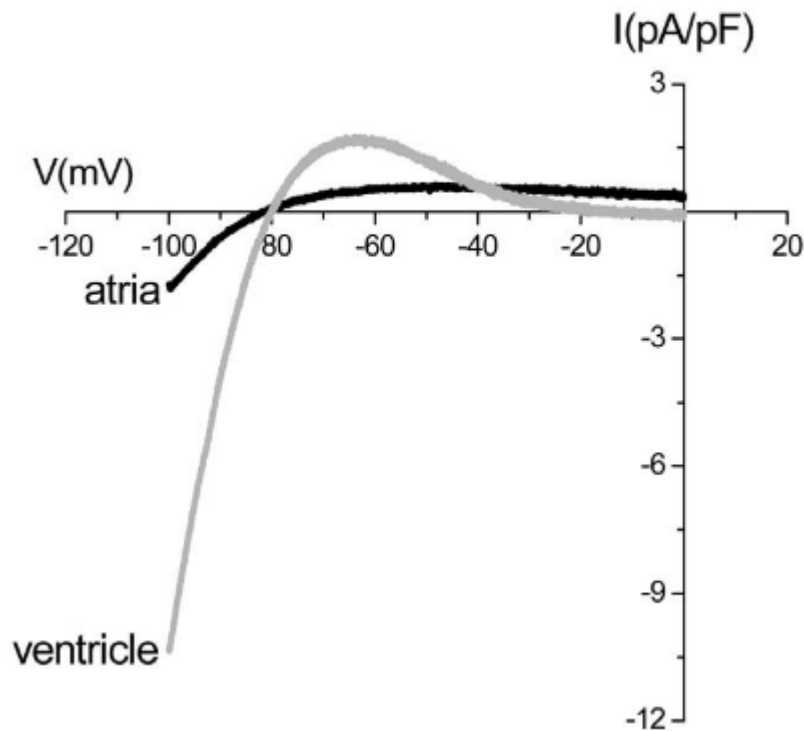


**Figure 1.5 - I/V (current-voltage) relationships of atrial and ventricular  $I_{k1}$ . Greater current density in ventricle than atria. Ventricular  $I_{k1}$  has a prominent negative slope conductance, which is less evident in atrial  $I_{k1}$ . Figure from Dhamoon and Jalife. (2005).**

Inwardly rectifying potassium channels, as illustrated (Figure 1.5), pass inward currents at potentials more negative than the reversal potential of  $K^+$  ( $E_k$ ) but allow significantly less current at more positive potentials (Dhamoon and Jalife, 2005).

### 1.5.1.1 The structure of $I_{k1}$

The Human Genome Organization named the genes encoding the inward rectifier subfamily *KCNJ* (Dhamoon and Jalife, 2005). Subfamily 2 members (Kir2.1, Kir2.2, and Kir2.3(Kir2.x)<sup>3</sup>) are the molecular correlates of  $I_{k1}$  in the heart.

Activation of  $I_{k1}$  does not depend on membrane potential ( $V_m$ ) alone but rather the difference between  $V_m$  and  $E_k$ , as extracellular  $K^+$  ( $[K^+]_o$ ) is changed (Dhamoon and Jalife, 2005, Luo and Rudy, 1991), The inward rectification is significantly marked for  $I_{k1}$ , which allows it to set a stable resting potential by carrying substantial current at negative potentials (Snyders, 1999). Upon depolarisation,  $I_{k1}$  channels inactivate almost immediately, remain closed throughout the plateau phase, with zero contribution at high potentials, and open again at potentials negative to  $-20mV$ . These characteristics reflect the voltage and  $[K^+]_o$  dependence (Luo and Rudy, 1991, Tamargo et al., 2004). Most importantly,  $I_{k1}$  stabilises the resting membrane potential and determine the cell input resistance.

$I_{k1}$  is an inwardly rectifying potassium current preferring inward over outward conductance due to block of the pore at depolarised membrane potentials by intracellular divalent cations such as  $Mg^{2+}$  and  $Ca^{2+}$  and by polyamines such as spermine and spermidine (Anumonwo and Lopatin, 2010). Kir2.1 is the predominant expressed protein in cardiac tissue out of all members of this family, however the exact role of  $I_{k1}$  in cardiac arrhythmias is poorly understood (Skarsfeldt et al., 2016).

### 1.5.1.2 Lack of $I_{k1}$ on hiPSC-CMs

A reduction in  $I_{k1}$  leads to the generation of spontaneous ventricular activity. It has been shown that Kir2.1 channel blockade results in increased frequency of spontaneous action potentials in isolated myocytes (Doss et al., 2012). *In silico* reduced  $I_{k1}$  initially caused mild prolongation of the most terminal part of the AP, with greater decreases resulting in the generation of spontaneous APs that are triggered by  $I_{NCX}$  (Tristani-Firouzi and Etheridge, 2010). Changes in  $I_{k1}$  have significant effects on the cardiac action potential morphology, the excitability of the heart, and thereby possibly contribute to or protect against cardiac arrhythmia (Schmitt et al., 2014).

$I_{k1}$  is almost non-existent in sinoatrial node cells, allowing for a relatively depolarised membrane potential ( $-50mV$ ) with respect to the ventricles ( $-80mV$ ), which have robust  $I_{k1}$  expression (Dhamoon and Jalife, 2005). In the SA node, the absence of  $I_{k1}$  allows for small inward currents to pass through the non-selective cation current ( $I_f$ ) to slowly depolarise the membrane during diastole which maintains the pacemaker activity.  $I_{k1}$  current density is six to ten times larger in the ventricles than in the atria, resulting in a more hyperpolarised resting membrane potential and faster phase 3 repolarisation in the

ventricles (Dhamoon and Jalife, 2005). The downregulation of  $I_{k1}$  produces membrane depolarisation, prolongation of the APD and both early and delayed after depolarisations, and mutations of *KCNJ2* encoding Kir2.1 result in dominant negative effects on the current (Tamargo et al., 2004). These have been associated with Andersen-Tawil syndrome – an inherited disease characterised by periodic paralysis, dysmorphic features, QT prolongation and ventricular arrhythmias (Tamargo et al., 2004, Doss et al., 2012).

In the past,  $I_{k1}$  has been blocked by non-specific compounds like RP-58866, MS-551, chloroquine, tamoxifen, or by cations such as barium and caesium. However, all these compounds affect other targets in addition to the Kir2.x currents. In isolated adult canine ventricular cardiomyocytes, pentamidine blocks the pore region of Kir2.1 from the cytoplasmic side (De Boer et al., 2010). Takanari et al. (2013) examined several analogues of pentamidine and found PA-6 has the highest affinity for cardiac  $I_{k1}$ . PA-6 is pentamidine with a phenyl-substituted alternative arrangement of the amidine group. It has provided improved blocking capacity (12.1% and 10.8% *re* for inward and outward currents, respectively) (Takanari et al., 2013).

Ma et al. (2011a) were the first to show that  $I_{k1}$  is present in hiPSC-CMs, which is likely to contribute to more negative MDP values. Despite its presence, high levels of  $I_f$  prevent a full resting membrane potential repolarisation, therefore contributing to automaticity. Kane et al. (2015a) suggests that  $APD_{90}$ - $APD_{30}$  correspondent to the time for repolarisation, presumably highly dependent of  $I_{k1}$ , independent of APD, could be representative of chamber-specificity through its connection to  $I_{k1}$  presence. When replotting data from Bett et al. (2013), another group (Kane et al., 2015a) showed that AP duration is fairly uniform after corrections for  $I_{k1}$ , and that there is no relationship between this distribution and the ventricular chamber-specificity presented by the group.

### 1.5.2 The presence of $I_f$

In 1993, DiFrancesco discovered an ion current which he thought was ‘funny’ in the SAN of the rabbit. This was unusual as it was hyperpolarisation-activated and carried by both sodium and potassium ions. Hence, he named it  $I_f$  (DiFrancesco, 1993, Gewirtz, 2009). This current is active in diastole between -50 and -20mV (Figure 1.6), when it inactivates, followed by the activation of the T-channel calcium current, which continues the process

of diastolic depolarisation, and therefore has a pivotal role in the generation of cardiac rhythms in pacemaker cells (Gewirtz, 2009, Tse et al., 2009).

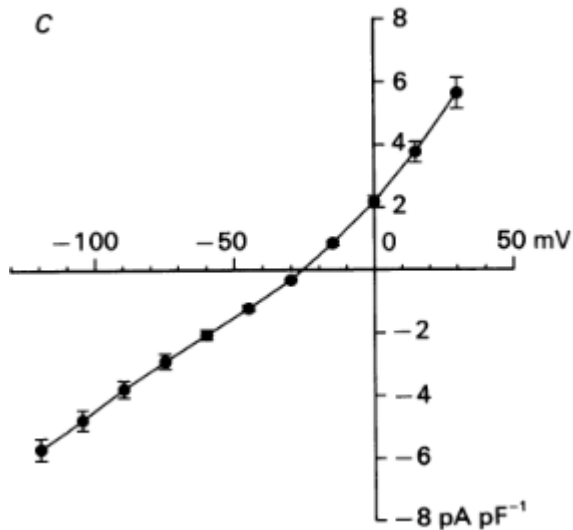


**Figure 1.6 - Fully activated I-V relationship for  $I_f$ . Figure from Zhou and Lipsius (1992).**

$I_f$  is a significant contributor to spontaneous pacemaker activity in the mammalian heart (Gewirtz, 2009).  $I_f$  is encoded by the hyperpolarisation-activated cyclic nucleotide-modulated (*HCN*) channel gene family (Tse et al., 2009). The approaches of  $I_{K1}$  suppression and  $I_f$  overexpression have been independently and, most commonly, exploited to convert normally quiescent CMs into spontaneously AP-firing cells as bioartificial pacemakers (Tse et al., 2009).  $I_{K1}$  synergistically interacts with  $I_f$  by maintaining the voltage changes within a range where *HCN* channels can most effectively operate during a dynamic cardiac cycle (Tse et al., 2009).

### 1.5.2.1 The presence of $I_f$ in hiPSC-CMs

The density of  $I_f$  in human ventricular myocytes is controversial (Hoppe et al., 1998). It has been reported that  $I_f$  is highly expressed in the foetal/neonatal heart and decreases with maturation. Re-expression is associated with cardiac hypertrophy and failure in rats (Stillitano et al., 2008). The relatively high density of  $I_f$  in hiPSC-CMs compared to adult ventricular cardiomyocytes (in adult rats the density is  $-1.97 \pm 0.56 \text{ pA/pF}$ ) (Fares et al., 1998, Stillitano et al., 2008) is a possible explanation for the automaticity of the first (Ma

et al., 2011b). In hiPSC-CMs, at voltages below -60mV,  $I_f$  undergoes time-dependent activation, and the gating properties resemble those of adult cardiomyocytes (Ma et al., 2011b).

### 1.5.3 Other pacemaker currents (NCX/Ca)

Expression of NCX in hiPSC-CMs is comparable to that in the adult human heart (Kane et al., 2015a, Kane et al., 2015b). However, the rate of decline of  $Ca^{2+}$  transients is extremely slow in hiPSC-CMs with both absolute values for SR  $Ca^{2+}$  uptake and NCX-mediated  $Ca^{2+}$  extrusion significantly reduced – hiPSC-CMs display significantly impaired diastolic  $Ca^{2+}$  removal (Kane et al., 2015a). This also stands in contrast to the consistent observation that hiPSC-CMs display a negative force-frequency response (FFR), a phenomenon observed in failing hearts, consistent with substantially reduced SR function (Kane et al., 2015a).

Further studies show that the contribution of SR  $Ca^{2+}$  flux is 60% in hiPSC-CMs, which is not different from that seen in adult rabbit ventricular CMs and human. While some studies report either a complete lack or small presence of caffeine-releasable SR  $Ca^{2+}$  stores, others report that these exist in 100% of hiPSC-CMs tested (Hwang et al., 2015). The reason for this difference can be attributable to variability in cardiac differentiation, dependence on chemically undefined growth factors and cytokines, or growth factors and cytokines failing to gain access to the embryoid body interior (Hwang et al., 2015). Hwang et al. (2015) found that SR  $Ca^{2+}$  stores and  $Ca^{2+}$  handling are day-dependent. Contributions from day 15 to day 21 suggest that SERCA and NCX contributions are similar, while non-NCX contribution decreases in day 21. These findings suggest that non-NCX pathways may be compensation for the decreased SERCA activity in early stages.

## 1.6 Gap junctional channels

Gap junction channels are intercellular conductors for exchange via diffusion of ions, metabolites, and second messengers. These are important in the heart as they establish electric and metabolic coupling between cardiomyocytes, important for impulse propagation. Gap junctions are composed of proteins called connexins (Cxs), which form low resistance channels that enable electrical coupling of adjacent myocytes and intercellular electrical communication (Wang et al., 2016). Cx43, Cx40, Cx45 and Cx37 are known to be expressed in the heart. Connexin 43 (Cx43) is the main Cx expressed in

the adult working myocardium of the ventricle in mouse (Wang et al., 2016) and human (Bruce et al., Vozzi et al., 1999, Bruce et al., 2008), encoded by the *Gjal* gene, and it has a mobility of 43kDa (Oyamada et al., 2013).

Alterations in the localisation, expression level and nature of Cx43 can cause abnormal conduction, leading to arrhythmias, therefore engraftment of Cx43-expressing myocytes can potentially reduce life-threatening post-infarct arrhythmias through the augmentation of intercellular coupling in a cardiac cell-based therapy (Roell et al., 2007).

In hiPSC-CMs, Cx43 is only expressed on the membranes of adjacent hiPSC-CMs which need communication or material exchange (Wang et al., 2016). Eng et al. (2016) found that chronic stimulation of hiPSC-CMs over prolonged periods of time (1 week) at 2Hz led to an increase in Cx43, and to an organisation of the sarcomere. When stimulation was stopped, these cells beating rate remained that of the stimulation.

In the HEK cell line produced for stable  $I_{K1}$  expression used for these studies (HEK stably expressing murine wildtype Kir2.1-GFP. HEK-KWGF), Cx43 was present, albeit in fairly low levels compared to rat neonatal cardiomyocytes (De Boer et al., 2006).

## **1.7 Alternative approach to changing electrical phenotype**

This immature status due to the lack of certain currents, as mentioned before (see section 1.5), calls for an external source of ionic channels and their currents. The Human embryonic kidney cell (HEK cell) line is of epithelial origin. They have been exposed to sheared fragments of human adenovirus type 5 (Ad5) DNA, to generate the widely used HEK293 cell line. These cells can be transfected with the necessary gene product to express exogenous proteins stably (Thomas and Smart, 2005). HEK cells can be sourced from the American Type culture collection (ATCC: Manassas, USA), which maintains not only the original Ad5 line, but also HEK293E, which has been transformed by the Epstein-Barr (EBNA1) virus, but also a HEK293T, which has been transformed with an SV40 virus (Thomas and Smart, 2005). It has been widely used as an expression tool for recombinant proteins for the past 25 years (Thomas and Smart, 2005).

These cells adhere to substrate when kept in culture at 37°C in a 5% CO<sub>2</sub> 95% air humidified incubator, and can be continuously cultured, passaged and frozen for future

use, although it is not recommended to go over 20-30 passages of the same cell vial obtained from ATCC (Thomas and Smart, 2005). At roughly 20-30 $\mu$ m in length, the cell is suitable for drug perfusion to all parts of the cell through whole-cell recording methods. The fidelity with which it can express exogenous receptors makes it a candidate for many kinds of transfections, allowing for the expression of proteins from other sources and for other purposes, such as  $I_{K1}$ . In 2006, De Boer et al. (2006) were successfully able to stably produce a current by expressing the protein in HEK293 by transfecting them with C-terminal GFP-tagged Kir2.1. Kir2.1 appears to be present at the plasma membrane, and exhibit the presence of high levels of  $I_{K1}$ , displaying an I-V curve characteristic of Kir2.1 channel densities. These cells also demonstrated the presence of Cx43, however the levels were fairly low. These cells are easy to maintain, and are defined as “immortal”, as they can be grown and passaged numerous times, thawed and re-frozen. When applied to HEK-KWGF cells, stably expressing GFP-tagged murine Kir2.1, pentamidine at 10 $\mu$ M inhibited outward current by approximately 45%. In contrast, under the same conditions, a 1000-fold lower concentration of PA-6 produced 83% block (Takanari et al., 2013). Furthermore, PA-6 did not significantly affect  $I_{NaV}$ ,  $I_{Ca-L}$ ,  $I_{to}$ ,  $I_{Kr}$ , and  $I_{Ks}$  at 200nmol/L (Takanari et al., 2013). So far, the role of  $I_{K1}$  has been investigated using Barium Chloride, however  $Ba^{2+}$  is not a specific blocker of  $I_{K1}$ , as it also blocks other inwardly  $K^+$  rectifiers. Furthermore,  $Ba^{2+}$  is toxic and not tolerated *in vivo* (De Boer et al., 2010).

## 1.8 Conclusion and aims

On the basis of this information, there are major benefits to be gained from achieving a more mature phenotype in hiPSC-CMs: (i) more adult-like tissue would provide a more appropriate screening material for pharmaceutical research; (ii) a more mature phenotype would help in the development of suitable tissue grafts that could be used as a future treatment for repair of the heart after an MI.

### 1.8.1 Aims

The overall aim of the project was to investigate techniques to improve the electrophysiology of hiPSC-CMs and study the consequences on EC coupling in this tissue. The main hypothesis tested was that lack of  $I_{K1}$  was the main cause of immature electrophysiology and that addition an  $I_{K1}$  component will regularise the hiPSC-CM electrophysiology. In particular, the project wishes to:

1. Determine, using pharmacological tools, the evidence for the relative roles of  $I_{k1}$  and  $I_f$  in the pacemaker mechanism in hiPSC-CMs;
2. Test the concept that co-culture of hiPSC-CMs with an  $I_{k1}$ -expressing HEK cell line is a viable method for restoring  $I_{k1}$  function in a controlled dose-dependent manner;
3. Examine, using voltage-sensitive dye signals, the extent to which co-culture with HEK cells influence electrical and mechanical behavior of hiPSC-CMs;
4. Investigate whether over-expression of Cx43 in HEK cells enhances the effect of  $I_{k1}$ -expressing HEK cells on hiPSC-CMs electrical activity in co-culture.

This work will use established and fully characterised cell lines, in particular commercial hiPSC-CMs that have previously been shown to lack  $I_{k1}$  and have  $I_f$  (Doss et al., 2012, Bett et al., 2013, Kane et al., 2015a). De Boer et al (2006) successfully stably expressed  $I_{k1}$  in an HEK line. These facts have been established in literature (De Boer et al., 2006, De Boer et al., 2010, Takanari et al., 2013), and, as such, the current work is based on this assumption.

## **2 General Methods**

## **2.1 Health and Safety**

All the experimental work was compliant with Health and Safety rules. COSHH forms and rules were in place for the use of substances hazardous to health.

## **2.2 Cell culture**

### **2.2.1 Pre-plating protocol**

96-well glass-bottom plates (MatTek, US) were coated with bovine fibronectin (Sigma Aldrich) diluted in DPBS (Dulbecco's phosphate-buffered saline) with  $\text{Ca}^{2+}$  and  $\text{Mg}^{2+}$  (Thermo Fisher, US) to a final concentration of  $10\mu\text{g/mL}$  and left either at  $37^{\circ}\text{C}$  5%  $\text{CO}_2$  75% humidity for a minimum of 3 hours when plating on the same day, or at  $4^{\circ}\text{C}$  if to be kept for longer periods of time. Fibronectin was left to settle for the period specified above, and the supernatant was removed during the plating prior to hiPSC-CMs being added. The same procedure was repeated for inserts (Ibidi, UK) in glass-bottom 6-well plates (MatTek). In the latter, the inserts were attached to glass-bottom culture petri dishes, and fibronectin was added as above.

### **2.2.2 Pluricytes® hiPSC-CMs handling and plating**

Pluricyte® hiPSC-CMs are spontaneously active cells which can be obtained commercially (Plurionics, Netherlands). They are readily available, having been pre-differentiated into cardiomyocytes – the factors used by this provider are unknown. hiPSC-CMs were kept at  $-180^{\circ}\text{C}$  in liquid nitrogen until ready to be used. The cells were thawed at  $37^{\circ}\text{C}$  for exactly 4 minutes in either a water bath or an incubator. The vial was then sterilised with 70% ethanol. The cells were quickly transferred to a 50mL tube in a sterile laminar flow hood, and the cryovial was rinsed with 1mL of Pluricyte® Cardiomyocyte medium (Plurionics, Netherlands). Pluricyte® Cardiomyocyte medium is a chemically defined medium designed to promote cardiomyocyte maturation and cell function. Another 1mL of Pluricyte® Cardiomyocyte medium was added to the cells in a drop-wise fashion every 5 seconds, while swirling the cells. Another 3.7mL of Pluricyte® Cardiomyocyte medium was added per manufacturer's instructions, drop-wise every 2-4 seconds. Once mixed, a cell count, using 0.4% trypan blue at 1:1 dilution with cell suspension, and a manual

haemocytometer, was performed for live cells, and total cell number for viability, and the cell density was adjusted as required.

This was done either by adding more medium, or by spinning the cardiomyocytes for 3 minutes at 250xg, and resuspending with adequate volume of Pluricyte® Cardiomyocyte medium. The next step was dependent on the purpose of the plating. If only hiPSC-CMs were to be used, then the fibronectin on the plate was removed by suction, and 100µL of cell suspension were added to the plate, to a final cell density of 25,000-40,000 cells/well. If the cells were to be used for co-culture with HEK293, then the tube containing the cells was kept at 37°C while the HEK293 were thawed (see 2.2.4). On day 1, 24h post-plating, the Pluricyte® Cardiomyocyte medium was refreshed, and then every 3-4 days.

### **2.2.3 Cor.4U® hiPSC-CMs (Axiogenesis, Germany) handling and plating**

Cor.4U® is a hiPSC-CM generated using the Yamanaka protocol (Takahashi et al., 2007) from human skin fibroblasts. These cells were initially cultured with puromycin to select for 100% purity of cardiomyocytes, as Cor.4U® are puromycin resistant to exposure for up to 2µg/mL for up to 24h, and this step hinders the outgrowth of fibroblasts. Cor.4U® hiPSC-CMs were thawed per manufacturer's instructions (Axiogenesis, Germany). The cells were transported in dry ice to a sterile laminar flow hood, and 500 µL Cor.4U medium with 2µg/mL puromycin at 37°C were added before the cryovial was placed in the waterbath until the frozen cell suspension detached. The cells were quickly transferred to 3mL Cor.4U containing puromycin, and the vial was rinsed with a further 1mL of medium, which was added to the tube containing the cells. A cell count was performed using 0.4% Trypan blue and a haemocytometer. Cell density was adjusted accordingly, by adding further medium for dilution, or by centrifuging at 250xg for 2min, and resuspending. As with Pluricyte® Cardiomyocytes, the next steps were dependent on the purpose.

### **2.2.4 General HEK293 handling**

Standard HEK293 (referred to as N hereafter) (courtesy of Professor George Baillie, University of Glasgow) and I<sub>k1</sub>-expressing HEK293 (thus referred to as I<sub>k1</sub>) (courtesy of Dr Van der Heyden, University Medical Center, Utrecht) cells were transferred to -80°C upon arrival. Prior to culturing, these cells were transported in dry ice, and then transferred to the

37°C waterbath until the cell suspension detached from the cryovial. The cells were then slowly transferred to DPBS -Ca<sup>2+</sup> -Mg<sup>2+</sup> and centrifuged at 250g x 2min. The supernatant was removed and the cells were resuspended in HEK medium. Serum-containing medium composed of DMEM (Sigma), 10% foetal bovine serum (Sigma), 1% non-essential amino acids (Gibco), 1% L-Glutamine and 1% penicillin-streptomycin (Sigma), and plated in T75cm<sup>2</sup> flasks, and kept at 35°C, 5% CO<sub>2</sub>, 75% humidity (Thomas and Smart, 2005) until 70-80% confluency was reached. The cells were passaged by washing with DPBS -Ca<sup>2+</sup> -Mg<sup>2+</sup> twice, and adding 0.05% Trypsin-EDTA for 4 minutes, until cells detached from flask. HEK medium was added to stop trypsin effects and cells were centrifuged at 250g x 2 minutes and resuspended in culture medium. HEK293, both sub-types, were frozen by resuspending in medium containing 10% DMSO, and being transferred in cryovials to dry ice, until frozen and then placed at -80°C. To plate these cells for experimental purposes, the thawing process was performed, but once resuspended in either HEK medium or hiPSC-CMs, as necessary, a cell count was done using 0.4% trypan blue and a haemocytometer. Once cell density was adjusted to the required, the cells were transferred to culture, where they were mixed in eppendorfs with hiPSC-CMs before being transferred to the plates.

## 2.3 Solutions used

Pluricyte and Cor.4U maintenance media were provided by each manufacturer, and the composition is unknown.

For voltage studies on cells other than Cor.4U cells, serum-free medium was prepared less than a week prior to experiments. The medium consists of DMEM (with phenol red) with 1mM sodium pyruvate and 10mM galactose.

BMCC is a serum-free medium manufactured by Axiogenesis (Germany). This medium is composed of 1.49mM CaCl<sub>2</sub>, 0.81mM MgSO<sub>4</sub>, 4.40mM KCl, 36mM NaHCO<sub>3</sub>, 77.59mM NaCl, 0.91mM NaH<sub>2</sub>PO<sub>4</sub>-H<sub>2</sub>O, 0.001mM Na<sub>2</sub>SeO<sub>3</sub>-5H<sub>2</sub>O, 0.0008mM KNO<sub>3</sub>, 25mM D-Glucose (dextrose), 25.03mM HEPES, 0.04mM Phenol red, and 1mM Sodium Pyruvate (C<sub>3</sub>H<sub>3</sub>NaO<sub>3</sub>). This medium was recreated with no K<sup>+</sup> (no addition of KCl, and renamed LBMCC, for K<sup>+</sup> studies.

It is worth noting that the medium used for serum-free experiments contains 44mM  $\text{HCO}_3$ , which, at 5%  $\text{CO}_2$  leads to a pH of 7.6.

HEK medium is prepared in DMEM (Sigma), 1% non-essential amino acids (Gibco), 1% L-Glutamine (Sigma), 1% penicillin-streptomycin (Sigma), 10% foetal bovine serum (Sigma). The medium was kept at 4°C for a maximum of 4 weeks.

## **2.4 Measuring voltage with dyes**

Voltage-sensitive dyes (VSDs) are important tools in cardiac electrophysiology, as their use allows for simultaneous recording of changes in the membrane potential from various sites (Larsen et al., 2012). There are two most common types of ratiometry: emission ratiometry and excitation ratiometry. In the first, the tissue is excited with a single wavelength band, while two emission bands are recorded, therefore, normally, two photodetectors carefully aligned to match the corresponding pixels in the image, are required. For the second, two excitation bands are used, but only one emission band is recorded. This reduces the complexity of the photodetector set up but poses a significant technical challenge in that the excitation sources must be rapidly switched in synchrony with the photodetector (Bachtel et al., 2011). Work was initially conducted using di-4-ANEPPS, and later changed to FluoVolt.

### **2.4.1 Cell culture loading with different dyes**

#### **2.4.1.1 Loading with di-4-ANEPPS**

Cell cultures were loaded with the VSD di-4-ANEPPS (Sigma-Aldrich) on the designated day. The dye was prepared in serum-free medium at 37°C (BMCC for Cor.4U CMs, and SFM for Pluricytes) at 5 $\mu\text{M}$  (unless specified otherwise). Cell culture maintenance medium was removed and dye-containing medium was added for 1 minute. This was replaced with 37°C serum-free medium.

### 2.4.1.2 Loading with FluoVolt

Cell cultures were loaded with FluoVolt (Life Technologies) on a designated day. The dyes was prepared as that on section 2.3.1.1 at 1:1000, with 1:100 PowerLoad, as per manufacturer's instructions. The cells were placed at 37°C 5% CO<sub>2</sub> for 25min, after which the medium was replaced with 37°C serum-free medium.

### 2.4.2 Di-4-ANEPPS

The voltage-sensitive dye, di-4-ANEPPS (Pyridinium 4-(2-(6-(dibutylamino)-2-naphthalenyl)ethenyl)-1-(3-sulfopropyl)- hydroxide, inner salt 90134-00-2), was used for initial experiments, as this is a well-known dye. Organic electrochromic dyes like those from the ANEPPS family are fast responding but show a rapid cellular phototoxicity that develops proportionally to the intensity and duration of the illumination and thus limits their use (Warren et al., 2010).

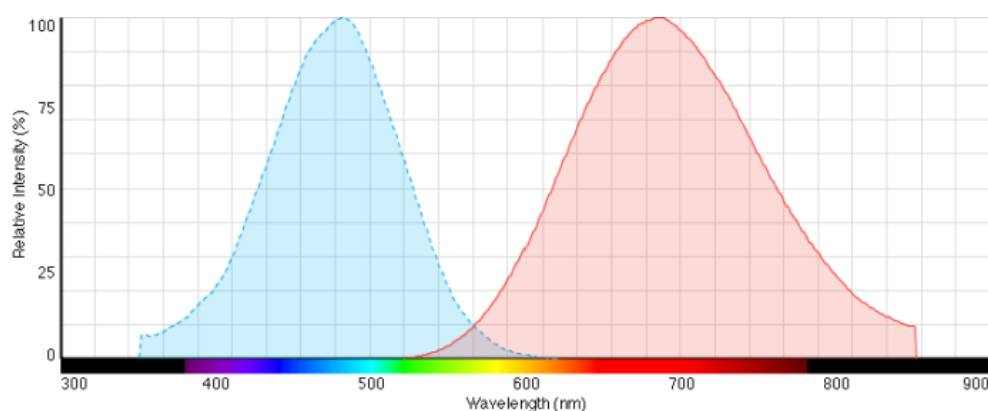


**Figure 2.1 - di-4-ANEPPS excitation/ emission spectrum. Excitation spectrum (blue) and emission spectrum (red) and relative fluorescence intensity. Figure from Thermo Fisher.**

Di-4-ANEPPS has an excitation peak of 475nm when membrane bound, its excitation range is 370-570nm, and its emission range is from 570-850nm, with an emission peak of 617nm when membrane bound.

CelloPTIQ (Clyde Biosciences, UK), a system built to record voltage, contractility and calcium, registers voltage by exciting the cells at 470nm and recording emission (Figure 2.2A) using two photomultipliers (PMTs): a short wavelength PMT (swPMT) and a long wavelength PMT (lwPMT). These register at <585nm and >585nm, respectively (Figure 2.2B). The output is a trace of APs, a result of ratio between swPMT and lwPMT (Figure 2.2C). From this trace, a number of variables can be analysed: the time for depolarisation (TRise), the different stages of repolarisation, from 20% to 90% (APD<sub>20-90</sub>), and the interval between each beat.

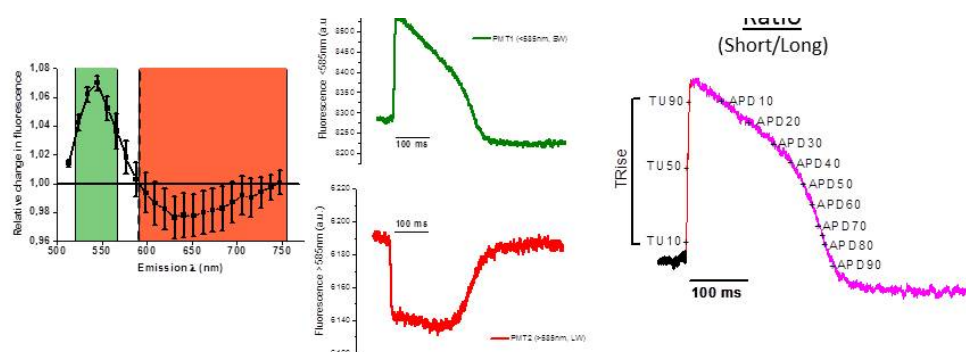


**Figure 2.2 – Ratiometric dye, di-4-ANEPPS, as measured by CelloPTIQ. A) Changes in fluorescence relative to different emission wavelengths, green channel fluoresces at wavelengths <585nm, whereas the red channel is >585nm; B) Example trace of fluorescence registered by the short wavelength photomultiplier (swPMT) at wavelengths <585nm produces (green), and by the long wavelength photomultiplier (lwPMT) >585nm (red); C) Example trace of an example trace resulting from the ratio between swPMT and lwPMT, and resulting parameters which can be recorded from it. Depolarisation duration (TRise) and repolarisation (APD) can be measured.**

### 2.4.3 FluoVolt

FluoVolt has an excitation/emission spectrum of 522/535nm (Figure 2.3), with a response change of up to 25% per 100mV. The dye is used in conjunction with PowerLoad, as this solution can be used in the presence of culture medium to reduce negative effects of replacing medium or loading in serum-free medium.

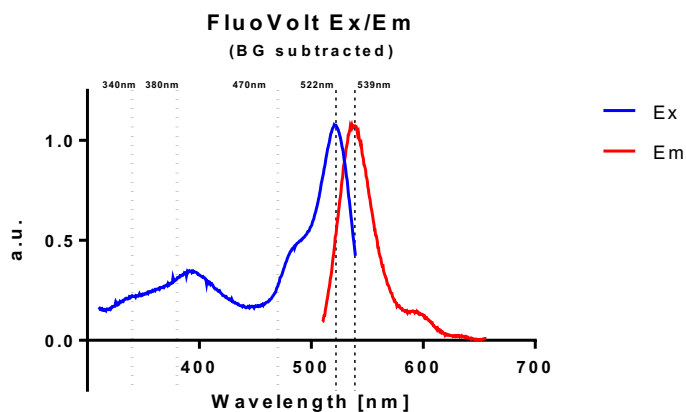


**Figure 2.3 – FluoVolt spectrum.** Excitation wavelength range (blue) represents the necessary wavelength to react with the fluorescent dye and elicit a response. The latter is emitted at a different range of wavelengths (red).

This dye has been shown to be well-adapted to record electrophysiological events in spontaneously beating monolayers of hiPSC-CMs seeded in 96-well plate formats (Bedut et al., 2016). The dye was diluted at desired concentration in serum-free medium or BMCC depending on the nature of the hiPSC-CMs. hiPSC-CMs and co-culture were initially loaded with 0.05 and 0.1% FluoVolt and 1% Powerload for 15-25min. Data showed that for the nature of these experiments, the most adequate concentration was 0.1% FluoVolt and 1% Powerload for 25min, as suggested by Bedut et al. (2016). The cells were then washed with fresh serum-free medium and allowed to recover from the media change for 30min before experiments were conducted.

## 2.5 Measuring calcium signals

A very successful approach to studying the role of  $\text{Ca}^{2+}$  in a specific cellular process has been the use of fluorescent  $\text{Ca}^{2+}$  indicators, which tend to exhibit altered fluorescent properties when bound with  $\text{Ca}^{2+}$ .  $\text{Ca}^{2+}$  indicators bind and interact only with freely diffusible  $\text{Ca}^{2+}$  ions (Paredes et al., 2008).

### 2.5.1 Fura-4F/AM

Fura dyes arise from the salicylaldehyde derivative XXV. The absorbance spectra for  $\text{Ca}^{2+}$  are in near UV, and the binding of calcium shifts all the absorbance spectra to shorter wavelengths. In all indicators from this family, both the calcium-free and calcium-bound

species fluoresce quite strongly. The fluorescence excitation spectra shifts to shorter wavelengths as  $[Ca^{2+}]$  increases, as much as the absorption spectra does (Grynkiewicz et al., 1985). Originally Fura dyes were designed for dual wavelength excitation and single-wavelength band emission fluorescence (Grynkiewicz et al., 1985, Wokosin et al., 2004), but single-wavelength excitation may not only provide an easy to calibrate  $Ca^{2+}$  signal, but also offer additional advantages when excited  $>365nm$  wavelengths (Wokosin et al., 2004).

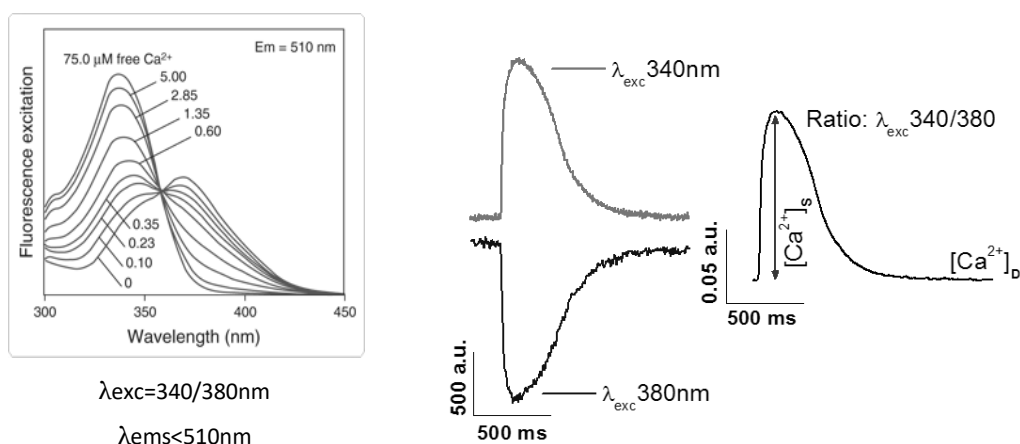


**Figure 2.4 -  $Ca^{2+}$  transient recording principle by CelLOPTIQ. A) Excitation/emission spectra for Fura-4F/AM. While unbound, Fura-4F/AM has a peak excitation of 380nm, and 340nm when  $Ca^{2+}$  bound; B) Representative traces of CaT recorded when excited at 340nm (grey) and at 380nm (black), and the resulting ratio trace from which time to peak (TPeak), amplitude, time to relaxation and interval between each CaT can be obtained.**

$Ca^{2+}$  indicator dyes were engineered with acetoxymethyl (AM) esters to facilitate hydrophilic dye loading into cells. These are sufficiently hydrophobic to be membrane permeable, allowing them to be passively loaded into cells simply by adding them to extracellular medium. Intracellular esterases then cleave the AM group and trap the dye inside the cells (Paredes et al., 2008).

Fura-4F/AM is a ratiometric calcium dye which excites at a range from 330-393nm, and thus emits at 476-590nm (Figure 2.4). This dye can be prepared using dimethylsulfoxide (DMSO) to slow the hydrolysis of esters, thus preserving the activity of the indicator until it is in the cytosol. Pluronic-F127 can also be used to help disperse the AM-linked indicator dyes into medium, as the AM groups have low solubility in aqueous solutions (Paredes et al., 2008). Fura-4F/AM was prepared in DMSO, unless otherwise stated, and added to cells in serum-free medium at a final concentration of  $6\mu M$ , and

incubated for 30min at 37°C, after which the medium was replaced by serum-free medium at 37°C.

## 2.6 Measuring movement/contraction

Contractility is an important feature in hiPSC-CMs, as these show spontaneous beating. To measure this, an open source software tool was used – MUSCLEMOTION, which allows for rapid and easy measurement of contractility from high speed movies in 1D in bright field microscopy (Sala et al., 2017). The videos are taken using HCLive, an acquisition software, which acquires data at 1,000Hz, 100 frames per second. Individual frames are uploaded in order to MUSCLEMOTION, and subsequently analysed.

### 2.6.1 MUSCLEMOTION

The principle behind the algorithm in this software is the assessment of contraction by quantifying absolute changes in pixel intensity between a reference frame and the frame of interest. For every pixel in the frame, each reference pixel is subtracted from the corresponding pixel of interest and the difference is presented as an absolute number. Unchanged pixels have low values (black), whereas pixels that have changed result in high values (white) (Figure 2.5A). The next step is the mean pixel intensity of the resulting image is measured – this is a measure of how much the pixels have moved compared to the reference frame (Figure 2.5B). Contraction velocity is determined by a measure of the relative displacement per interframe interval.

hiPSC-CMs exhibit concentric contraction, and the area of contraction for hiPSC-CMs monolayers is distributed heterogeneously throughout the whole field. MUSCLEMOTION can automatically identify and select the reference frame and increase the signal-to-noise ratio, and is valid under a range of illumination conditions without changing temporal parameters (Sala et al., 2017).

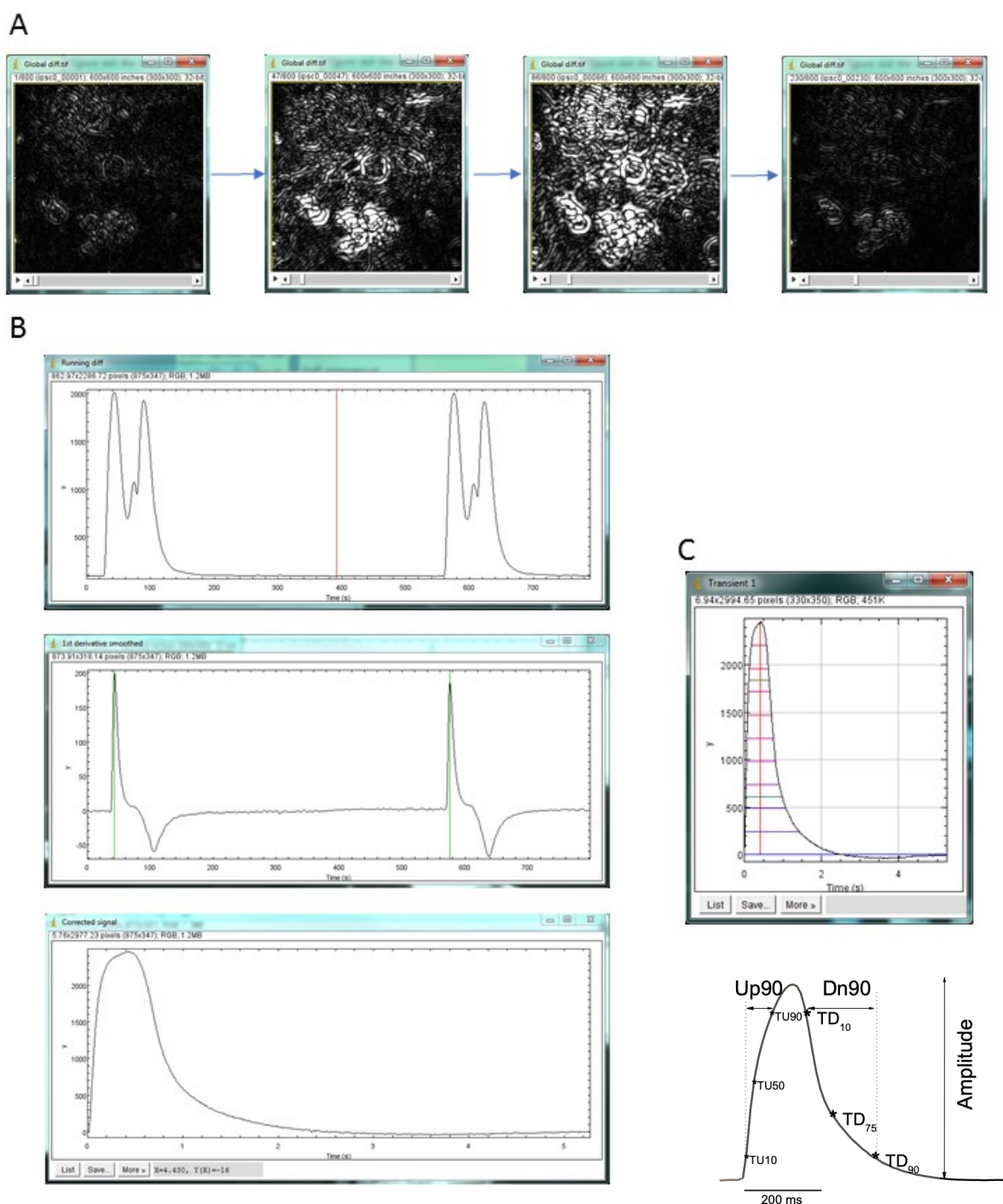


**Figure 2.5 – Contractility measurements from hiPSC-CMs using MUSCLEMOTION. A)** Frames showing the changes in pixel colour because of cell contraction from black to white, and back as the cell relaxes; **B)** Different calculations applied to pixel changes showing the subtracted differences from reference pixel and pixel of interest, the first derivative subsequently calculated, and the resulting corrected signal. MUSCLEMOTION measures differences between frames, thus producing ‘Running differences’, and a derivative, from which the outcome is a corrected signal; **C)** The final result is a transient which shows the different measurements taken from the contractility trace.

MUSCLEMOTION provides a range of variables: interval between each contraction, measured from peak to peak; contraction duration; time to contraction (Up<sub>90</sub>); time to relaxation (Dn<sub>90</sub>) (Figure 2.5C).

## 2.7 Integration of voltage, contractility and calcium measurements on CelLOPTIQ

CelLOPTIQ is a photometry system with camera-based cell motion. The sample/cell plate is placed in a motorised, incubated stage kept at 37°C, 5% CO<sub>2</sub>, 75% humidity. A white light (bright field) passes through a condenser to illuminate the substrate. The stage can be controlled using a joystick, or via the software CelLOPTIQ. Under the incubated stage there is a 40x objective with an area of view of 270µm, and a working distance of 2mm. A 470nm LED illuminates the cells via a 500nm long pass (LP) filter. Two other LEDs are connected to the system, one exciting at 340nm and the other at 380nm for calcium measurements. The signal collected is then passed through two PMTs: <535nm and >535nm 800LP, which then outputs the data onto a computer in the form of 2 channels.

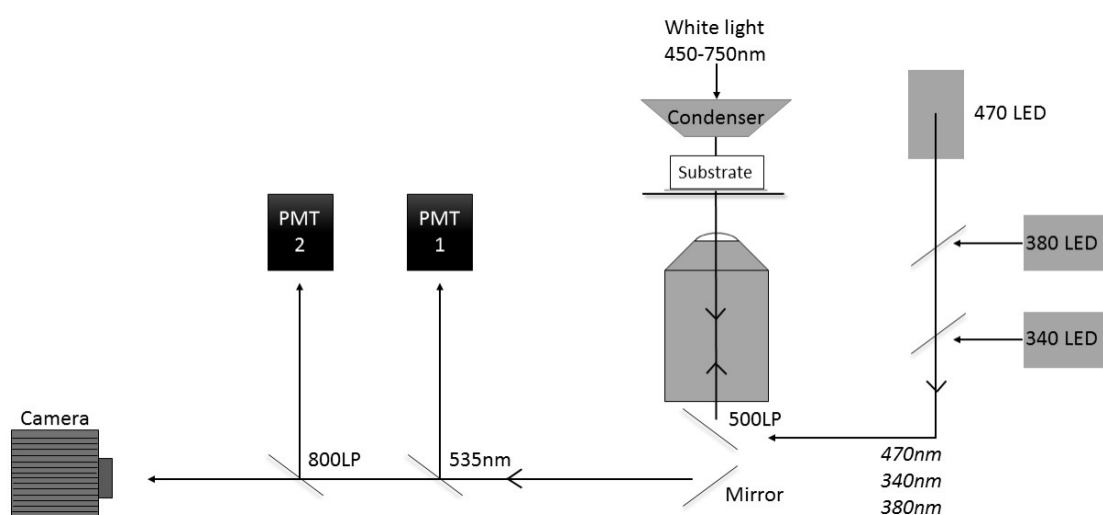


**Figure 2.6 – Settings for CelLOPTIQ.** Excitation light was directed at the specimen from a 470, 340 or 380nm LED and passed through dichroic mirrors which allow the intended wavelength to pass through to a 500LP filter. The light excites the substrate and reflects onto a mirror. This is then collected by two PMTs, one collects <585nm and the other >585nm. Bright field images are collected by a camera using MUSCLEMOTION.

A camera is plugged in to record contractility using bright field. This is connected to a second computer with MUSCLEMOTION software. To record voltage, data is captured at 10kHz for 10-20s, for calcium 500Hz for each wavelength, and contractility has a 100Hz frame rate.

Voltage data is collected by the two PMTs, whereas calcium is only captured by PMT 1 due to the range of wavelengths Fura-4F/AM emits.

Voltage and contractility can be recorded simultaneously using filters. For the nature of the experiments in this project, voltage was recorded first, and the coordinates used for each recording were saved. Contractility was later recorded from the saved coordinates.

## 2.7.1 Analysis using CelloPTIQ

### 2.7.1.1 Di-4-ANEPPS

Analysis of traces obtained from di-4-ANEPPS dyed cells was conducted using CelloPTIQ. The ratio obtained from the two individual channels (Figure 2.7) was filtered and a baseline was fitted and subtracted. This accounts for the bleaching that results from dye loss. From the ratio, there is an average trace output which shows the different variables being measured.

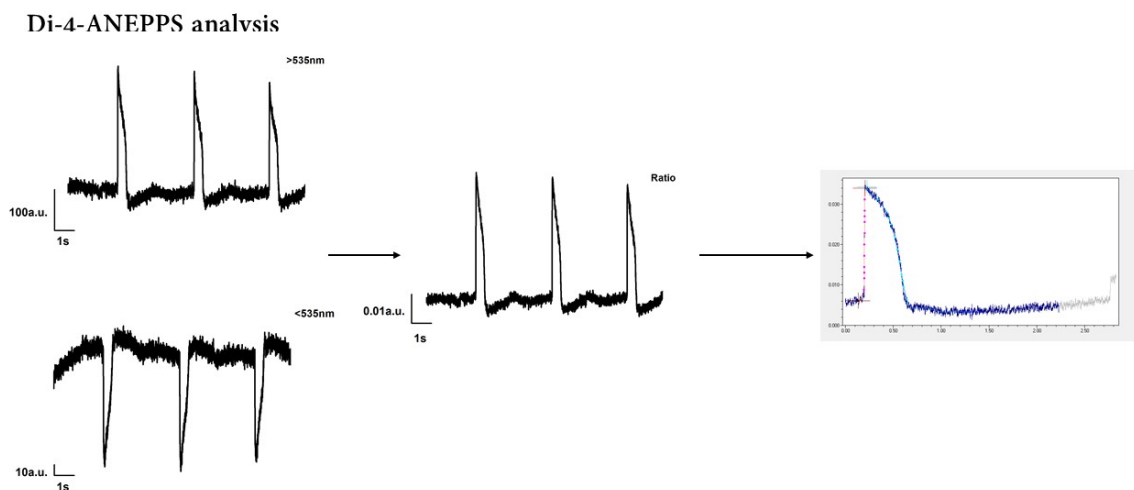


**Figure 2.7 - Example traces obtained from hiPSC-CMs dyed with di-4-ANEPPS. The two first traces are the voltage traces captured by the two PMTs, at >585 and <585nm. From these an output of a ratio trace is created, thus allowing for an average trace to be further analysed.**

The output single AP trace is analysed for interval between each AP, depolarisation time (TRise) and the duration of the various stages of repolarisation, from 20% to 90%.

### 2.7.1.2 FluoVolt

FluoVolt signals are measured in a single wavelength, as the dye is not ratiometric. Baseline is fitted and subtracted, and the trace is filtered to reduce the noise (Figure 2.8). The average AP is further analysed for the different variables (see heading 2.7.1.1).

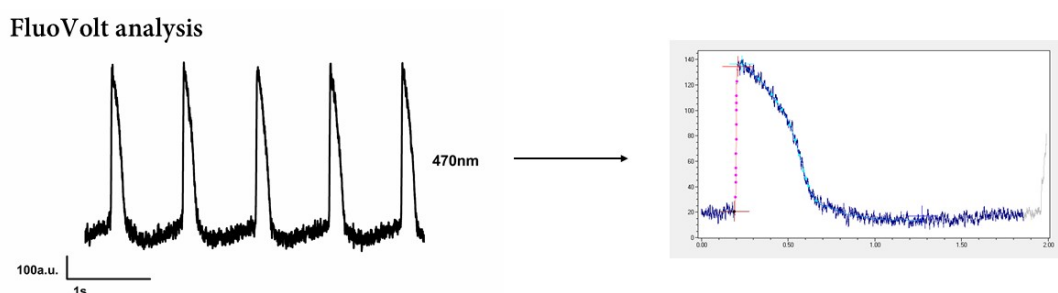


Figure 2.8 - FluoVolt analysis

### 2.7.1.3 Fura-4F/AM

To record  $\text{Ca}^{2+}$  transients, only one PMT is used, thus the output is two traces, one recorded from the 340nm excitation LED, and the other from the 380nm excitation LED (Figure 2.9). A ratio trace is calculated from  $\lambda_{\text{exc}} 340/380\text{nm}$ . A single CaT is further analysed to obtain time to peak (TPeak) and time to repolarise.

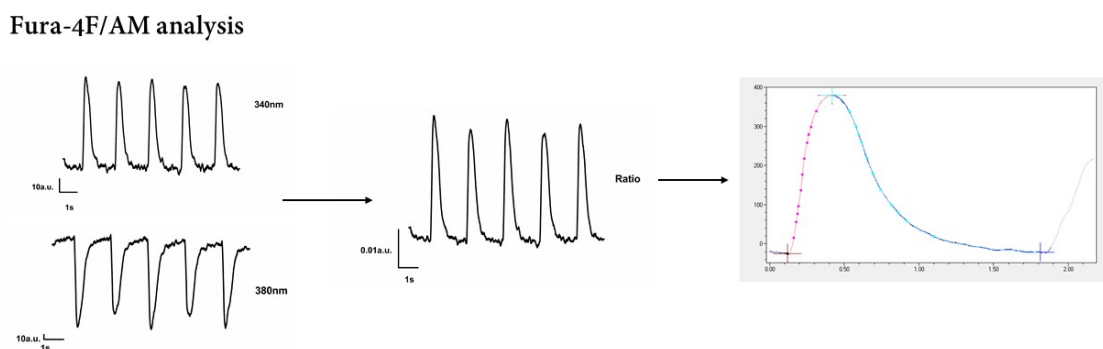
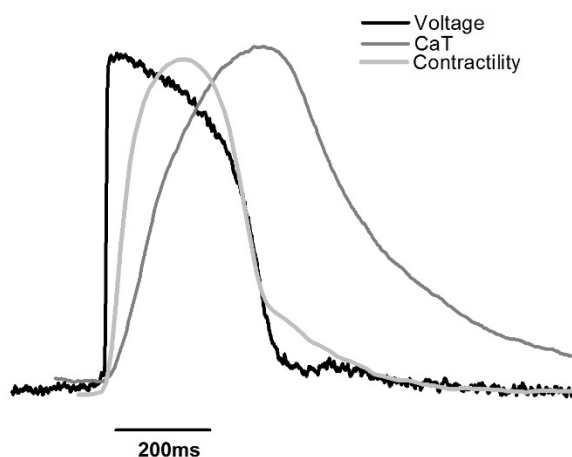


Figure 2.9 - Fura-4F/AM analysis

Measurement of the three conditions: voltage, calcium signalling and contractility on the CelLOPTIQ platform provides an in-depth understanding of electrophysiological changes in single-cell and in clusters.



**Figure 2.10 - Correlation of the three different conditions measured using CelLOPTIQ: Voltage, calcium signalling and contractility.**

Recording from the same cell or same area within a monolayer of cells contributes greatly towards establishing the effects incurred by addition of cells/drugs on all three measurements, also on how these correlate. An example trace (Figure 2.10) shows a calcium transient starting and leading to depolarisation on an action potential and the timeline necessary for this to incur – and reach full contraction. Also visible is the repolarisation stage of the AP and the calcium transient decline as the cell returns to a relaxed state (resting membrane potential).

## 2.7.2 Signal-to-noise calculations

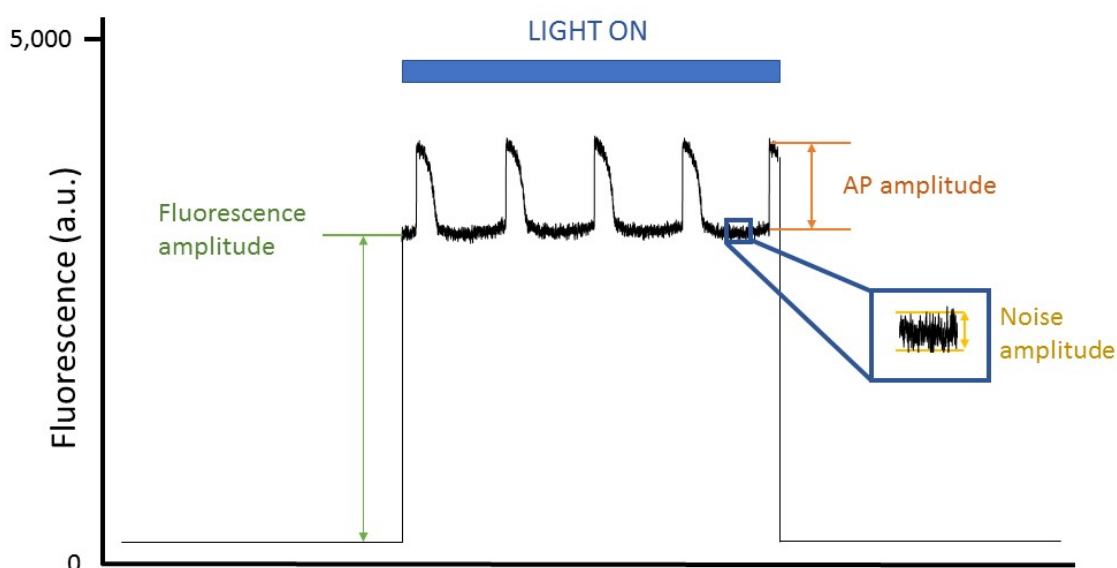


**Figure 2.11 – Signal-to-noise can be calculated by measuring the fluorescence amplitude collected from 470nm excitation using a voltage-sensitive dye and/or the AP amplitude. There is little or no fluorescence on CelloPTIQ while the excitation light is off, and this increases immediately when the light is on (blue). The fluorescence amplitude can be measured as a baseline for the AP trace (green), and AP amplitude corresponds to the size of the AP minus the baseline (orange). The noise amplitude is measured from the bottom to the highest point of the noise between each AP (yellow).**

Recordings were obtained from different cell cultures to study the effects of the presence of different cell types in co-culture and how it affects SNR. Voltage measurements were done in the presence of a voltage-sensitive dye, FluoVolt, and the following parameters were measured (Figure 2.11) once the 470nm light was on:

- Fluorescence amplitude
- AP amplitude
- Noise amplitude

### 2.7.2.1 Conversion of fluorescence to photons/pixel

As mentioned before, it is important to distinguish the SNR from the cell culture from that of the system used for recordings itself. As such further measurements were taken using fluorescein. Fluorescein was prepared at different concentrations: 0.3, 0.6, 1.25, 2.5, 3.8, 5.3, 5.6, 6.3, 7.5, 8.9, 9.5, 10.3, 10.6, 11.3, 12.5, 13.8 and 14.5 $\mu$ M and added to a 96-well glass-bottom plate diluted in Krebs. Krebs is composed of 120mM NaCl, 20mM HEPES, 5.40mM KCl, 0.52mM NaH<sub>2</sub>PO<sub>4</sub>, 3.5mM MgCl<sub>2</sub>6H<sub>2</sub>O, 20mM taurine, 20mM creatine and

11.1mM glucose, with a pH of 7.4 at 37°C. Control wells were prepared solely with distilled water. The plate was then transferred to CelloPTIQ and kept at 37°C. Fluorescein was then excited at 470nm and traces were recorded and analysed using OriginPro 7.5. The mean of the noise amplitude was then measured and analysed and the standard deviation (SD) was calculated for each of the wells containing the different concentrations of fluorescein.

Mean was corrected by subtracting the fluorescence obtained from water:

$$\text{Mean (zero sub)} = \text{Mean (fluorescein)} - \text{Mean (water)}$$

Variance was calculated as  $SD^2$ . Since  $\sigma^2 = \mu$  (variance = mean), the conversion factor from arbitrary fluorescence units to photons can be obtained by plotting  $\sigma^2$  vs  $\mu$  and taking the gradient of the line of best fit (Macquaide, 2004). The gradient obtained was then used to scale the mean and variance:

$$\mu(\text{scaled}) = \text{Mean (zero sub)} \times \text{Slope}$$

$$\sigma^2(\text{scaled}) = (\sigma^2 \times \text{Slope})^2$$

Plotting  $\sigma^2$  (scaled) vs  $\mu$  (scaled) will provide a new gradient and equation which allows for the correction for noise from the system where  $\sigma^2 = \mu$ .

### 2.7.2.2 Cell loading with voltage-sensitive dyes

Cor.4U hiPSC-CMs were cultured alone or at 1:1 ratios with HEKs (standard – N; I<sub>k1</sub>-overexpressing) in glass-bottom 96-well plates. On day 4 in culture the cells were loaded with the voltage-sensitive dye, FluoVolt, at 1:1000 as well as PowerLoad at 1:100. FluoVolt was diluted in serum-free medium, BMCC, and loaded onto the cells for 25min at 37°C 5% CO<sub>2</sub>. The supernatant was removed and replaced with BMCC at 37°C. The plates were directly transferred to CelloPTIQ's incubated stage and allowed to settle for 30 minutes prior to recordings.

Data was collected at 10kHz, with an excitation of 470nm and collection at 535nm.

### 2.7.2.3 SNR calculations

The amplitude of the noise was measured as shown on (Figure 2.11), as well as the amplitude of the AP. Baseline (fluorescence amplitude) corresponds to the fluorescence existent in the medium and cell membrane, which is obtained by turning the 470nm LED on, and measuring the resting period of the AP.

The correction factor for Poisson noise previously described was applied to the 3 different amplitudes measured. This allows the data to be presented as photon/pixel.

The SNR can thus be calculated for the AP and for the total fluorescent signal. To calculate the first the following equation was used:

$$SNR (AP) = \frac{\textit{Amplitude of AP}}{\textit{Amplitude of noise}}$$

The SNR for the fluorescence was calculated as follows:

$$SNR (Fluo) = \frac{\textit{Amplitude of fluorescence}}{\textit{Amplitude of noise}}$$

The equations above allow for the investigation of whether SNR is affected by co-culture and if different cell types affect the SNR differently.

## 2.8 Statistical analysis

Statistical analysis was performed using GraphPad statistical software. All data was presented as mean  $\pm$  standard error of the mean. N refers to number of wells recorded for each dataset. Comparisons between groups of data were performed using Student's t-tests, which were paired where appropriate. Multiple comparison tests were performed using repeated measures two-way ANOVA with Dunnett's multiple comparison post-hoc test. A p-value of less than 0.05 was considered statistically significant. Where data is presented as percentage from baseline, statistical analysis was done on raw data.

### **3 Characterisation of human induced pluripotent stem cell-derived cardiomyocytes**

## 3.1 Introduction

### 3.1.1 Pacemaker current blockade

The pacemaker mechanism of the heart, which was previously believed to be the decaying of an outward potassium current,  $I_{k2}$ , was shown to be a “funny” current discovered in SAN cells, in the late 1970’s (Difrancesco, 1981a). (Difrancesco, 1981a) spent the next years closely studying this current, which was later given the name of  $I_f$ , providing a new interpretation of pacemaking: the pacemaker depolarisation was generated by activation of the inward  $I_f$  during diastole (Difrancesco, 1993, Difrancesco, 2010). During the depolarised part of the AP, at positive voltages,  $I_f$  is completely turned off, no contribution is available.  $I_f$  is a current carried by both  $Na^+$  and  $K^+$ . During repolarisation/diastole, when the voltage hyperpolarises below  $-40/-45mV$ , which is the  $I_f$  activation threshold, the current switches on and increases, first opposing, and then stopping the repolarisation process, and finally initiating the diastolic depolarisation (Bucchi et al., 2002, Difrancesco, 1981a, Difrancesco, 1981b).  $I_f$  contribution ends when the  $Ca^{2+}$ -dependent processes take over, and the threshold for the L-type  $Ca^{2+}$  current activation and AP firing is reached in the late part of the diastolic depolarisation (Difrancesco, 2010). f-channels are modulated by intracellular cAMP by an action involving direct cAMP binding to channel proteins and not mediated by a phosphorylation mechanism (Difrancesco and Tortora, 1991).

The relevance of  $I_f$  in the control of heart rate makes it an important pharmacological target, and several f-channel blocker molecules have been developed, such as ivabradine (Bois et al., 1996). This has been shown to induce heart rate slowing with limited inotropic side effects. In vitro studies have shown that threshold concentrations of ivabradine at which effects start to be visible on the  $I_{CaL}$  and on  $I_{Kr}$  range between 3 and  $10\mu M$ , whereas a half-block concentration of  $2.8\mu M$  was found for  $I_f$ , indicating substantial selectivity (Bois et al., 1996). Bucchi et al. (2002) investigated the effects of ivabradine on native f-channels in rabbit SAN cells and found that it blocks f-channels when they are open, meaning the block is strongly use-dependent. This block is exerted preferentially when the current deactivates on depolarisation and is relieved when it activates on hyperpolarisation.

### 3.1.2 Inward rectifying current blockade

The inward rectifying current ( $I_{K1}$ ) plays an important role in the repolarisation in cardiomyocytes (Dhamoon and Jalife, 2005), displaying its importance in phase 4 of the cardiac action potential, and phase 3. It is responsible for maintaining a stable resting membrane potential, and for the late phase of cardiac repolarisation, where it constitutes a part of the repolarisation reserve currents. Changes in  $I_{K1}$  have significant effects on the cardiac action potential morphology, the excitability of the heart, and thereby possibly contribute to or protect against cardiac arrhythmia (Schmitt et al., 2014).

So far, the role of  $I_{K1}$  has been investigated using Barium Chloride, however  $Ba^{2+}$  is not a specific blocker of  $I_{K1}$ , as it also blocks other inwardly  $K^+$  rectifiers. Furthermore,  $Ba^{2+}$  is toxic and not tolerable *in vivo* (De Boer et al., 2010, Skarsfeldt et al., 2016).

PA-6 has a known  $IC_{50}$  in a range of 12 to 15nM, and 200nM blocked more than 90% of all  $K_{ir2.x}$  channels in a voltage-independent manner (Skarsfeldt et al., 2016). Its effects show a prolonged AP at 50, 100 and 200nM. At higher concentrations (10 $\mu$ M), it leads to an increased expression of Kir2.1. Furthermore, PA-6 did not significantly affect  $I_{Nav}$ ,  $I_{Ca-L}$ ,  $I_{to}$ ,  $I_{Kr}$  and  $I_{Ks}$  at 200nmol/L (Takanari et al., 2013). In an intact heart Langendorff preparation,  $I_{K1}$  inhibition in the ventricles with 200nM of PA-6 prolonged  $APD_{90}$  and increased the vERP, as well as the variability in the ventricular APD. (Skarsfeldt et al., 2016) reported that loss of  $I_{K1}$  leads to an increased risk of ventricular arrhythmia, which may be supported by at least three different parameters: (1)  $APD_{90}$  dispersion; (2) prolonged vERP; (3) reduced sodium channel availability caused by a depolarised RMP.

PA-6, a pentamidine analogue was used to study the availability of  $I_{K1}$  in hiPSC-CMs. PA-6 has a time-dependent inhibition of  $I_{K1}$ , as the binding site is in the cytosolic part of the channel, leading to the onset of the current inhibition to be slow when the drug is applied to the extracellular solution. Maximal effect is seen 20min after the application of PA-6 (De Boer et al., 2006, Skarsfeldt et al., 2016).

### 3.1.3 Potassium availability and uptake

As previously mentioned, determining the amount of  $K^+$  channels in hiPSC-CMs is challenging. One possibility for studying this is to manipulate the available extracellular  $K^+$ . Different cell providers use different media compositions, resulting in different concentrations of different compounds.  $K^+$  is added in the form of potassium chloride (KCl) at 4.4mM (Axiogenesis, Germany) to 5.3mM (Cellular Dynamics, USA). This study was conducted by measuring the effects of standard availability of  $K^+$  at 4.4mM, and then removing KCl from the medium altogether, and slowly re-introducing  $K^+$ .

### 3.1.4 SERCA blockade

Thapsigargin is a plant-derived sesquiterpene lactone, from the plant *Thapsia garganica*, which binds to the Ca-ATPase on the endoplasmic reticulum (ER) and empties the intracellular calcium stores as a consequence of inhibiting the uptake pathway (Jones and Sharpe, 1994, Lytton et al., 1991) Ca-ATPase activity is important and required for calcium sequestration into the ER, and therefore important for the homeostasis of cytosolic calcium (Jones and Sharpe, 1994). This drug interacts directly with the endoplasmic reticulum (ER), the major intracellular  $Ca^{2+}$  store, thus inducing  $Ca^{2+}$ -release. Thapsigargin is a specific inhibitor of SERCA in striated muscle. It has been shown that the drug decreases the  $V_{max}$  of the transport reaction without affecting the apparent affinity of the enzyme for  $Ca^{2+}$ , as the number of active ATPase molecules diminishes as a function of the thapsigargin concentration (Wrzosek et al., 1992).

### 3.1.5 Ryanodine-receptor calcium release

Ryanodine is a highly specific modulator of RyR-mediated  $Ca^{2+}$  release and as such has been used to determine the contribution of RyR-mediated  $Ca^{2+}$  release to cell function or to modulate the properties of RyR channels within the cell (Thomas and Williams, 2012).

The variable delay between the addition and action of ryanodine reflects the slow rate of association of ryanodine with its binding site on the channel protein. When ryanodine eventually binds, it produces dramatic effects on both the gating and the ion-handling properties of the channel. High concentrations of ryanodine (high micromolar and above)

also induce the occurrence of the high open probability ( $P_o$ ), reduced conductance, modified state described above. However, in the continued presence of ryanodine the channel closes and does not revert to either the ryanodine-modified state or normal channel gating within the time frame of a single-channel experiment (Tinker et al., 1996). The implication of this is that should intracellular concentrations of ryanodine reach levels sufficient to permit interaction with low affinity sites (following a transient increase in SR  $Ca^{2+}$  permeability, when ryanodine-bound RyR channels will exist in the high  $P_o$ , reduced conductance state),  $Ca^{2+}$  permeability will be reduced as channels close on occupation of the low affinity sites (Thomas and Williams, 2012). Inhibition of  $Ca^{2+}$  efflux was observed when ryanodine concentrations were higher than  $10\mu M$  (Meissner, 1986). Ryanodine can both increase and decrease  $Ca^{2+}$  permeability of cardiac SR membranes, increased at  $0.01-10\mu M$  and decreased at  $1-300\mu M$  (Meissner, 1986, Lattanzio et al., 1987).

### **3.1.6 Other potential mechanisms for spontaneous activity**

Due to the commercial origin of the hiPSC-CMs used for this study, there is a lack of information with regards to the media composition. Studies using the adrenaline antagonist, atenolol, have shown no effect on hiPSC-CMs (Peters et al., 2014), which suggests that adrenaline is not present in medium or part of the maintenance of the differentiated cardiomyocyte.

### **3.1.7 Aims of this chapter**

To assess the availability of certain ion channels and contribute towards a characterisation of electrophysiological behaviour of hiPSC-CMs. To do so, commonly used channel blockers were administered to hiPSC-CMs and the effects on electrophysiology and/or contractility were assessed.

## **3.2 Methods**

### **3.2.1 Ivabradine – $I_f$ block**

Cor.4U cells were plated (see Ch2. General Methods) in glass-bottom petri dishes (MatTek) at 22,000 cells/well. The cells were kept in culture for 6 days. On day 6 the cells

were loaded with 6 $\mu$ M di-4-ANEPPS for 1 minute in serum-free medium, and fresh medium was used to wash the dye. Graphite electrodes were fitted onto the well, and 40mV, 0.2ms pulses were used to stimulate the cells at different frequencies. Voltage was recorded (CelloPTIQ, Clyde Biosciences, UK) for 10s per cell, at 10,000Hz. The vehicle (DMSO) was added to control petri dishes at final concentrations of 0.004%, 0.008% and 0.02%. Increasing concentrations of ivabradine were added cumulatively at 1, 3 and 10 $\mu$ M final concentration, and recordings were taken 30 minutes after each addition.

### **3.2.2 Barium Chloride – non-specific I<sub>k1</sub> block**

Cor.4U hiPSC-CMs were plated following the protocol previously mentioned (see General Methods) in 96-well, glass-bottom plates (MatTek) at 25,000 cells/well. The cells were maintained for 4 days, at which point they were transferred to BMCC and loaded for 20-25min with the voltage-sensitive dye, FluoVolt at 1:1000, diluted in 1:100 PowerLoad. The medium was then replaced with fresh BMCC, and the cells were left to settle for 30min before voltage recordings were taken. BaCl<sub>2</sub> was prepared in distilled water. A range of different concentrations of BaCl<sub>2</sub> were added, from 30 $\mu$ M to 1mM final concentrations. Distilled water was used as a control at  $\leq$ 0.06%.

Contraction (HCImage, property of Hamamatsu) was recorded at 100fps, for each well from which voltage was recorded as above. Contraction was recorded again post addition of increasing concentrations of BaCl<sub>2</sub>. The drug was left to take effect for 30min before recordings were taken. This data was analysed using CelloPTIQ and ImageJ, respectively.

### **3.2.3 PA-6 - I<sub>k1</sub> block**

Cor.4U hiPSC-CMs were plated at 25,000cells/well in a 96-well glass-bottom plate (MatTek). On day 4 post-plating, these cells were loaded with 1:1000 FluoVolt, 1:100 PowerLoad for 25 minutes in BMCC. The medium was replaced by fresh, 37°C BMCC, and the cells were allowed 15-30min to settle. Voltage was recorded using CelloPTIQ. PA-6 was added at 100, 150 and 200 $\mu$ M final concentrations. Voltage was recorded again 30 minutes after the drug was added. Analysis was done using CelloPTIQ and GraphPad, statistical analysis was paired t-tests.

### 3.2.4 Potassium Chloride – K<sup>+</sup> depletion and re-introduction

We studied the availability of K<sup>+</sup> channels by depleting all the K<sup>+</sup> sources, and slowly re-introducing KCl to the cell media. BMCC, serum-free medium (Axiogenesis, Germany), was recreated without KCl (BMCC-KCl) or any other K<sup>+</sup> sources. The BMCC-KCl was composed of 1.49mM CaCl<sub>2</sub>, 0.81mM MgSO<sub>4</sub>, 36mM NaHCO<sub>3</sub>, 77.59mM NaCl, 0.91mM NaH<sub>2</sub>PO<sub>4</sub>-H<sub>2</sub>O, 0.0001mM Na<sub>2</sub>SeO<sub>3</sub>-5H<sub>2</sub>O, 0.0008mM KNO<sub>3</sub>, 25mM D-Glucose dextrose, 25.03mM HEPES, 1mM Sodium Pyruvate. Cor.4U cells were plated at 25,000 cells/well in a 96-well plate, and maintained in Cor.4U medium for 8 days. On day 8, the cells were loaded for 1 minute with 6μM di-4-ANEPPS prepared in standard BMCC medium, and fresh BMCC was added after. The cells were left to settle for 30 minutes, after which voltage and contraction were measured. The medium was then replaced with BMCC-KCl, and voltage and contraction were measured again. KCl was added in increasing concentrations every 30 minutes, starting at 0.5mM, followed by 1mM, and in 1mM steps after, up to 8mM. Voltage and contraction were measured between each step. Unpaired t-tests were done comparing each concentration to initial preparation in standard BMCC. Data are shown as mean±SEM.

### 3.2.5 Thapsigargin

The cells were exposed to 6μM di-4-ANEPPS for 1 minute in BMCC, 6μM of Fura-4F/AM for 30 minutes in BMCC, then BMCC without dye was used to replace the medium with dye at 37°C. The plate was transferred to an incubated stage at 37°C, 5% CO<sub>2</sub>, 70% humidity (CelloPTIQ) and the cells were allowed to rest for 10 minutes before recordings were taken. A baseline recording was taken for voltage. Thapsigargin was added in BMCC to create final concentrations of 1, 3, 10 and 30μM to Cor.4U hiPSC-CMs plated at 25,000cells/well in a 96-well format, on day 7. Calcium and voltage recordings were taken 30 minutes after drug addition. Data were analysed with paired t-tests comparing baseline and drug using GraphPad Prism and presented as percentage of baseline±SEM, where baseline is 100%. Unpaired t-tests were conducted to compare control and drug for calcium measurements, data shown as mean±SEM.

### 3.2.6 Ryanodine

On day 8 in culture, Cor.4U hiPSC-CMs were loaded with FluoVolt at 1:1000 and 1:100 PowerLoad, and 6 $\mu$ M Fura-4F/AM in BMCC. The dyes were left for 25min before being replaced with BMCC at 37°C. The culture was left inside the incubated stage in CelloPTIQ for 15 minutes to settle, after which the baseline voltage and calcium transients were recorded for a minimum of 8 seconds. Ryanodine was prepared in DMSO, and further diluted to final concentrations of 3 $\mu$ M or 10 $\mu$ M in BMCC in culture. Thirty minutes after addition, voltage and calcium were recorded. Data were analysed using paired t-tests comparing baseline and drug using GraphPad Prism and presented as percentage of baseline $\pm$ SEM, where baseline is 100%. Unpaired t-tests were conducted to compare control and drug in calcium recordings, data shown as mean $\pm$ SEM.

## 3.3 Results

### 3.3.1 Ivabradine – I<sub>f</sub> block

Blocking I<sub>f</sub> is known to have an effect on APD. Lees-Miller et al (2015) showed a prolongation in APD<sub>90</sub> in a dose-dependent manner, with a large effect at 10 $\mu$ M ivabradine in isolated cardiomyocytes. In hiPSC-CMs, there was also a prolongation of APD in the presence of ivabradine, as shown by an example trace (Figure 3.1A). Cycle length (CL) was prolonged at all concentrations, compared to a DMSO control, from 81 $\pm$ 6% to 155 $\pm$ 13% from baseline at 1 $\mu$ M, 78 $\pm$ 7% to 194 $\pm$ 31% at 3 $\mu$ M, and 72 $\pm$ 6% to 186 $\pm$ 22% at 10 $\mu$ M ivabradine (**Error! Reference source not found.B**). Repolarisation was affected by ivabradine, and this was observed at 75% and 90% of repolarisation before reaching resting membrane potential. Shown as percentage of baseline obtained pre-treatment, APD<sub>75</sub> was significantly longer than control, 161 $\pm$ 15% of baseline at 1 $\mu$ M, 213 $\pm$ 19% at 3 $\mu$ M, and 358 $\pm$ 41% at 10 $\mu$ M ivabradine, compared to vehicle (81 $\pm$ 6%, 77 $\pm$ 7% and 72 $\pm$ 6% from baseline) (**Error! Reference source not found.C**). The same effect was present at 90% of repolarisation at ivabradine concentrations  $\geq$ 3 $\mu$ M, where it increased to 200 $\pm$ 28% and 348 $\pm$ 62% from baseline for 3 and 10 $\mu$ M, respectively, compared to 86 $\pm$ 21% and 91 $\pm$ 11% from baseline for control (**Error! Reference source not found.D**).

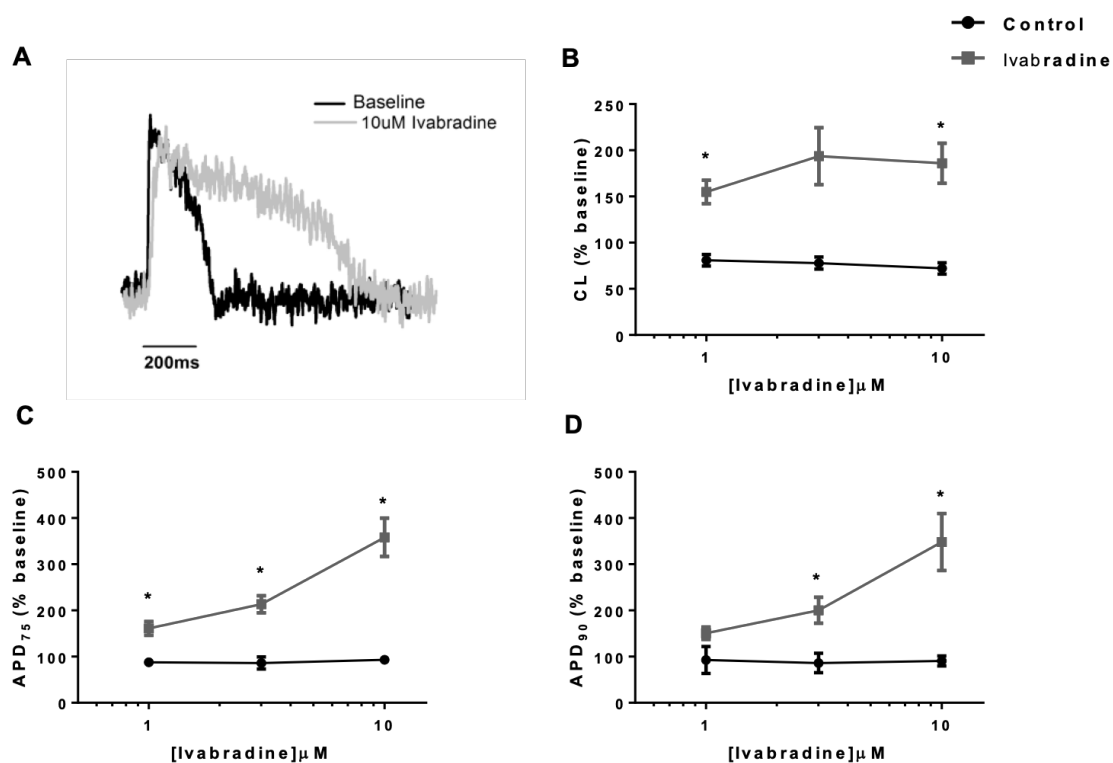


**Figure 3.1** - The effects of a pacemaker current inhibitor on hiPSC-CMs. Voltage changes as a result of the addition of ivabradine at 1, 3 and 10  $\mu\text{M}$ . **A)** Example traces of a single AP before (black) and after addition of 10  $\mu\text{M}$  ivabradine (grey); **B)** Cycle length changes on a control (DMSO) and ivabradine; **C)** repolarisation phase, at 75%, changed with cumulative additions of ivabradine; **D)** effects on 90% of repolarisation. Paired t-test, \* $p < 0.05$ ,  $n = 10$ .

The effects of ivabradine were further studied by electrically stimulating these cells at increasing frequencies. At spontaneous rates and 1 Hz, CL was prolonged in the presence of 1, 3 and 10  $\mu\text{M}$  ivabradine (Figure 3.2A, circles, solid line). At 2 Hz, cells stopped responding to pacing after 3  $\mu\text{M}$  ivabradine (Figure 3.2A, triangles, solid line), whereas at 3 Hz they became unresponsive after 1  $\mu\text{M}$  (Figure 3.2A, inverted triangles, solid line). Cells in vehicle were responsive to stimulation, except at the highest concentrations of DMSO (3  $\mu\text{M}$  and 10  $\mu\text{M}$ ), at which they stopped responding at 3 Hz (Figure 3.2A). AP was prolonged during the repolarisation phase at 75% in the presence of ivabradine at spontaneous rates and 1 Hz (Figure 3.2B). The same behaviour was shown for 90% of the repolarisation phase (Figure 3.2C). The effects on CL were further analysed by determining whether the effect was due to changes in diastolic interval (DI) or repolarisation time (APD<sub>90</sub>). Results show that APD<sub>90</sub> was prolonged at the highest concentration, but there were no changes in diastolic interval (DI) (Figure 3.2D).

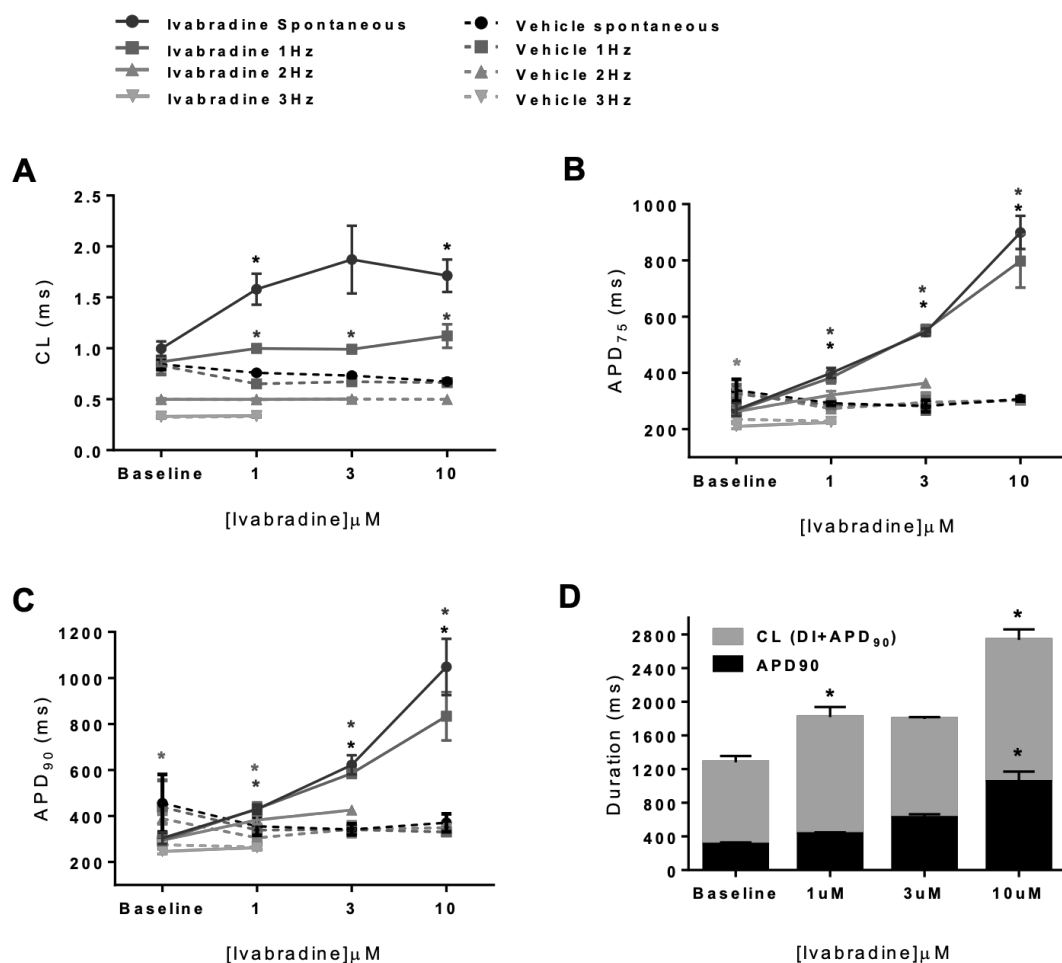


**Figure 3.2 - The effects of ivabradine on hiPSC-CMs at different pacing frequencies.** hiPSC-CMs were electrically stimulated at increasing frequencies in the presence of ivabradine or a vehicle (DMSO). A) effects of increasing concentrations of ivabradine on cycle length at a range of pacing frequencies; B) effects on APD<sub>75</sub>; and C) effects on APD<sub>90</sub>; D) prolongation of cycle length as a result of possible changes in diastolic interval and/or APD<sub>90</sub>. CL is shown as the absolute value from DI+APD<sub>90</sub> (grey + black). Unpaired t-test comparing baseline vs drug effect for each beating frequency. Data shown as mean±SEM: \*p<0.05, n=4.

Ivabradine is a potent and specific blocker of  $I_f$  in SA-nodal cells, at concentrations as high as 10 μM (Bucchi et al., 2002). Although an effect was seen for CL in this study, this was a result of prolongation of APD<sub>90</sub> at 10 μM. On hiPSC-CMs, 10 μM ivabradine has no effect on spontaneous beating frequency, thus  $I_f$  is either absent or its kinetics are too slow and activation-voltage too negative (Zhang et al., 2015).

### 3.3.2 Barium Chloride – non-specific $I_{K1}$ block

The presence of  $I_{K1}$  in hiPSC-CMs was studied by using a known inhibitor: BaCl<sub>2</sub>. The effects of this inhibitor are shown in an example trace (Figure 3.3A) where a prolongation

of the APD is visible, but with no consequences on interval between APs. Addition of BaCl<sub>2</sub> to hiPSC-CMs did not affect interval between spontaneous beats (Figure 3.3B). Diastolic interval (Figure 3.3C) did not change at 30μM or 100μM BaCl<sub>2</sub> but was shortened from 519.3±50.2ms to 355.7±22.6ms from baseline at 300μM, and further shortened from 400.3±14.2ms to 270.7±12.7ms from baseline at 1mM BaCl<sub>2</sub>. The vehicle did not produce an effect from baseline. The duration of the repolarisation was significantly affected at concentrations of 100μM and higher of BaCl<sub>2</sub>. At 50% of repolarisation (Figure 3.3D), there was no effect at 30μM BaCl<sub>2</sub>, but a significant prolongation from 149.1±6.4ms baseline to 178.6±9.4ms, and also to 169.7±5.2ms (p<0.05) at 100μM, compared to 157.2±7.8ms in vehicle. Further effects when APD<sub>50</sub> at 300μM BaCl<sub>2</sub>, when it was longer at 169.7±5.2ms compared to 145.7±8.0ms vehicle (p<0.05), and 172.4±3.9ms compared to 148.1±16.1ms of vehicle at 1mM BaCl<sub>2</sub> (p<0.05). At 75% of repolarisation (Figure 3.3E), concentrations above 30μM led to prolongation. 100μM BaCl<sub>2</sub> increased APD<sub>75</sub> to 220.0±10.7ms from 178.7±6.7ms baseline, opposed to 189.7±9.1ms of the vehicle (p<0.05), 300μM prolonged from 196.4±38.1ms to 219.1±6.6ms, compared to 176.7±9.6ms of vehicle (p<0.05), and 1mM increased from 156.8±9.1ms to 212.7±4.3ms, compared to 178.8±18.7ms for vehicle (p<0.05). A similar effect was observed for 90% of repolarisation (Figure 3.3F), where 30μM BaCl<sub>2</sub> had no effect, but 100μM increased APD<sub>90</sub> from 204.8±6.5ms baseline to 251.5±10.2ms, and DMSO did not affect at 218.8±11.3ms (p<0.05). 300μM BaCl<sub>2</sub> prolonged APD<sub>90</sub> to 258.8±8.5ms (p<0.05) and 1mM prolonged to 244.6±4.1ms (p<0.05) from 228.0±43.3ms and 176.3±10.2ms, respectively, but the vehicle had no effect.

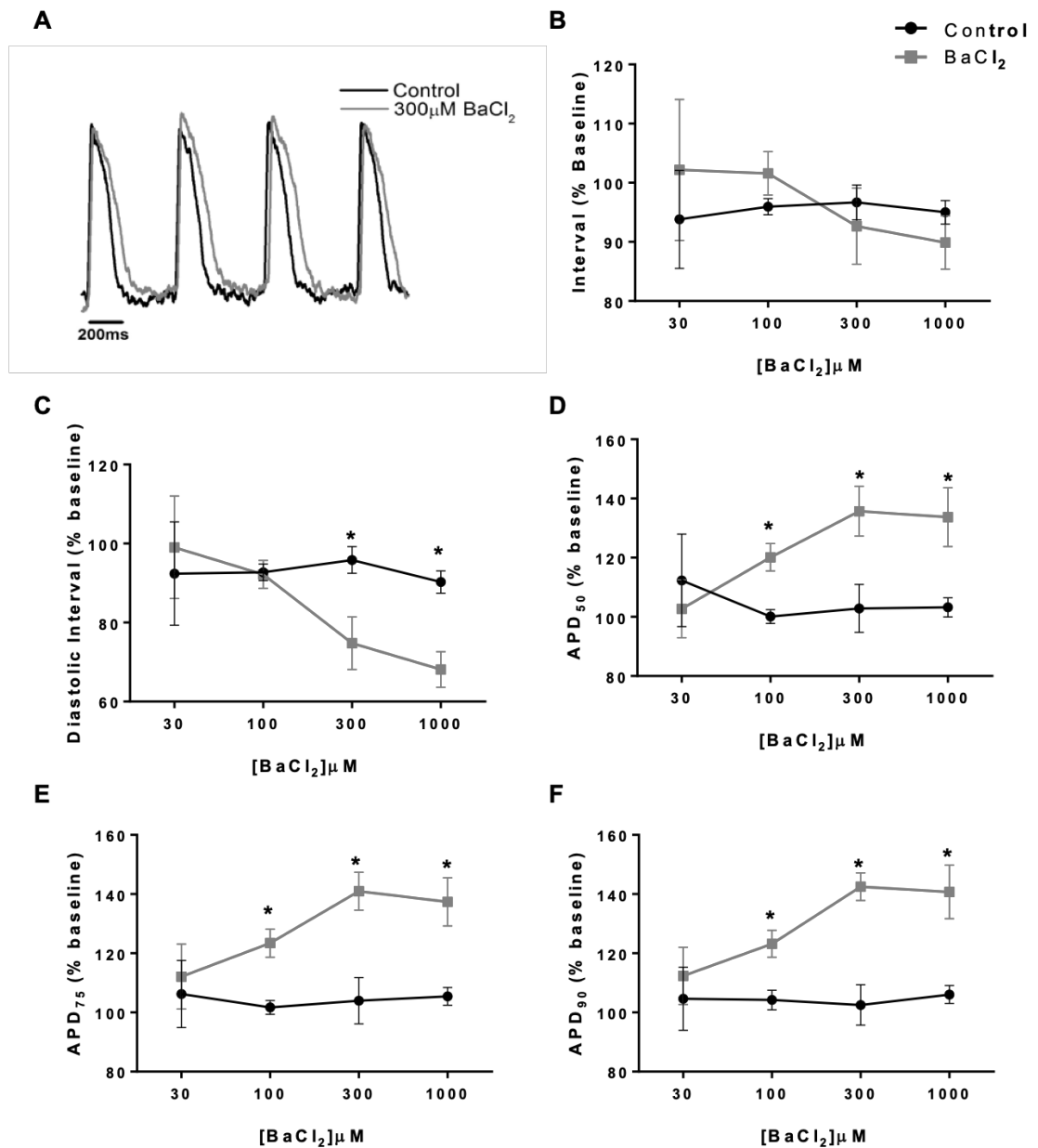


**Figure 3.3 - Barium chloride affects electrophysiological behaviour in hiPSC-CMs.** The effects of BaCl<sub>2</sub> were investigated at spontaneous rates at a different range of concentrations. **A)** Example trace of the effects of 300 μM BaCl<sub>2</sub> (grey) on voltage compared to control (black) over time; **B)** changes in interval between beats at increasing concentrations, compared to a DMSO control; **C)** changes in diastolic interval; **D)** Action potential duration at 50% of repolarisation; **E)** Action potential duration at 75% of repolarisation; **F)** Action potential duration at 90% of repolarisation. Unpaired t-test comparing control to drug, \*p<0.05, n=5.

The effect on APD is associated with an action on I<sub>k1</sub>, previously seen in ventricular myocardium in guinea pig hearts (Poelzing and Veeraraghavan, 2007). The changes in diastolic interval are not associated with a possible effect of I<sub>k1</sub> block, but could be due to off-target effects (Hoeker et al., 2017). Barium is known to alter calcium-mediated

inactivation of the L-type  $\text{Ca}^{2+}$  channel (Poelzing and Veeraraghavan, 2007). This data shows that  $\text{BaCl}_2$  is non-specific and thus inhibits more than the  $I_{k1}$  current. The effects on APD could be representative of the lack of  $I_{k1}$  in hiPSC-CMs.

### 3.3.3 PA-6

$I_{k1}$  presence was studied using PA-6, a pentamidine analogue which has been shown to block  $I_{k1}$  on isolated cardiomyocytes. When applied to hiPSC-CMs, it had no effect on electrophysiological behaviour. All parameters: interval between beats, diastolic interval, various stages of repolarisation, remained unchanged at different concentrations of PA-6 (Figure 3.4).

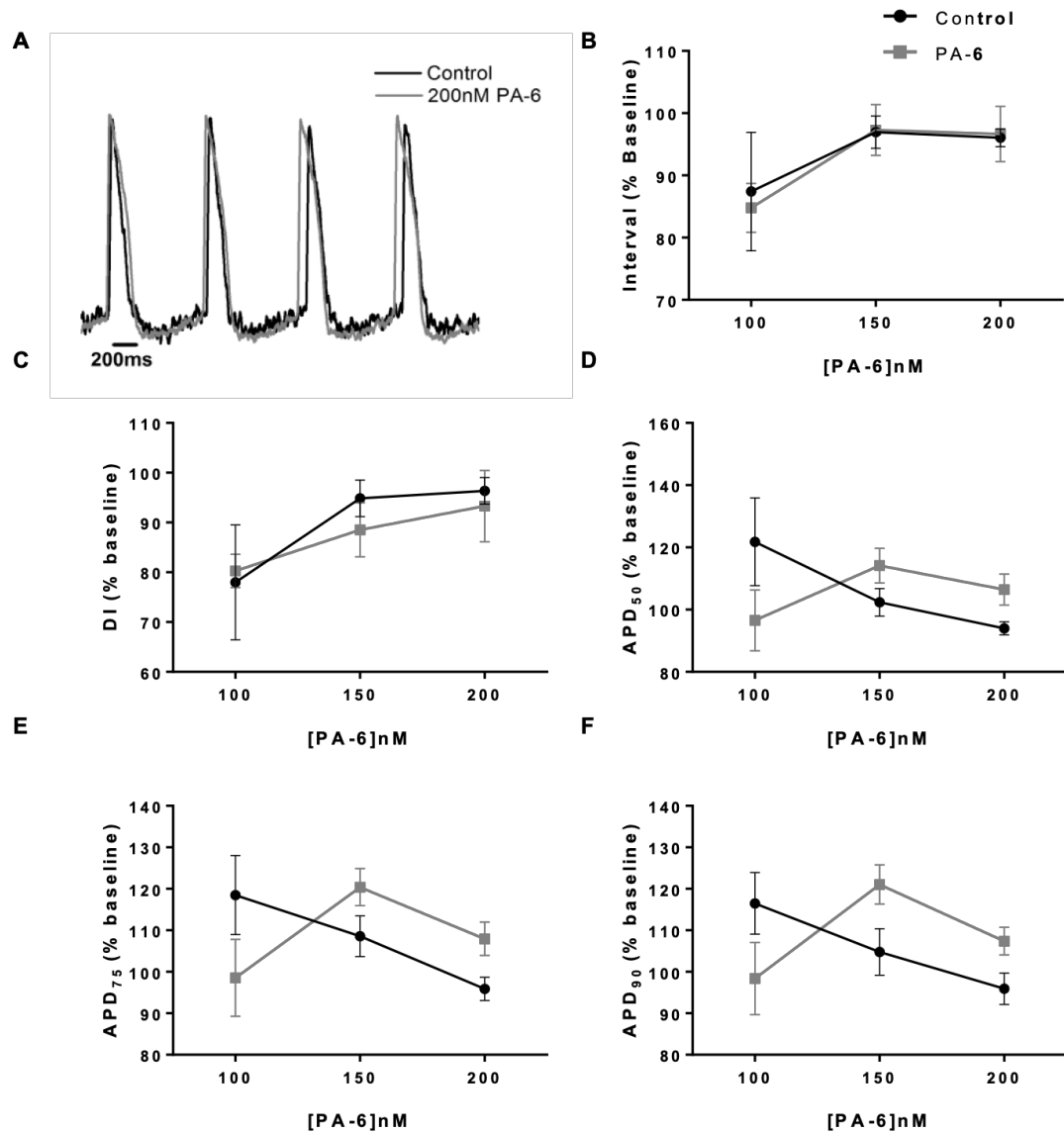


**Figure 3.4 - The effects of PA-6 at 100, 150 and 200nM on voltage in hiPSC-CMs at increasing concentrations. A) example trace of voltage traces obtained with FluoVolt over a time course in the presence of PA-6 or vehicle; B) the effects of PA-6 on interval shown as percentage of baseline; C) the effects of the drug on diastolic interval; D, E and F) the effects on the repolarisation phase, namely 50%, 75% and 90% of its duration, respectively (APD<sub>50</sub>, 75, 90). Unpaired t-test, n=6 for PA-6 and n=4 for vehicle.**

Interval remained unchanged at  $810.45 \pm 60.62$ ms and  $776.20 \pm 34.17$ ms ( $833.73 \pm 53.37$ ms and  $806.29.70$ ms baseline, respectively) in the presence of 150 and 200nM PA-6, whereas the vehicle stayed at  $888.63 \pm 28.12$ ms and  $817.73 \pm 23.17$ ms for the increasing DMSO, respectively ( $917.70 \pm 30.40$  and  $832.00 \pm 31.26$ ms for baseline, respectively) (Figure 3.4B). Diastolic interval remained unaffected (Figure 3.4C). Repolarisation time did not differ from the control at the different depolarisation stages. APD<sub>50</sub> was  $170.9 \pm 6.6$ ms,

192.4±12.37ms, and 166.7±3.7ms in the presence of 100, 150 and 200nM PA-6, respectively, compared to baseline (187.1±21.4ms, 170.3±13.1ms, and 158.1±7.1ms). DMSO APD<sub>50</sub> was 170.2±12.6ms, 141.2±9.3ms and 118.3.0ms in the presence of the vehicle (Figure 3.4D) (baseline: 144.5±15.8ms, 138.1±7.9ms and 124.9±4.3ms, respectively). APD<sub>75</sub> and APD<sub>90</sub> were not different from the vehicle (Figure 3.4E & F). Other studies in animal models have seen a prolongation of the APD in a dose-dependent manner with PA-6 (Hoeker et al., 2017, Takanari et al., 2013). The lack of an effect of an I<sub>kl</sub> blocker in our study is suggestive of the lack or low availability of I<sub>kl</sub> in hiPSC-CMs.

### 3.3.4 Potassium depletion and re-introduction

The availability of K<sup>+</sup> channels was further investigated by depleting external K<sup>+</sup> and slowly re-introducing. The effects resulting from the depletion and re-introduction will provide insight into the availability of potassium channels in hiPSC-CMs.

Baseline was recorded in the presence of 4.4mM of KCl to record the effect of the standard serum-free medium in the culture. Changes in voltage (Figure 3.5) and contractile behaviour (Figure 3.6) were recorded.

Voltage behaviour at baseline was recorded, when hiPSC-CMs were still in BMCC medium containing 4.4mM KCl, where interval was 2201.00±37.46ms. Figure 3.5A and B show a representation of the effects seen on depletion and after K<sup>+</sup> was re-introduced back to the starting concentration of K<sup>+</sup>, respectively. Interval (Figure 3.5C) was unaffected by the removal of KCl from the extracellular medium, although there was a slight decrease in interval showing that cell beating got faster. During initial re-introduction there was a prolongation in interval between APs, but started shortening once K<sup>+</sup> content reached 3mM, where it decreased to 1705.85±40.61ms, and stabilised. APD<sub>50</sub> (Figure 3.5D) shortened significantly from 414.14±6.65ms to 181.62±44.07ms upon removal of KCl from the extracellular medium. Addition of 0.5mM did not return APD<sub>50</sub> to baseline values but remained short at 191.37±54.04ms. Further addition of KCl led to recovery with APD<sub>50</sub> to 371.10±60.05ms at 1mM, and stably at that range of interval throughout increasing concentrations, except for shortening at 4, 5 and 8mM (368.96±18.04ms, 356.34±13.30ms, 343.70±27.86ms, respectively). APD<sub>75</sub> (Figure 3.5E) was not affected by the removal of extracellular K<sup>+</sup>, but a shortening was observed at 4mM to 499.68±19.12ms, also at 7mM

and 8mM ( $488.72 \pm 15.34$ ms and  $491.65 \pm 5.95$ ms, respectively).  $APD_{90}$  was unaffected by changes to the extracellular medium (Figure 3.5F).

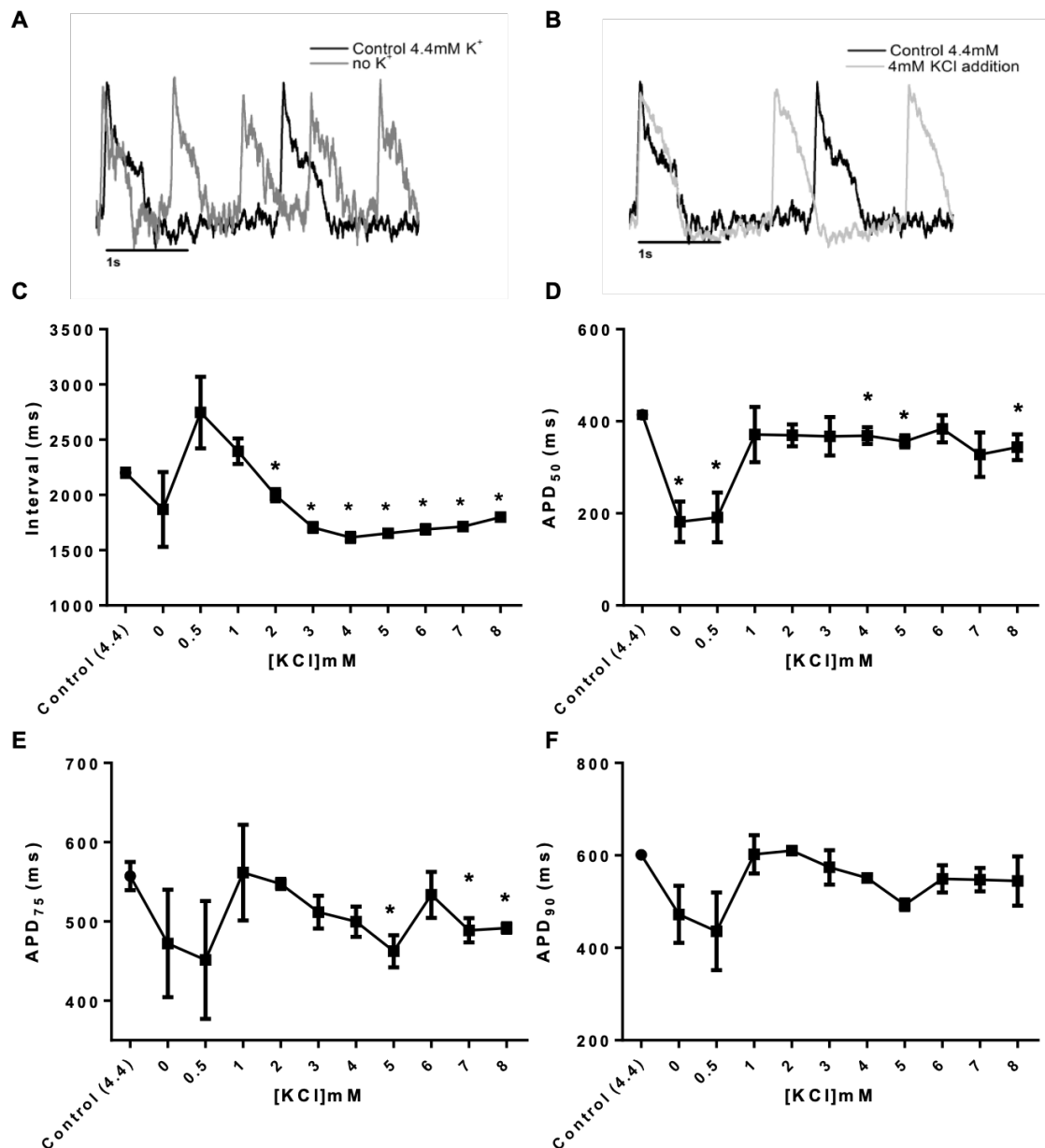


**Figure 3.5 –  $K^+$  depletion and re-introduction affects voltage in hiPSC-CMs.** A) example of voltage traces over a time course in the absence of  $K^+$  (grey) compared to control cells kept in 4.4mM  $KCl$  (black); B) example of voltage traces over a time course when the extracellular medium reaches 4mM  $KCl$  (grey) compared to control cells kept in 4.4mM  $KCl$  (black); C) the effects of removal and reintroduction of  $K^+$  on interval; D, E and F) the effects on the repolarisation phase, namely 50%, 75% and 90% of its duration, respectively ( $APD_{50, 75, 90}$ ). Unpaired t-test, \* $p < 0.05$ ,  $n = 6$ .

Contractility was not significantly affected by the removal of KCl (Figure 3.6A and B), as interval decreased from  $1818.94 \pm 114.02$ ms in BMCC to  $1431.07 \pm 174$ ms with no  $K^+$ , thus starting to increase the frequency of cell contraction (Figure 3.6C). Re-introduction of  $K^+$  at 0.5mM started increasing the interval between the start of each cell contraction to  $2181.67 \pm 36$ ms, and further significantly increased it past BMCC levels to  $2286.94 \pm 100.07$ ms when the BMCC-KCl reached 1mM. Interval reached a plateau at higher concentrations than 1mM. 2mM brought the interval down to  $1859.88 \pm 289.30$ ms, stayed at  $1668.33 \pm 40.02$ ms at 3mM,  $2058.92 \pm 342.73$ ms at 4mM,  $1623.61 \pm 48.13$ ms at 5mM,  $1538.13 \pm 119.26$ ms at 6mM,  $1692.92 \pm 20.46$ ms at 7mM, and  $1817.62 \pm 50.88$ ms at 8mM (Figure 3.6C). Time for contraction was substantially higher upon removal of  $K^+$  ( $131.83 \pm 18.71$ ms,  $p < 0.05$ ) compared to the time before its removal ( $82.17 \pm 11.65$ ms). At all other concentrations of KCl, time for contraction was not different from that of BMCC (Figure 3.6D). Time for relaxation in the presence of 4.4mM BMCC was  $428.23 \pm 40.07$ ms and did not change with  $K^+$  depletion and re-introduction (Figure 3.6E). The 50% of contraction duration was registered at  $412.46 \pm 21.42$ ms and was not affected by the absence of  $K^+$ , nor by its re-introduction.

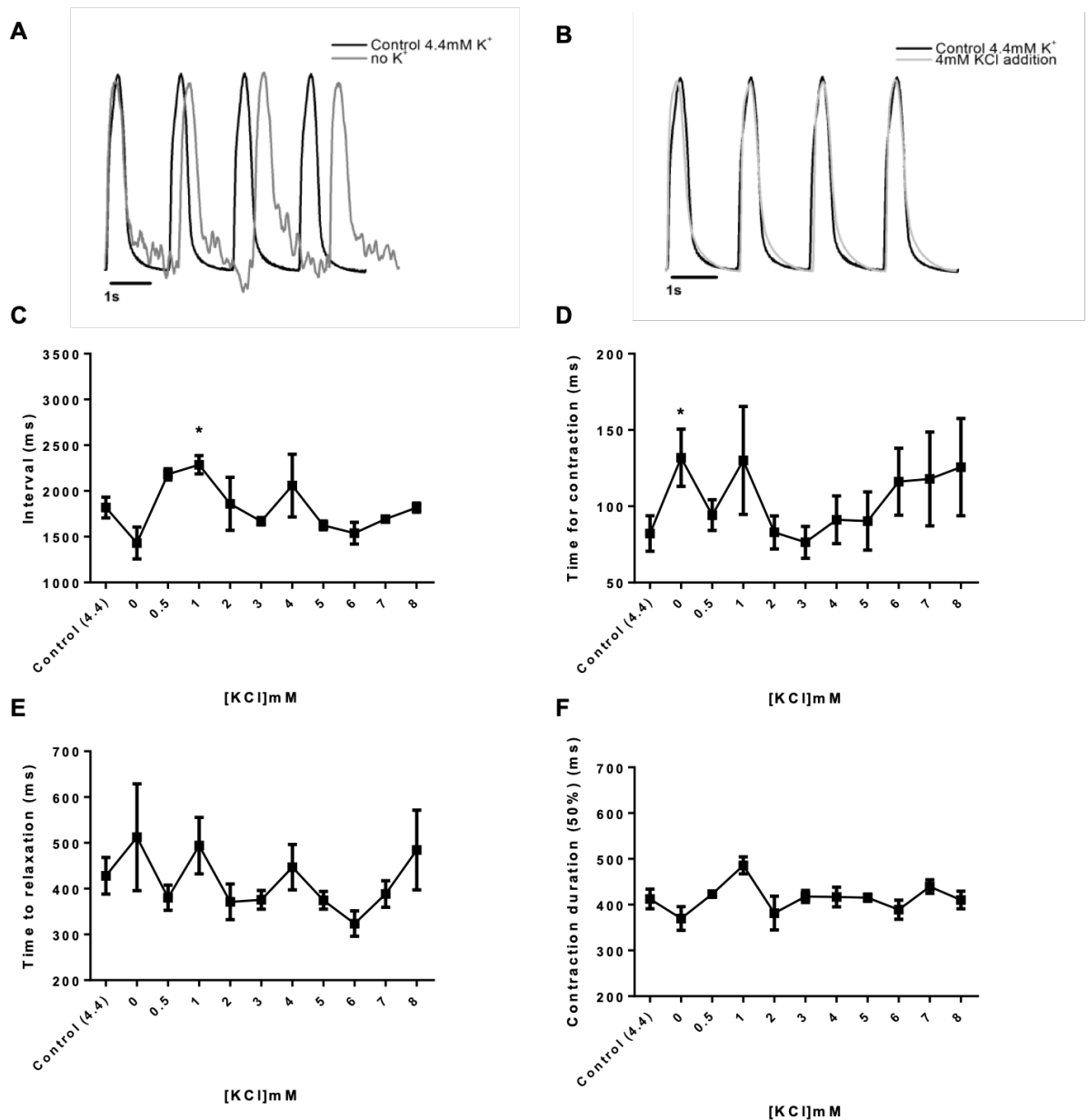


**Figure 3.6 –  $K^+$  depletion and re-introduction affects contractile behaviour.** A) example of contraction traces over a time course in the absence of  $K^+$  (grey) compared to control cells kept in 4.4mM  $KCl$  (black); B) example of contraction traces over a time course when the extracellular medium reaches 4mM  $KCl$  (grey) compared to control cells kept in 4.4mM  $KCl$  (black); C) the effects of removal and reintroduction of  $K^+$  on interval; D) effects on time for full contraction; E) effects on relaxation time; F) the effects on 50% of contraction duration. Unpaired t-test, \* $p < 0.05$ ,  $n = 6$ .

The effects of the removal of potassium sources from the medium show that interval is unaffected. Its reintroduction increased the interval between each beat, but it reached normal levels at 2mM for contractility, whereas the interval on voltage was significantly

shorter. The lack of an effect on interval upon removal of extracellular  $K^+$  could be a result of the lack of available potassium channels in hiPSC-CMs.

### 3.3.5 Thapsigargin

Addition of thapsigargin to hiPSC-CMs had effects on interval as it was prolonged to  $2484 \pm 127$ ms with  $3 \mu\text{M}$  compared to  $1747 \pm 81$ ms in the vehicle control. A higher concentration ( $10 \mu\text{M}$ ) did not further prolong interval keeping it at  $2480 \pm 150$ ms, whereas control stayed at  $1709 \pm 66$ ms (Figure 3.7B). Diastolic interval was significantly longer in the presence of thapsigargin compared to vehicle, as it reached  $2002.0 \pm 125.3$ ms and  $2010.0 \pm 148.8$ ms at 3 and  $10 \mu\text{M}$ , compared to  $1408.2 \pm 81.9$ ms and  $1354.7 \pm 73.9$ ms for corresponding concentrations of DMSO (Figure 3.7C).  $\text{APD}_{50}$  was greatly prolonged to  $349.9 \pm 10.9$ ms in the lowest concentration of thapsigargin,  $3 \mu\text{M}$ , compared to control ( $272.6 \pm 2.5$ ms,  $p < 0.05$ ). At  $10 \mu\text{M}$ , the prolongation was smaller to  $321.6 \pm 8.8$ ms, whereas control was  $274.4 \pm 9.2$ ms (Figure 3.7D).  $\text{APD}_{75}$  prolonged to  $424.8 \pm 10.4$ ms at  $3 \mu\text{M}$ , while control did not change, remaining at  $309.9 \pm 2.3$ ms. At  $10 \mu\text{M}$   $\text{APD}_{75}$  was prolonged significantly to  $395.2 \pm 6.2$ ms and remained at  $311.5 \pm 9.5$ ms for control (Figure 3.7E). The same effect was seen for  $\text{APD}_{90}$ , where it was prolonged to  $481.1 \pm 6.7$ ms and  $459.8 \pm 4.5$ ms, for  $3 \mu\text{M}$  and  $10 \mu\text{M}$ , respectively. Control stayed at  $338.3 \pm 1.6$ ms and  $354.2 \pm 16.0$ ms (Figure 3.7F).

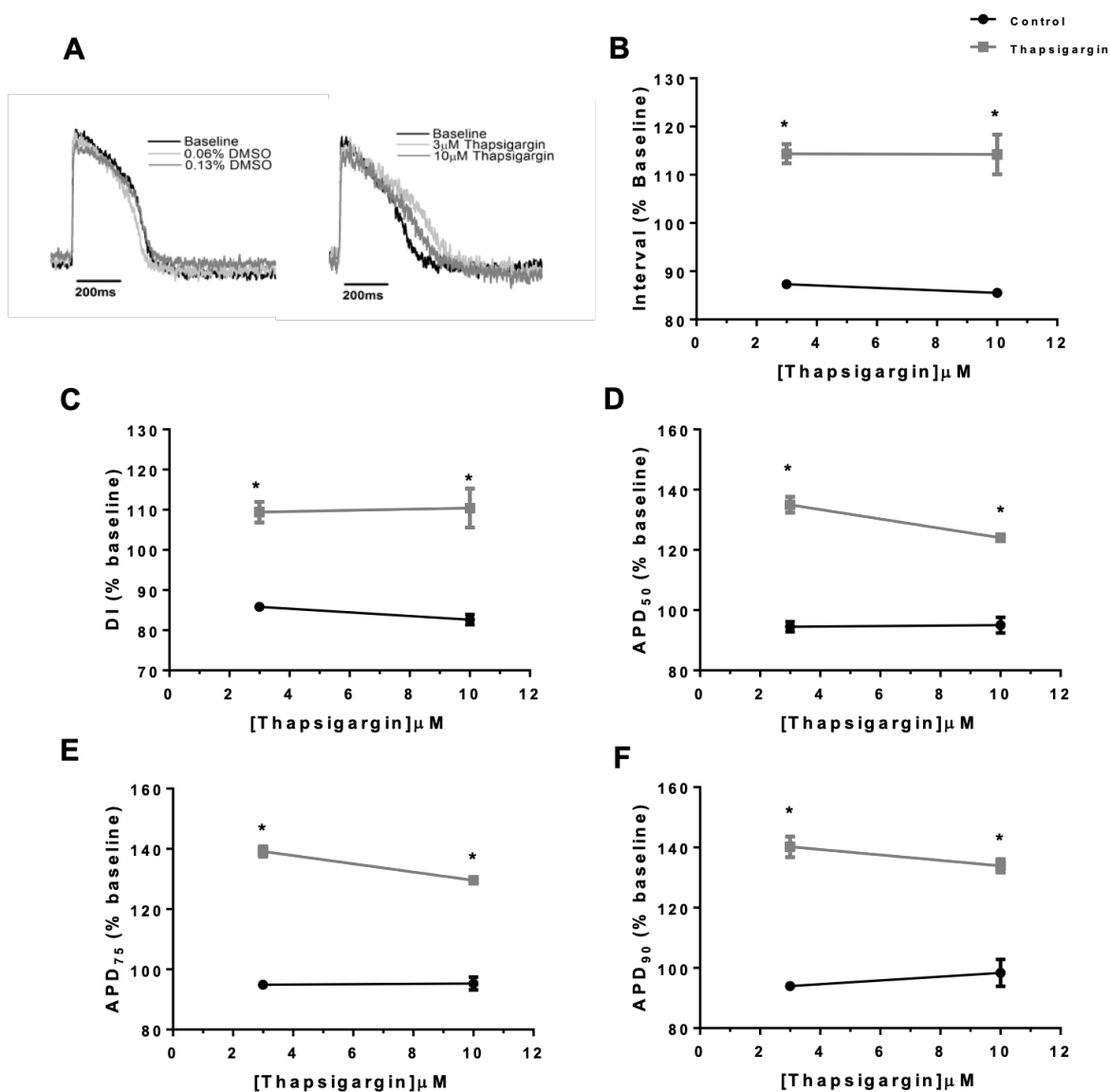


**Figure 3.7 – The effects of thapsigargin on hiPSC-CMs' electrophysiological behaviour. A)** example traces of the effects of a vehicle (DMSO) at 0.06% and 0.12% and thapsigargin at 3 and 10 $\mu\text{M}$ ; **B)** the effects on interval shown as percentage from baseline for vehicle and thapsigargin; **C)** diastolic interval affected by thapsigargin; **APD** at 50, 75 and 90% of repolarisation are affected by thapsigargin. Unpaired t-test, \* $p < 0.05$ ,  $n = 6$ .

The effects on calcium signalling were also studied (Figure 3.8). At 3 $\mu\text{M}$ , thapsigargin significantly prolonged interval ( $1916.00 \pm 72.25\text{ms}$ ) compared to baseline ( $1754.63 \pm 76.97\text{ms}$ ) and vehicle ( $1730.93 \pm 20.90\text{ms}$ ) (Figure 3.8A). The presence of DMSO alone had a strong effect on interval as it decreased interval from  $1902.28 \pm 24.71\text{ms}$ . The reason for this is unknown as these concentrations are frequently used. It is possible that these cells had damaged membranes from handling. Amplitude did

not change in the presence of thapsigargin, but DMSO decreased the amplitude of the CaT in the vehicle from  $0.057 \pm 0.01$  a.u. to  $0.042 \pm 0.008$  a.u. (Figure 3.8B). Time to reach peak of the CaT was significantly longer ( $255.00 \pm 14.15$  ms) compared to baseline ( $198.50 \pm 25.32$  ms) and control ( $172.50 \pm 7.04$  ms) (Figure 3.8C). Decay time was prolonged in the presence of thapsigargin ( $891.13 \pm 22.67$  ms) but decreased in the vehicle ( $594.10 \pm 14.22$  ms) compared to baseline ( $673.90 \pm 41.71$  ms in thapsigargin, and  $721.20 \pm 5.19$  ms in vehicle) (Figure 3.8D).

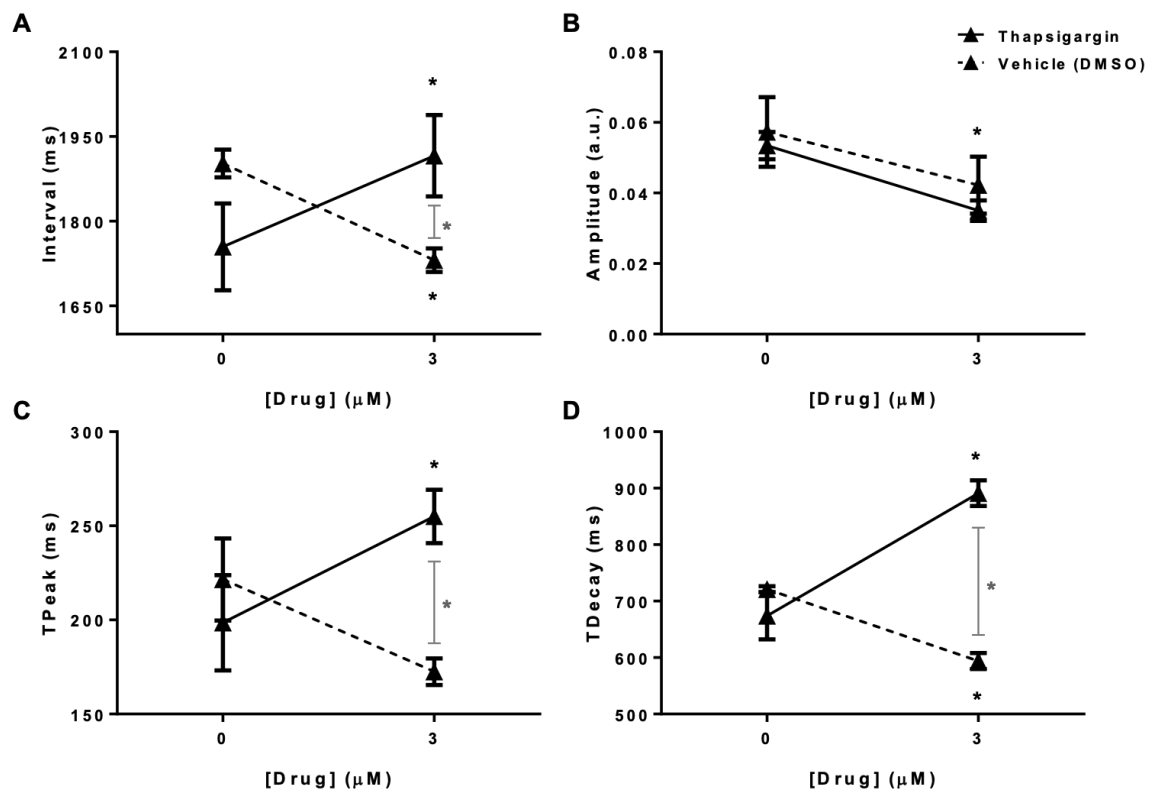


**Figure 3.8 - Calcium handling is affected by thapsigargin.** A) Interval changes in DMSO control (dashed line) and in the presence of thapsigargin (solid line) from baseline to  $3\mu\text{M}$ ; B) effects on CaT amplitude for control and thapsigargin; C) effects on time to reach the peak of the CaT; D) time to decay from peak. Paired t-test comparing baseline to drug or vehicle, unpaired t-tests comparing vehicle to drug. Asterisks compare  $3\mu\text{M}$  to baseline, and asterisks with vertical line compare thapsigargin and DMSO,  $*p < 0.05$ ,  $n = 4$ .

Thapsigargin has been shown to inhibit  $I_{\text{NCX}}$  at concentrations as low as  $5\mu\text{M}$  in some hiPSC-CMs, suggesting that  $\text{Ca}^{2+}$  release from the SR plays a critical part in the spontaneous activity of these cells (Zhang et al., 2015). On  $\text{Ca}^{2+}$  behaviour, thapsigargin acted slowly to progressively decrease the amplitude of whole-cell  $[\text{Ca}^{2+}]_i$  transients,

eventually leading to their complete inhibition (Itzhaki et al., 2011). This agrees with the data from this study, suggesting that the SR plays a critical role in the spontaneous activity of hiPSC-CMs.

### 3.3.6 Ryanodine

Ryanodine was added to hiPSC-CMs at 3 and 10 $\mu$ M for 30min before recording. Electrophysiology (Figure 3.9A) was greatly affected by the drug at both concentrations as interval was prolonged to 2958.4 $\pm$ 104.9ms from baseline (2117.5 $\pm$ 98.1) compared to control (1957.0 $\pm$ 77.3ms,  $p$ <0.05) at 3 $\mu$ M, and to 2695.1 $\pm$ 77.0ms compared to control (1918.1 $\pm$ 77.7ms,  $p$ <0.05) at 10 $\mu$ M (Figure 3.9B). Diastolic interval was also significantly longer at 3 $\mu$ M, 2424.3 $\pm$ 104.5ms (baseline: 1772.1 $\pm$ 94.3ms), compared to the vehicle (1626.0 $\pm$ 84.1ms,  $p$ <0.05), and at 10 $\mu$ M, 2153.8 $\pm$ 80.5ms (vehicle was 1592.4 $\pm$ 76.1ms,  $p$ <0.05) (Figure 3.9C). APD<sub>50</sub> was significantly longer in the presence of ryanodine, where at 3 $\mu$ M it was 435.0 $\pm$ 11.9ms with baseline at 266.4 $\pm$ 6.0ms (control was 245.9 $\pm$ 8.6ms,  $p$ <0.05), and at 10 $\mu$ M 426.2 $\pm$ 11.6ms (compared to control 241.4 $\pm$ 8.2ms,  $p$ <0.05) (Figure 3.9D). A similar effect was seen on APD<sub>75</sub>, which prolonged to 500.2 $\pm$ 13.1ms for both 3 $\mu$ M and 10 $\mu$ M, compared to 294.6 $\pm$ 8.0ms and 288.9 $\pm$ 7.2ms ( $p$ <0.05) for DMSO control (Figure 3.9E). Same occurred for APD<sub>90</sub>, where at 3 $\mu$ M it prolonged to 534.2 $\pm$ 12.7ms, and at 10 $\mu$ M to 541.3 $\pm$ 10.4ms, whereas vehicle was 331.0 $\pm$ 10.7ms and 325.7 $\pm$ 9.8ms ( $p$ <0.05) (Figure 3.9F). Baseline for APD<sub>90</sub> was 345.4 $\pm$ 7.5ms.

Ryanodine inhibition of the SR affected all voltage parameters at both tested concentrations. This indicates that the calcium clock might play an important role in spontaneous activity, as suggested in section 3.3.5. To further study this, calcium recordings were taken.

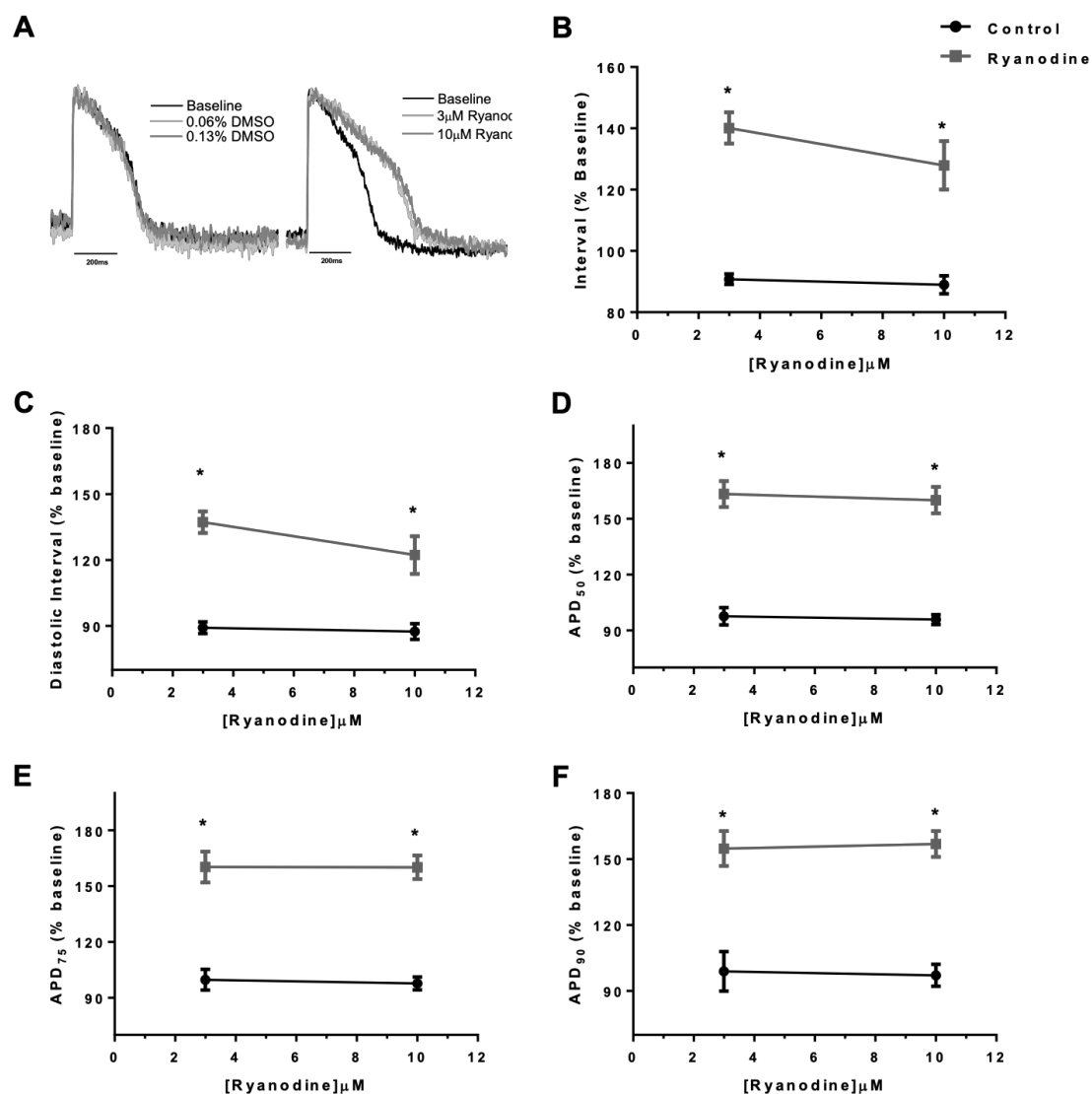


**Figure 3.9 - Ryanodine affects electrophysiological behaviour in hiPSC-CMs.** A) Example trace of the effects on the action potential shape of the vehicle at two different concentrations, matching the percentage of DMSO in ryanodine preparation (left), and of the effects of the two concentrations of ryanodine (right); B) Interval is affected by ryanodine, shown as percentage from baseline, where baseline is 100%; C) Effects of ryanodine and vehicle in diastolic interval; D, E and F) APD at 50, 75 and 90% of repolarisation are affected by ryanodine. Unpaired t-test, \* $p < 0.05$ ,  $n = 6$ .

The effects on calcium signalling with  $3\mu\text{M}$  ryanodine showed a prolongation in the interval between each CaT from  $1626 \pm 25.3\text{ms}$  at baseline to  $2174.93 \pm 68.96\text{ms}$ . It was also significantly longer than the vehicle at  $1386.45 \pm 122.31\text{ms}$  (Figure 3.10A). The CaTamp was significantly decreased from  $0.036 \pm 0.004\text{a.u.}$  to  $0.014 \pm 0.0006\text{a.u.}$  in the presence of  $3\mu\text{M}$  of ryanodine. The vehicle decreased amplitude from  $0.042 \pm 0.007\text{a.u.}$  to  $0.028 \pm 0.007\text{a.u.}$  (Figure 3.10B). The effects seen from the presence of DMSO alone are unknown. It is possible that the concentration used was high, or that there was some

damage to cell membrane, as these are standard concentrations. Time to reach the peak of CaT did not change from baseline but was significantly longer ( $230.00 \pm 24.51$ ms) than the vehicle control ( $149.00 \pm 17.29$ ms) (Figure 3.10C). Decay time was significantly longer ( $1045.69 \pm 98.62$ ms) in the presence of ryanodine compared to baseline ( $717.45 \pm 49.43$ ms) and vehicle ( $566.05 \pm 23.77$ ms) (Figure 3.10D).

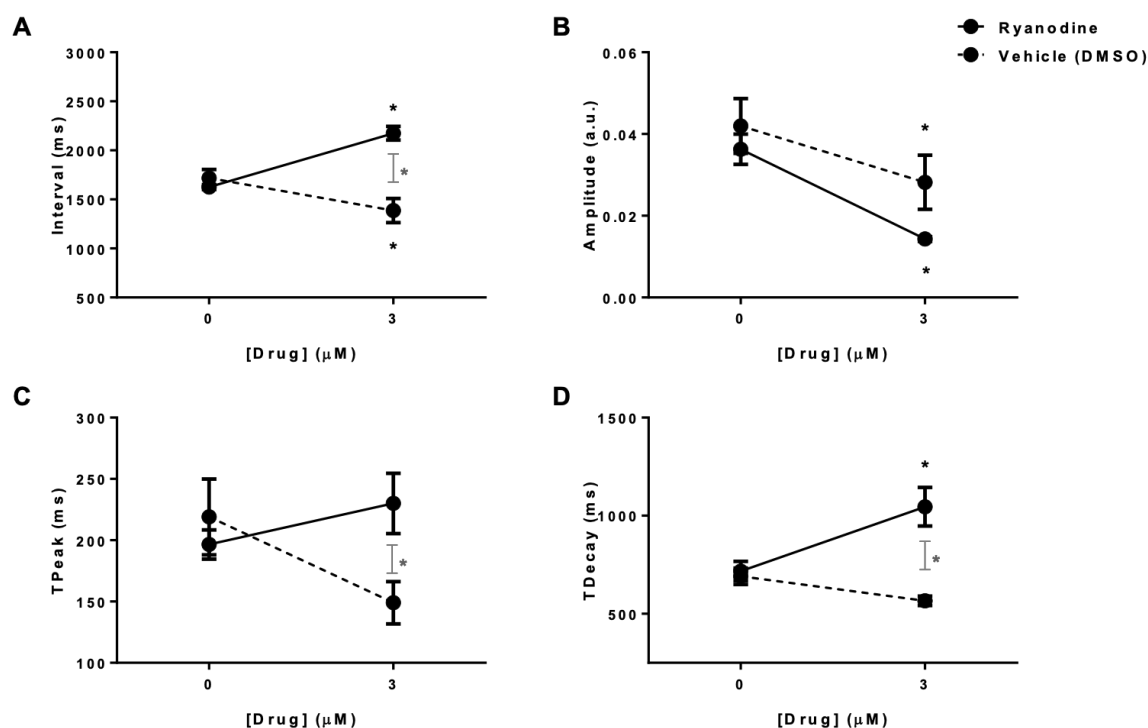


**Figure 3.10 - Calcium handling in hiPSC-CMs is affected by ryanodine. A)** Interval changes in DMSO control (dashed line) and in the presence of ryanodine (solid line) from baseline to  $3\mu\text{M}$ ; **B)** effects on CaT amplitude for control and ryanodine; **C)** effects on time to reach the peak of the CaT; **D)** time to decay from peak. Paired t-test comparing baseline to drug or vehicle, unpaired t-tests comparing vehicle to drug,  $*p < 0.05$ ,  $n=4$ .

Application of ryanodine leads to a significant reduction of  $\text{Ca}^{2+}$  release, previously observed in reduction of CaT amplitude and frequency on hiPSC-CMs and rabbit SAN cells, ESC-CMs, and mouse ESC-CMs (Itzhaki et al., 2011).

## 3.4 Discussion

### 3.4.1 $I_f$ and its contribution towards spontaneous activity

Ivabradine, a well-known pacemaker current blocker, affected mainly action potential duration. Previous studies have shown that block of hiPSC-CMs with ivabradine had no

effect on spontaneous activity (Zhang et al., 2015). The observed cycle length prolongation in this study can be a result of an effect on  $I_f$ , thus showing a partial block of the pacemaker current, or changes in APD, showing a non-specific target. APD was, in fact, prolonged in a dose-dependent manner, increasing significantly at  $10\mu\text{M}$ . The effect was previously reported in isolated cardiomyocytes, which was associated with non-specificity for  $I_f$ , but rather with a blockade of hERG1 in the same range of concentrations, where ivabradine blocked hERG-A with an  $\text{IC}_{50}$  of  $6.8\mu\text{M}$  and hERG-B with an  $\text{IC}_{50}$  of  $3.7\mu\text{M}$  (Lees-Miller et al., 2015). Zhang et al. (2015) reported that  $I_f$  was expressed more robustly in hiPSC-CMs than in neonatal cells, but it only activated at potentials negative to  $-80\text{mV}$ , and if it were to contribute to the generation of spontaneous activity, it would have to carry significant inward current at voltages positive to  $-70\text{mV}$ . This could mean it is either absent, or the kinetics are slow, and thus the activation-voltage too negative.

The data obtained showed that lower concentrations of ivabradine ( $1\mu\text{M}$ ) affects diastolic interval and has little effect on APD, suggesting that it is having an effect on spontaneous activity. Higher concentrations prolonged APD, which is no longer a characteristic effect on  $I_f$ , suggesting that other channels might be blocked instead due to non-specificity. This data suggests that, in hiPSC-CMs,  $I_f$  plays a role in spontaneous activity, albeit small.

### 3.4.2 $I_{k1}$ presence in hiPSC-CMs

$\text{BaCl}_2$  is a non-specific  $I_{k1}$  blocker, known to also block other inwardly  $\text{K}^+$  rectifiers (De Boer et al., 2010). In this study it affected the diastolic interval and repolarisation time but had no consequence in interval. While repolarisation changes can be explained by effects on  $I_{k1}$ , the effects on diastolic interval are possibly due to off-target effects (Hoeker et al., 2017). Therefore, determining the contribution of  $I_{k1}$  towards the spontaneous activity of hiPSC-CMs using  $\text{BaCl}_2$  is not ideal, and other methods need to be used. For this purpose, a second test was done using the  $I_{k1}$  inhibitor: PA-6. Although effects on APD have been seen in adult animal hearts, where it is prolonged in a dose-dependent manner, no effect was seen on hiPSC-CMs, as the electrophysiological behaviour of hiPSC-CMs' remained unchanged at a range of PA-6 concentrations. This could be an indicator of the low availability of this current and Kir2.1 in these cells, which is consistent with what has previously been found:  $I_{k1}$  density is four-times lower than what has been reported in human adult CMs (Ma et al., 2011a).

Another approach to determining the availability of  $K^+$  channels and rectifying currents was to remove all the extracellular  $K^+$  and observe the electrophysiological and contractile behaviour exhibited by the cells. Removal of  $K^+$  had no effect on interval, but led to a shortening of medium repolarisation, but re-introduction led to a shortening of the interval past initial duration. Contractile behaviour remained unaltered. The lack of response upon removal of the  $K^+$  source is an indicator of the low availability of the  $I_{K1}$  current.

### **3.4.3 SERCA and other potential contributions towards spontaneous activity**

To study the contribution of SERCA to the electrophysiological behaviour of hiPSC-CMs, thapsigargin was added at widely-used concentrations. This had a strong effect on interval, diastolic interval and APD, prolonging all variables. It also led to a decrease in CaTamp and increase in time to reach peak and decay. The effects are suggestive that  $Ca^{2+}$  release from the SR plays a critical role in spontaneous activity in these cells (Zhang et al., 2015).

Ryanodine, a RyR antagonist, is associated with a reduction in calcium release in adult cardiomyocytes, but also in hiPSC-CMs. Addition of this drug at 3 and  $10\mu\text{M}$  led to a prolongation in interval between each AP and CaT, prolonged DI, APD, time to reach peak of CaT and time of CaT decay. The effects seen on amplitude and interval demonstrate that hiPSC-CMs have ryanodine-sensitive SR  $Ca^{2+}$  stores capable of unloading  $Ca^{2+}$  via RyR-mediated  $Ca^{2+}$  release and contributing to whole-cell  $[Ca^{2+}]_i$  transients (Itzhaki et al., 2011).

In the presence of thapsigargin or ryanodine, both the diastolic interval and APD were prolonged, and this increase cannot be separated. Thapsigargin and ryanodine slow the calcium transient rise and fall, and the slow rate of decay may influence the repolarisation, thus affecting the APD. In hiPSC-CMs, the SR affects only the rate of rise and decay, but not the amplitude of the calcium transient, suggesting that the SR capacity is much lower than that in the adult CM. One possible explanation is that the SR release inactivates  $I_{Ca}$  via  $Ca^{2+}$  inactivation, and, without SR, there is no inactivation of the LTCC, therefore L-type  $Ca^{2+}$  increases, and so does APD.

### 3.4.4 Conclusion

hiPSC-CMs have come a long way, but still lack very important channels and currents to resemble adult CMs. Channel and current antagonists: ivabradine, PA-6, BaCl<sub>2</sub>, thapsigargin and ryanodine were used to investigate the mechanisms which contribute towards the spontaneous activity in hiPSC-CMs. I<sub>f</sub> is not a major contributor towards spontaneous activity in hiPSC-CMs but plays an important part in initiating depolarisation in adult cells. Another distinguishing, yet lacking feature is that there is low availability or absence of I<sub>k1</sub> current, important in maintaining a stable resting membrane potential and in late repolarisation. SERCA plays an important role in spontaneous activity and hiPSC-CMs release Ca<sup>2+</sup> via RyR. The differences in electrophysiology between hiPSC-CMs and adult CMs have to be known in order to further improve hiPSC-CMs.

The spontaneous activity of hiPSC-CMs has been widely studied, but no comprehensive research has been done into the contribution of different ion channels and currents. This study was the first to use pharmacological tools to determine the roles of SERCA, RyR, I<sub>k1</sub> and I<sub>f</sub> to spontaneous activity.

## **4 Co-culture of hiPSC-CMs and HEK293**

## 4.1 Introduction

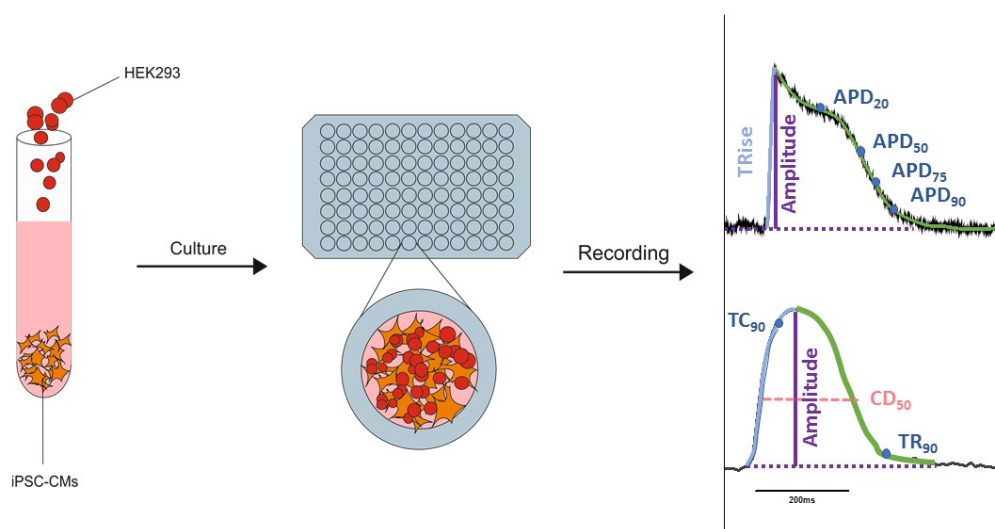


**Figure 4.1- Principle of co-culture of hiPSC-CMs and HEK293.** hiPSC-CMs and HEK293 are thawed and suspended in cell maintenance medium and mixed at desired densities before being plated in a 96-well format. The cells are maintained for 4 days, and contractile (bottom trace) and electrophysiological (top trace) behaviour are measured on the last day. Different parameters are measured, such as amplitude of voltage and contraction signal, APD and time for contraction and relaxation.

Several studies have elaborated on the use of *HCN* ion channels in the construction of biological pacemakers.  $I_{k1}$  stabilises the resting membrane potential between  $-75$  and  $-90$ mV. Inward rectification is established by increasing potassium conductivity at hyperpolarisation, while the  $I_{k1}$  channels close upon membrane depolarising. As mentioned before, HEK293 cells can be genetically engineered to express specific ion channels and currents, normally not present. De Boer et al. (2006) developed a stable HEK293 cell line expressing murine wildtype Kir2.1-GFP. To create these cells, HEK293 were transfected with a pcDNA3-Kir2.1-GFP, which produced a C-terminal GFP-tagged Kir2.1 (De Boer et al., 2006).

Despite the low amount of connexin-43, a protein responsible for establishing gap junctions in heart tissue, HEK can attach and couple with other cells, as shown by De Boer et al. (2006), where the group co-cultured HEK293 and adult cardiomyocytes. Developing a co-culture protocol where HEK are introduced into an existing and well-established hiPSC-CMs culture could provide the means to introduce the lacking  $I_{k1}$  and lower the

resting membrane potential to a stable value, such as -75 to -90mV. For this purpose, a co-culture protocol was developed where HEK293 and hiPSC-CMs are cultured collectively in a 96 well plate, and optimised cell culture medium. The cells are then maintained for a determined period of time and the necessary measurements are taken.

Co-culture was also done using hiPSC-CMs and human cardiac fibroblasts (HCF), as the latter are naturally present in the heart. This protocol will provide understanding into the effects of co-culture on hiPSC-CMs electrophysiological and contractile behaviours.

### **4.1.1 Aims**

The aims of this chapter were to introduce an external source of  $I_{K1}$  using  $I_{K1}$ -overexpressing HEK cells and assess the effects on electrophysiology and contractility on co-culture with hiPSC-CMs. The hypothesis was that the presence of  $I_{K1}$  to hiPSC-CMs' culture will impact the spontaneous activity.

## **4.2 Methods**

### **4.2.1 HEK293 proliferation assay**

The rate of HEK proliferation was measured using two different methods: manual count using 0.4% trypan blue and haemocytometer and by MTT assay. Both standard and  $I_{K1}$ -expressing HEK293 were plated in 48-well plastic plates (Corning) at 50,000 cells/mL, 1mL per well, the density necessary to create a uniform monolayer. Cell counts were performed at 24h, 48h and 72h. To perform cell counting, the cells were washed 2x in PBS at RT, and then 0.5% trypsin-EDTA was added for 3min until cells were detached. The effect of trypsin was blocked with HEK293 culture medium, and the cell suspension was centrifuged at 1050rpm for 1 minute. The cells were resuspended in HEK293 medium, and a small sample was taken and mixed at 1:1 with 0.4% trypan blue. A cell count was performed using a manual haemocytometer.

A second method was performed using an MTT (3-(4,5-dimethylthiazol-2-yl)-2,5-diphenyl tetrazolium bromide) assay. This reagent is cleaved by living cells, as it requires active mitochondria to cleave the tetrazolium ring, yielding purple MTT formazan crystals. The purple solution is spectrophotometrically measured. Absorbance is measure at 570nm and

background absorbance measured at 690nm is subtracted. The cells were cultured as before in 96 well plastic plates at 125,000 cells/mL, 200 $\mu$ L per well (final density 25,000 cells/well), to match the new diameter in the well. On each measurement day, the culture was incubated with 10 $\mu$ L of the MTT assay for 3h at 37°C. After incubation, the medium is replaced with MTT solvent and absorbance was measured within 30min. As controls, unloaded cells were measured in the presence of the MTT solvent, and empty wells were also recorded with MTT solvent alone.

#### **4.2.2 Co-culture of Pluricyte hiPSC-CMs and HEK293**

Pluricyte hiPSC-CMs are available commercially. Initial studies were performed with these cells and develop a co-culture protocol, and later protocols were switched to Cor.4U CMs. Following manufacturer's recommendations, these cells were seeded at either 30,000 cells/well or 40,000 cells/well in 96 well plates in Pluricyte maintenance medium. The ratios used ranged from 1:2 to 1:20 HEK:hiPSC. The cell cultures were maintained in Pluricyte culture medium, and the contractile behaviour was recorded using HCLive, daily for 6 days. The ratio of HEK:hiPSC was subsequently changed to ratios of 1:5, 1:10, 1:15, 1:20, 1:30, 1:100 and 1:300 and final density was raised to 40,000 cells/well total. This was done to overcome quiescence from the addition of high densities of HEK. Contractility was recorded for 12 days since the cultures were no longer quiescent. On the last day, the cultures were electrically stimulated at 40V, pulse set for 2ms duration. Spontaneous rates were recorded once the electrodes were fitted, and subsequent recordings were taken starting at 1Hz and increasing frequencies. Data was analysed on ImageJ and CelloPTIQ and processed in GraphPad Prism 7.

#### **4.2.3 Co-culture of Cor.4U hiPSC-CMs and HEK293**

Cor.4U hiPSC-CMs are also a commercial cell line, and the most abundantly used in this lab. The standard protocol for plating is described in Ch. 2 (General Methods). These cells were cultured at 25,000 cells/well in 200 $\mu$ L. Firstly, the most appropriate HEK:hiPSC-CM ratio to be used between cells was established, dependent on when the effect of  $I_{K1}$  was most visible. Cor.4U were thawed and cell count was performed (see Ch.2), cell density was adjusted to 125,000 cells/mL, and were transferred to separate sterile eppendorfs so that different densities of HEK could later be added and mixed. HEK293, both standard

and  $I_{K1}$ -expressing, were thawed in HEK medium, centrifuged at 1050rpm for 2min, and then resuspended in Cor.4U maintenance medium, at which point a cell count was performed and cell density adjusted accordingly.

#### **4.2.3.1 Different densities**

Initially a range of HEK:hiPSC-CM ratios were tested to determine the most appropriate, starting with low densities of HEK293 and contractility were measured daily for 4 days. On the last day, the cells were loaded with the voltage-sensitive dye, FluoVolt, at 1:1000, along with the accompanying PowerLoad at 1:100, for 25min, diluted in BMCC. The dye was removed and replaced with BMCC at 37°C. The culture was allowed to settle for 30min before any recordings were taken, in an incubated stage (CelloPTIQ, Clyde Biosciences, UK) at 37°C 5%CO<sub>2</sub>. A voltage signal was found for each well or area, and subsequently recorded for 10s with 470nm excitation. Contractility recordings were taken immediately after for 8s, at 1000fps using HCImage Live, of the same cell or area. Subsequent work was done at 1:1 HEK:hiPSC.

#### **4.2.4 The effects of different media in cell proliferation and co-culture**

HEK293 cells are an immortal cell line which proliferates in an exponential manner. Understanding of the proliferation rates in these cells is important, as there is a need for knowledge regarding the cell density during the recorded periods. For this effect, several different protocols were followed to either arrest the cell growth or reduce it. Co-culture at two different ratios: 1:3 and 1:1, was plated as normal, but split into different media: BMCC, a serum-free medium; Low-serum medium, a modified HEK medium containing 5% FBS; Mitomycin C, an anti-mitotic agent. For the latter, HEK293 were previously plated in T25cm<sup>2</sup> flasks for a minimum period of 48h, and 10µg/ml of mitomycin C in DMSO was added for 3h, and cells were kept at 37°C. Mitomycin C was then washed 3x with PBS, and the cells were returned to an incubated chamber in HEK medium, for 24h minimum before being used for co-culture with hiPSC-CMs. This granted enough time to prevent the anti-mitotic agent being extruded from the cells when in co-culture, and, therefore, possibly affecting hiPSC-CMs.

hiPSC-CMs were thawed as standard (see General Methods), split into different conical tubes, centrifuged at 1050rpm for 2min, and re-suspended in the different media. Cell

counts were performed, and cell density adjusted accordingly. HEK293 which had undergone growth arrest (GA) were washed 2x with PBS, and 0.05% Trypsin-EDTA at RT was added for 4min, and the culture kept at 37°C in the meantime. Trypsin-EDTA was blocked by adding 3x volume of HEK medium. The cells were transferred to sterile conical centrifuge tubes, and centrifuged at 1050rpm for 2 min. The cells were then resuspended in Cor.4U medium, and a cell count was performed using Trypan Blue and a haemocytometer. HEK293 to test different maintenance media were plated from frozen conditions. These cells were thawed at 37°C until pellet detached from the cryovial. They were then transferred to conical centrifuge tubes containing 2ml of PBS at RT and centrifuged at 1050rpm for 2min. The cells were resuspended in different media: Cor.4U, HEK medium with 5% FBS, or BMCC.

Once in co-culture, these cells were kept in standard Cor.4U medium. Contractility was recorded daily from day 4 to day 8, post-plating. The effects of each method of cell growth-containment was assessed based on contractility parameters, such as interval between contractions (Int), time for contraction ( $Up_{90}$ ), time for relaxation ( $Dn_{90}$ ), and amplitude of contraction (Amp). The same cell or area, if possible, were recorded each day, which made quiescence noticeable. Statistical analysis was done using a one-way ANOVA using a Bartlett's test, comparing baseline (day 4) and the following days. On day 8, the cultures were loaded with 1:1000 FluoVolt, 1:100 PowerLoad for 25min in BMCC. Voltage was recorded, and subsequently analysed on CelloPTIQ (Clyde Biosciences, UK).

#### **4.2.5 Blocking of $I_{K1}$ in co-culture with HEK- $I_{K1}$**

Co-culture of hiPSC-CMs with HEK (normal and  $I_{K1}$ ) was prepared with Cor.4U cells. On day 4 the culture was loaded with a voltage-sensitive dye, 1:1000 FluoVolt and 1:100 PowerLoad for 25min. The dye was prepared in BMCC. The medium was replaced with fresh BMCC at 37°C, and cells incubated for 30min before recording. Baseline recordings for voltage and contractility were taken at 37°C, 5% CO<sub>2</sub>, 75% humidity using CelloPTIQ and HCImageLive, for 10s. PA-6, an  $I_{K1}$  inhibitor, was added to the cells at 200nM and left for 30min. Recordings for voltage and contractility were repeated. Contractility analysis was performed in ImageJ, and voltage analysis was done on CelloPTIQ.

## 4.2.6 Co-culture of hiPSC-CMs with human cardiac fibroblasts

Human cardiac fibroblasts (HCF) were introduced to hiPSC-CMs culture using the same plating protocol. HCF were initially thawed in PBS (with  $\text{Ca}^{2+}$  and  $\text{Mg}^{2+}$ ) and re-suspended in DMEM with 10% foetal bovine serum, 1% penicillin-streptomycin, 1% non-essential amino acids, and 1% L-glutamine. The cells were then transferred to T75cm<sup>2</sup> flasks and maintained in culture until 70% confluency. At this stage, cells were lifted using 0.05% trypsin-EDTA for 4min, which was then blocked with medium. The cells were re-suspended in medium or Cor.4U, depending on intended purpose. Cor.4U hiPSC-CMs were thawed and adjusted for desired densities: 25,000, 24,750, 24,375 and 23,750 cells/well. HCF, upon being re-suspended in Cor.4U, were adjusted for the desired density so that they composed 50, 5, 2.5 or 1% of the co-culture (1:1, 1:20, 1:40, 1:100 HCF:hiPSC, respectively). The 2 cell lines were gently mixed and plated in previously 1:100 fibronectin coated 96-well glass-bottom plates. The co-cultures were maintained for 5 days in Cor.4U and medium was changed daily. On day 5 the cells were loaded for 25min with 1:1000 FluoVolt and 1:100 PowerLoad prepared in 37°C serum-free medium BMCC. Voltage and contractility were recorded using CelloPTIQ and HCImage Live, and analysed on CelloPTIQ and ImageJ, respectively.

## 4.3 Results

### 4.3.1 HEK293 proliferation assay

HEK293 proliferation in  $I_{\text{K1}}$ -expressing cells was compared to the proliferation of two standard HEK293 cell lines from two different providers: Prof. Van der Heyden and Prof. George Baillie (see Ch.2). Cell counts showed that over the period of 72h there were no significant changes in cell numbers from the initial plating density (Figure 4.2).

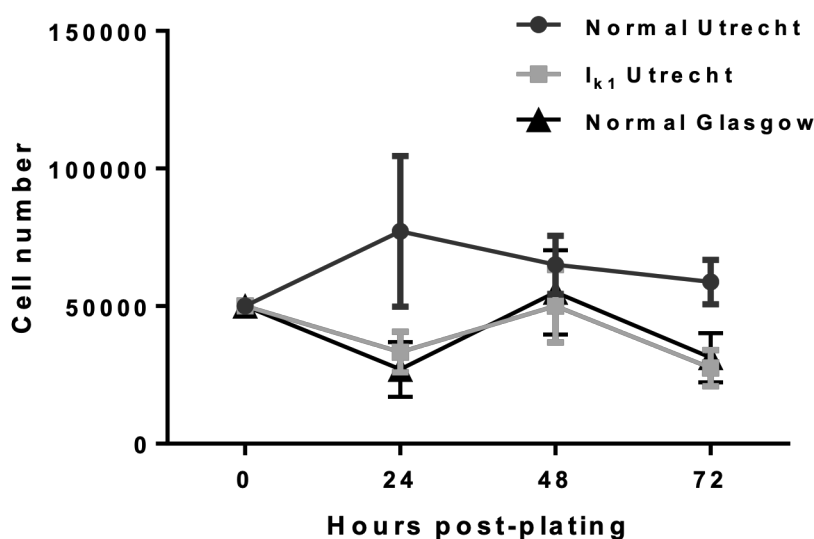


Figure 4.2 – HEK293 cells do not proliferate over 72h. Cells were plated at 50,000 cells/well and manual cell counts were performed on subsequent days to 72h. Three HEK293 cell lines were measured: standard HEK293 obtained from Utrecht University (Normal Utrecht); HEK293 stably expressing  $I_{k1}$  from Utrecht University ( $I_{k1}$  Utrecht); standard HEK293 from Glasgow University (Normal Glasgow). One-way ANOVA,  $n=7$ , all comparisons were not significant.

Cell proliferation was also observed using an MTT assay every 24h for 72h. Cell numbers did not change throughout the timeline, as shown by proliferation (absorbance units).

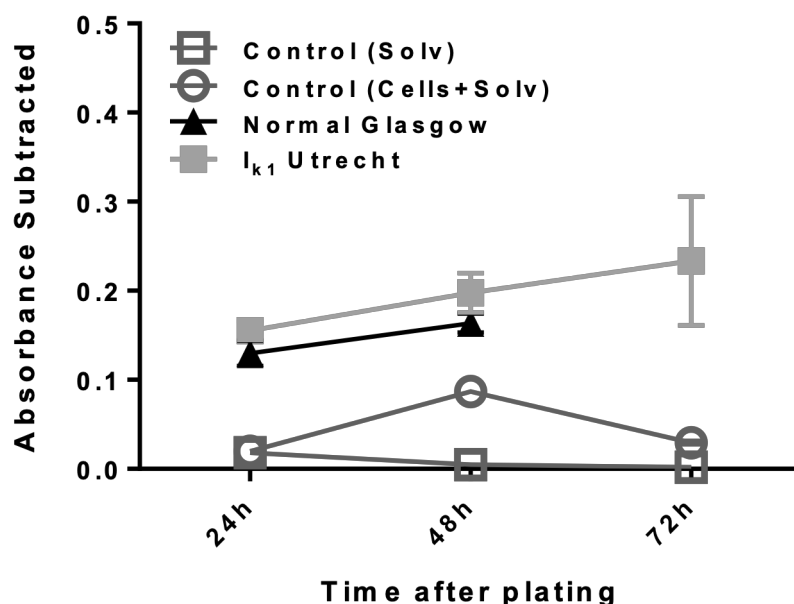
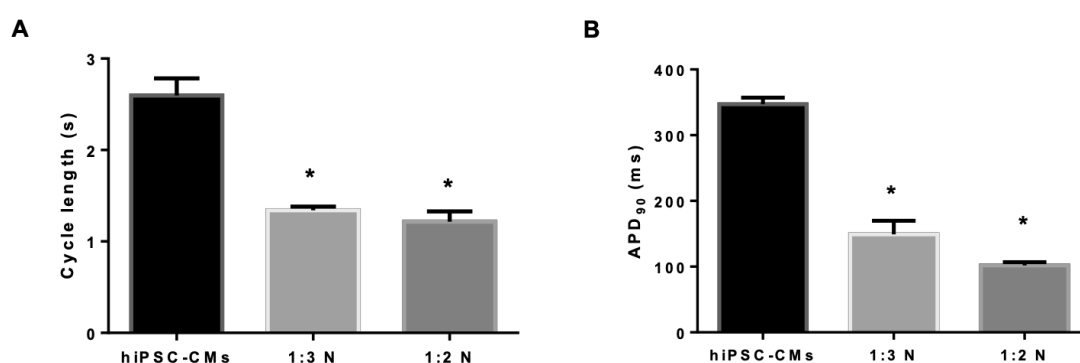


Figure 4.3 - Cell proliferation assay using an MTT assay. Absorbance was measured from cultured monolayers every 24h on normal HEK from Glasgow University and  $I_{k1}$ -expressing HEK from Utrecht University, and from control wells which did not contain MTT, but only the solvent and cells. One-way ANOVA,  $n=4$ , no comparisons were statistically different.

Data shows that cells plated at a density which forms a monolayer remain at the same density after 72h in culture. It is possible that, as cells reach 100% confluency, some cells might detach, but attached cells keep proliferating, at least for a short period of time.

### 4.3.2 Pluricyte co-culture with HEK293

The addition of HEK293 to Pluricyte hiPSC-CMs was done gradually. These cells were prone to contamination and quiescence upon introduction of HEK. Introduction of  $I_{K1}$ -HEK led to immediate quiescence (cells not showing spontaneous activity), thus all data shown was obtained from co-culture with standard HEK293.



**Figure 4.4 – Pluricyte hiPSC-CMs were cultured with Normal HEK (N) to a final density of 30,000 cells/well in a 96 well glass-bottom plate. Voltage measurements were done from the monolayer upon loading all co-cultures with voltage-sensitive dye, di-4-ANEPPS. Co-cultures with  $I_{K1}$ -HEK were quiescent. A) Cycle length recorded from hiPSC-CMs and co-cultured HEK:hiPSC; B) APD<sub>90</sub> in co-culture. Unpaired t-test comparing co-cultures with hiPSC-CM culture, n=14 hiPSC, n=5 HEK:hiPSC. \*p<0.05**

Figure 4.4 shows the effects of the presence of untransfected HEK cells (N) in co-culture at 1:3 and 1:2 HEK:hiPSC. The presence of HEK at 1:3 and 1:2 HEK:hiPSC led to shorter CL and APD<sub>90</sub>. Further decreasing the amount of HEK in culture did not reverse the effect seen in higher densities, as quiescence still occurred (Figure 4.5).

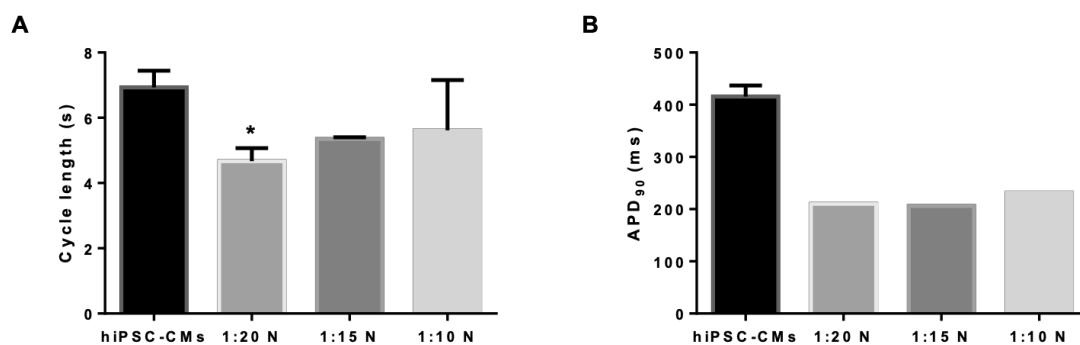


**Figure 4.5 - Pluricytes were cultured with HEK to a final density of 40,000 cells/well in a 96 well glass-bottom plate. Voltage measurements were done upon loading culture with voltage-sensitive dye, di-4-ANEPPS. A) cycle length recorded from hiPSC-CMs and co-culture HEK:hiPSC; B) APD<sub>90</sub> in co-culture (n=1 for co-culture due to poor SNR). Unpaired t-test, n=10 hiPSC, n=5 HEK:hiPSC. \*p<0.05.**

When the final density of hiPSC-CMs plus HEK was increased to 40,000 cells/well (Figure 4.5), signal-to-noise ratio (see Ch. 6) worsened, thus making analysis challenging. This resulted in a single AP being analysable for APD<sub>90</sub>.

Due to the sensitivity of Pluricytes to the addition of HEK to the culture, future experiments were done using a different cell line: Cor.4U.

### 4.3.3 Cor.4U co-culture with HEK293

Introduction of HEK into a Cor.4U culture was done slowly. Smaller percentages of HEK in culture were initially introduced: 1:300 and 1:100 HEK:hiPSC. There was no effect on contractile behaviour (Figure 4.6).

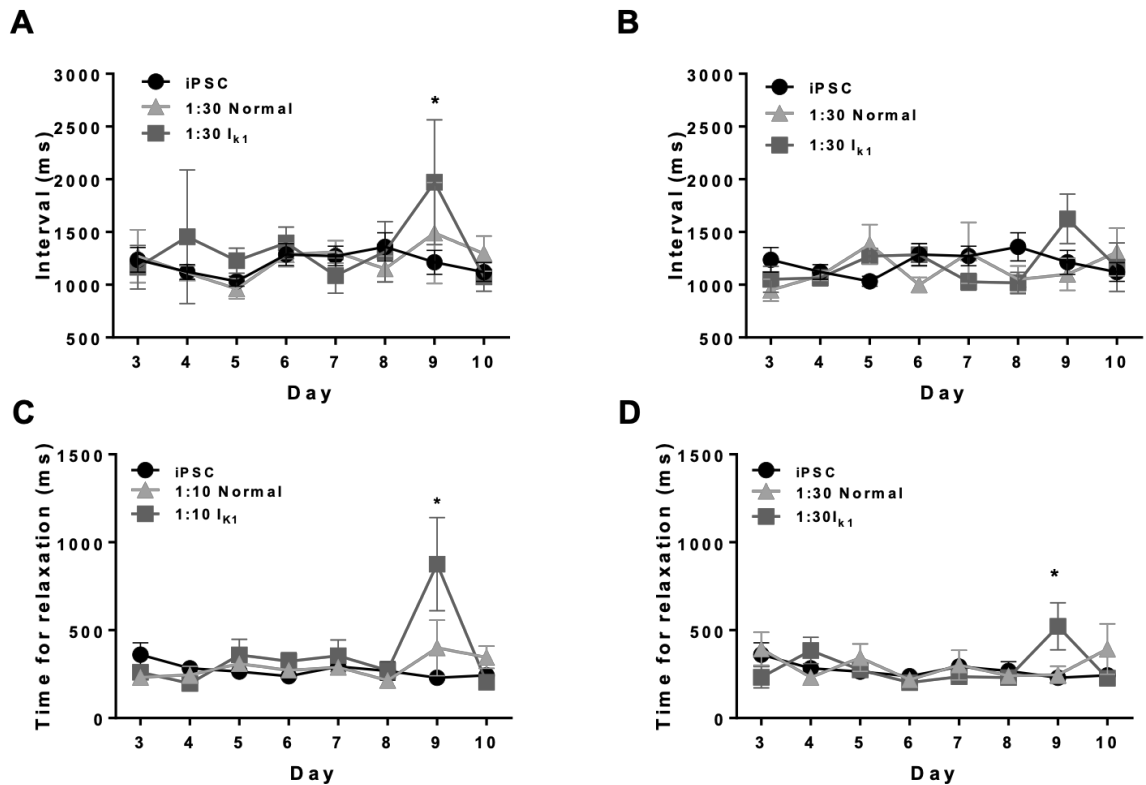


**Figure 4.6 - Different co-culture densities Cor.4U. Contractility was recorded daily for 7 days, starting on day 3 post-plating. Co-culture was done using both I<sub>k1</sub> or normal HEK and hiPSC-CMs. 2-way ANOVA, \*p<0.05.**

When the density of either I<sub>k1</sub>- and N-HEK increased to 30% (1:30) (Figure 4.7A) and 10% (1:10) (Figure 4.7B), there was no change in interval throughout the 5 days of observation of contractile behaviour. Density was further increased to 1:3, and on day 5 post-plating, there was a prolongation of interval in the presence of I<sub>k1</sub> HEK cells (Figure 4.7C). This went from 827.84±65.83ms on day 4 to 932.89±58.70ms on day 5 and a further prolongation to 994.64±69.73ms on day 6, 1102.86±67.53ms on day 7 and 1068.92±83.16ms on day 8. hiPSC-CM control for 1:3 interval remained constant at 907.77±46.54ms on day 3 to 859.48±41.37ms on day 10 (Figure 4.7C). The strongest effect of the presence of I<sub>k1</sub>-expressing HEK293 cells was seen at 1:1 ratio, where interval was severely prolonged and visible from day 3 until day 8 (Figure 4.6D). On day 3, interval was 1401.96±143.65ms, compared to hiPSC-CMs at 907.77±46.54ms. This increased further on day 4 to 1646.73±96.54ms.

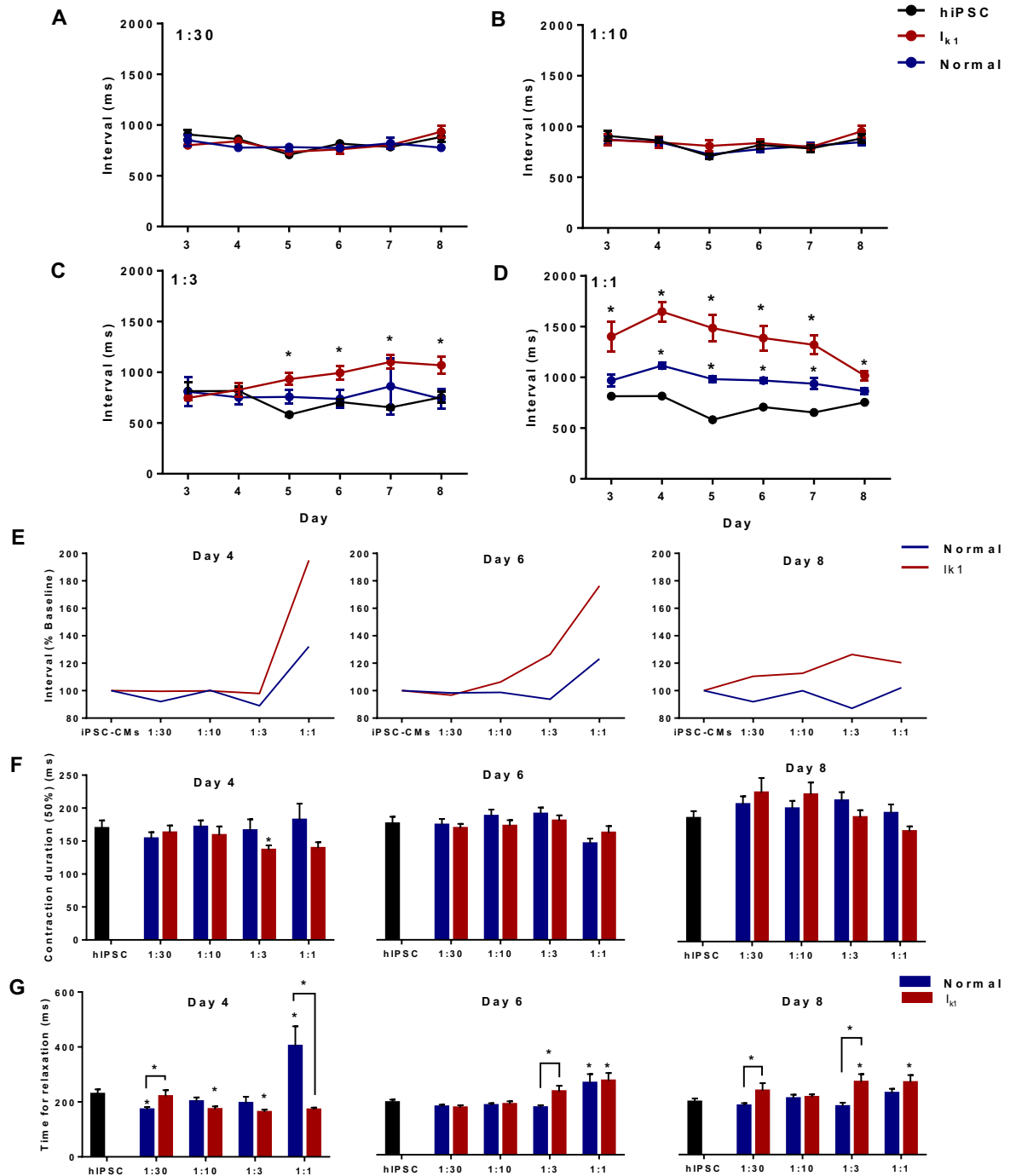


**Figure 4.7 - The effects of co-culture of iPSC-CMs with an increasing density of HEK293, for both  $I_{k1}$ -expressing ( $I_{k1}$ ) and untransfected (Normal) cells timeline. A,B,C,D) interval changes on HEK:hiPSC ratios of 1:30 1:10, 1:3 and 1:1 over 5 days; E) interval as percentage from baseline (standard hiPSC-CM culture) for the range of ratios. Left panel – day 4, middle panel – day 6, right panel – day 8; F) 50% of contraction duration on days 4, 6 and 8; G) time for relaxation on days 4, 6 and 8 comparing hiPSC-CMs culture, normal and  $I_{k1}$ . One-way ANOVA with Bartlett's test, \* $p < 0.05$ ,  $n = 51$ .**

Co-culture of HEK293 and hiPSC-CMs is a novel technique to attempt introducing the normally unavailable  $I_{K1}$  in hiPSC-CMs to a co-culture. Smaller ratios of  $I_{K1}$ -expressing HEK:hiPSC-CM in co-culture, such as 1:10 and 1:30 do not affect the interval between each contraction (Figure 4.7A and B). An effect was seen once the ratio was raised to 1:3 as the interval was prolonged significantly in the presence of  $I_{K1}$ -expressing HEK after day 4, and still visible effect on day 8 (Figure 4.7C). Further increasing it to 50% led to an increase in interval in the presence of both normal and  $I_{K1}$ -expressing HEK293 on all observed days (Figure 4.7D). The biggest effect on interval was seen on day 4 post-plating at a 1:1 density, followed by 1:3. Time for relaxation on day 4 was affected by the presence of  $I_{K1}$  HEK. 1:30N, or normal (N) HEK, was shorter at  $172.1 \pm 9.3$ ms whereas hiPSC-CMs was  $228.9 \pm 17.0$ ms. At 1:10, time for relaxation was shorter in the presence of  $I_{K1}$  compared to hiPSC-CMs ( $173.1 \pm 10.6$  vs  $228.9 \pm 17.0$ ms, respectively). 1:1 culture interval was severely prolonged in day 4 in normal co-culture compared to hiPSC-CMs and  $I_{K1}$  with a TR of  $403.8 \pm 71.5$ ms (hiPSC-CMs:  $228.9 \pm 17$ ms,  $I_{K1}$ :  $171.5 \pm 7.6$ ms). The effect was reduced on day 6, but still prolonged ( $262.0 \pm 32.0$ , hiPSC:  $190.8 \pm 9.8$ ms).  $I_{K1}$  co-culture at 1:1 also prolonged TR ( $269.8 \pm 28.2$ ms). On day 8, there was no difference in TR between hiPSC-CM controls and co-culture with control HEK cells at any of the ratios, but co-culture with  $I_{K1}$ -expressing HEK cells caused prolongation at some ratios. This effect was most visible at a ratio of 1:1 where TR was  $264.0 \pm 26.2$ ms, compared to  $192.6 \pm 11.9$ ms in hiPSC-CMs. Further studies on the effects of the co-culture were conducted on day 4 in either 1:1 or 1:3 densities.

#### 4.3.3.1 Different media affect contractile behaviour and cell numbers

The effects of different media in co-culture were studied. To prevent HEK proliferation, co-cultures were maintained in either serum-free medium or HEK underwent a growth arrest protocol before plating in a co-culture. The effects of different media were then studied to investigate changes in electrophysiological and contractile changes.

Despite it previously being established that HEK293 do not increase in numbers once they have been cultured when plated in a confluent monolayer, it is important to know the growth of these cells once in co-culture. Co-culture's contractility behaviour at a 1:1 ratio HEK:hiPSC with  $I_{K1}$ -expressing or N-HEK was monitored over 8 days (

Table 4.1). All cell cultures first exhibited spontaneous contractile activity on day 3, thus day 4 was the first day of recordings, in which co-culture showed that maintaining cells in serum-free medium (BMCC) was leading to quiescence (42% in presence of normal HEK, 31% in presence of  $I_{K1}$  HEK). Quiescent wells were recorded as normal, and quiescence incidence was calculated from total well number. Normal cells were not fully active, with only 50% showing spontaneous activity in maintenance medium. On day 5, 1:1N cells which underwent growth arrest with mitomycin C showed a prolongation in interval from  $1086 \pm 85$ ms on day 4 to  $1649 \pm 132$ ms. Serum-free medium led to a decrease in 50% of contraction duration from  $157 \pm 8$ ms to  $105 \pm 11$ ms in 1:1N. Time for contraction decreased greatly in maintenance medium in 1:1 $I_{K1}$  on the same day, with a decline from  $70 \pm 5$ ms to  $49 \pm 6$ ms. On day 6, 1:1N in maintenance medium and serum-free medium became quiescent, as well as 1:1 $I_{K1}$  on serum-free medium. There were no further changes observed. On day 7 1:1N which had undergone growth arrest became fully quiescent, and 1:1 $I_{K1}$  from the growth arrest group saw a decrease in contraction duration at 50% from  $191 \pm 13$ ms to  $166 \pm 10$ ms.

**Table 4.1 – Maintenance of co-cultures of HEK:hiPSC-CMs in different media. Contractile behaviour was recorded daily from day 4 post-plating to day 8. TC = time for contraction; TR = time for relaxation; CD=contraction duration. Q = quiescent. Arrows show prolongation (↑) or reduction (↓) of the different time variables measured. One-way ANOVA with Bartlett's test comparing to day 4 (baseline) \*p<0.05, \*\*p<0.01, \*\*\*p<0.005, n=8.**

Day	Culture type	HEK293 line	Medium	Interval (ms±SEM)	TC (ms)	TR (ms±SEM)	CD50% (ms±SEM)	Percentage of quiescence (%)
4	hiPSC-CMs		Maintenance medium	881±54	68±8	245±26	194±12	0
			Growth arrest	1086±85	67±13	307±24	255±12	0
	1:1	Normal	Maintenance medium	1050	55	339	142	50
			Serum-free medium	580±33	52±5	195±23	157±8	42
			Growth arrest	1183±96	65±7	321±37	242±20	0
		I <sub>k1</sub>	Maintenance medium	1814±364	70±5	524±110	223±21	0
Serum-free medium	1672±234		67±8	405±43	209±14	31		
5	hiPSC-CMs		Maintenance medium	1271±220	46±3	111±7	174±20	0
			Growth arrest	1649±132 ↑**	51±3	489±55	266±17	63
	1:1	Normal	Maintenance medium	812±1	67±4	384±89	169±1	71
			Serum-free medium	495±47	45±6	161±33	105±11 ↓**	0
			Growth arrest	1034±99	49±6	417±51	204±19	13
		I <sub>k1</sub>	Maintenance medium	1416±159	49±6 ↓*	417±51	204±19	0
Serum-free medium	1723±428		56±3	365±87	220±44	25		
6	hiPSC-CMs		Maintenance medium	834±114	51±12	289±91	192±59	0
			Growth arrest	1200	58	935	401	88
	1:1	Normal	Maintenance medium	Q	Q	Q	Q	100
			Serum-free medium	Q	Q	Q	Q	100
			Growth arrest	1331±153	50±3	425±72	191±13	0
		I <sub>k1</sub>	Maintenance medium	1143±97	53±6	317±38	213±20	0
Serum-free medium	Q		Q	Q	Q	100		
7	hiPSC-CMs	N/A	Maintenance medium	754±17	56±11	194±40	150±27	0
			Growth arrest	Q	Q	Q	Q	100
	1:1	Normal	Maintenance medium	Q	Q	Q	Q	100
			Serum-free medium	Q	Q	Q	Q	100
			Growth arrest	1274±139	55±6	401±68	166±10 ↓*	6
		I <sub>k1</sub>	Maintenance medium	1986±588	56±4	685±237	208±14	0
Serum-free medium	Q		Q	Q	Q	100		
8	hiPSC-CMs		Maintenance medium	1315±481	40±1	459±234	260±5	0
			Growth arrest	1901±141 ↑**	56±5	1164±161 ↑***	308±126	88
	1:1	Normal	Maintenance medium	835±1	69±1	547±13	138±1	13
			Serum-free medium	Q	Q	Q	Q	100
			Growth arrest	2010±214 ↑**	55±7	754±146 ↑***	231±32	88
		I <sub>k1</sub>	Maintenance medium	1423±8	49±6	374±7	260±5	0
Serum-free medium	Q		Q	Q	Q	100		

Data shows that, although only HEK293 underwent growth arrest, this treatment affected the cell culture greatly leading to full quiescence, and unresponsiveness to electrical field stimulation (data not shown). Cultures maintained in serum-free medium never recovered, and as such, maintaining cells without serum merely to contain HEK293 growth appears to be unfeasible.

Voltage recordings of spontaneous beating and 1Hz pacing on day 8 showed that 1:1 cultures were quiescent in BMCC and unresponsive to electrical pacing (Figure 4.7A). Interval at spontaneous rates was shortened from  $1312.34 \pm 286.37$ ms on hiPSC-CMs alone to  $818.98 \pm 40.67$ ms and  $1005.10 \pm 98.40$ ms at 1:3 densities in the presence of normal HEK293 and  $I_{K1}$ -expressing HEK293, respectively, when maintained in Cor.4U medium. Maintenance in BMCC had the opposite effect for the same densities, where interval was prolonged to  $2353.03 \pm 97.52$ ms in 1:3N and  $2548.58 \pm 75.76$ ms in 1:3 $I_{K1}$  (Figure 4.8A). When paced at 1Hz, interval decreased greatly in 1:3N kept in Cor.4U ( $481.22 \pm 1.11$ ms) from baseline (hiPSC-CMs,  $894.16 \pm 55.41$ ms). This was significantly smaller than the effect seen when the cells were maintained in BMCC ( $953.88 \pm 38.16$ ms). When cultured at 1:3, with  $I_{K1}$  HEK293, interval was significantly longer in BMCC than in Cor.4U ( $1023.62 \pm 21.65$  vs  $788.85 \pm 91.69$ ms) (Figure 4.8B). APD<sub>50</sub> at spontaneous rates reduced in 1:1 $I_{K1}$  to  $138.53 \pm 5.89$ ms from  $230.13 \pm 19.68$ ms in hiPSC-CMs. 1:3N in Cor.4U also led to a shortening to  $163.55 \pm 17.29$ ms, which was significantly shorter than the effect seen in BMCC ( $301.08 \pm 50.06$ ms). 1:3 $I_{K1}$  in Cor.4U was significantly shorter than BMCC ( $172.53 \pm 15.19$  vs  $335.18 \pm 58.51$ ms) (Figure 4.8C).

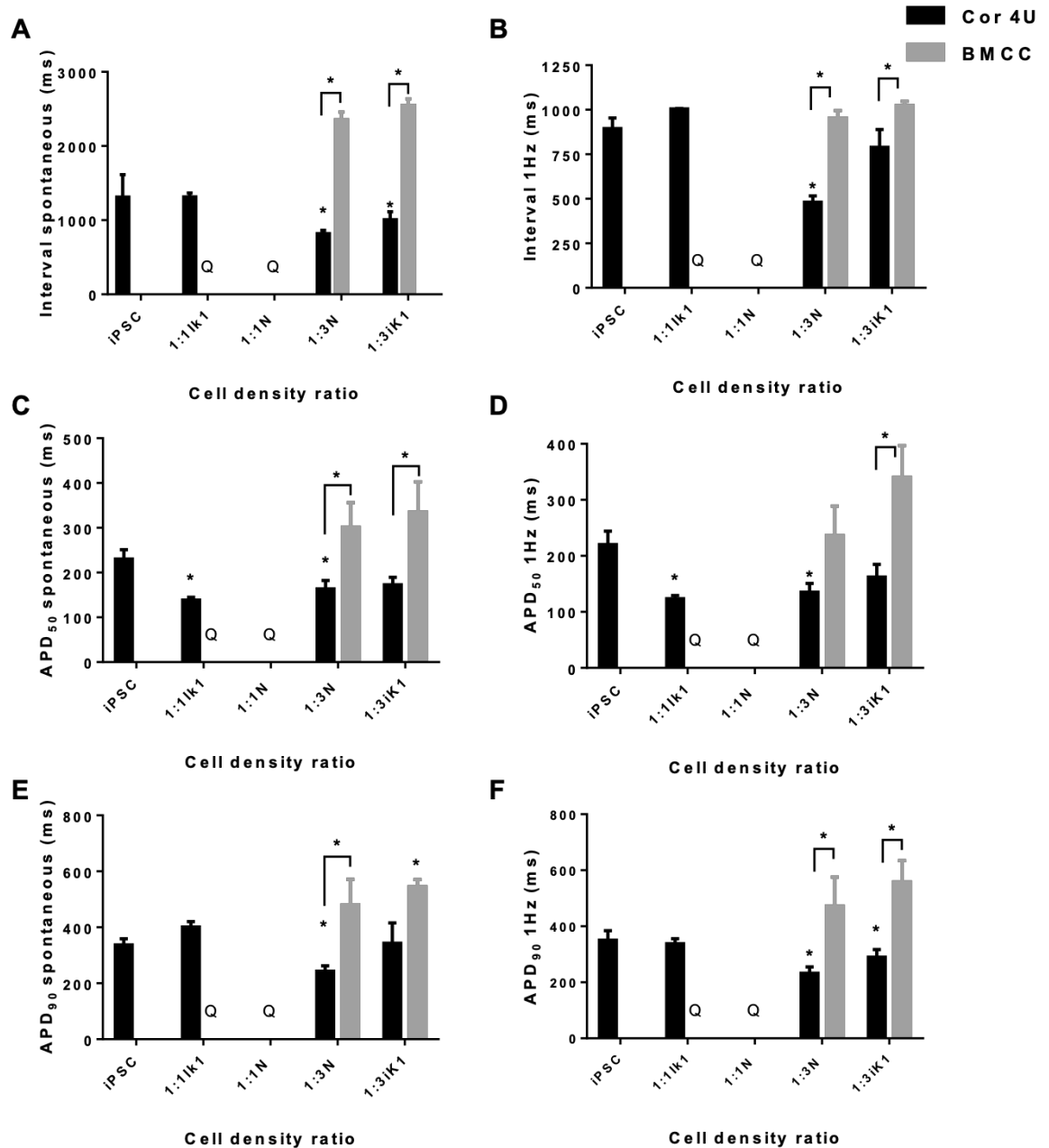


**Figure 4.8 – Electrophysiology of HEK:hiPSC-CM co-cultures on day 8 after maintenance in different serum-containing or serum-free media. A) Interval at spontaneous rates in maintenance medium (Cor.4U) and serum-free medium (BMCC) in co-cultures with  $I_{K1}$  and N-HEK at different ratios HEK:hiPSC; B) Interval at 1Hz in the different media; C) Action potential duration at 50% of repolarisation for different ratios and media at spontaneous rates; D) APD<sub>50</sub> when paced at 1Hz; E) Action potential duration at 90% of repolarisation in different media and at different HEK:hiPSC ratios at spontaneous rates; F) 90% of repolarisation at 1Hz at 1:1 and 1:3 ratios in BMCC and Cor.4U. Q = quiescent. Unpaired t-test, \* $p < 0.05$ ,  $n = 6$ .**

When the cultures were paced at 1Hz, APD<sub>50</sub> was shortened in 1:1 $I_{K1}$  in Cor.4U from  $220.03 \pm 22.52$ ms in hiPSC-CMs, to  $123.43 \pm 5.15$ ms. The same occurred in 1:3N, which

shortened to  $135.18 \pm 14.02$ ms in Cor.4U.  $APD_{50}$  prolonged in BMCC in 1:3 $I_{k1}$  compared to when the culture was maintained in Cor.4U ( $340.27 \pm 51.63$ ms vs  $162.23 \pm 20.67$ ms) (Figure 4.8D).  $APD_{90}$  at spontaneous rates was shortened in 1:3N to  $242.90 \pm 17.44$ ms when maintained in Cor.4U compared to hiPSC-CMs,  $337.07 \pm 20.8$  ms, but prolonged in 1:3 $I_{k1}$  in BMCC,  $544.70 \pm 18.10$ ms. 1:3N in BMCC was significantly longer in  $APD_{90}$  at  $479.70 \pm 79.14$ ms (Figure 4.8E). When paced at 1Hz, cells at 1:3 maintained in Cor.4U shortened significantly compared to hiPSC-CMs, where Normal shortened to  $232.04 \pm 20.44$ ms, and  $I_{k1}$  to  $289.50 \pm 24.91$ ms, whereas hiPSC-CMs remained at  $350.50 \pm 30.51$ ms. When the same cultures were in BMCC,  $APD_{90}$  was prolonged in comparison to Cor.4U cultures. 1:3N prolonged to  $471.90 \pm 84.95$ ms, and 1:3 $I_{k1}$  prolonged to  $558.30 \pm 62.03$ ms (Figure 4.8F).

The use of serum-free medium and growth-arresting HEK prior to co-culture plating led to high incidence of quiescence.

#### 4.3.3.2 Co-culture at 1:1 ratio of HEK:hiPSC-CM: effects on day 4

To get further insight into the effects of co-culture at 1:1 HEK to hiPSC-CMs, contractility and voltage measurements were done on day 4 after plating, the day where the strongest effect of the presence of  $I_{k1}$ -expressing HEK cells was previously seen (Figure 4.7C). Example traces of the effects of the co-culture on contractility showed a big effect on the amplitude of the contraction (Figure 4.9A and B) in both the presence of  $I_{k1}$ -expressing and control HEK. Amplitude of the contraction was greatly affected in co-culture, where, at spontaneous rates, it was  $1439.1 \pm 130.6$ a.u. in the presence of  $I_{k1}$ -expressing HEK cells and  $1166.2 \pm 77.5$ a.u. in presence of control HEK293, opposed to  $783.7 \pm 61.7$ a.u. in hiPSC-CMs. The effect was still present at increasing pacing frequencies. At 1Hz, the amplitude of the contraction in  $I_{k1}$  culture was  $1269.8 \pm 130.4$ a.u., at 2Hz  $1334.1 \pm 115.7$ a.u. and at 3Hz  $1284.7 \pm 94.5$ a.u. In normal co-culture, at 1Hz the amplitude was  $1181.3 \pm 89.9$ a.u., at 2Hz  $1096.9 \pm 78.7$ a.u. and at 3Hz  $1004.1 \pm 81.6$ a.u.. The amplitude was significantly higher than that observed in hiPSC-CMs, where at 1Hz amplitude was  $760.8 \pm 63.4$ a.u., 2Hz  $738.2 \pm 57.1$ a.u., and at 3Hz  $658.8 \pm 56.3$ a.u.

Time for contraction was not affected in co-culture at spontaneous nor at increasing pacing frequencies (Figure 4.9D).

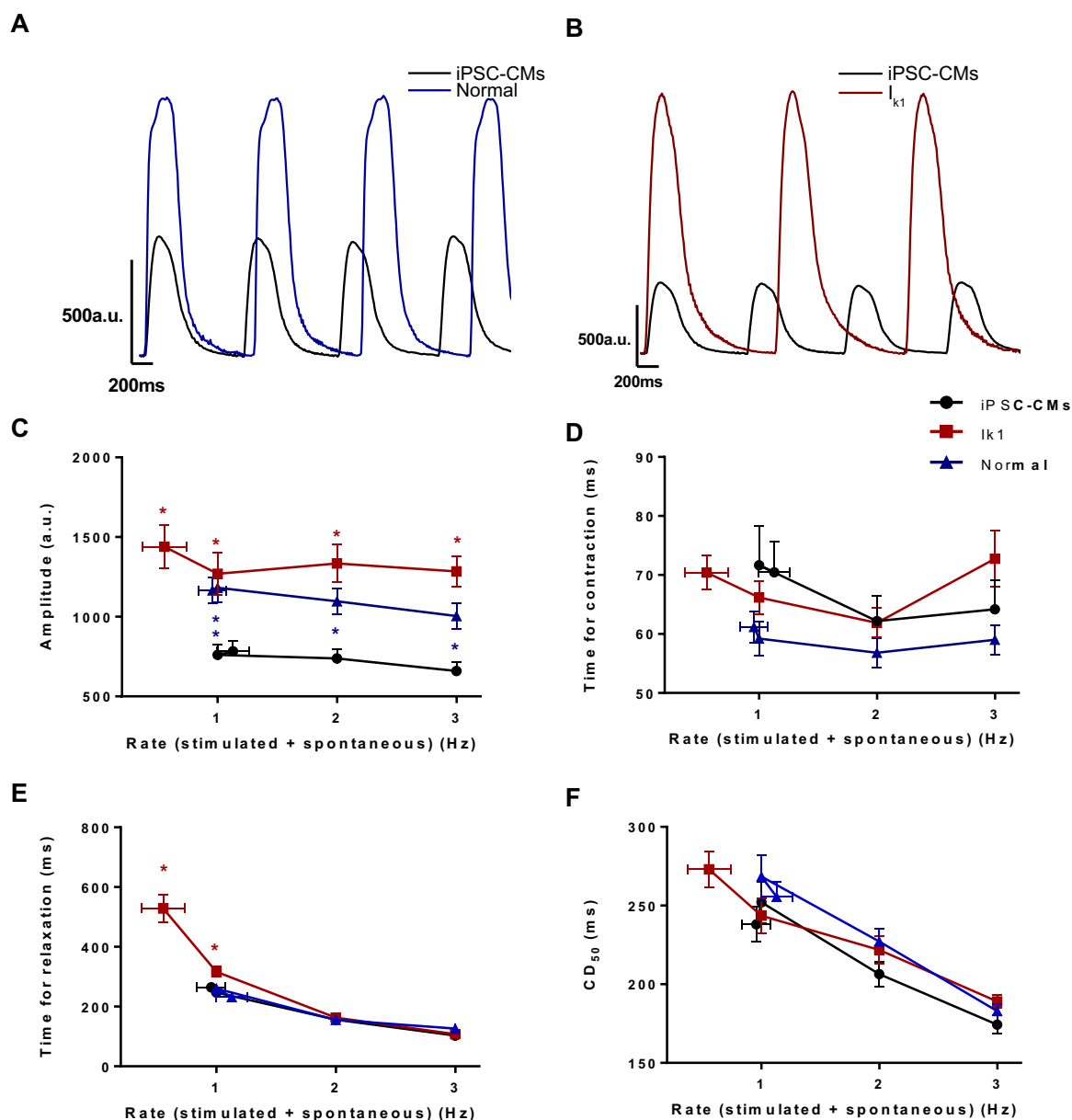
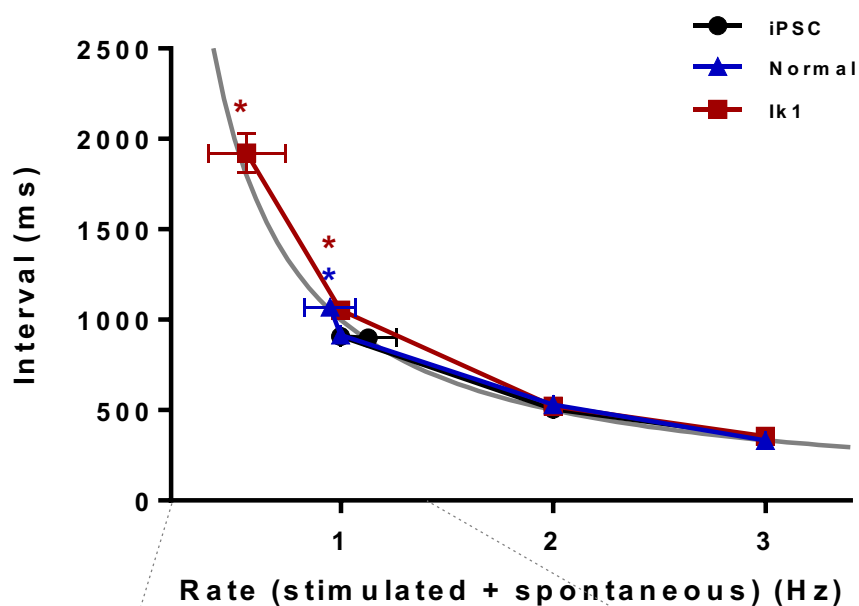


**Figure 4.9 - Contractile behaviour is affected by the presence of HEK293 at 1:1 ratio with hiPSC-CM.** A) Example trace of contractility changes in the presence of control HEK293; B) example trace of contractility in co-culture with  $I_{K1}$ -expressing HEK293; C) amplitude of the contraction is affected by the presence of HEK293 at spontaneous rates and electrically paced; D) time for contraction; E) time for relaxation; F) contraction duration. One-way ANOVA, \* $p < 0.05$ ,  $n = 16$ , horizontal error bars represent the mean  $\pm$  SEM for spontaneous rate.

Time for relaxation was significantly longer in the presence of  $I_{K1}$  HEK293 cells at spontaneous rates and 1 Hz. At spontaneous rates it was prolonged to  $528.3 \pm 44.1$  ms and at 1 Hz it was  $316.5 \pm 17.1$  ms, whereas hiPSC-CMs had a relaxation time of  $231.4 \pm 11.5$  ms and  $260.6 \pm 14.0$  ms, respectively (Figure 4.9E). 50% of contraction duration was not affected in co-culture at spontaneous and pacing rates (Figure 4.9F).

A



B

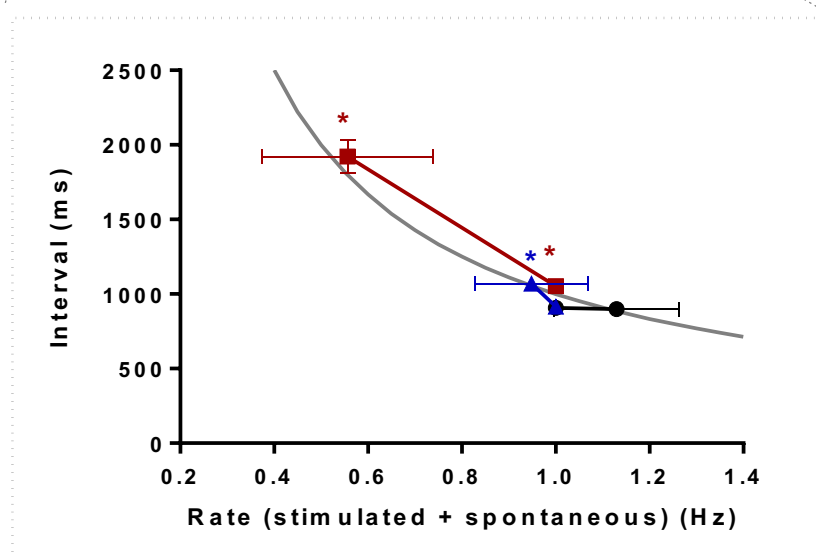


**Figure 4.10 - The effects of 1:1 co-culture on contraction interval.** Contractile behaviour was monitored at spontaneous rates and during electrical stimulation. **A)** interval at spontaneous rates and increasing frequencies of stimulation, on hiPSC-CMs and co-culture with normal HEK293 and  $I_{K1}$  HEK293; **B)** spontaneous rates (horizontal error bar) and 1Hz are greatly affected by the presence of HEK293 in culture. One-way ANOVA, \* $p < 0.05$ ,  $n = 16$ .

Spontaneous rates were considered, where hiPSC-CMs were contracting at  $1.13 \pm 0.13$  Hz, 1:1 $I_{K1}$  at  $0.56 \pm 0.18$  Hz and 1:1N at  $0.95 \pm 0.12$  Hz. The effects on interval of the contraction

appear to fit an exponential decay curve throughout the various stimulation frequencies (Figure 4.10). At 1Hz, co-culture in the presence of  $I_{K1}$ -expressing HEK showed that the culture was not following the stimulus, thus leading to a longer interval (Figure 4.10B). Interval on hiPSC-CMs at spontaneous rates was  $899.5 \pm 21.2$ ms, which was not different from that seen at 1Hz at  $906.5 \pm 27.6$ ms. Higher frequencies such as 2Hz and 3Hz led to the expected shortening in interval to  $506.2 \pm 4.7$ ms and  $348.3 \pm 15.7$ ms, respectively. 1:1 $I_{K1}$  culture's interval was much longer at spontaneous rates, staying at  $1922.2 \pm 105.7$ ms, and  $1052.4 \pm 29.8$ ms at 1Hz. Higher frequencies were unaffected by the presence of  $I_{K1}$  or HEK293 cells. At spontaneous rates there was a prolongation of interval in the presence of Normal HEK293 to  $1069.3 \pm 22.0$ ms but was not affected at higher frequencies (Figure 4.10).

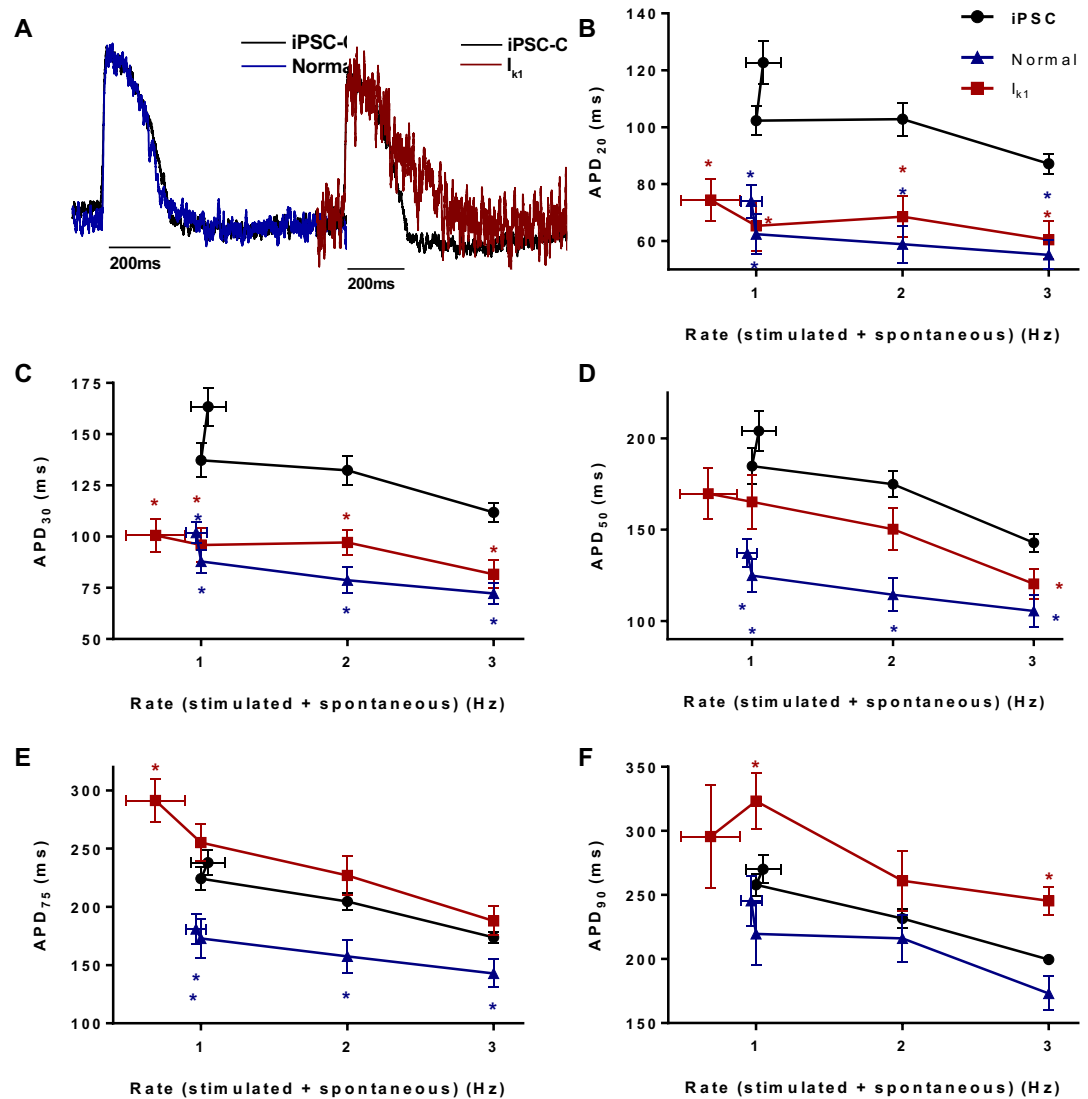


**Figure 4.11 - Electrophysiological behaviour is affected by the presence of HEK at 1:1 HEK:hiPSC. A) Example trace of AP changes in the presence of normal HEK293 and in co-culture with  $I_{K1}$ -expressing HEK293; B) effects on early repolarisation (20%) at spontaneous rate and electrical stimulation; C) effects on early repolarisation (at 30%); D) mid-repolarisation (50%); E) late repolarisation, 75% of APD; F) late repolarisation at 90% of full repolarisation. One-way ANOVA, \* $p < 0.05$ ,  $n = 16$ .**

Simultaneously to the contractility measurements, voltage measurements were taken in cells previously loaded with FluoVolt. Very early repolarisation phase, at 20%, was shortened compared to the effect seen in hiPSC-CMs. At spontaneous rates, APD<sub>20</sub> reduced in the presence of  $I_{K1}$  to  $74.4 \pm 7.1$  ms, and at 1 Hz to  $65.4 \pm 8.4$  ms, at 2 Hz to  $68.4 \pm 6.9$  ms, and at 3 Hz to  $60.5 \pm 6.5$  ms. This is in comparison to hiPSC-CMs, which were  $122.7 \pm 7.4$  ms at spontaneous rates,  $102.3 \pm 4.9$  ms at 1 Hz,  $102.3 \pm 5.6$  ms at 2 Hz, and

87.2±3.4ms. A similar effect was seen in the presence of normal (standard) HEK293. At spontaneous rates APD<sub>20</sub> was reduced to 73.9±5.5ms, at 1Hz to 62.2±6.7ms, at 2Hz 58.9±6.2ms, and at 3Hz 55.1±4.9ms (Figure 4.11B). APD<sub>30</sub> (Figure 4.11C) showed a similar effect, where, at spontaneous rates, early repolarisation shortened in the presence of I<sub>k1</sub> HEK293 to 100.5±7.7ms, at 1Hz to 95.8±8.2ms, at 2Hz to 97.2±6.0ms, and at 3Hz to 81.6±6.7ms. hiPSC-CMs cultured alone showed a longer APD<sub>30</sub>, where, at spontaneous rates, it was 163.3±9.1ms, at 1Hz 137.2±7.9ms, at 2Hz 132.4±6.8ms, and at 3Hz 111.7±4.3ms. The presence of normal HEK293 also shortened early repolarisation, at spontaneous rates it was 101.9±4.9ms, at 1Hz it shortened to 87.8±5.4ms, at 2Hz 78.7±6.0ms, and at 3Hz 72.3±5.0ms (Figure 4.11C). Mid-repolarisation (APD<sub>50</sub>) in the presence of I<sub>k1</sub> HEK was unaffected compared to hiPSC-CMs but was significantly shorter in the presence of normal HEK. Normal HEK presence shortened APD<sub>50</sub> at all rates, dropping to 137.0±7.4ms at spontaneous rates, 124.8±8.8ms at 1Hz, 114.4±8.7ms at 2Hz and 105.5±8.4ms at 3Hz, compared to hiPSC-CMs where spontaneous rates resulted in an APD<sub>50</sub> of 204.0±10.5ms, at 1Hz 184.8±9.3ms, at 2Hz 174.9±7.0ms and at 3Hz 142.9±4.8ms. In the presence of I<sub>k1</sub>-expressing cells, APD<sub>50</sub> was significantly shorter at 3Hz, where it was 120.3±7.9ms (Figure 4.11D).

APD<sub>75</sub>, start of late repolarisation, was not affected in the presence of I<sub>k1</sub> HEK when paced, but was significantly prolonged at spontaneous rates, where it reached 291.3±17.9ms, compared to the duration in hiPSC-CMs of 237.9±10.6ms. At this rate, normal co-culture had a much smaller APD<sub>75</sub> of 181.0±12.7ms. At pacing frequencies, there were no effects of the presence of I<sub>k1</sub> in the culture. In the presence of normal HEK APD<sub>75</sub> was severely shorter at 1, 2 and 3Hz, where it shortened to 172.9±16.0ms, 157.5±13.7ms, and 142.9±11.6ms, respectively, compared to hiPSC-CMs where it was 224.3±9.5ms, 204.6±7.1ms, and 173.8±4.3ms (Figure 4.11E). APD<sub>90</sub> did not change at spontaneous rates, nor in the presence of normal HEK, but was prolonged at 1Hz and 3Hz in the presence of I<sub>k1</sub> cells. Late repolarisation prolonged to 323.3±20.4ms and 245.4±10.4ms, compared to hiPSC-CMs, where 1Hz was 257.8±8.2ms and at 3Hz was 199.6±3.3ms (Figure 4.11F).

Interval (Figure 4.12) was greatly affected by at 1:I<sub>k1</sub>, where, at spontaneous rates it prolonged to 1515.87±76.64ms, compared to 963.48±23.68ms in hiPSC-CMs. At 1Hz, the co-culture did not follow the stimulation, which led to a prolongation of the interval to

992.77±12.95ms, compared to 868.50±40.86ms in hiPSC-CMs. Also, at spontaneous rates, 1:1N was longer at 1039.25±19.05ms. At 2 and 3Hz interval in hiPSC-CMs was 500.04±0.034ms and 333.71±0.73ms, which did not differ in co-culture.

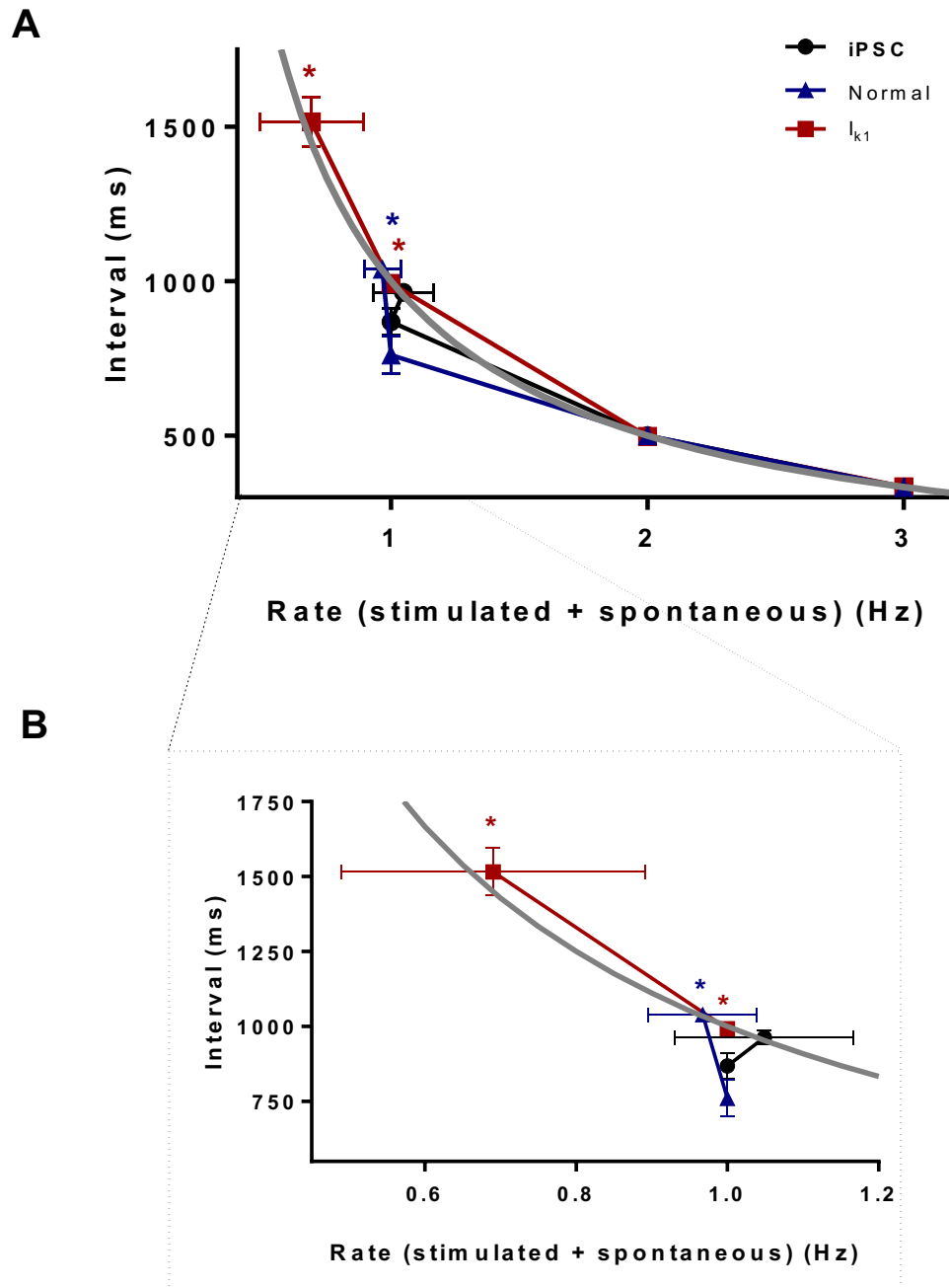


**Figure 4.12 - The effects of 1:1 HEK:hiPSC co-culture on electrophysiological interval. Electrophysiological behaviour was monitored at spontaneous rates and during electrical stimulation. A) Interval at spontaneous rates and increasing frequencies of stimulation, on hiPSC-CMs and co-culture with normal HEK293 and  $I_{k1}$  HEK293; B) spontaneous rates (horizontal error bar) and 1Hz are greatly affected by the presence of HEK293 in culture. One-way ANOVA, \* $p < 0.05$ ,  $n = 16$ .**

A closer look at the effects of the co-culture in spontaneous rates, as measured by voltage showed that the frequency of spontaneous beating in 1:1I<sub>kl</sub> is much slower than rates in hiPSC-CMs. I<sub>kl</sub>-expressing HEK slowed the co-culture to  $0.69 \pm 0.20$ Hz, whereas Normal HEK led to a smaller slowing to  $0.97 \pm 0.07$ Hz, compared to hiPSC-CMs frequency of  $1.05 \pm 0.12$ Hz (Figure 4.12).

#### **4.3.4 High densities of HEK293 affect amplitude of contraction**

A further look into the effects on contractile behaviour showed that the contraction in the presence of HEK cells is greatly affected, leading to an increase in the amplitude of each cell contraction (Figure 4.9C). This effect is visible at spontaneous rates and during electrical pacing. The causes for this effect are unknown and further investigation is needed.

### 4.3.5 $I_{K1}$ antagonist PA-6 has no effect on 1:1 co-culture

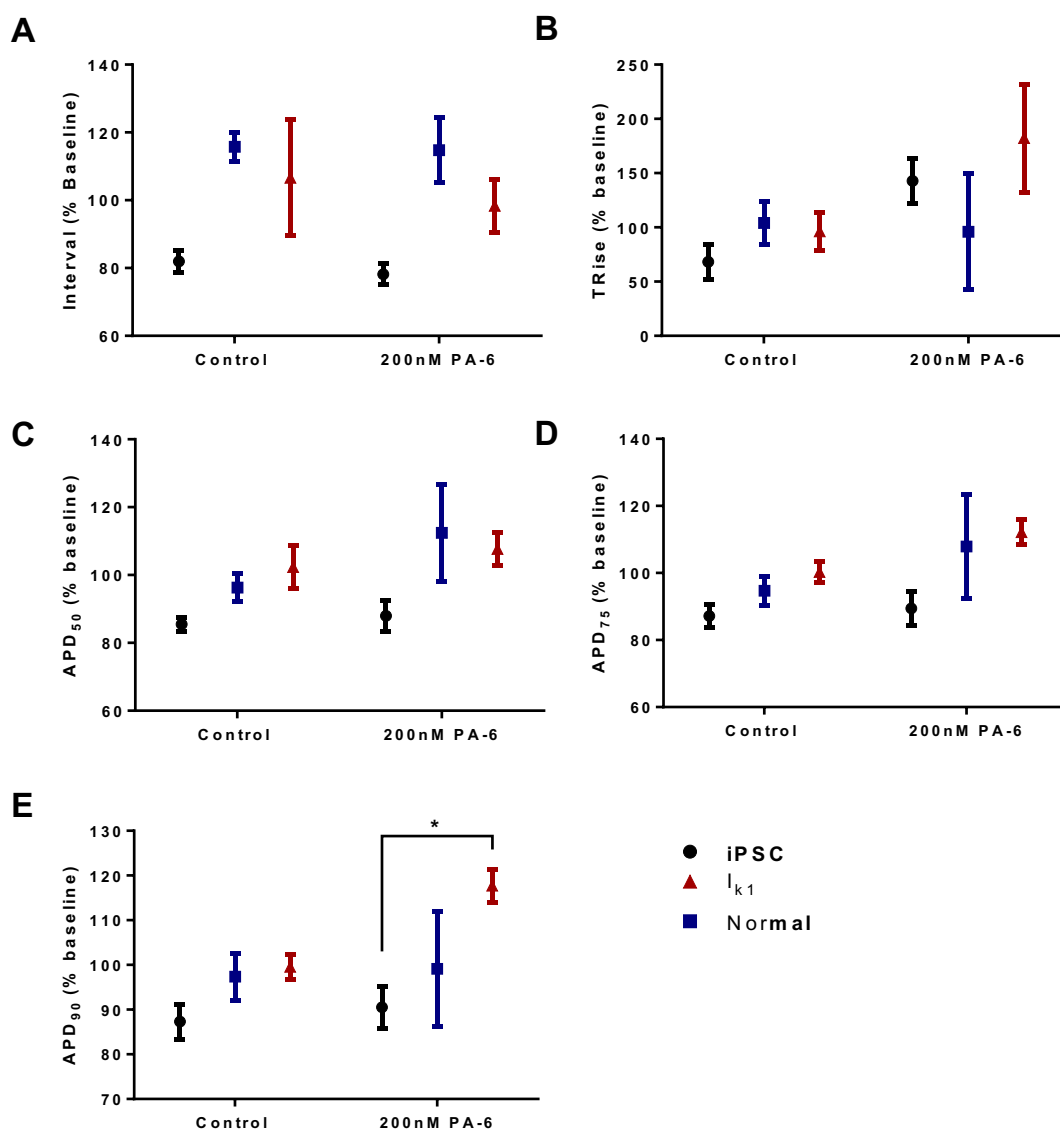


**Figure 4.13 – Effects on voltage of  $I_{K1}$  blockage in HEK:hiPSC-CM co-culture.** hiPSC-CMs and co-cultures in the presence of  $I_{K1}$ -expressing and standard (Normal) HEK293 were loaded with FluoVolt and voltage was measured on day 4. A) interval was recorded as percentage from baseline for control (0.002% DMSO) and in the presence of 200nM PA-6; B) effects on time to reach peak of the AP; C) 50% of the repolarisation phase; D) 75% of repolarisation; E) 90% of repolarisation. One-way ANOVA comparing the effects of PA-6 on hiPSC-CMs alone and both co-cultures, and also comparing the effects of PA-6 within each co-culture,  $n=5$ ,  $*p<0.05$ .

Inhibition of  $I_{K1}$  with the antagonist PA-6 did not greatly alter electrophysiology on 1:1 co-culture (Figure 4.12). APD<sub>90</sub> was prolonged in the presence of  $I_{K1}$  cells in the co-culture compared to the effect seen in hiPSC-CMs as it prolonged from  $90.5\pm 4.7\%$  from baseline to  $117.7\pm 3.6\%$  from baseline. Inhibition of  $I_{K1}$  in normal co-culture did not alter

electrophysiology. This shows that  $I_{K1}$  is either not present or present in small densities as inhibition of  $I_{K1}$  has been shown to prolong APD and the effective refractory period (Takanari et al., 2013, Skarsfeldt et al., 2016).

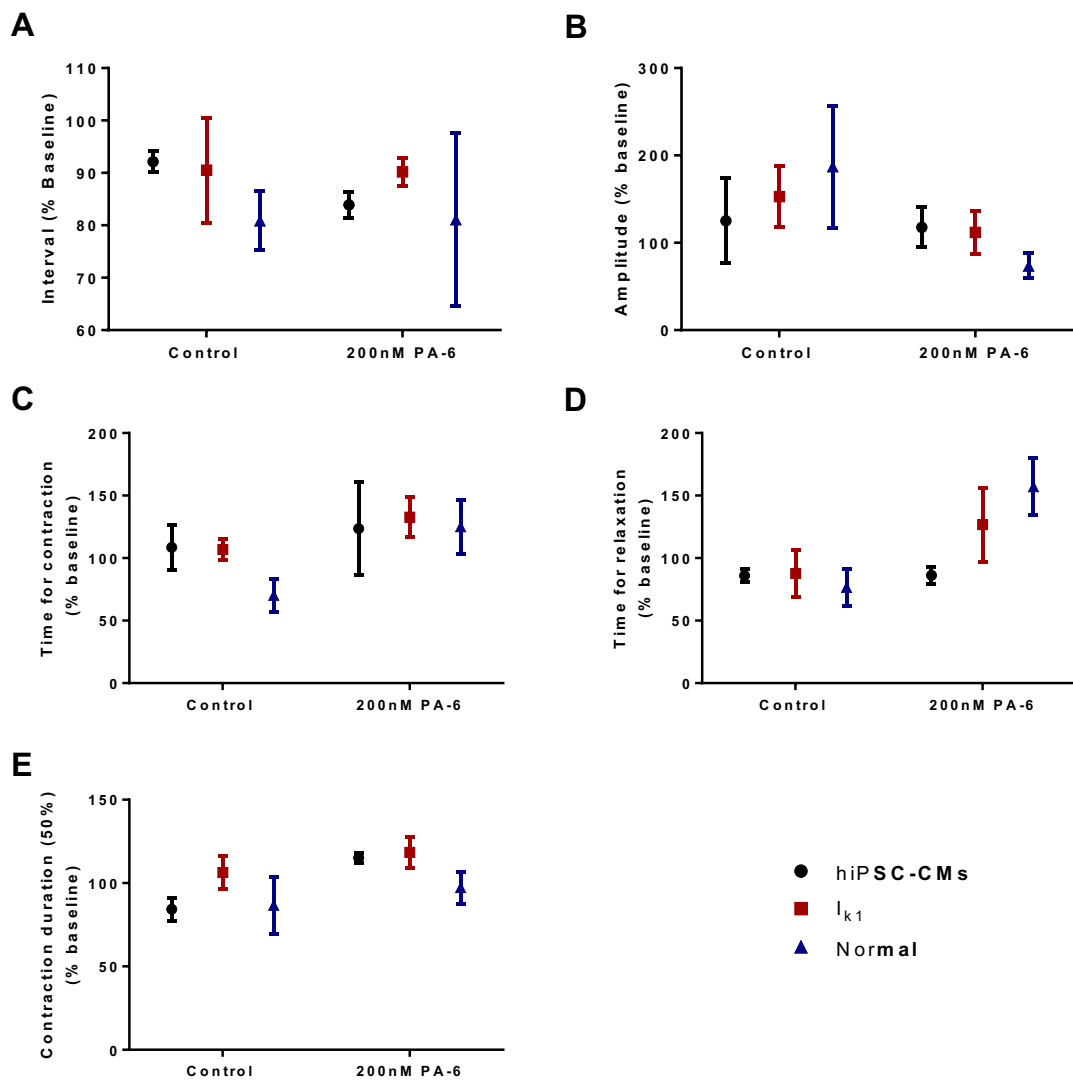


**Figure 4.14 – Effects on contraction of  $I_{K1}$  antagonist, PA-6. hiPSC-CMs and co-cultures in the presence of  $I_{K1}$ -expressing and standard (Normal) HEK293 were loaded with FluoVolt and voltage was measured on day 4. A) interval was recorded as percentage from baseline for control (0.002% DMSO) and in the presence of 200nM PA-6; B) effects on amplitude of the contraction; C) time for contraction to reach 90% of peak; D) time for 90% of relaxation; E) Contraction duration at 50%. One-way ANOVA,  $n=5$ ,  $*p<0.05$ .**

Contractility was not affected by the presence of 200nM PA-6 in co-culture.

These observations go in line with what was previously seen in isolated rat and guinea pig hearts, where the main effect of 200nM PA-6 was prolongation of the ventricular action

potential duration at 90% repolarisation (Hoeker et al., 2017, Skarsfeldt et al., 2016). In rat hearts this prolongation is in the order of 14% (Skarsfeldt et al., 2016) whereas in guinea pig it leads to 4x longer APD<sub>90</sub> (Hoeker et al., 2017). The effect seen in hiPSC-CMs relates with these observations, and it has previously been shown that this concentration inhibits  $I_{K1}$  by 77-100% while having no effect on  $I_{Na}$ ,  $I_{Ca}$ ,  $I_{to}$ ,  $I_{Kr}$  or  $I_{Ks}$  (Takanari et al., 2013). (Hoeker et al., 2017) developed a protocol to lower  $[K^+]_o$  to 2mmol/L which resulted in prolonged APD by approximately 25% in guinea pig ventricle. Further addition of 200nM PA-6 resulted in further prolongation.

#### **4.4 Investigating the effects of co-culture using human cardiac fibroblasts**

To further understand the effects of co-culture on the amplitude of the contraction, hiPSC-CMs were cultured with a different cell type, human cardiac fibroblasts (HCF). The latter show different elasticity from that seen in HEK (Kuznetsova et al., 2007), thus providing further insight into the effects previously seen on amplitude of the contraction in co-culture with HEK. Cardiac fibroblasts display multiple overlapping phenotypes depending on their spatial location (Herum et al., 2017). HCF mechanosensitivity is demonstrated by HCFs' rapid transformation to a profibrotic myofibroblast phenotype when they are grown in different matrices (Herum et al., 2017).

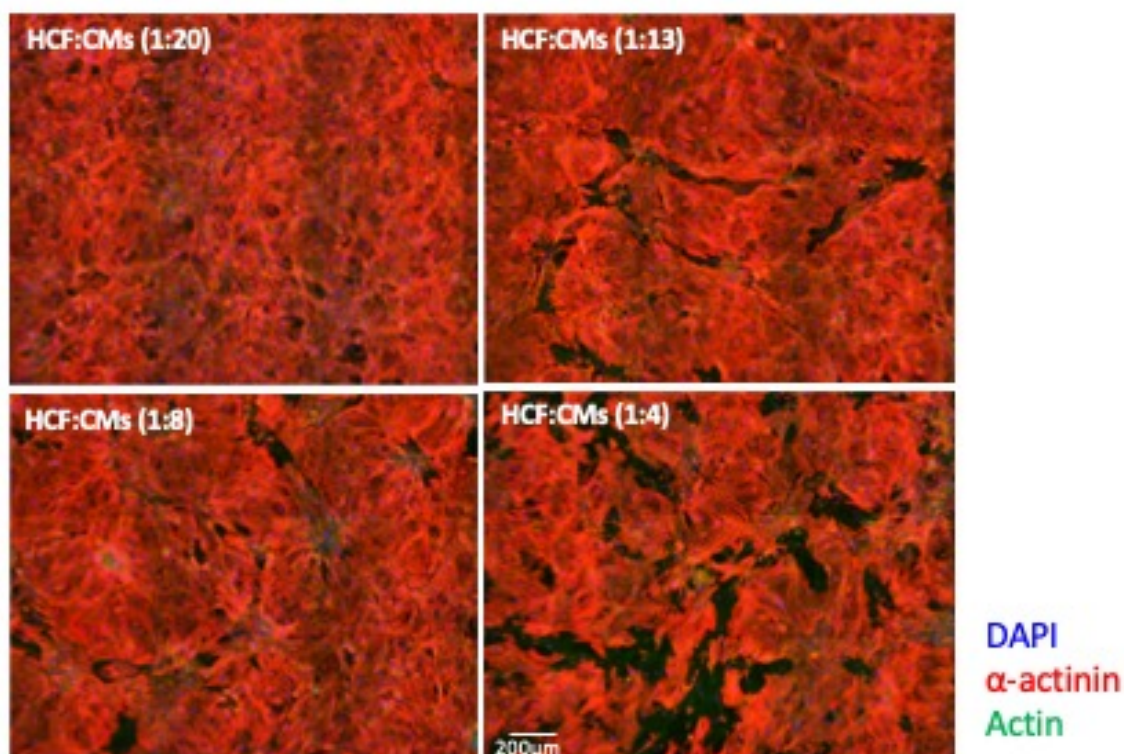


**Figure 4.15 - Co-culture of hiPSC-CMs with HCF at different ratios. HCF were co-cultured with hiPSC-CMs at 1:20, 1:13, 1:8 and 1:4 HCF:CMs. Co-culture was stained for nucleus (DAPI),  $\alpha$ -actinin and actin. Immunocytochemistry figure courtesy of Dr Maria Hortigon-Vinagre.**

The effects of the presence of HCF in a co-culture were observed via electrophysiological analysis. Co-cultures at different ratios of HCF:hiPSC were loaded with the voltage-sensitive dye FluoVolt and different parameters of the AP were measured (Figure 4.16). When 50% of the co-culture consisted of fibroblasts, the interval was prolonged to  $872.43 \pm 30.01$ ms compared to  $791.72 \pm 13.60$ ms in hiPSC-CMs. The 50% of repolarisation phase was affected in 1:1 and 1:20, where the former was shortened to  $185.90 \pm 5.93$ ms and the latter prolonged to  $237.55 \pm 7.45$ ms compared to hiPSC-CMs of  $208.10 \pm 3.35$ ms.

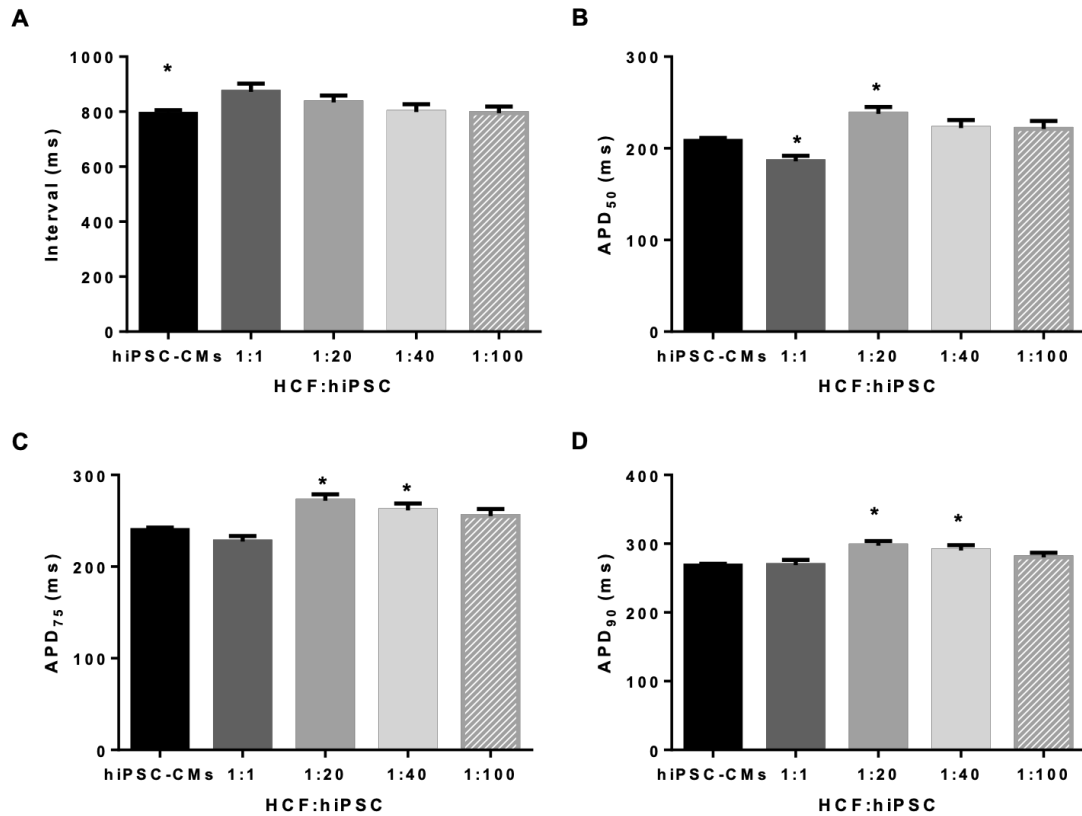


**Figure 4.16 – The effects on voltage of co-culture of HCF with hiPSC-CMs. Different ratios HCF:hiPSC-CMs starting at 1:1, 1:20, 1:40 and 1:100, at a final density of 25,000 cells/well, loaded with FluoVolt. A) Changes on interval between APs; B) time for 50% of repolarisation changes; C) effects of different ratios on 75% of time to repolarisation; D) Effects of different ratios on time to 90% of repolarisation. Unpaired t-test, n=6, \*p<0.05.**

75% of repolarisation was prolonged in 1:20 and 1:40 to  $271.75 \pm 7.14$ ms and  $261.43 \pm 7.50$ ms, respectively, while hiPSC-CMs exhibited an APD<sub>75</sub> of  $239.93 \pm 2.73$ ms. APD<sub>90</sub> was also prolonged in 1:20 and 1:40 to  $297.20 \pm 6.66$ ms and  $290.32 \pm 7.46$ ms compared to hiPSC-CMs at  $268.15 \pm 2.80$ ms.

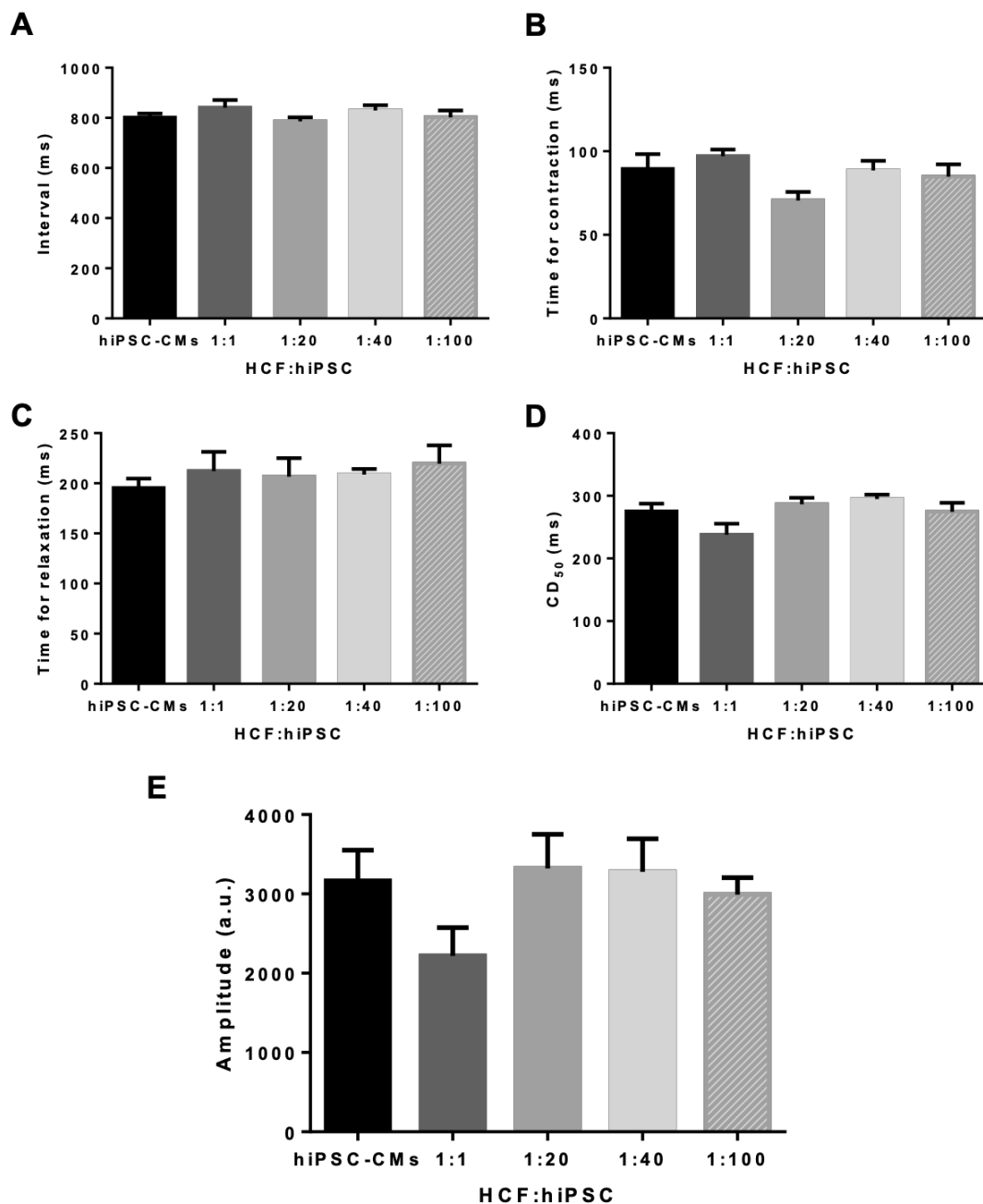


**Figure 4.17 - The effects on contractile behaviour of co-culture of fibroblasts with hiPSC-CMs. Different ratios HCF:hiPSC-CMs starting at 1:1, 1:20, 1:40 and 1:100, at a final density of 25,000 cells/well, loaded with FluoVolt. A) Changes on interval between APs at different cell:cell ratios; B) Time to 90% of contraction; C) Effects of different ratios on time to 90% of relaxation; D) Effects of different ratios on 50% of contraction duration; E) the effects on amplitude of the contraction. Unpaired t-test, n=6, \*p<0.05.**

Contractility remained unaffected by the presence of HCFs; most importantly there were no changes to amplitude of the contraction (Figure 4.17).

### Contractility in 1:1 HCF vs 1:1 HEK co-culture with hiPSC-CMs

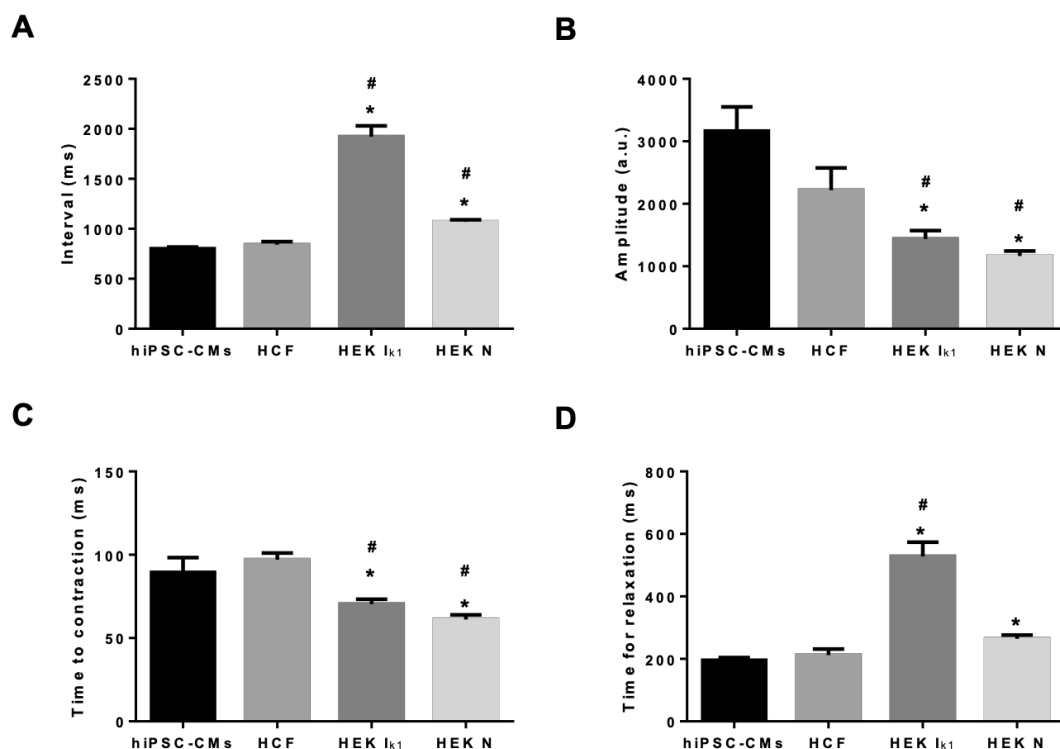


**Figure 4.18 - Contractile behaviour is affected differently in co-culture with different cell lines. Co-culture of hiPSC-CMs with HEK (I<sub>k1</sub> and normal) or with HCF at 1:1 were monitored and contractile behaviour was recorded on day 4 *in vitro* in BMCC. A) Interval between contractions did not differ in HCF co-culture from baseline behaviour (hiPSC-CMs), but HEK co-culture was prolonged; B) The amplitude of the contraction was unaffected in presence of HCF, but reduced in presence of HEK; C) Time to contraction was shorter in co-culture with HEK, but there were no effects on HCF; D) Time for relaxation was affected solely on HEK co-culture. Unpaired t-test, (\*) HEK vs hiPSC-CMs, (#) HEK vs HCF co-culture; \*p<0.05, #p<0.05.**

As shown in Figure 4.11 and illustrated in Figure 4.18, co-culture with I<sub>k1</sub>-expressing cells caused a prolongation of the normalised APD<sub>50</sub> and <sub>75</sub> but not APD<sub>20</sub> (Figure 4.17E and Figure 4.11) compared to co-culture with N-HEK. In additional measures, the amplitude of the signal was estimated to be reduced by 50% when compared with co-culture with normal HEK. As shown in Figure 4.18E, the net result of these two changes is to suggest an abbreviated AP that has a similar repolarisation time. This net change could only be verified with the use of microelectrodes to measure absolute voltages from two co-culture systems. One hypothesis is that these changes in AP shape are consistent with a large expression of I<sub>k1</sub> that would limit the extent of depolarisation of the AP. This is in contrast with the data from Bett et al. (2013) which showed reduced rates of rise and shortening of

APD when  $I_{k1}$  is introduced via dynamic clamping to a single hiPSC-CM cell. One hypothesis that arises from these changes in AP shape is that the  $Ca^{2+}$  current triggered by the AP would be substantially reduced which in turn would reduce contraction amplitude. Data from contraction measurements suggested the opposite, that, if anything, contraction amplitude was increased. These changes in electrophysiology and contractility are difficult to reconcile and require further investigation. The cause of these differences between the current study and that of Bett et al. (2013) is not clear, but the electrophysiology reported in this thesis is on a syncytium of cells where the electrical activity of the surrounding cells affects the overall AP shape and therefore may influence the final outcome of increased  $I_{k1}$  function. The effects on rise time and APD due to the syncytial nature of cardiac tissue has been reported previously for ventricle (Myles et al., 2015, Kelly et al., 2018). Co-culture of hiPSC-CMs with HCF does not affect electrophysiology or contractile behaviour.

## Electrophysiology in 1:1 HCF vs 1:1 HEK co-culture with hiPSC-CMs

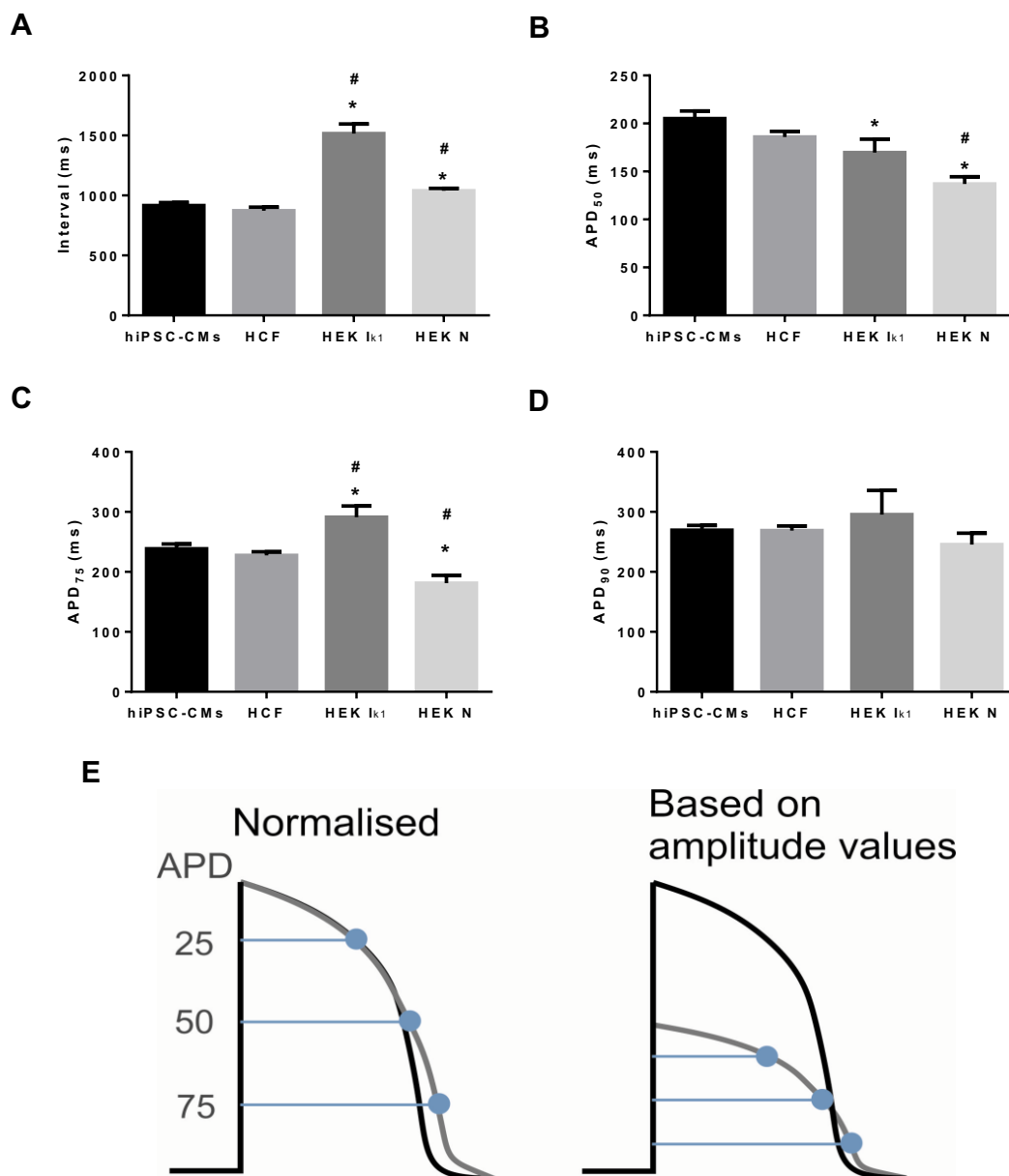


**Figure 4.19** – Electrophysiology is only affected in co-culture with HEK. Co-culture of hiPSC-CMs with HEK (I<sub>k1</sub> and normal) or with HCF at 1:1 were loaded with FluoVolt in BMCC and voltage recordings were taken. **A)** Interval between APs did not differ in HCF co-culture from baseline behaviour (hiPSC-CMs), but HEK co-culture was prolonged; **B)** APD<sub>50</sub> was unaffected in presence of HCF, but reduced in presence of HEK; **C)** APD<sub>75</sub> was longer in HEK-I<sub>k1</sub> and shorter in HEK-N, but there were no effects on HCF; **D)** APD<sub>90</sub> was not altered in either co-culture; **E)** Diagrammatic representation of the change in amplitude associated with I<sub>k1</sub> overexpression (grey) compared to N-HEK (black). Incorporating a change in AP amplitude gained from SNR measurements. Unpaired t-test, (\*) HEK vs hiPSC-CMs, (#) HEK vs HCF co-culture; \*p<0.05, #p<0.05.

Further effects were seen on electrophysiology, as early to mid-repolarisation was shorter in the presence of both HEK cell types in co-culture, but late repolarisation was longer in

the presence of  $I_{K1}$ -HEK. Figure 4.19E shows a diagram of one of the possible reasons for this effect on APD. It is possible that, due to lower AP amplitude, the APD values are shifted as represented. If Amplitude is lower, this could also represent a shorter APD<sub>25</sub> and 50.

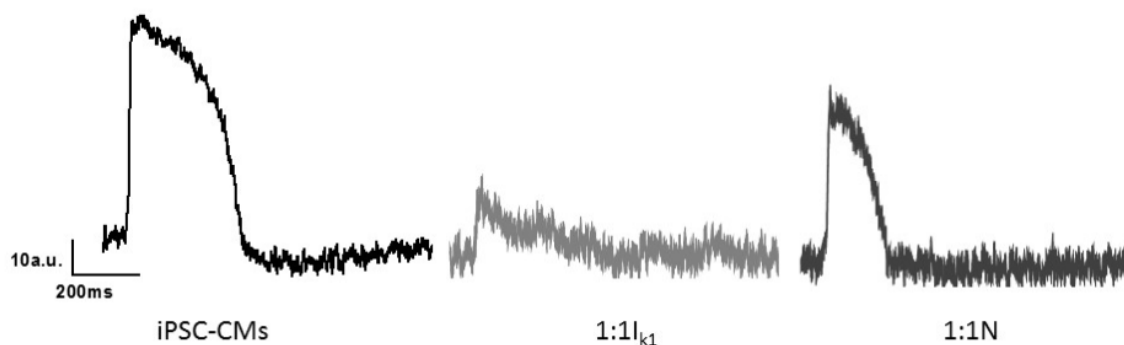


**Figure 4.20 - Example AP traces obtained from a plating. The different AP morphologies occur when different cell types are co-cultured. A standard AP obtained from Cor.4U hiPSC-CM monolayer (black, left) can be compared to an AP obtained from hiPSC-CMs are co-cultured with  $I_{K1}$ -HEK (light grey, middle) and normal-HEK (dark grey, right).**

The shape of the AP was affected differently in the presence of  $I_{K1}$  or N HEK (Figure 4.20). The mechanisms which led to this change are unknown. This was further investigated in chapter 6.

## 4.5 Discussion

Co-culture of hiPSC-CMs with HEK293 is an alternative method for the incorporation of an ion channel into a cell line which does not express it. HEK overexpressing  $I_{K1}$  were co-cultured with hiPSC-CMs as a way to possibly contribute towards a more stable resting membrane potential in the latter, and thus providing further insight into the mechanisms which contribute towards spontaneous activity in these cells.

HEK proliferation rates were investigated using 2 alternative methods: MTT assay and haemocytometer counts. Before introducing these cells into culture, it was important to determine how quickly they proliferate. The assays demonstrated that once the culture is at full confluency, the number of cells remains stably at plating densities. This could be due to potential cell loss, as the cells detach from the culture plate once confluency is reached. These assays provide some insight into cell number and growth rates but were shown to be fallible. To perform cell counts using haemocytometers and trypan blue, cells had to first

be detached from the plates using trypsin, which leads to cell loss due to its nature. The cells had to then be spun, thus leading to further cell loss. The MTT assay measured absorbance without need for cell detachment or disturbance. As the number of HEK293 did not vary when confluency was reached, ensuing experiments where these cells were introduced into co-culture with hiPSC-CMs were done with no concern for proliferation, and assuming that the number of HEK in culture did not vary over the 4 days in culture.

Incorporation of HEK to culture with hiPSC-CMs was done gradually to determine the cell densities to be used for results of the effect of  $I_{K1}$  and attempt on reducing the effects of presence of HEK alone. Two hiPSC-CM cell lines were used: Pluricytes and Cor.4U. Due to the nature of these experiments, it was determined that for current work Cor.4U was more suitable. The different ratios vary from the absence of any effect from  $I_{K1}$  to the effect of the presence of HEK in general. When the cells were plated at ratio of 1:10 (HEK:hiPSC) there were no changes in interval between spontaneous beats, but time for relaxation was affected. A decrease in time for relaxation was observed on day 4 in vitro in the presence of HEK- $I_{K1}$  compared to hiPSC-CMs but this effect was lost by day 8. Higher densities of HEK, such as 33% or 50%, led to prolongations of the interval in  $I_{K1}$  culture from day 3, and in the presence of HEK in general from day 5, respectively. In cultures at a ratio of 1:3 interval remains unaffected for 2 days, and differences start to be seen on day 5, and further increases in interval are seen in the  $I_{K1}$  culture over time. Time for relaxation at this ratio in  $I_{K1}$  culture is shortened on day 4 but remains unaffected in normal culture. On day 8 this ratio prolongs time for relaxation in the  $I_{K1}$  culture while normal co-culture remains unaffected. In 1:1 co-culture there was a prolongation of the interval between each contraction from day 3 in vitro in both  $I_{K1}$  and normal co-culture but this effect is diminished by day 8. Time for relaxation at day 4 was prolonged in normal co-culture compared to hiPSC and  $I_{K1}$  co-culture. On day 8, however, time for relaxation returned to that of hiPSC-CMs, and prolonged in  $I_{K1}$  co-culture. These effects led to a closer investigation of the mechanisms which contribute towards these on day 4.

Co-cultures were maintained for 8 days and contractile behaviour was monitored daily from day 4. HEK which had been growth arrested before plating showed a high incidence of quiescence, and the same effect was seen when the cells were maintained in serum-free medium. The purpose of this research was to investigate the most adequate medium to use in culture to contain HEK293 proliferation.

An investigation on the effects of 1:1 co-culture showed that the amplitude of the contraction increases greatly in the presence of HEK, with a stronger effect on the  $I_{K1}$  culture. The causes for this are unknown. Further research into this matter was done by adding human fibroblasts rather than HEK to co-culture. These have a Young's elastic modulus of 4-5kPa, compared to that seen in cardiomyocytes, which is in the order of 90-110kPa (Kuznetsova et al., 2007). HEK have a Young's modulus of  $\approx 20$ Pa (Blumlein et al., 2017). This allowed us to determine whether HEK's elasticity was the contributor towards the increase in amplitude of the contraction. The lack of an effect on amplitude in co-culture with HCF indicates that cell elasticity is not the contributor towards what was observed in HEK co-culture with hiPSC-CMs. As such, the mechanism which led to this remains unknown.

At spontaneous rates a prolongation of the time for relaxation was observed in the presence of  $I_{K1}$ . Most importantly, the presence of  $I_{K1}$  led to a prolongation of the interval at spontaneous rates to approximately twice the control interval. A prolongation was seen at a smaller scale in the presence of normal HEK at spontaneous rates. At 1Hz there was a small prolongation of interval in  $I_{K1}$ , as these cells did not fully follow the pacing. When observing the electrophysiological behaviour, early repolarisation was shortened in the presence of HEK in general (Figure 4.11). This effect started reversing in the presence of  $I_{K1}$  mid-repolarisation. During late repolarisation the action potential duration was prolonged in  $I_{K1}$  presence and unaffected in normal HEK.

When  $I_{K1}$  was blocked in co-culture using PA-6, electrophysiology remained mostly unaffected except for APD<sub>90</sub> which was prolonged. The same effect was previously observed by (Hoeker et al., 2017) in guinea pig ventricle with same dose of PA-6 (200nM) and in rat ventricle (Skarsfeldt et al., 2016). This is representative of phase 3 of the cardiac AP, for which  $I_{K1}$  is active to pump  $K^+$  out so the cell returns to its resting membrane potential.

Co-culture of hiPSC-CMs with HEK overexpressing  $I_{K1}$  showed that this current is introduced into culture. This method can be used for the addition of different proteins that hiPSC-CMs do not express or express in small amounts. HEK are not present in the heart and, as such, it would be better to use naturally existing cells such as fibroblasts, if these can be stably transfected with the intended protein. The effects seen from using HEK in co-culture (either  $I_{K1}$  or N) were further investigated in chapter 6 (see appendix).

### 4.5.1 Conclusion

At certain ratios of HEK:hiPSC there was a prolongation in interval between beats, suggesting that  $I_{k1}$  is now present in culture, but it also had effects on AP shape. The causes of these effects are unknown and are further investigated in later chapters. Co-culture with HCF provides a more natural route, as the latter are present in the heart, unlike HEK. An improvement to the co-culture protocol would be to overexpress  $I_{k1}$  in HCF and use these for the co-culture strategy.

## **5 Co-culture of hiPSC-CMs and Cx43 and I<sub>k1</sub>-overexpressing HEK293**

## 5.1 Introduction

Gap junctions connect most mammalian cells. These are agglomerates of multiple intercellular channels which connect the cytoplasm of adjacent cells thus providing both electrical and mechanical coupling (Van Veen et al., 2001).

Gap junctional intercellular communication (GJIC) refers to the diffusion and exchange of intracellular molecules of less than 1–1.5 kDa (i.e., small ions, second messengers, amino acids, metabolites, and peptides, etc.) between neighbouring cells and involves in the regulation of diverse cellular (Ke et al., 2017).

Electrical coupling has a key role in excitable tissues, such as smooth and cardiac muscle, where the propagation of the electrical impulse is mediated by passage of ions through gap junction channels. Each gap junction channel is composed of 12 connexin (Cx) molecules, assembled from 2 hexameric hemichannels (connexons) (Figure 5.1); one of each is delivered by both participating cells (Van Veen et al., 2001).

Propagation of the action potential from cell to cell is mediated by current flow through gap junction channels, primarily located in the intercalated disk (ID) at the end-to-end intercellular connections. Connexins are proteins which form gap junctions and hemichannels. There are 21 types known to exist in humans, and the permeability and signalling properties of the individual gap junctions and hemichannels are defined by their specific connexins (Ribeiro-Rodrigues et al., 2017).

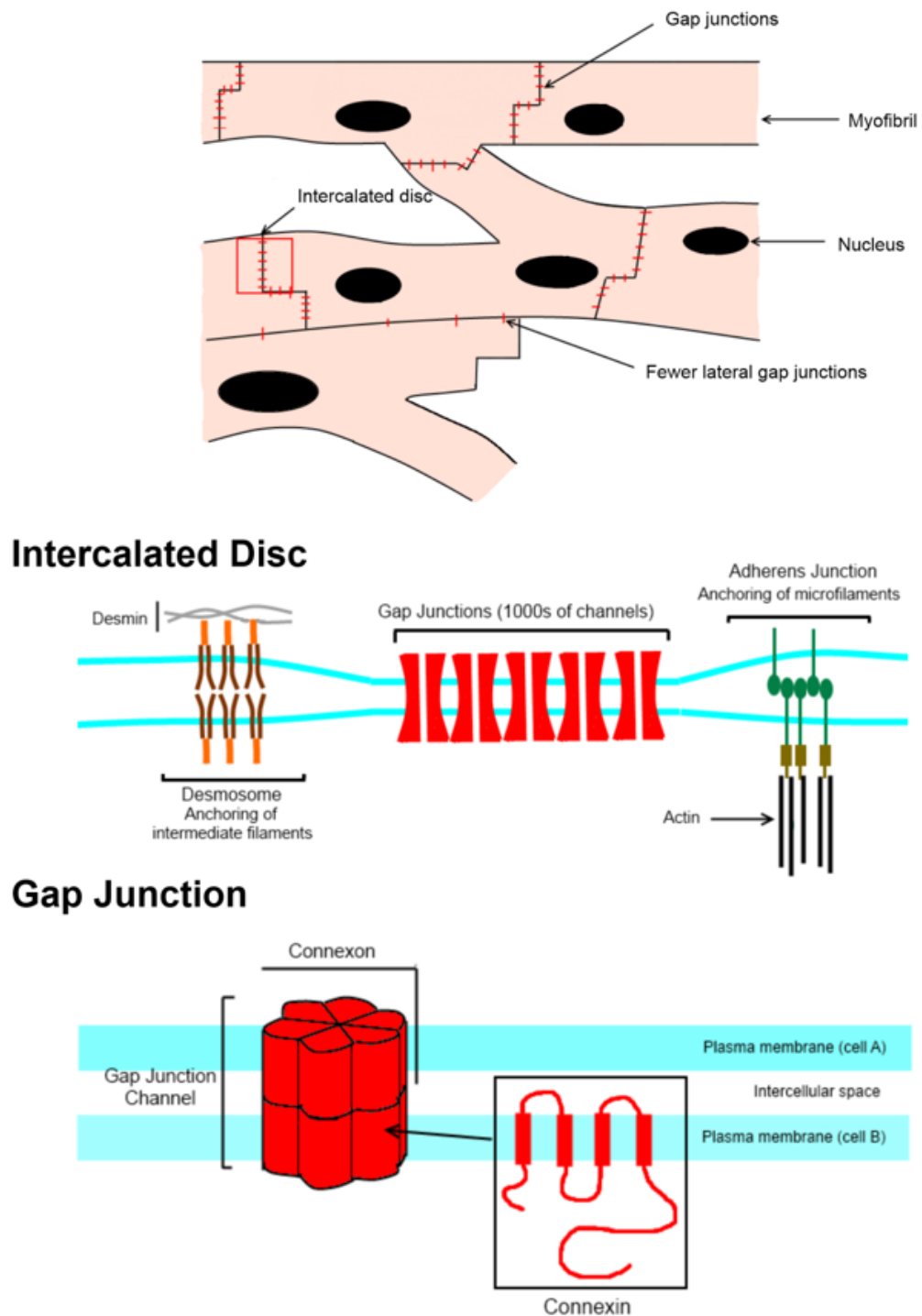


**Figure 5.1 - Gap junctions and the intercalated disc.** Diagram showing the communication of cardiomyocytes via intercalated disks. These disks contain gap junction (GJ) plaques – made up of thousands of GJ channels – through which adjacent cells communicate, alongside physical junctions, such as desmosomes and adherens junctions. GJ channels are composed of connexon dimers, with one connexon provided by each of the adjacent cells. Each connexon is composed of 6 connexins. (Image courtesy of Dr Annabel Campbell, 2016).

In mammalian hearts the gap junctions are most commonly made of connexin40 (Cx40), connexin43 (Cx43) and connexin45 (Cx45) (Van Veen et al., 2001).

### 5.1.1 Connexin expression in hiPSC-CMs

Cardiomyocytes generated from hiPSC have been shown to express cardiac proteins essential to the development of an adult ventricular myocyte phenotype, such as connexin-43 and myosin chain complexes, when cultured in vitro (Citro et al., 2015). There have not been many studies done on the expression of Cx43 on hiPSC-CMs. Different cell providers report that Cx43 is present (Ncardia, Herron et al., 2016), and is taken as a cardiac marker, but no specific amount is reported as this can vary depending on the extracellular matrix used for the cell culture (Herron et al., 2016).

During the reprogramming, single cells gather together and finally form compact colonies with tight cellular association in an ESC-like state (Ke et al., 2017). It has been reported that adherens junctions, gap junctions (GJs), focal adhesions and tight junctions were involved in complicated intercellular crosstalk that occurs during reprogramming. Ke et al. (2017) reported that Cx43 is involved in the generation of hiPSCs but the roles of the other Cxs in the reprogramming process are still unknown.

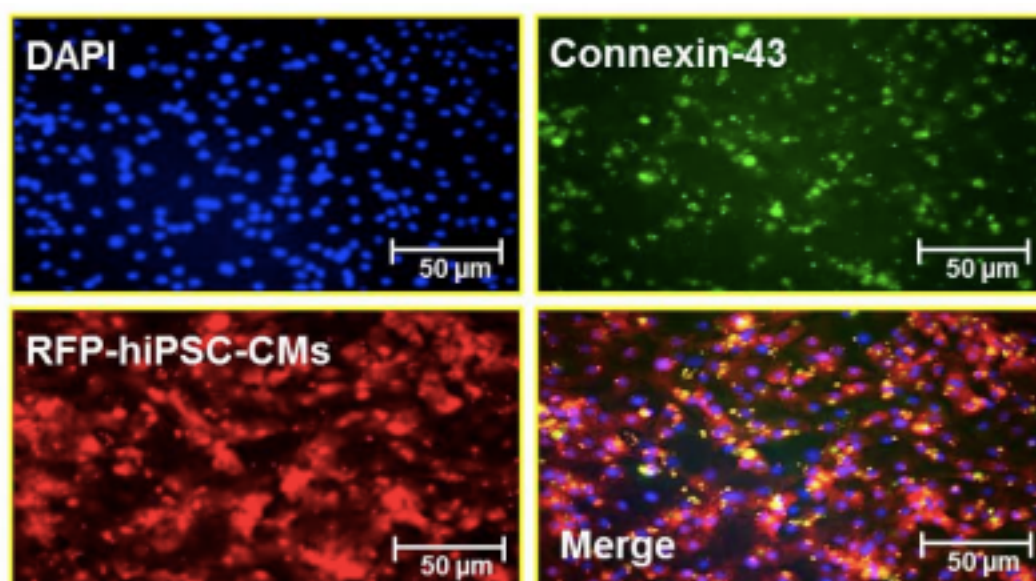


**Figure 5.2 - CDI hiPSC-CMs express Cx43 (green).** Immunohistological staining shows expression of Cx43; RFP (red fluorescence protein, red color), an hiPSC-CM marker; DAPI (blue color). Figure from (Citro et al., 2015).

A study by Citro et al. (2015) showed that, using Cx43 as a cardiac marker during the differentiation process, this is indeed present (Figure 5.2) in hiPSC-CMs obtained from a

commercial provider – CDI (Cellular Dynamics International, Maddison, USA), but fails to quantify it.

### 5.1.2 Connexin expression in HEK293

HEK293 cells genetically engineered to stably express both  $I_{K1}$  and  $I_{Na}$  developed membrane excitability, wherein on reaching an excitation threshold by current injection, they reproducibly fired an ‘all-or-none’ AP (Kirkton and Bursac, 2011). The resulting slow and unorganised AP propagation was supported by weak endogenous cell coupling, that likely originated from expression of connexin-45 rather than connexin-43 gap junctions. The same group found that when these HEK293 expressing both currents are stably transfected with a plasmid encoding Cx43, functional intercellular coupling was dramatically enhanced compared with endogenous HEK293 coupling. When confluent 2D monolayers were electrically stimulated these cells showed rapid, spatially uniform AP propagation (Kirkton and Bursac, 2011).

### 5.1.3 Aims

The two cell lines used for co-culture, hiPSC-CMs and HEK (both  $I_{K1}$  and normal) have been shown to express little to no Cx43 (Citro et al., 2015, Patel et al., 2014), which is responsible for cell-to-cell communication in the adult heart. It was hypothesised that, in  $I_{K1}$ -HEK transfected with Cx43 ( $I_{K1}$ -Cx43) co-culture, improved coupling would affect APD as more  $I_{K1}$  is available for restoring the cell to its resting membrane potential. To ensure proper electrical coupling between HEK293 and hiPSC-CMs, the first were transfected with a plasmid overexpressing Cx43 before being co-cultured. Electrophysiological and contractile behaviour were monitored.

## 5.2 Methods

### 5.2.1 Transfection protocol

HEK293 were plated in 6-well plastic plates at 250,000 cells/well in HEK medium (see Ch2. General methods). The cells were allowed to proliferate to 70% confluency before plasmid transfection, normally achieved in 48h. The plasmid pcDNA3.1 with Cx43 (courtesy of Prof Stuart Nicklin, University of Glasgow) was mixed with Xfect Reaction Buffer (Takara Bio, USA) at different volumes and vortexed for 5 seconds. The manufacturer of the transfection reagent recommends 2.5 $\mu$ g to 7.5 $\mu$ g of DNA per well.

HEK293 expressing  $I_{k1}$  were transfected with 2.5 and 5 $\mu$ g of pcDNA3.1. At this point Xfect Polymer was added and vortexed for 10s. The plasmid solution was incubated for 10 minutes at room temperature to allow nanoparticle complexes to form. It was then spun down for 1 second to collect the contents at the bottom of the tube so that only the supernatant nanoparticle complex solution was added dropwise - 100 $\mu$ L per well – to the well containing cells and HEK maintenance medium (see Ch. 2). The plate was incubated at 37°C for 4.5h and the nanoparticle complexes were aspirated the next day. The medium was replaced with 3 mL fresh HEK medium and the plate returned to the incubator until ready to use.

Cultures were transfected with the plasmid, a mock-transfection where only the Xfect kit was added, or not transfected. All cells were washed twice with DPBS at room temperature and fixed with 4% paraformaldehyde (PFA) for 15 minutes (see section 5.2.2). The cultures were fixed 24h and 96h post-transfection to check duration of Cx43 expression using immunocytochemistry.

### 5.2.2 Immunocytochemistry

HEK to be used for immunocytochemistry were plated and transfected with a Cx43 plasmid in 6-well glass-bottom plates (MatTek) using the protocol above. Existing medium was removed from the cells, and they were washed 3 times with 1 mL PBS (-Ca<sup>2+</sup> -Mg<sup>2+</sup>). The cells were fixed for 15 minutes at RT with 4% PFA and washed 3 times with 0.1% PBST (PBS + 0.1% Tween20). The cells were then permeabilised with 0.1% Triton X-100 diluted in PBS for 10 minutes at RT. The cells were washed 3 times in PBST for 5 minutes each wash and blocked for 60 minutes with 10% goat serum in PBS. The block was removed, and the cells were incubated overnight with 1:200 anti-connexin 43 antibody (Merck, Germany) in PBST + 10% goat serum. The cells were then washed 3 times in PBST at RT with 5 minutes for each wash and incubated for 1h with anti-rabbit Ig-Alexa 647 at 1:200 dilution in PBST + 10% goat serum. The stain was removed and PBST with 1:1000 DAPI was added for 3 minutes. The cells were then washed 3 times with PBST before imaging using a confocal microscope with 40x magnification. Images were edited using ImageJ (NIH).

### 5.2.3 Co-culture with Cx43-transfected HEK

HEK293 overexpressing  $I_{k1}$  and control HEK293 cells were plated at 350,000 cells/well in a 6-well plate in HEK medium and incubated for 24h, to reach 70% confluency. Cells were transfected with 5 $\mu$ g pcDNA3.1-Cx43 plasmid as detailed above; after removing transfection reagent and replacing with fresh medium, the cells were incubated overnight.

Cor.4U hiPSC-CMs were thawed following manufacturer's instructions (see Ch2. General Methods) and cell density was adjusted to 250,000 cells/mL. 100 $\mu$ L of hiPSC-CMs were transferred to each well of a fibronectin-coated 96-well glass bottom plate. HEK293 transfected with Cx43 were harvested by trypsinisation and resuspended in Cor.4U medium at 250,000 cells/ml. 100 $\mu$ L of HEK cell suspension (Normal and  $I_{k1}$ ) were transferred to wells containing hiPSC-CMs, thus achieving a 1:1 ratio.

Co-culture was maintained in Cor.4U medium for 4 days. On day 4 the cells were loaded with 1:1000 FluoVolt and 1:100 PowerLoad prepared in BMCC, for 25min at 37°C. Voltage and contractility were measured using CelloPTIQ and HCImage, respectively. Voltage analysis was done on CelloPTIQ and GraphPad Prism 6. Contractility was analysed on ImageJ and data processed on GraphPad Prism 6.

## 5.3 Results and discussion

### 5.3.1 Setting the transfection protocol

To initially establish which concentration of plasmid to use for future experiments two recommended concentrations were used, 2.5 and 5 $\mu$ g for increased expression of Cx43 on HEK. When the cells were transfected with 2.5 $\mu$ g in 6 well plates, Cx43 transfected HEK did not express Cx43 well at 96h (Figure 5.3A). Ensuring the majority of the HEK express Cx43 over 96h is important as measurements in co-culture are taken at this time point. Increasing the plasmid concentration to 5 $\mu$ g in both normal and  $I_{k1}$  HEK resulted in a transfection which was present for 4 days (Figure 5.3B). Figure 5.3B shows that small amounts of Cx43 are present in both  $I_{k1}$  and N-HEK in a control, but that it is possible to successfully express this connexin and maintain expression for 96h.

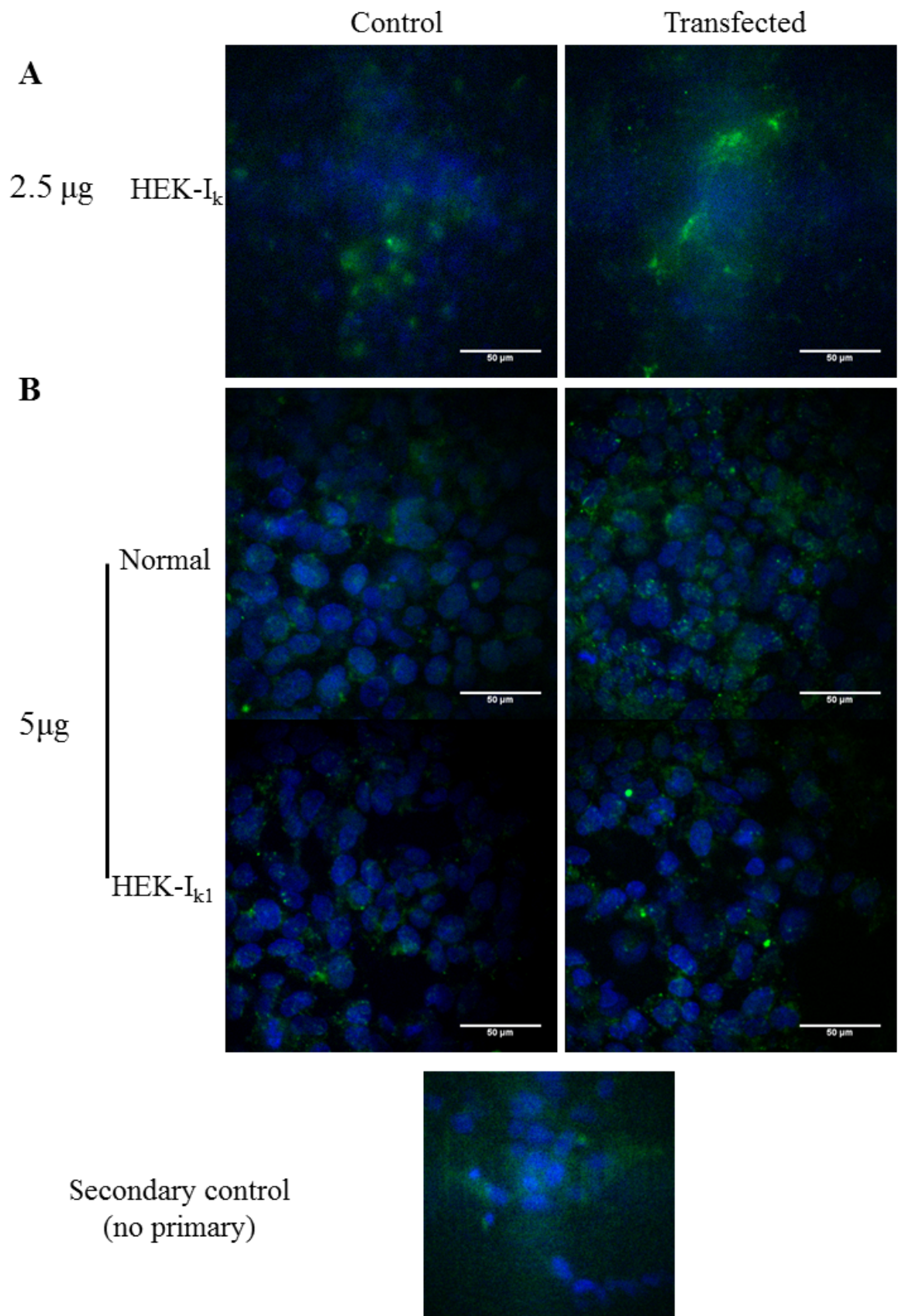


**Figure 5.3 - Cx43 expression on HEK, normal and  $I_{k1}$ -expressing on day 4 post-transfection with 2.5  $\mu$ g and 5  $\mu$ g of plasmid. Green – Cx43, blue – nuclear stain, DAPI. A) Increased expression with 2.5  $\mu$ g of Cx43 plasmid 96h after transfection shows a non-specific stain; B) Staining of both normal and  $I_{k1}$  HEK with 5  $\mu$ g Cx43 plasmid in a 6-well format shows expression of Cx43 is still present 96h after transfection.**

Transfection using higher amount of plasmid led to cell death (data not shown). Lower amounts of plasmid did not alter Cx43 expression in either cell type (data not shown). Taking the durability and success of the transfection into consideration future work was done using HEK293 transfected with 5 $\mu$ g of Cx43 plasmid in 6 well plates.

### **5.3.2 Co-culture overexpressing Cx43**

It was hypothesised that increasing Cx43 expression would increase interval, amplitude of the AP and decrease APD<sub>50</sub> and APD<sub>90</sub> further than that seen in 1:1 co-culture of hiPSC-CMs with I<sub>k1</sub>-HEK. Therefore, the effect of Cx43-expressing HEK293 (HEK-Cx43), normal, or I<sub>k1</sub>-expressing, on hiPSC-CM voltage was determined. HEK-Cx43 co-cultured with hiPSC-CMs at a 1:1 ratio and functional measurements were performed on day 4 post-plating.

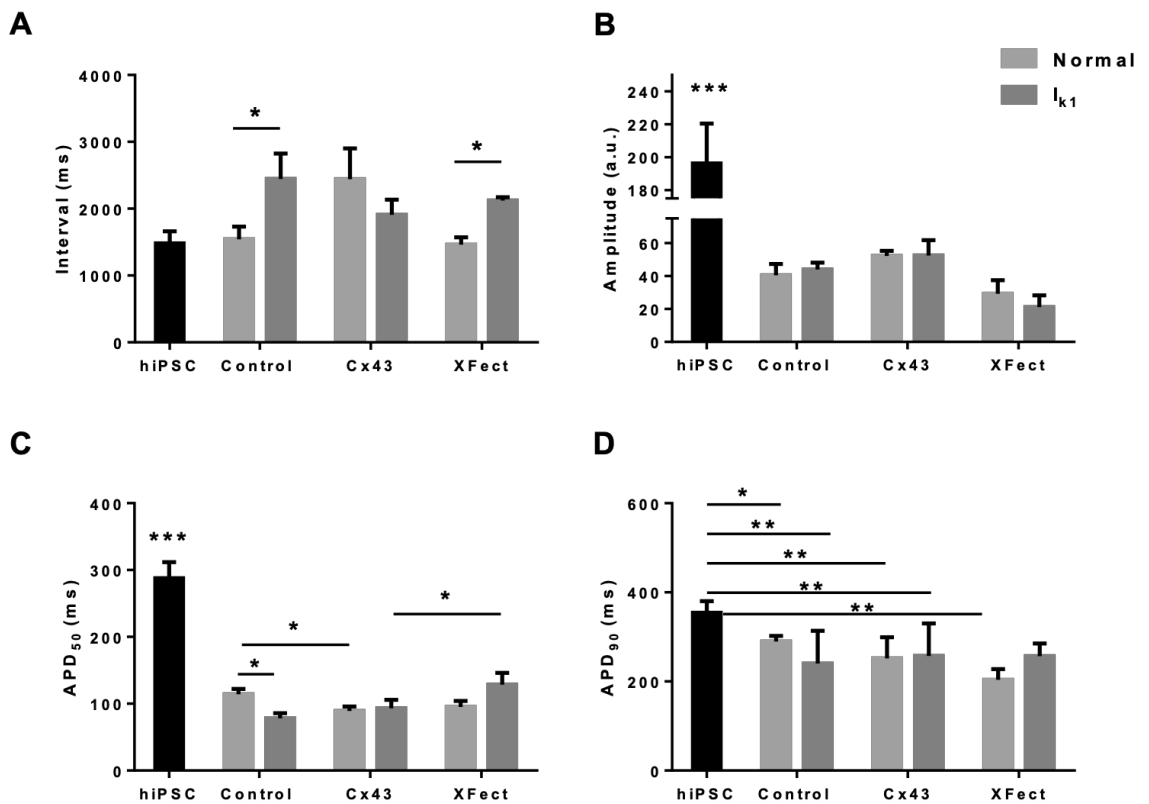


**Figure 5.4 - Electrophysiological effects of co-culture of HEK-Cx43 with and without  $I_{k1}$  expression on hiPSC-CMs.** HEK were transfected with 5 $\mu$ g of Cx43 plasmid or underwent a mock transfection (XFect). Control wells were maintained in standard media for 4 days. Voltage measurements were done on cells loaded with FluoVolt on day 4. A) Interval was prolonged in the presence of HEK- $I_{k1}$  but not on transfected cells; B) The amplitude of the AP was greater in hiPSC-CMs, but not different in co-culture; C) APD<sub>50</sub> was longer in hiPSC-CMs compared to co-culture; D) APD<sub>90</sub> was significantly shorter in co-culture compared to hiPSC-CMs with the exception of XFect cells. One-way ANOVA comparison hiPSC-CMs vs co-culture, unpaired t-test comparing different co-cultures: \*\*\* $p < 0.001$ , \*\* $p < 0.01$ , \* $p < 0.05$ ,  $n = 8$ .

The effect of co-culture on interval previously seen in 1:1 HEK:hiPSC was maintained, where it was prolonged in the  $I_{k1}$ -overexpressing culture compared to Normal control (2445 $\pm$ 379ms vs 1543 $\pm$ 187ms). This effect was also present in co-cultures with cells that were mock-transfected but not in co-cultures with cells expressing Cx43 (2123 $\pm$ 48ms vs 1460 $\pm$ 110ms). There was no effect of Cx43-transfected cells in either cell type (Figure 5.4A). The amplitude of the voltage trace was significantly larger in hiPSC-CM controls

( $196 \pm 24$  a.u.) compared to co-culture (Figure 5.4B). This effect is further investigated in Ch. 6.

Closer inspection of the effects on  $APD_{50}$  (Figure 5.4C) showed that this variable is significantly longer in hiPSC-CMs ( $288 \pm 24$  ms) compared to co-cultures. Within each co-culture  $APD_{50}$  is longer in normal control compared to  $I_{K1}$  control ( $114 \pm 8$  ms vs  $78 \pm 8$  ms), but also longer than Normal-Cx43 ( $89 \pm 7$  ms).  $I_{K1}$ -Cx43 had a shorter  $APD_{50}$  than  $I_{K1}$  mock-transfected (XFect) ( $93 \pm 13$  vs  $129 \pm 18$  ms).

$APD_{90}$  was significantly longer in hiPSC-CMs ( $321 \pm 19$  ms) alone compared to most co-cultures: Normal control ( $201 \pm 27$  ms);  $I_{K1}$ - control ( $159 \pm 46$  ms); Normal Cx43 ( $163 \pm 33$  ms);  $I_{K1}$ -Cx43 ( $175 \pm 46$  ms); Normal-XFect ( $139 \pm 28$  ms);  $I_{K1}$ -XFect ( $193 \pm 40$  ms).

These cultures were further paced at different frequencies and different aspects of the AP were analysed.

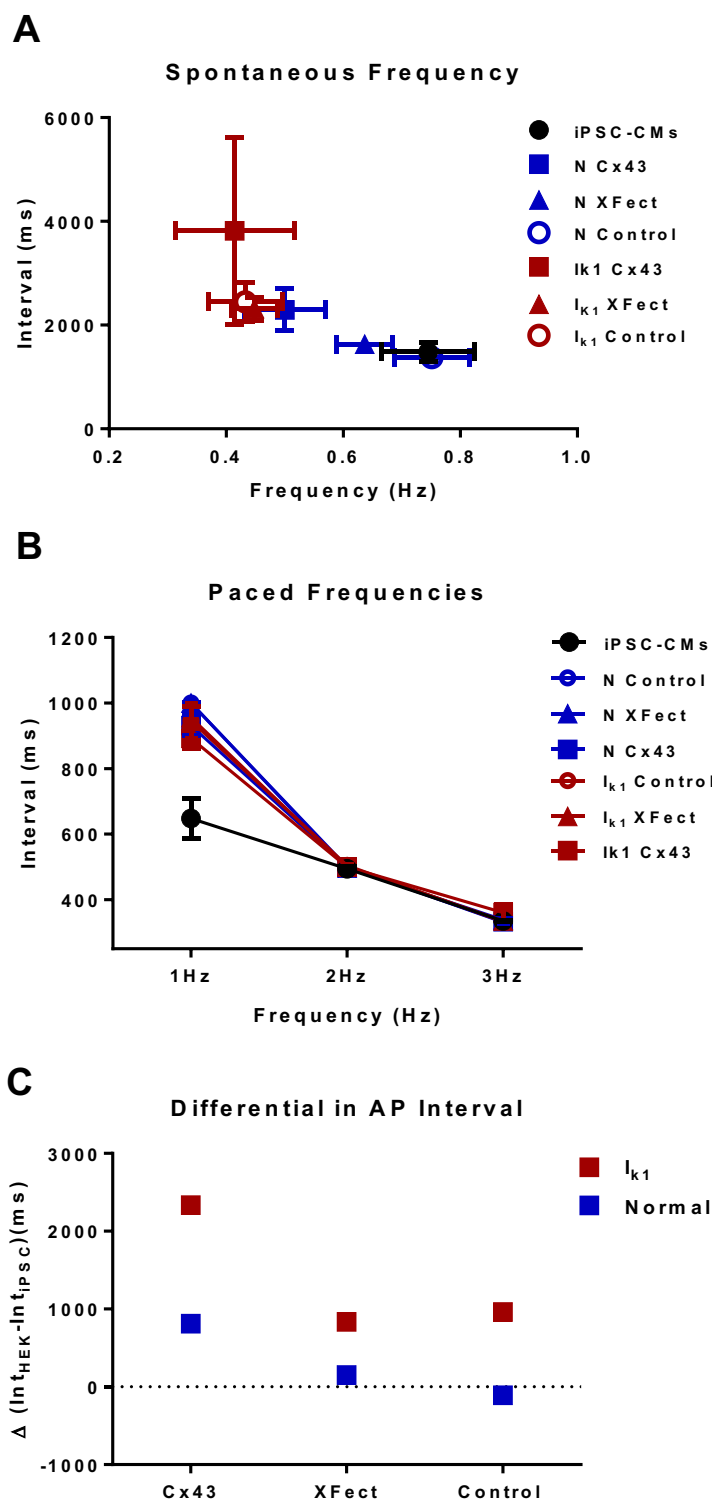


**Figure 5.5 - Voltage in the Cx43-overexpressing co-culture at spontaneous rates and increasing pacing frequencies.** HEK were transfected with  $5\mu\text{g}$  of Cx43 plasmid. Voltage was measured upon loading the co-culture with FluoVolt on day 4. **A)** Co-culture with expression of Cx43 affected interval in spontaneous beating; **B)** Interval was shorter in hiPSC-CM culture compared to  $I_{k1}$ -Cx43 (\*),  $I_{k1}$  XFect (\*),  $I_{k1}$  control (\*), N-Cx43 (\*), N XFect (\*), N control (\*) when paced at 1Hz. At 2 and 3Hz interval decreased equally in all conditions; **C)** The differential between  $I_{k1}$ /Normal co-culture and hiPSC-CMs in the three different conditions: Cx43 expression, XFect treatment, and control. hiPSC-CMs (black),  $I_{k1}$  (red), Normal (blue). One-way ANOVA, \* $p < 0.05$ ,  $n = 8$ .

Spontaneous data showed that although these co-cultures were beating at different frequencies (Figure 5.5A), these were not significantly different. When all co-cultures were paced at 1Hz, the interval was significantly slower compared to hiPSC-CMs. Interval at 1Hz in hiPSC-CMs was  $648 \pm 62$ ms, whereas in  $I_{k1}$ -Cx43 it was  $892 \pm 31$ ms (\* $p < 0.05$ ), in  $I_{k1}$ -XFect it was  $956 \pm 33$ ms (\* $p < 0.05$ ), in  $I_{k1}$ -Control it was  $946 \pm 55$ ms (\* $p < 0.05$ ). In Normal co-culture, in N-Cx43 interval was  $931 \pm 32$ ms (\* $p < 0.05$ ), in N-XFect it was  $1000 \pm 0.8$ ms (\* $p < 0.05$ ) and in N-control it was  $1000 \pm 0.2$ ms (\* $p < 0.05$ ). Despite all cultures being paced in an exact manner, it was found that 1Hz is very approximate to the intrinsic rate in hiPSC-CMs, and for this reason the pacing was not completely followed as there was occasional spontaneous beats (Figure 5.5B).

When the pacing frequency was increased to 2 and 3Hz, all cultures followed electrical stimulation and no changes were observed.

The differential (Figure 5.5C) was calculated from the mean interval in either HEK co-culture (i.e.  $I_{k1}$  or normal) and mean interval from hiPSC-CMs was subtracted. When the co-cultures overexpressed Cx43 the differential was higher, thus sustaining a bigger effect than that seen in control cultures. The increased expression of Cx43 led to a bigger change in interval than that seen in controls.

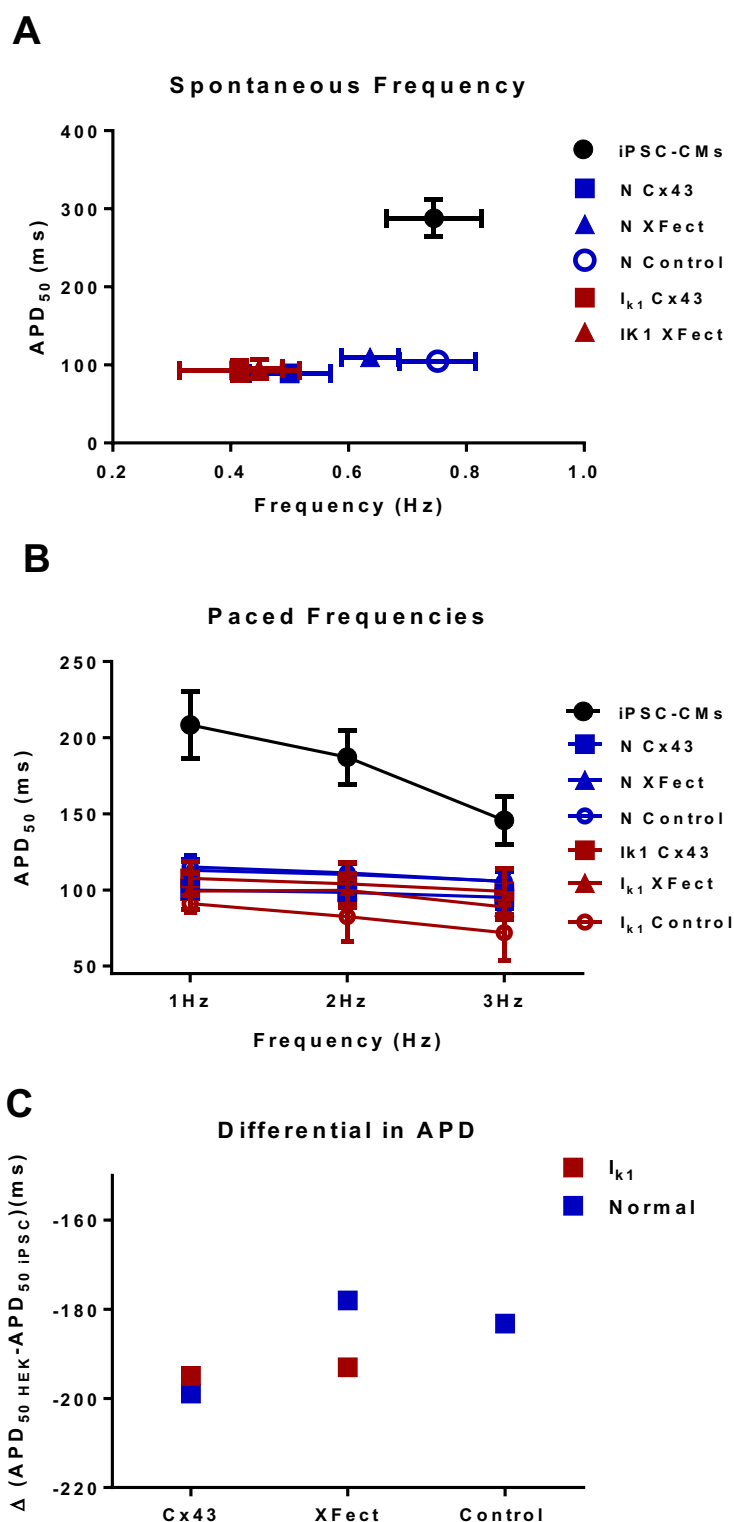


**Figure 5.6 - Voltage in the Cx43-overexpressing co-culture at spontaneous rates and increasing pacing frequencies. HEK were transfected with 5 $\mu$ g of Cx43 plasmid. Voltage was measured upon loading the co-culture with FluoVolt on day 4. A) Co-culture with increased expression of Cx43 affected APD<sub>50</sub> in spontaneous beating, where hiPSC-CM had a prolonged APD<sub>50</sub>; B) APD<sub>50</sub> was longer in hiPSC-CMs at different pacing frequencies compared to all conditions; C) The differential between I<sub>k1</sub>/Normal co-culture and hiPSC-CMs in the three different conditions: Cx43 expression, XFect treatment, and control. hiPSC-CMs (black), I<sub>k1</sub> (red), Normal (blue). One-way Anova, \*p<0.05, n=8.**

Spontaneous data showed APD<sub>50</sub> (Figure 5.6A) was significantly longer in hiPSC-CMs (288±24ms) compared to I<sub>k1</sub>-Cx43, I<sub>k1</sub>-XFect, I<sub>k1</sub>-control, N-Cx43, N-XFect, and N-control (93±13ms, 95±13ms, 78±8ms, 89±7ms, 110±9ms, and 105±5ms, \*p<0.05). When the co-cultures were paced at 1Hz, APD<sub>50</sub> remained longer in hiPSC-CMs. APD<sub>50</sub> at 1Hz (Figure 5.6B) in hiPSC-CMs was 208±22ms, whereas in I<sub>k1</sub>-Cx43 it was 108±11ms (\*p<0.05), in I<sub>k1</sub>-XFect it was 99±12ms (\*p<0.05), in I<sub>k1</sub>-Control it was 91±6ms (\*p<0.05). In Normal co-culture, in N-Cx43 APD<sub>50</sub> was 100±4ms (\*p<0.05), in N-XFect it was 113±7ms (\*p<0.05) and in N-control it was 115±7ms (\*p<0.05). When the cultures were paced at 2Hz the same effect was seen. APD<sub>50</sub> at 2Hz in hiPSC-CMs was 187±18ms, whereas in I<sub>k1</sub>-Cx43 it was 104±14ms (\*p<0.05), in I<sub>k1</sub>-XFect it was 100±11ms (\*p<0.05), in I<sub>k1</sub>-Control it was 83±16ms (\*p<0.05). In Normal co-culture, in N-Cx43 APD<sub>50</sub> was 99±4ms (\*p<0.05), in N-XFect it was 110±7ms (\*p<0.05) and in N-control it was 111±7ms (\*p<0.05). When the cultures were further electrically paced at 3Hz, APD<sub>50</sub> was shorter in I<sub>k1</sub>-XFect (89±8ms) compared to hiPSC-CMs (146±16ms).

The difference in APD<sub>50</sub> between HEK co-cultures and hiPSC-CMs alone showed that APD<sub>50</sub> is similarly shorter in all co-cultures (Figure 5.6C), which might be representative of the presence of HEK rather than related to I<sub>k1</sub> or Cx43 expression.

The effects seen were due to co-culturing hiPSC-CMs and HEK, and not attributable to the transfection protocol or increased expression of Cx43.

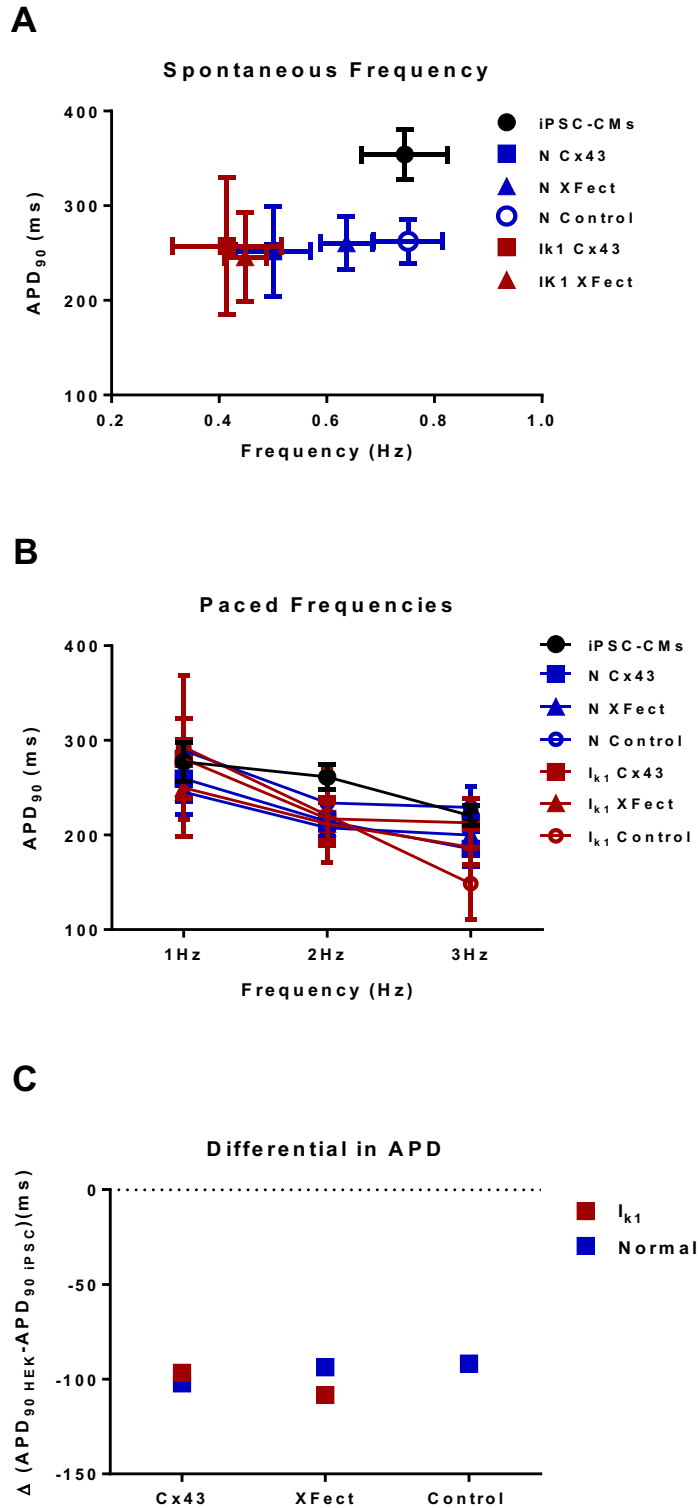


**Figure 5.7** - Voltage in the Cx43-overexpressing co-culture at spontaneous rates and increasing pacing frequencies. HEK were transfected with 5 $\mu$ g of Cx43 plasmid. Voltage was measured upon loading the co-culture with FluoVolt on day 4. **A)** Co-culture with increased expression of Cx43 affected APD<sub>50</sub> in spontaneous beating, where hiPSC-CM had a prolonged APD<sub>90</sub>; **B)** APD<sub>90</sub> was longer in hiPSC-CMs at different pacing frequencies compared to all conditions; **C)** The differential between I<sub>k1</sub>/Normal co-culture and hiPSC-CMs in the three different conditions: Cx43 overexpression, XFect treatment, and control. hiPSC-CMs (black), I<sub>k1</sub> (red), Normal (blue). One-way Anova, \*p<0.05, n=8.

APD<sub>90</sub> was not affected (Figure 5.7A) by the increased expression of Cx43. Despite APD<sub>90</sub> being shorter in co-cultures (Figure 5.7C) this was not significant.

## 5.4 Discussion and conclusion

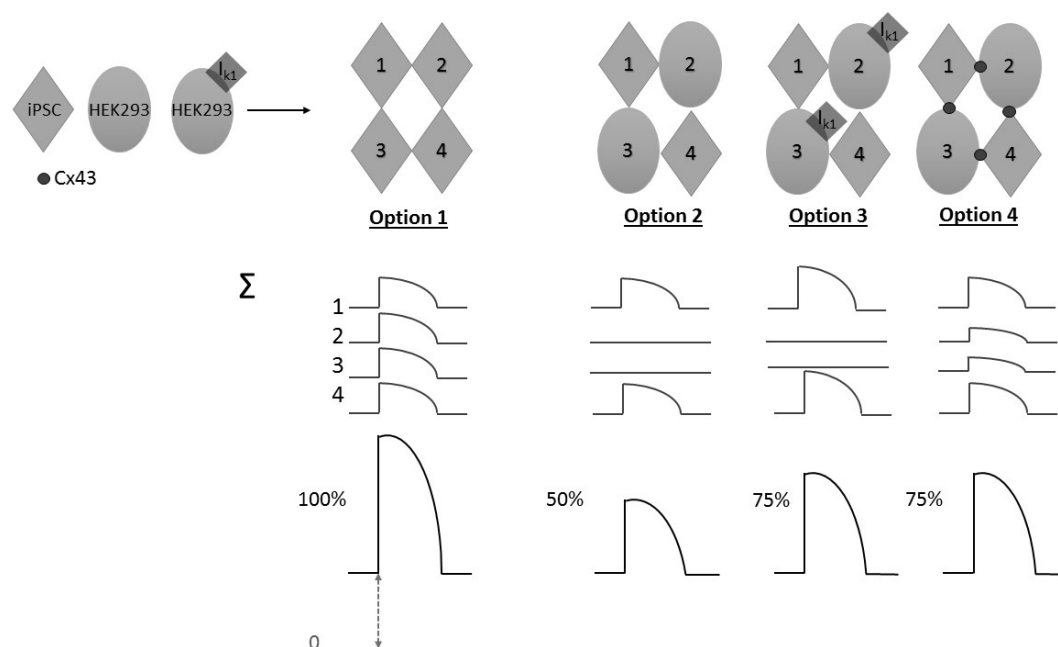


**Figure 5.8 – The contribution of the different cell types to the AP shape and size are unknown. It was hypothesised that: Option 1) all cells in the field of view contribute towards the AP thus generating an amplitude of 100%; Option 2) HEK do not contribute towards the AP and it results in an amplitude of 50%; Option 3) In the presence of  $I_{k1}$  the hiPSC-CMs generate a larger AP leading to an amplitude of 75%; Option 4) Better connexions through overexpressing Cx43 results in small AP generation by HEK and the AP is 75% of its full amplitude.**

Stable transfection of HEK with a plasmid expressing Cx43 can be achieved with 5 $\mu$ g, and expression is still present 96 hours after transfection. The addition of HEK-Cx43 to co-culture with hiPSC-CMs altered the electrophysiological and contractile behaviour, which was present when co-culture used two different HEK-Cx43 cell lines:  $I_{k1}$  and Normal. In fact, the presence of cells which underwent a mock transfection using Xfect but not the plasmid, showed altered electrophysiological behaviour. The mechanisms which underlie this change are unknown, as are the Xfect components.

The intensity of the AP signal represents the amount of dye in cell in field of view. When the signal intensity increases, so does signal to noise. This is a result of measuring function using photomultipliers (PMTs), Poisson distributed. The Poisson noise is characteristic

variance of the signal directly proportional to the amplitude of the signal. It is important to notice that variance is not equal to mean amplitude because this is not measured in terms of photons (see Ch.6).

Increased expression of Cx43 did not increase the interval between each AP further from what occurred in co-culture with  $I_{k1}$ -HEK previously. It was hypothesised that Cx43 expression in both  $I_{k1}$  and N-HEK would increase the amplitude of the AP as this would show that there were better cell-to-cell connections. Cx43 has been shown to enable adhesion between cells from different tissues and even species (Cotrina et al., 2008). Cx43 forms gap junctions, the channels that allow for that electrical charge to move between one cell and the next (Agullo-Pascual and Delmar, 2012).

Amplitude did not change in co-cultures and hiPSC-CMs from that seen in 1:1 co-culture before Cx43 increased expression. Figure 5.8 shows the hypothesised effect where, dependant on contribution from HEK towards the AP shape and size, the resulting trace would be affected. Observing the amplitude obtained from the hiPSC-CMs, it is clear that it is larger and that most, if not all, cells contribute electrically towards the AP size. When the amplitude is shorter, this could be due to either only hiPSC-CMs being electrically active, and as such the amplitude is only 50% of iPSC AP, or there is little contribution and the AP is at 75% of its full size. As amplitude was not affected in Cx43 expression, electrical coupling was not improved.

It was also hypothesised that, in  $I_{k1}$ -Cx43 co-culture, the attempt to improve coupling from Cx43 expression in HEK would decrease APD, as more  $I_{k1}$  is available for restoring the cell to its resting membrane potential. Co-culture appears to affect APD but that effect is not linked to  $I_{k1}$  or Cx43 expression. It is to be noted that overexpression of  $I_{k1}$  has previously shown that in co-culture it prolongs interval and decreases APD (see Ch. 4). This effect was not enhanced by Cx43 expression.

Figure 5.8 represents the hypothesised causes for the effects on AP amplitude seen on co-culture. As AP amplitude remains larger in hiPSC-CMs culture it is possible that this is due to HEK not generating an electrical discharge which contributes towards the AP. It had been originally hypothesised that this could be a result of lack of connexins linking the two cell types (Option 2). This study discovered that increasing connexin-43 expressing did not increase the amplitude and as such option 4 is not viable. Overexpression of  $I_{k1}$  was

expected to improve the electrical behaviour in hiPSC-CMs but the opposite happened where the AP amplitude was lower in this co-culture. This is further explored in Ch. 6.

In conclusion, increased expression of Cx43, responsible for electrical mechanical coupling, did not improve cell-to-cell communication between HEK and hiPSC-CMs. Further work is recommended to investigate the advantages of overexpression of this connexin in hiPSC-CMs.

### **5.4.1 Limitations**

This work was conducted at the end of the project. Time constraints did not allow for further investigation to be done. Future work needs to be done to further study the transfection of HEK293 using a Cx43 plasmid, and how this subsequently affects hiPSC-CM culture. A closer inspection at the effects of the Xfect transfection kit would provide insight into the effects seen. Immunocytochemistry and electron microscopy could help better understand the success of the Cx43 transfection into HEK. Quantification of Cx43 available in untransfected HEK and post transfection in HEK is needed to better understand the consequences of co-culture with both cell lines.

## **6 Discussion and Conclusion**

## 6.1 Discussion and Conclusion

hiPSC-CMs have an immature phenotype, where they resemble and behave like neonatal cardiomyocytes rather than fully developed adult CMs. Different drugs which block specific ion channels were used to help characterise these cells and to determine the contribution of the different ionic currents.

## 6.2 Ionic currents and channels in hiPSC-CMs

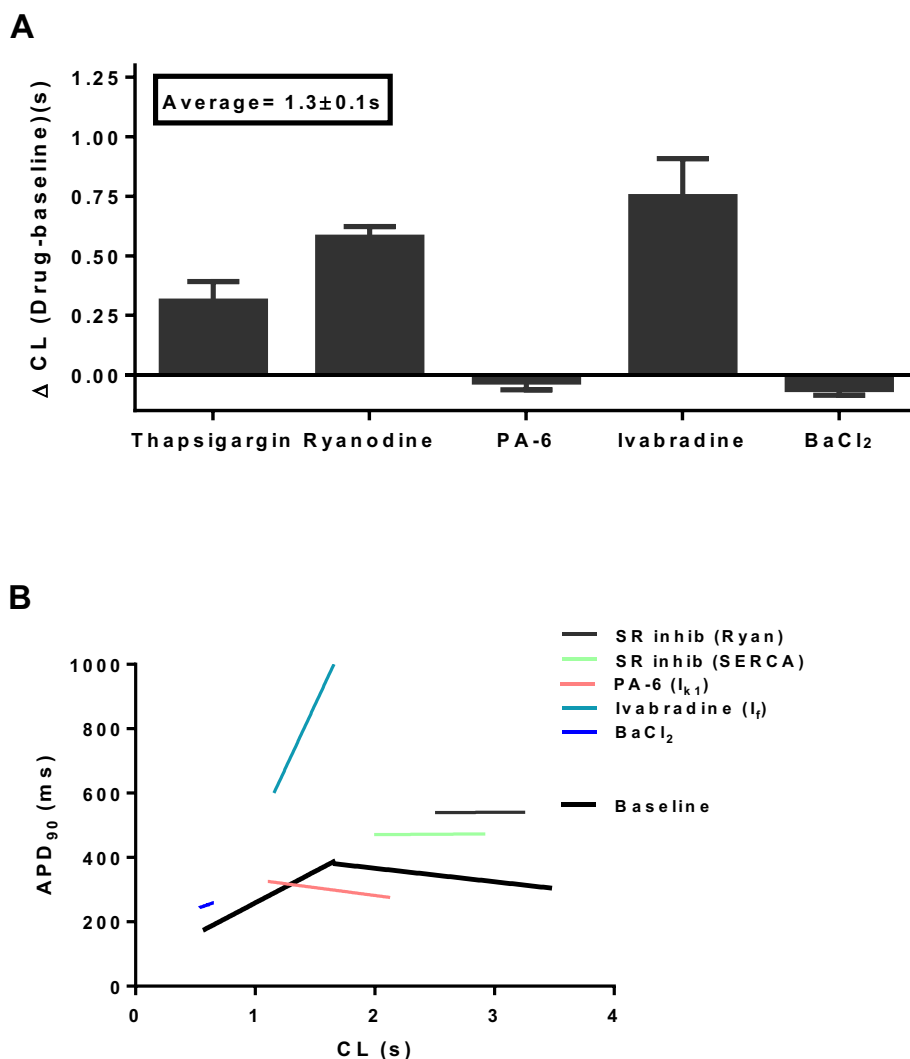


**Figure 6.1 - Different ion channel blockers elicit different effects on CL and APD<sub>90</sub>.** A) The effect of the drug on CL was subtracted from CL baseline. Average value for CL in hiPSC-CMs was  $1.3 \pm 0.1$  s; B) CL vs APD<sub>90</sub> plot. Baseline obtained from hiPSC-CMs from all experimental work (black) was used to assess the standard effects on APD at different CLs. SERCA (thapsigargin) and ryanodine receptor (ryanodine) inhibition results were plotted, along with I<sub>k1</sub> block (PA-6), I<sub>f</sub> (ivabradine) and non-specific I<sub>k1</sub> blocker (BaCl<sub>2</sub>) to establish a comparison.

When the drug effect on CL was plotted as  $\Delta CL = Drug\ effect - Baseline$  it is possible to see the changes in this variable (Figure 6.1A).

To further inspect the effects of the drugs used for different channel blocking the CL all data was plotted as CL vs APD<sub>90</sub> (Figure 6.1B). A plot of the baseline showed that CLs vary greatly in hiPSC-CMs and can range from ~0.5s to ~3.5s depending on factors such as days in culture. From 0.5 to 1.5s APD<sub>90</sub> increases steeply but stabilises at higher CLs and even starts decreasing slightly. When SR was inhibited either by SERCA or Ryanodine receptor inhibition the CL lengthened, and APD<sub>90</sub> prolonged to an extent expected with the prolongation of CL. Ivabradine prolonged CL but had an additional effect on APD<sub>90</sub> beyond that expected from CL alone. The latter effect could be due to the non-specific effects of ivabradine on repolarising currents including I<sub>kr</sub>. Inhibition of I<sub>k1</sub> via PA-6 and BaCl<sub>2</sub> had minimal effects on spontaneous rate and APD. These effects show the extent to which the CL is affected by different ionic channels. Literature reports that I<sub>f</sub> and I<sub>k1</sub> exist in either small densities, or not at all (Kane et al., 2015a). These results have implications for mechanisms underlying spontaneous activity in hiPSC-CMs, and relative contribution of background ionic currents, and show that there appears to be no functional I<sub>k1</sub> as part of the background currents. I<sub>f</sub> appears to have a significant role in spontaneous rates in commercial hiPSC-CMs alongside a role for Ca<sup>2+</sup> cycling via the SR. These results, along with parallel studies in sino-atrial nodal cells, showed an interaction between I<sub>f</sub> and Ca<sup>2+</sup> cycling in mechanisms for spontaneous activity.

In agreement with literature, the current study shows that the contribution of the SR to EC-coupling is minimal and that the inhibition of SR significantly slows the rate of rise and decay of Ca<sup>2+</sup> (see Ch.3) (Itzhaki et al., 2011). The overall picture supports the view that addition of I<sub>k1</sub> would be an important supplement to background physiology that would inevitably reduce spontaneous rate of the preparation, but the effect on APD is uncertain. Computer simulations and dynamic clamping of single cells suggest that I<sub>k1</sub> injection led to AP shortening (Verkerk et al.). Interestingly when I<sub>k1</sub> is expressed in HEK with mRNA transfection the APD was prolonged.

### 6.3 Co-culture of hiPSC-CMs with I<sub>k1</sub>-HEK

In an effort to develop techniques to regulate I<sub>k1</sub> in hiPSC-CMs, studies were done to investigate co-culture with an I<sub>k1</sub>-HEK cell line. Low relative amounts of HEK in co-

culture with hiPSC-CMs appear to have no significant effects on electrophysiology and contractility. However, at a 1:1 HEK:hiPSC ratio, effects were observed in both mechanical and electrical behaviour. When the co-culture involved  $I_{K1}$ -expressing HEK the effects on spontaneous rate were observed at 1:3 but were strongest at 1:1 even after allowances for effects of untransfected HEK.

The most notable effect was prolongation of interval (Figure 4.18A and Figure 4.19A), and occasional quiescence. This is consistent with a functional  $I_{K1}$  hyperpolarising the membrane potential and counteracting the effect of cellular mechanisms of spontaneous electrical activity.

Within the intact myocardium the fibroblasts are normally present in higher numbers to cardiomyocytes (Fan et al., 2012), but in this study co-culture with HEK cells were necessary as this was the only cell line available stably expressing  $I_{K1}$ . As shown in Figure 4.18, there were no effects of co-culture with HCF and untransfected HEK, it was only when  $I_{K1}$  was overexpressed that effects were seen. The latter effects suggest that electrical links between the two cell types were present. Measurements of contractility (Figure 4.19) indicate that co-culture with HCF has no significant effects while co-culture with HEK substantially reduced the movement signal interpreted as contraction (regardless of  $I_{K1}$  expression or not). The reason for the differences is unknown and requires further investigation. Some of the possible reasons for the marked differences between HEK and HCF are:

- Different mechanical properties of cells
- Different degree of coupling between cell types
- The co-culture changes the contractile phenotype of hiPSC-CMs
- Mechanical interactions between cells may limit the extent of movement associated with contraction.

## **6.4 Connexin overexpression in HEK293 does not alter electrophysiology in co-culture**

In an effort to improve electrical coupling between HEK and hiPSC-CMs to address the concern that this may be limiting the ability of HEK- $I_{K1}$  to alter hiPSC-CMs

electrophysiology, a strategy was developed to overexpress Cx43 in HEK cells. Increasing Cx43 protein did not affect electrophysiological behaviour beyond that seen with normal HEK cells, suggesting that: either (i) Cx43 and electrical coupling was not limiting in normal HEK co-culture; or (ii) although Cx43 protein was identified in HEK cells that protein was not functional – further work would be required to show that Cx43 overexpression successfully increased connexion function between HEK- $I_{k1}$  and hiPSC-CMs.

## 6.5 Co-culture affects Signal-to-noise ratio

The extent to which both HEK cells were electrically coupled was assessed indirectly by the size of the FluoVolt signal in different co-culture conditions. The data suggest that co-culture resulted in the loss of AP amplitude in relative terms, as would be expected from dye with non-specific membrane binding properties linked to a mixed population of excitable cells. Surprisingly the 1:1 culture with  $I_{k1}$ -HEK showed even smaller amplitudes than that in co-culture with the non- $I_{k1}$  cell line. This last result suggests that overexpression of  $I_{k1}$  reduced the amplitude of the AP in hiPSC-CMs which accompanies the change in AP shape.

The signal intensity represents the amount of dye in the cell in the field of view. When the signal intensity increases, so does signal-to-noise (SNR). This is a result of measuring function using photomultipliers (PMTs) which produces a signal that is Poisson distributed. Poisson noise is characterised by having a variance that is directly proportional to the amplitude of the signal.

As shown in Appendix, a separate analysis of the signals was performed to compare the amplitude of the AP signal with the associated noise. The amplitude of the signal measured from the base of the AP to the peak relative to the total fluorescence signal is a direct representation of fraction of the membrane responding with an action potential. In parallel experiments, the PMT signal was calibrated in terms of photon flux (photons/sec) based on the relationship between signal magnitude and associated variance of the noise (see Appendix). As a consequence of these measurements, signal amplitude was compared with the magnitude of the total fluorescence to estimate the fraction of the membrane signal supporting an action potential. The signal amplitude was smaller in 1:1 co-culture of HEK expressing  $I_{k1}$  with hiPSC-CMs (1:1 $I_{k1}$ ) ( $24.2 \pm 3.4$  photon/pixel) compared to 1:1 co-

culture of standard HEK with hiPSC-CMs (1:1N) ( $51.3 \pm 2.6$  photon/pixel). A smaller AP amplitude was also seen in 1:1N compared to hiPSC-CMs ( $63.7 \pm 3.3$  photon/pixel) (Supplementary figure 3B).

The amplitude of the noise (Figure 2.11) was measured for all three cultures. This variable is directly proportional to the amount of membrane due to the Poisson nature of the PMT signal. It was shown that the amplitude of the noise was larger in co-culture, where for 1:1 $I_{k1}$  it was  $78.5 \pm 1.5$  photon/pixel and  $82.5 \pm 1.3$  photon/pixel for 1:1N. The amplitude of the noise in hiPSC-CMs is  $65.7 \pm 0.9$  photon/pixel (**Error! Reference source not found. 3 C**). Since the number of cells is equal in both co-culture conditions, the number of cells are equal and approximately twice that in iPSC-alone, this suggests that there were more membranes available for staining in co-culture, but the total staining was less than that expected assuming the cells were of equal size. But for  $I_{k1}$  and N groups, total staining was approximately the same. One simple explanation for the lack of proportionality associated with total cell number is simply that HEK cells were smaller in volume than iPSC-CMs.

An alternative explanation is that the dye was not being taken into the membrane in HEK cells to the same extent as iPSC-CMs. The effects on amplitude and noise amplitude were used to study SNR of the AP. This showed that SNR is much lower in co-culture, especially in  $I_{k1}$ . The analysis of SNR relative to AP size suggests that the AP amplitude is smaller in the  $I_{k1}$ :hiPSC co-culture than in a culture with normal HEK cells. This suggests that the presence of  $I_{k1}$  affects the amplitude of the AP signal within the hiPSC-CMs. This, along with the change in AP shape, suggests that electrical coupling between the two cell types was sufficient to modulate the hiPSC-CM electrophysiology.

## 6.6 Conclusion

The mechanisms which lead to spontaneous activity in hiPSC-CMs are still unknown. The absence of a functional  $I_{k1}$  would contribute to an unstable membrane potential but cannot account for the full mechanism. When  $I_{k1}$  was externally added via HEK, it induced a slowing of the spontaneous rate, but did not halt it completely. There is evidence for the contribution of the  $Ca^{2+}$  clock and for a role for  $I_f$ . It is likely that the contribution of these three factors varies in different cell brands of hiPSC-CMs and differentiation protocols. In summary, co-culture of hiPSC-CMs with  $I_{k1}$ -HEK provides an alternative way of

introducing  $I_{K1}$  into the immature hiPSC-CMs, but not without consequences. Incorporation can be done in a controlled manner, by changing the cell density, but higher densities affect other aspects of electrophysiology and SNR of potentiometric dyes. A more suitable cell type for this co-culture approach may be HCF.

This work has studied, using pharmacological tools, the contribution of different ionic currents and channels to spontaneous activity in hiPSC-CMs. It was also pioneer in co-culturing hiPSC-CMs and HEK, for which there are consequences.

## **6.7 Future directions**

### **6.7.1 Co-culture strategies**

Future work should look to develop more natural co-cultures with  $I_{K1}$ -expressing cells, for example using fibroblasts, as the latter are naturally present in the adult heart. The data suggested that knowledge of the overall electrical characteristics of the cell are important in predicting the outcome of co-culture. Thus future work should include assessment of whole cell electrophysiology with and without additional components such as  $I_{K1}$ . Important additional information will come from techniques that allow separate voltage measurements in fibroblasts and cardiomyocytes.

### **6.7.2 Expression strategies**

Methods for the monitoring and manipulation of specific proteins need revision and improvement: (i) key experiments in the future should look further into methods of efficient transfection of hiPSC-CMs; (ii) techniques that allow accurate quantification of expression of mRNA or protein; (iii) direct measurement of cell-to-cell coupling for hiPSC-CMs to fibroblasts would give insight into how these two cell types interact.

### **6.7.3 Alternative geometries of cells in culture**

3D structures are getting more attention due to their relevance for comparison with adult heart morphology (Archer et al., 2018, Scuderi and Butcher, 2017). For co-culture to be viable for a 3D model, the effects of coupling with  $I_{K1}$  in a larger scale model would need to be studied.

#### **6.7.4 Methods to control spontaneous rate**

The consequence of successfully coupling a slave-cell containing  $I_{k1}$  and hiPSC-CMs is that spontaneous rate is decreased, and chronically this could have de-differentiation effects on hiPSC-CMs. This side effect can be solved in the longer term by electrically stimulating these cells using optogenetic strategies.

## Appendix

The signal-to-noise ratio (SNR) is the amplitude squared of a signal or the signal variance divided by the variance of the system noise. However, the standard concept of SNR cannot be applied to the cardiac action potential as these are electrical discharges. The Poisson regression model is suitable for studying the SNR for non-Gaussian systems because it provides an analogue of the square of the multiple correlation coefficient ( $R^2$ ) used to measure the goodness of the fit in linear regression analysis (Czanner et al., 2015).

At low light levels and high sample rates, noise due to statistical fluctuations in light emission/collection becomes more evident. This phenomenon is called photon noise – the inherent natural variation of the incident photon flux (Macquaide, 2004). Variation in the signal when measuring light follows a Poisson distribution which is similar to a normal or Gaussian distribution, except it is for discrete values, rather than continuous ones, and applies only to non-negative quantities. A Poisson distribution has the property that its variance is equal to its mean:

$$\sigma^2 = \mu$$

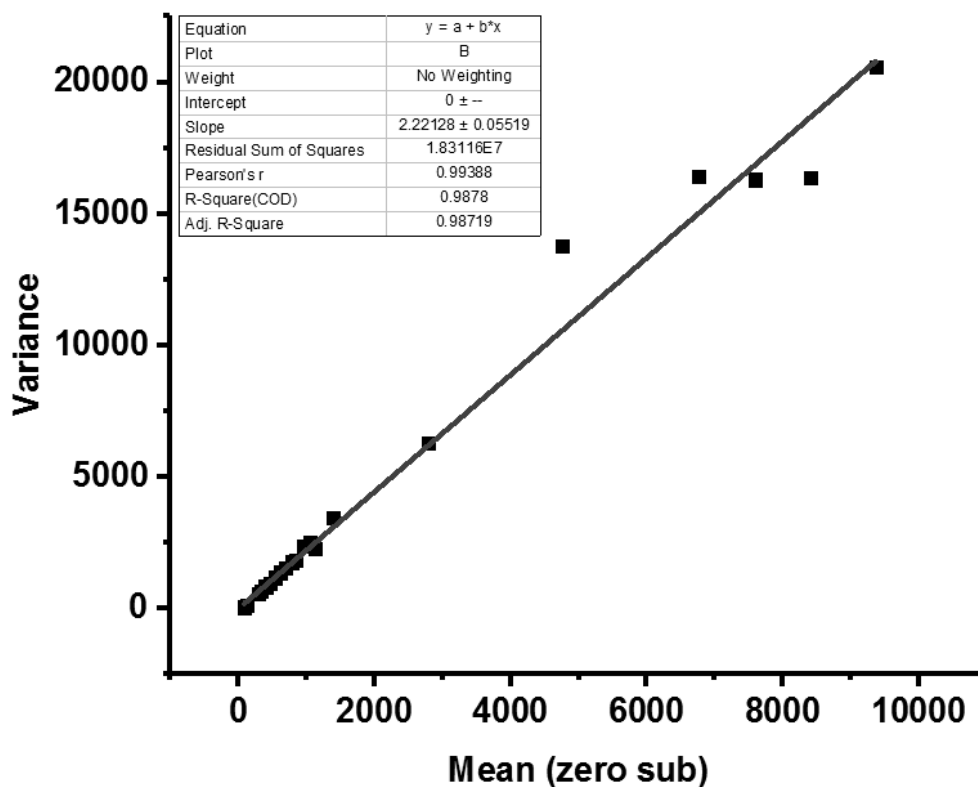
Thus, it can be assumed that the histogram of the signal from one pixel over time will be Poisson distributed. To achieve this, the signal must first be converted to photons/pixel (Macquaide, 2004).

It is important to notice that variance is not equal to mean amplitude because this is not measured in terms of photons.

### Poisson distribution of fluorescence

#### Poisson distribution

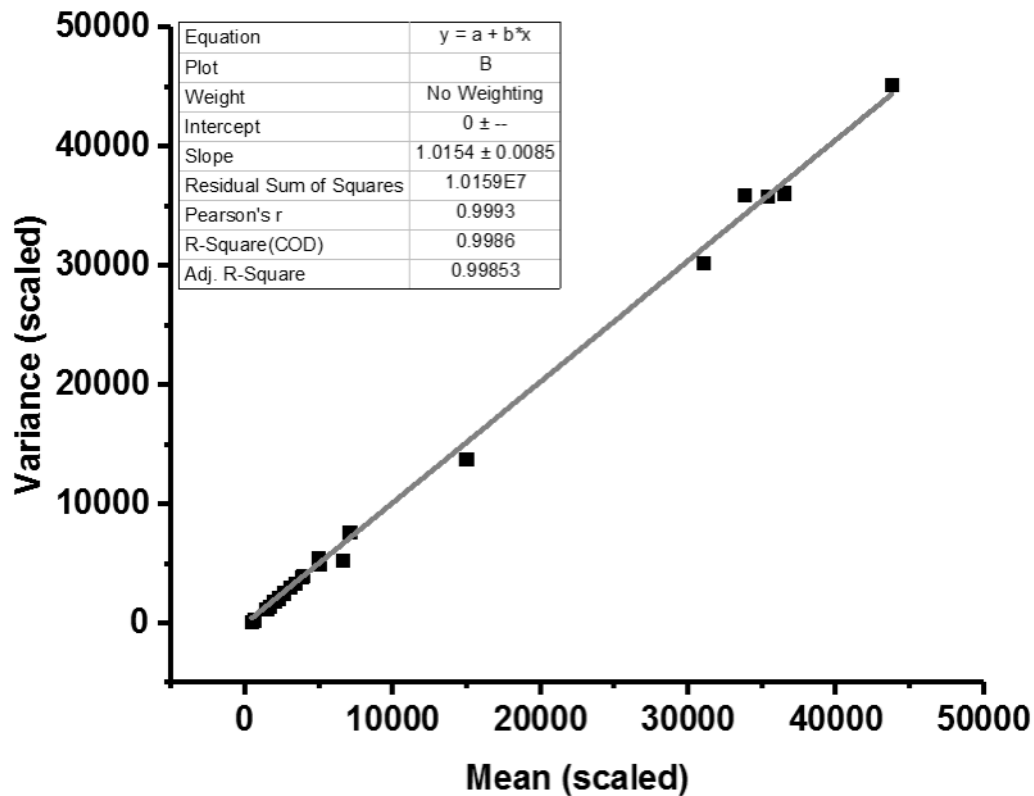
Measurements taken with fluorescein for measuring the system's noise were plotted as mean (zero subtracted) vs variance. A linear regression line was fitted and a slope of  $2.22 \pm 0.06$  ( $n=4$ ) was obtained (Supplementary figure 1).



**Supplementary Figure 1 - Variance vs Mean (zero sub).** Data was obtained from increasing fluorescein concentrations. The control (or zero value) was obtained from measuring water. Graph showing change in variance with increasing signal amplitude. The grey line shows the best fit for this relationship. This yields an estimated conversion factor of  $2.22 \pm 0.06$ .

It is now possible to use this conversion factor to calculate the number of photons collected per pixel.

The slope from Supplementary figure 1 was then used to correct both the variance and the mean, thus referred to as variance scaled and mean scaled. When this conversion factor is applied, and data is re-graphed, a slope of 1 is achieved (Supplementary figure 2).



**Supplementary Figure 2 – Variance (scaled) vs Mean (scaled).** Applying the slope (2.22) as a correction factor will create a slope of 1, where  $\sigma^2 = \mu$ .

The application of this conversion factor means the data is now expressed as photons/pixel (Macquaide, 2004).

This correction factor can now be applied to data obtained from CelLOPTIQ, which means it will be corrected for Poisson noise.

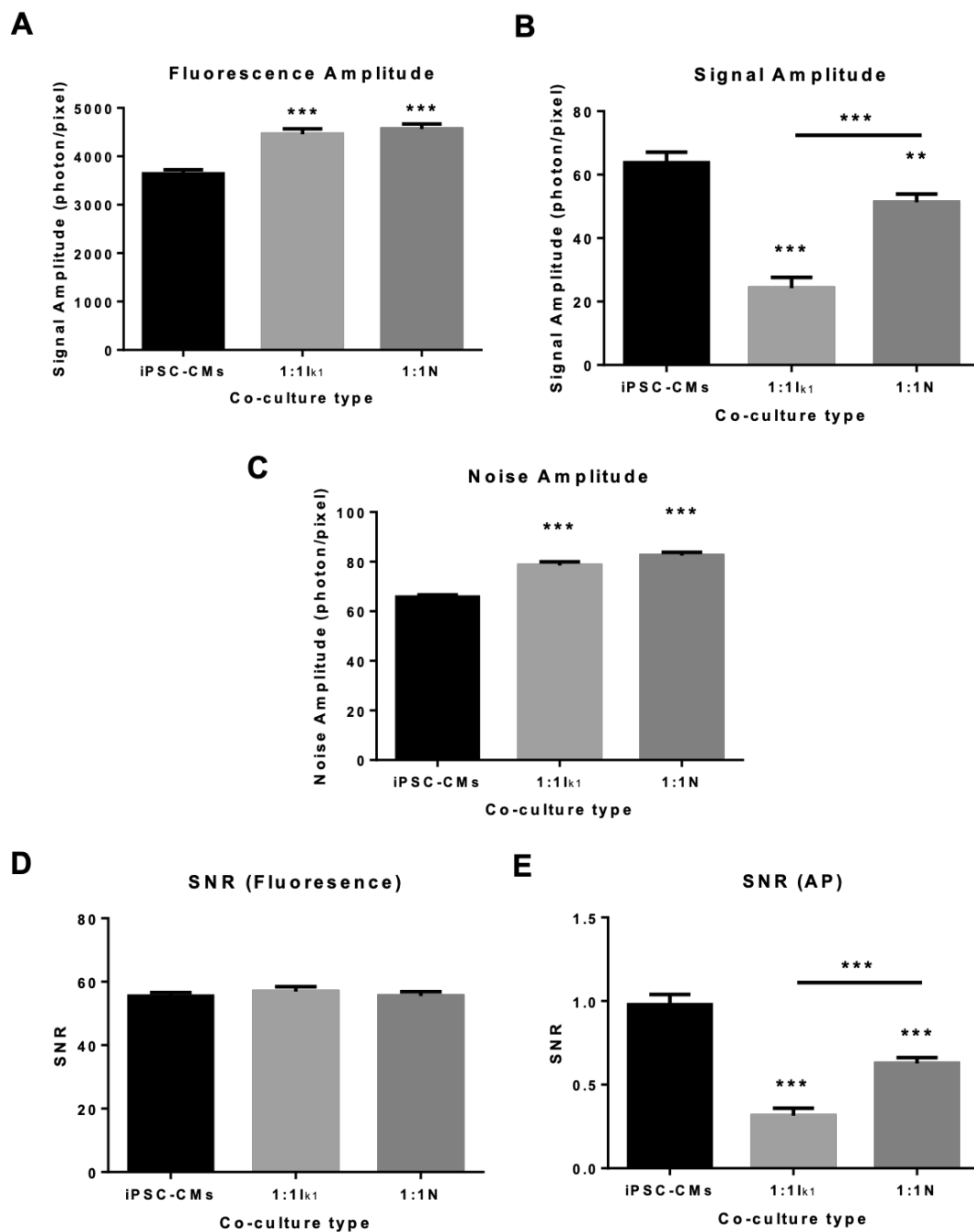
### Signal to noise

When hiPSC-CMs are co-cultured with HEK cells at 1:1 there are consequences not only to electrophysiology but also to the SNR. This is especially visible in 1:1 $I_{k1}$  co-culture (Figure 4.20), but also in 1:1N to a smaller extent.

The fluorescence amplitude was measured from zero to the value reached once the light was on (Figure 2.11). This was larger in co-culture, where the value obtained in  $I_{k1}$  was  $4456 \pm 115$  photon/pixel and  $4565 \pm 103$  photon/pixel in Normal, compared to hiPSC-CMs ( $3641 \pm 82$  photon/pixel) (Supplementary figure 3A).

The SNR was calculated for the fluorescence magnitude in the different types of co-culture. SNR (fluo) did not change (Supplementary figure 3D).

The SNR for the AP shows that the values are much smaller for 1:1I<sub>k1</sub> co-culture where they are  $0.3 \pm 0.05$  compared to hiPSC-CMs ( $0.9 \pm 0.06$ ) and 1:1N ( $0.6 \pm 0.04$ ). Comparing the two different co-cultures, it is clear that 1:1I<sub>k1</sub> is also smaller than 1:1N (Supplementary figure 3E).



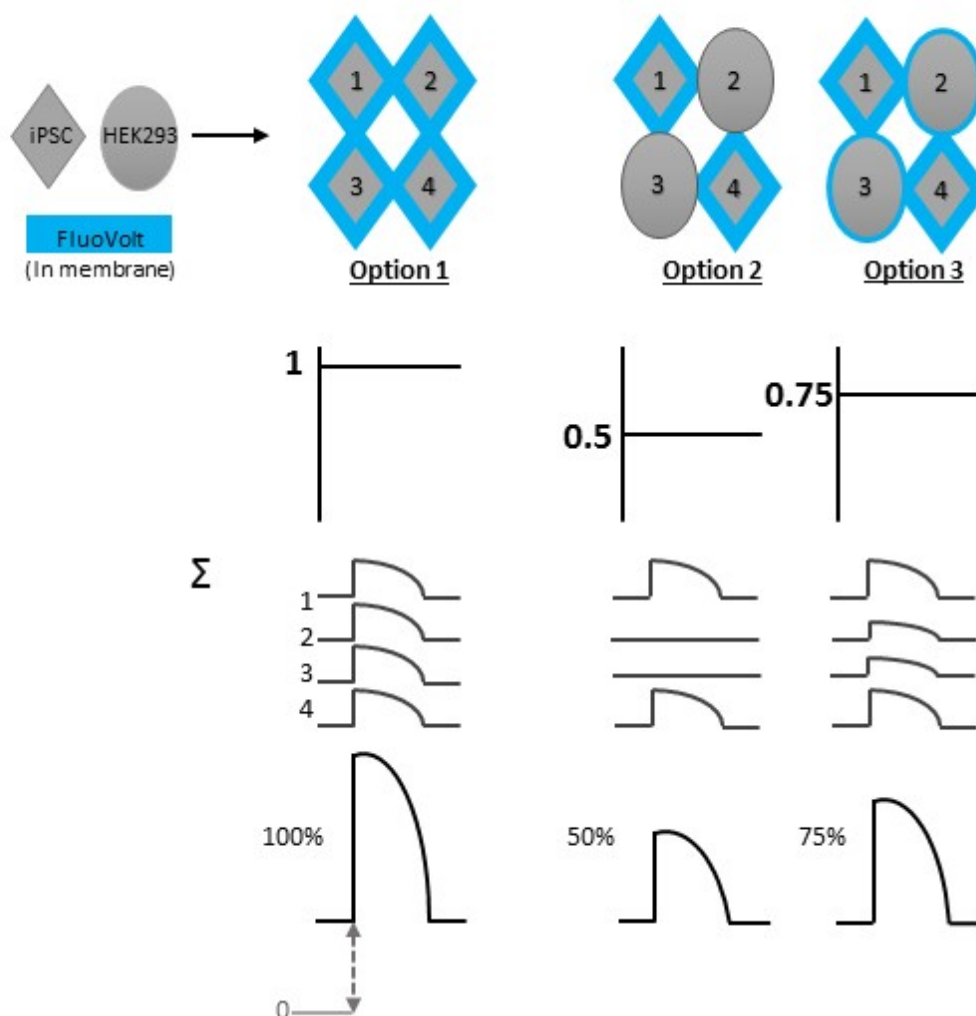
**Supplementary Figure 3– SNR obtained from analysing voltage traces from co-cultures with  $I_{K1}$ -HEK and N-HEK compared to that from hiPSC-CM culture. A) Amplitude of the baseline fluorescence when the light is on, measured from zero to the resting phase of the AP; B) The amplitude of the signal/AP measured from baseline to peak of AP; C) Amplitude of the noise in baseline; D) SNR of the fluorescence; D) SNR of the AP. Unpaired t-test comparing co-culture to hiPSC-CMs, and between different co-cultures; \*\*\* $p < 0.001$ , \*\* $p < 0.01$ ,  $n = 16$  (Corrected for Poisson noise).**

The increased fluorescence (fluorescence amplitude) is a demonstration of the higher cell number in culture.

The effects seen on SNR(AP) show that when  $I_{k1}$  is introduced to a co-culture with hiPSC-CMs the SNR is lower, which translates into noisier signals. This effect is also seen in N-HEK although to a smaller extent. This is related to the effects seen on signal amplitude and to noise amplitude, where the latter was larger in co-culture. This indicates that either the  $I_{k1}$  co-culture increased AP amplitude in hiPSC-CMs or the HEK cells with  $I_{k1}$  are better coupled to hiPSC-CMs.

### **Interpretation of changes in SNR**

Measuring the photon noise led to a conversion factor which can now be applied to future measurements to help obtain more accurate results which take the photon/pixel into account.



**Supplementary Figure 4 – AP amplitudes are affected in co-culture.** It is unknown how much dye hiPSC-CM and HEK membranes absorb and how this affects the AP. Option 1 suggests that the membranes of hiPSC-CMs take up dye, which results in every cell in the imaging field contributing towards the AP equally creating a large AP (AP at 100% of its height with fluorescence equal to 1). Option 2 refers to co-culture where HEK do not take up voltage-sensitive dye at all, leading to fluorescence being 0.5 and the AP amplitude only 50% of standard. Option 3 suggests that HEK might take up some dye, but to a smaller extent than hiPSC thus resulting in a slightly larger AP at 75% of its normal size.

SNR analysis shows that the AP amplitude is greatly affected in co-culture. The amplitude in  $I_{k1}$ -co-culture was smaller than that seen on normal co-culture, and even smaller than that in hiPSC-CMs. It is possible that the smaller amplitude in  $I_{k1}$  is related to option 2 (Supplementary figure 4), where the HEK membrane does not take up the voltage-sensitive dye, thus resulting in no contribution towards the amplitude. This would lead to a smaller AP. It was also observed that the AP obtained from normal co-culture is slightly larger than that in  $I_{k1}$ , but smaller than that in hiPSC-CMs. As such option 3 was stipulated where HEK membranes take up some dye, but to a smaller extent thus giving a smaller

contribution towards the AP. The reason for this remains unknown but there is strong evidence that it could be related to the dye uptake into the membrane.

## List of References

- Agullo-Pascual, E. & Delmar, M. 2012. The “non-canonical” functions of Cx43 in the heart. *The Journal of membrane biology*, 245, 477-482.
- Anumonwo, J. M. & Lopatin, A. N. 2010. Cardiac strong inward rectifier potassium channels. *J Mol Cell Cardiol*, 48, 45-54.
- Archer, C. R., Sargeant, R., Basak, J., Pilling, J., Barnes, J. R. & Pointon, A. 2018. Characterization and Validation of a Human 3D Cardiac Microtissue for the Assessment of Changes in Cardiac Pathology. *Scientific Reports*, 8, 10160.
- Avilion, A. A., Nicolis, S. K., Pevny, L. H., Perez, L., Vivian, N. & Lovell-Badge, R. 2003. Multipotent cell lineages in early mouse development depend on SOX2 function. *Genes Dev*, 17, 126-40.
- Bachtel, A. D., Gray, R. A., Stohlman, J. M., Bourgeois, E. B., Pollard, A. E. & Rogers, J. M. 2011. A novel approach to dual excitation ratiometric optical mapping of cardiac action potentials with di-4-ANEPPS using pulsed LED excitation. *IEEE Trans Biomed Eng*, 58, 2120-6.
- Bedada, Fikru b., Chan, Sunny s.-K., Metzger, Stefania k., Zhang, L., Zhang, J., Garry, Daniel j., Kamp, Timothy j., Kyba, M. & Metzger, Joseph m. 2014. Acquisition of a Quantitative, Stoichiometrically Conserved Ratiometric Marker of Maturation Status in Stem Cell-Derived Cardiac Myocytes. *Stem Cell Reports*, 3, 594-605.
- Bedut, S., Seminatore-Nole, C., Lamamy, V., Caignard, S., Boutin, J. A., Nosjean, O., Stephan, J. P. & Coge, F. 2016. High-throughput drug profiling with voltage- and calcium-sensitive fluorescent probes in human iPSC-derived cardiomyocytes. *Am J Physiol Heart Circ Physiol*, 311, H44-53.
- Bers, D. M. 2002. Cardiac excitation-contraction coupling. *Nature*, 415, 198-205.
- Bers, D. M. 2008. Calcium Cycling and Signaling in Cardiac Myocytes. *Annual Review of Physiology*, 70, 23-49.
- Bett, G. C. L., Kaplan, A. D., Lis, A., Cimato, T. R., Tzanakakis, E. S., Zhou, Q., Morales, M. J. & Rasmusson, R. L. 2013. Electronic “expression” of the inward rectifier in cardiocytes derived from human-induced pluripotent stem cells. *Heart Rhythm*, 10, 1903-1910.
- Blaustein, M. P. & Lederer, W. J. 1999. Sodium/calcium exchange: its physiological implications. *Physiol Rev*, 79, 763-854.
- Blumlein, A., Williams, N. & Mcmanus, J. J. 2017. The mechanical properties of individual cell spheroids. *Scientific Reports*, 7, 7346.
- Bois, P., Bescond, J., Renaudon, B. & Lenfant, J. 1996. Mode of action of bradycardic agent, S 16257, on ionic currents of rabbit sinoatrial node cells. *Br J Pharmacol*, 118, 1051-7.
- Bruce, A. F., Rothery S Fau - Dupont, E., Dupont E Fau - Severs, N. J. & Severs, N. J. Gap junction remodelling in human heart failure is associated with increased interaction of connexin43 with ZO-1.
- Bruce, A. F., Rothery S Fau - Dupont, E., Dupont E Fau - Severs, N. J. & Severs, N. J. 2008. Gap junction remodelling in human heart failure is associated with increased interaction of connexin43 with ZO-1.
- Bucchi, A., Baruscotti, M. & DiFrancesco, D. 2002. Current-dependent Block of Rabbit Sino-Atrial Node I(f) Channels by Ivabradine. *The Journal of General Physiology*, 120, 1-13.
- Cao, N., Liu, Z., Chen, Z., Wang, J., Chen, T., Zhao, X., Ma, Y., Qin, L., Kang, J., Wei, B., Wang, L., Jin, Y. & Yang, H.-T. 2012. Ascorbic acid enhances the cardiac differentiation of induced pluripotent stem cells through promoting the proliferation of cardiac progenitor cells. *Cell Res*, 22, 219-236.

- Caspi, O., Itzhaki, I., Kehat, I., Gepstein, A., Arbel, G., Huber, I., Satin, J. & Gepstein, L. 2009. In vitro electrophysiological drug testing using human embryonic stem cell derived cardiomyocytes. *Stem Cells Dev*, 18, 161-72.
- Citro, L., Naidu, S., Hassan, F., Kuppusamy, M. L., Kuppusamy, P., Angelos, M. G. & Khan, M. 2015. Comparison of Human Induced Pluripotent Stem-Cell Derived Cardiomyocytes with Human Mesenchymal Stem Cells following Acute Myocardial Infarction. *PLOS ONE*, 9, e116281.
- Cotrina, M. L., Lin, J. H. C. & Nedergaard, M. 2008. Adhesive Properties of Connexin Hemichannels. *Glia*, 56, 1791-1798.
- Czanner, G., Sarma, S. V., Ba, D., Eden, U. T., Wu, W., Eskandar, E., Lim, H. H., Temereanca, S., Suzuki, W. A. & Brown, E. N. 2015. Measuring the signal-to-noise ratio of a neuron. *Proceedings of the National Academy of Sciences*, 112, 7141.
- Da Rocha, A. M., Campbell, K., Mironov, S., Jiang, J., Mundada, L., Guerrero-Serna, G., Jalife, J. & Herron, T. J. 2017. hiPSC-CM Monolayer Maturation State Determines Drug Responsiveness in High Throughput Pro-Arrhythmia Screen. *Scientific Reports*, 7, 13834.
- Darr, H., Mayshar, Y. & Benvenisty, N. 2006. Overexpression of NANOG in human ES cells enables feeder-free growth while inducing primitive ectoderm features. *Development*, 133, 1193-201.
- De Boer, T. P., Nalos, L., Stary, A., Kok, B., Houtman, M. J., Antoons, G., Van Veen, T. A., Beekman, J. D., De Groot, B. L., Opthof, T., Rook, M. B., Vos, M. A. & Van Der Heyden, M. A. 2010. The anti-protozoal drug pentamidine blocks KIR2.x-mediated inward rectifier current by entering the cytoplasmic pore region of the channel. *Br J Pharmacol*, 159, 1532-41.
- De Boer, T. P., Van Veen, T. A., Houtman, M. J., Jansen, J. A., Van Amersfoorth, S. C., Doevendans, P. A., Vos, M. A. & Van Der Heyden, M. A. 2006. Inhibition of cardiomyocyte automaticity by electrotonic application of inward rectifier current from Kir2.1 expressing cells. *Med Biol Eng Comput*, 44, 537-42.
- Denning, C. & Anderson, D. 2008. Cardiomyocytes from human embryonic stem cells as predictors of cardiotoxicity. *Drug Discovery Today: Therapeutic Strategies*, 5, 223-232.
- Denning, C., Borgdorff, V., Crutchley, J., Firth, K. S. A., George, V., Kalra, S., Kondrashov, A., Hoang, M. D., Mosqueira, D., Patel, A., Prodanov, L., Rajamohan, D., Skarnes, W. C., Smith, J. G. W. & Young, L. E. 2016. Cardiomyocytes from human pluripotent stem cells: From laboratory curiosity to industrial biomedical platform(). *Biochimica et Biophysica Acta*, 1863, 1728-1748.
- Dhamoon, A. S. & Jalife, J. 2005. The inward rectifier current (IK1) controls cardiac excitability and is involved in arrhythmogenesis. *Heart Rhythm*, 2, 316-324.
- Difrancesco, D. 1981a. A new interpretation of the pace-maker current in calf Purkinje fibres. *J Physiol*, 314, 359-76.
- Difrancesco, D. 1981b. A study of the ionic nature of the pace-maker current in calf Purkinje fibres. *The Journal of Physiology*, 314, 377-393.
- Difrancesco, D. 1993. Pacemaker Mechanisms in Cardiac Tissue. *Annual Review of Physiology*, 55, 455-472.
- Difrancesco, D. 2010. The Role of the Funny Current in Pacemaker Activity. *Circulation Research*, 106, 434-446.
- Difrancesco, D. & Tortora, P. 1991. Direct activation of cardiac pacemaker channels by intracellular cyclic AMP. *Nature*, 351, 145-7.
- Dillmann, W. H. 2002. Cellular action of thyroid hormone on the heart. *Thyroid*, 12, 447-52.
- Doss, M. X., Di Diego, J. M., Goodrow, R. J., Wu, Y., Cordeiro, J. M., Nesterenko, V. V., Barajas-Martinez, H., Hu, D., Urrutia, J., Desai, M., Treat, J. A., Sachinidis, A. & Antzelevitch, C. 2012. Maximum Diastolic Potential of Human Induced Pluripotent Stem Cell-Derived Cardiomyocytes Depends Critically on I<sub>Kr</sub>. *PLoS ONE*, 7, e40288.

- Du, D. T., Hellen, N., Kane, C. & Terracciano, C. M. 2015. Action potential morphology of human induced pluripotent stem cell-derived cardiomyocytes does not predict cardiac chamber specificity and is dependent on cell density. *Biophys J*, 108, 1-4.
- Eng, G., Lee, B. W., Protas, L., Gagliardi, M., Brown, K., Kass, R. S., Keller, G., Robinson, R. B. & Vunjak-Novakovic, G. 2016. Autonomous beating rate adaptation in human stem cell-derived cardiomyocytes. *Nat Commun*, 7, 10312.
- Fan, D., Takawale, A., Lee, J. & Kassiri, Z. 2012. Cardiac fibroblasts, fibrosis and extracellular matrix remodeling in heart disease. *Fibrogenesis & Tissue Repair*, 5, 15-15.
- Fares, N., Bois, P., Lenfant, J. & Potreau, D. 1998. Characterization of a hyperpolarization-activated current in dedifferentiated adult rat ventricular cells in primary culture. *J Physiol*, 506 (Pt 1), 73-82.
- Fujiwara, M., Yan, P., Otsuji, T. G., Narazaki, G., Uosaki, H., Fukushima, H., Kuwahara, K., Harada, M., Matsuda, H., Matsuoka, S., Okita, K., Takahashi, K., Nakagawa, M., Ikeda, T., Sakata, R., Mummery, C. L., Nakatsuji, N., Yamanaka, S., Nakao, K. & Yamashita, J. K. 2011. Induction and Enhancement of Cardiac Cell Differentiation from Mouse and Human Induced Pluripotent Stem Cells with Cyclosporin-A. *PLoS ONE*, 6, e16734.
- Gewirtz, H. 2009. 'Funny' current: If heart rate slowing is not the best answer, what might be? *Cardiovasc Res*, 84, 9-10.
- Gibson, J. K., Yue, Y., Bronson, J., Palmer, C. & Numann, R. 2014. Human stem cell-derived cardiomyocytes detect drug-mediated changes in action potentials and ion currents. *Journal of Pharmacological and Toxicological Methods*, 70, 255-267.
- Giles, Wayne r. & Noble, D. 2015. Rigorous Phenotyping of Cardiac iPSC Preparations Requires Knowledge of Their Resting Potential(s). *Biophysical Journal*, 110, 278-280.
- Gintant, G., Sager, P. T. & Stockbridge, N. 2016. Evolution of strategies to improve preclinical cardiac safety testing. *Nature Reviews Drug Discovery*, 15, 457.
- Goversen, B., Van Der Heyden, M. A. G., Van Veen, T. A. B. & De Boer, T. P. 2017. The immature electrophysiological phenotype of iPSC-CMs still hampers in vitro drug screening: Special focus on IK1. *Pharmacology & Therapeutics*.
- Grynkiewicz, G., Poenie, M. & Tsien, R. Y. 1985. A new generation of Ca<sup>2+</sup> indicators with greatly improved fluorescence properties. *J Biol Chem*, 260, 3440-50.
- Hayakawa, T., Kunihiro, T., Ando, T., Kobayashi, S., Matsui, E., Yada, H., Kanda, Y., Kurokawa, J. & Furukawa, T. 2014. Image-based evaluation of contraction-relaxation kinetics of human-induced pluripotent stem cell-derived cardiomyocytes: Correlation and complementarity with extracellular electrophysiology. *J Mol Cell Cardiol*.
- Herron, T. J., Rocha, A. M. D., Campbell, K., Ponce-Balbuena, D., Willis, B. C., Guerrero-Serna, G., Liu, Q., Klos, M., Musa, H., Zarzoso, M., Bizy, A., Furness, J., Anumonwo, J., Mironov, S. & Jalife, J. 2016. Extracellular Matrix Mediated Maturation of Human Pluripotent Stem Cell Derived Cardiac Monolayer Structure and Electrophysiological Function. *Circulation. Arrhythmia and electrophysiology*, 9, 10.1161/CIRCEP.113.003638 e003638.
- Herum, K. M., Choppe, J., Kumar, A., Engler, A. J. & Mcculloch, A. D. 2017. Mechanical regulation of cardiac fibroblast profibrotic phenotypes. *Molecular Biology of the Cell*, 28, 1871-1882.
- Himmel, H. M. 2013. Drug-induced functional cardiotoxicity screening in stem cell-derived human and mouse cardiomyocytes: Effects of reference compounds. *Journal of Pharmacological and Toxicological Methods*, 68, 97-111.
- Hoeker, G. S., Skarsfeldt, M. A., Jespersen, T. & Poelzing, S. 2017. Electrophysiologic effects of the I(K) (1) inhibitor PA-6 are modulated by extracellular potassium in isolated guinea pig hearts. *Physiological Reports*, 5, e13120.

- Hoekstra, M., Mummery, C. L., Wilde, A. A., Bezzina, C. R. & Verkerk, A. O. 2012. Induced pluripotent stem cell derived cardiomyocytes as models for cardiac arrhythmias. *Front Physiol*, 3, 346.
- Hoppe, U. C., Jansen, E., Sudkamp, M. & Beuckelmann, D. J. 1998. Hyperpolarization-activated inward current in ventricular myocytes from normal and failing human hearts. *Circulation*, 97, 55-65.
- Hwang, H. S., Kryshtal, D. O., Feaster, T. K., Sánchez-Freire, V., Zhang, J., Kamp, T. J., Hong, C. C., Wu, J. C. & Knollmann, B. C. 2015. Comparable calcium handling of human iPSC-derived cardiomyocytes generated by multiple laboratories. *Journal of Molecular and Cellular Cardiology*, 85, 79-88.
- Itskovitz-Eldor, J., Schuldiner, M., Karsenti, D., Eden, A., Yanuka, O., Amit, M., Soreq, H. & Benvenisty, N. 2000. Differentiation of human embryonic stem cells into embryoid bodies compromising the three embryonic germ layers. *Mol Med*, 6, 88-95.
- Itzhaki, I., Rapoport, S., Huber, I., Mizrahi, I., Zwi-Dantsis, L., Arbel, G., Schiller, J. & Gepstein, L. 2011. Calcium Handling in Human Induced Pluripotent Stem Cell Derived Cardiomyocytes. *PLoS ONE*, 6, e18037.
- Ivashchenko, C. Y., Pipes, G. C., Lozinskaya, I. M., Lin, Z., Xiaoping, X., Needle, S., Grygielko, E. T., Hu, E., Toomey, J. R., Lepore, J. J. & Willette, R. N. 2013. Human-induced pluripotent stem cell-derived cardiomyocytes exhibit temporal changes in phenotype. *Am J Physiol Heart Circ Physiol*, 305, H913-22.
- Jensen, J., Hyllner, J. & Bjorquist, P. 2009. Human embryonic stem cell technologies and drug discovery. *J Cell Physiol*, 219, 513-9.
- Jiang, Z., Han, Y. & Cao, X. 2014. Induced pluripotent stem cell (iPSCs) and their application in immunotherapy. *Cellular and Molecular Immunology*, 11, 17-24.
- Jones, K. T. & Sharpe, G. R. 1994. Thapsigargin Raises Intracellular Free Calcium Levels in Human Keratinocytes and Inhibits the Coordinated Expression of Differentiation Markers. *Experimental Cell Research*, 210, 71-76.
- Jonsson, M. K., Vos, M. A., Mirams, G. R., Duker, G., Sartipy, P., De Boer, T. P. & Van Veen, T. A. 2012. Application of human stem cell-derived cardiomyocytes in safety pharmacology requires caution beyond hERG. *J Mol Cell Cardiol*, 52, 998-1008.
- Jonsson, M. K. B., Van Veen, T. A. B., Goumans, M.-J., Vos, M. A., Duker, G. & Sartipy, P. 2009. Improvement of cardiac efficacy and safety models in drug discovery by the use of stem cell-derived cardiomyocytes. *Expert Opinion on Drug Discovery*, 4, 357-372.
- Kane, C., Couch, L. & Terracciano, C. M. 2015a. Excitation-contraction coupling of human induced pluripotent stem cell-derived cardiomyocytes. *Frontiers in Cell and Developmental Biology*, 3.
- Kane, C., Couch, L. & Terracciano, C. M. N. 2015b. Excitation-contraction coupling of human induced pluripotent stem cell-derived cardiomyocytes. *Frontiers in Cell and Developmental Biology*, 3.
- Ke, Q., Li, L., Yao, X., Lai, X., Cai, B., Chen, H., Chen, R., Zhai, Z., Huang, L., Li, K., Hu, A., Mao, F. F., Xiang, A. P., Tao, L. & Li, W. 2017. Enhanced generation of human induced pluripotent stem cells by ectopic expression of Connexin 45. *Scientific Reports*, 7, 458.
- Kelly, A., Salerno, S., Connolly, A., Bishop, M., Charpentier, F., Stølen, T. & Smith, G. L. 2018. Normal interventricular differences in tissue architecture underlie right ventricular susceptibility to conduction abnormalities in a mouse model of Brugada syndrome. *Cardiovascular Research*, 114, 724-736.
- Khan, J. M., Lyon, A. R. & Harding, S. E. 2013. The case for induced pluripotent stem cell-derived cardiomyocytes in pharmacological screening. *British Journal of Pharmacology*, 169, 304-317.

- Kirkton, R. D. & Bursac, N. 2011. Engineering biosynthetic excitable tissues from unexcitable cells for electrophysiological and cell therapy studies. *Nature Communications*, 2, 300.
- Klein, I. & Ojamaa, K. 2001. Thyroid hormone and the cardiovascular system. *New England Journal of Medicine*, 344, 501-509.
- Kruger, M., Sachse, C., Zimmermann, W. H., Eschenhagen, T., Klede, S. & Linke, W. A. 2008. Thyroid hormone regulates developmental titin isoform transitions via the phosphatidylinositol-3-kinase/ AKT pathway. *Circ Res*, 102, 439-47.
- Kuznetsova, T. G., Starodubtseva, M. N., Yegorenkov, N. I., Chizhik, S. A. & Zhdanov, R. I. 2007. Atomic force microscopy probing of cell elasticity. *Micron*, 38, 824-833.
- Lahmers, S., Wu, Y., Call, D. R., Labeit, S. & Granzier, H. 2004. Developmental control of titin isoform expression and passive stiffness in fetal and neonatal myocardium. *Circ Res*, 94, 505-13.
- Lahti, A. L., Kujala, V. J., Chapman, H., Koivisto, A. P., Pekkanen-Mattila, M., Kerkela, E., Hyttinen, J., Kontula, K., Swan, H., Conklin, B. R., Yamanaka, S., Silvennoinen, O. & Aalto-Setälä, K. 2012. Model for long QT syndrome type 2 using human iPS cells demonstrates arrhythmogenic characteristics in cell culture. *Dis Model Mech*, 5, 220-30.
- Larsen, A. P., Sciuto, K. J., Moreno, A. P. & Poelzing, S. 2012. The voltage-sensitive dye di-4-ANEPPS slows conduction velocity in isolated guinea pig hearts. *Heart rhythm : the official journal of the Heart Rhythm Society*, 9, 1493-1500.
- Lattanzio, F. A., Jr., Schlatterer, R. G., Nicar, M., Campbell, K. P. & Sutko, J. L. 1987. The effects of ryanodine on passive calcium fluxes across sarcoplasmic reticulum membranes. *J Biol Chem*, 262, 2711-8.
- Lees-Miller, J. P., Guo, J., Wang, Y., Perissinotti, L. L., Noskov, S. Y. & Duff, H. J. 2015. Ivabradine prolongs phase 3 of cardiac repolarization and blocks the hERG1 (KCNH2) current over a concentration-range overlapping with that required to block HCN4.
- Li, Y., McClintick, J., Zhong, L., Edenberg, H. J., Yoder, M. C. & Chan, R. J. 2005. Murine embryonic stem cell differentiation is promoted by SOCS-3 and inhibited by the zinc finger transcription factor Klf4. *Blood*, 105, 635-7.
- Luo, C. H. & Rudy, Y. 1991. A model of the ventricular cardiac action potential. Depolarization, repolarization, and their interaction. *Circulation Research*, 68, 1501-26.
- Lytton, J., Westlin, M. & Hanley, M. R. 1991. Thapsigargin inhibits the sarcoplasmic or endoplasmic reticulum Ca-ATPase family of calcium pumps. *J Biol Chem*, 266, 17067-71.
- Ma, J., Guo, L., Fiene, S. J., Anson, B. D., Thomson, J. A., Kamp, T. J., Kolaja, K. L., Swanson, B. J. & January, C. T. 2011a. High purity human-induced pluripotent stem cell-derived cardiomyocytes: electrophysiological properties of action potentials and ionic currents. *American Journal of Physiology-Heart and Circulatory Physiology*, 301, H2006-H2017.
- Ma, J., Guo, L., Fiene, S. J., Anson, B. D., Thomson, J. A., Kamp, T. J., Kolaja, K. L., Swanson, B. J. & January, C. T. 2011b. High purity human-induced pluripotent stem cell-derived cardiomyocytes: electrophysiological properties of action potentials and ionic currents. *American Journal of Physiology - Heart and Circulatory Physiology*, 301, H2006-H2017.
- Macquaide, N. 2004. *Spontaneous Ca<sup>2+</sup> waves in rabbit cardiac myocytes: a modelling study*. University of Glasgow.
- McLaren, A. 2001. Ethical and social considerations of stem cell research. *Nature*, 414, 129-131.
- Meissner, G. 1986. Ryanodine activation and inhibition of the Ca<sup>2+</sup> release channel of sarcoplasmic reticulum. *J Biol Chem*, 261, 6300-6.
- Myles, R. C., Wang, L., Bers, D. M. & Ripplinger, C. M. 2015. Decreased inward rectifying K(+) current and increased ryanodine receptor sensitivity synergistically contribute to sustained focal arrhythmia in the intact rabbit heart. *The Journal of Physiology*, 593, 1479-1493.

- Nakagawa, M., Koyanagi, M., Tanabe, K., Takahashi, K., Ichisaka, T., Aoi, T., Okita, K., Mochiduki, Y., Takizawa, N. & Yamanaka, S. 2008. Generation of induced pluripotent stem cells without Myc from mouse and human fibroblasts. *Nat Biotech*, 26, 101-106.
- Ncardia. 2014-2015. *Pluricyte® Cardiomyocytes* [Online]. Available: [https://ncardia.com/files/documents/manuals/PluricyteCardiomyocyte\\_Manual\\_v2.pdf](https://ncardia.com/files/documents/manuals/PluricyteCardiomyocyte_Manual_v2.pdf).
- Nie, Z., Hu, G., Wei, G., Cui, K., Yamane, A., Resch, W., Wang, R., Green, Douglas r., Tessarollo, L., Casellas, R., Zhao, K. & Levens, D. 2012. c-Myc Is a Universal Amplifier of Expressed Genes in Lymphocytes and Embryonic Stem Cells. *Cell*, 151, 68-79.
- Niwa, H., Miyazaki, J.-I. & Smith, A. G. 2000. Quantitative expression of Oct-3/4 defines differentiation, dedifferentiation or self-renewal of ES cells. *Nat Genet*, 24, 372-376.
- Opitz, C. A., Leake, M. C., Makarenko, I., Benes, V. & Linke, W. A. 2004. Developmentally regulated switching of titin size alters myofibrillar stiffness in the perinatal heart. *Circ Res*, 94, 967-75.
- Oyamada, M., Takebe, K. & Oyamada, Y. 2013. Regulation of connexin expression by transcription factors and epigenetic mechanisms. *Biochimica et Biophysica Acta (BBA) - Biomembranes*, 1828, 118-133.
- Paredes, R. M., Etzler, J. C., Watts, L. T. & Lechleiter, J. D. 2008. Chemical Calcium Indicators. *Methods (San Diego, Calif.)*, 46, 143-151.
- Parikh, S. S., Blackwell, D. J., Gomez-Hurtado, N., Frisk, M., Wang, L., Kim, K., Dahl, C. P., Fiane, A., Tonnessen, T., Kryshtal, D. O., Louch, W. E. & Knollmann, B. C. Thyroid and Glucocorticoid Hormones Promote Functional T-Tubule Development in Human-Induced Pluripotent Stem Cell-Derived Cardiomyocytes.
- Park, I.-H., Zhao, R., West, J. A., Yabuuchi, A., Huo, H., Ince, T. A., Lerou, P. H., Lensch, M. W. & Daley, G. Q. 2008. Reprogramming of human somatic cells to pluripotency with defined factors. *Nature*, 451, 141-146.
- Patel, D., Zhang, X. & Veenstra, R. D. 2014. Connexin hemichannel and pannexin channel electrophysiology: How do they differ? *FEBS letters*, 588, 1372-1378.
- Peters, M. F., Abi-Gerges, N., Lamore, S. D., Zhang, X., Abassi, Y. A. & Scott, C. W. 2014. An Impedance-Based Cellular Assay Using Human iPSC-Derived Cardiomyocytes to Quantify Modulators of Cardiac Contractility. *Toxicological Sciences*, 142, 331-338.
- Poelzing, S. & Veeraraghavan, R. 2007. Heterogeneous ventricular chamber response to hypokalemia and inward rectifier potassium channel blockade underlies bifurcated T wave in guinea pig. *American Journal of Physiology-Heart and Circulatory Physiology*, 292, H3043-H3051.
- Ribeiro-Rodrigues, T. M., Martins-Marques, T., Morel, S., Kwak, B. R. & Girão, H. 2017. Role of connexin 43 in different forms of intercellular communication – gap junctions, extracellular vesicles and tunnelling nanotubes. *Journal of Cell Science*, 130, 3619.
- Robertson, C., Tran, D. D. & George, S. C. 2013. Concise Review: Maturation Phases of Human Pluripotent Stem Cell-Derived Cardiomyocytes. *Stem cells (Dayton, Ohio)*, 31, 10.1002/stem.1331.
- Robertson, J. A. 2001. Human embryonic stem cell research: ethical and legal issues. *Nat Rev Genet*, 2, 74-78.
- Roell, W., Lewalter, T., Sasse, P., Tallini, Y. N., Choi, B.-R., Breitbach, M., Doran, R., Becher, U. M., Hwang, S.-M., Bostani, T., Von Maltzahn, J., Hofmann, A., Reining, S., Eiberger, B., Gabris, B., Pfeifer, A., Welz, A., Willecke, K., Salama, G., Schrickel, J. W., Kotlikoff, M. I. & Fleischmann, B. K. 2007. Engraftment of connexin 43-expressing cells prevents post-infarct arrhythmia. *Nature*, 450, 819.
- Sala, L., Van Meer, B. J., Tertoolen, L. G. J., Bakkers, J., Bellin, M., Davis, R., Denning, C., Dieben, M. A. E., Eschenhagen, T., Giacomelli, E., Grandela, C., Hansen, A., Holman, E. R., Jongbloed, M. R. M., Kamel, S. M., Koopman, C. D., Lachaud, Q., Mannhardt, I., Mol, M. P. H.,

- Orlova, V. V., Passier, R., Ribeiro, M. C., Saleem, U., Smith, G. L., Mummery, C. L. & Burton, F. L. 2017. Versatile open software to quantify cardiomyocyte and cardiac muscle contraction in vitro and in vivo. *bioRxiv*.
- Scheel, O., Frech, S., Amuzescu, B., Eisfeld, J., Lin, K. H. & Knott, T. 2014. Action potential characterization of human induced pluripotent stem cell-derived cardiomyocytes using automated patch-clamp technology. *Assay Drug Dev Technol*, 12, 457-69.
- Schmitt, N., Grunnet, M. & Olesen, S. P. 2014. Cardiac potassium channel subtypes: new roles in repolarization and arrhythmia. *Physiol Rev*, 94, 609-53.
- Scuderi, G. J. & Butcher, J. 2017. Naturally Engineered Maturation of Cardiomyocytes. *Frontiers in cell and developmental biology*, 5, 50-50.
- Silva, J., Nichols, J., Theunissen, T. W., Guo, G., Van Oosten, A. L., Barrandon, O., Wray, J., Yamanaka, S., Chambers, I. & Smith, A. 2009. Nanog is the gateway to the pluripotent ground state. *Cell*, 138, 722-37.
- Skarsfeldt, M. A., Carstensen, H., Skibsbye, L., Tang, C., Buhl, R., Bentzen, B. H. & Jespersen, T. 2016. Pharmacological inhibition of IK1 by PA-6 in isolated rat hearts affects ventricular repolarization and refractoriness. *Physiol Rep*, 4.
- Snyders, D. J. 1999. Structure and function of cardiac potassium channels. *Cardiovasc Res*, 42, 377-390.
- Stillitano, F., Sartiani, L., Depaoli, P., Mugelli, A. & Cerbai, E. 2008. Expression of the hyperpolarization-activated current,  $I_f$ , in cultured adult rat ventricular cardiomyocytes and its modulation by hypertrophic factors. *Pharmacological Research*, 57, 100-109.
- Sumi, T., Tsuneyoshi, N., Nakatsuji, N. & Suemori, H. 2007. Apoptosis and differentiation of human embryonic stem cells induced by sustained activation of c-Myc. *Oncogene*, 26, 5564.
- Takahashi, K., Tanabe, K., Ohnuki, M., Narita, M., Ichisaka, T., Tomoda, K. & Yamanaka, S. 2007. Induction of pluripotent stem cells from adult human fibroblasts by defined factors. *Cell*, 131, 861-72.
- Takahashi, K. & Yamanaka, S. 2006. Induction of Pluripotent Stem Cells from Mouse Embryonic and Adult Fibroblast Cultures by Defined Factors. *Cell*, 126, 663-676.
- Takanari, H., Nalos, L., Stary-Weinzinger, A., De Git, K. C., Varkevisser, R., Linder, T., Houtman, M. J., Peschar, M., De Boer, T. P., Tidwell, R. R., Rook, M. B., Vos, M. A. & Van Der Heyden, M. A. 2013. Efficient and specific cardiac IK(1) inhibition by a new pentamidine analogue. *Cardiovasc Res*, 99, 203-14.
- Tamargo, J., Caballero, R., Gomez, R., Valenzuela, C. & Delpon, E. 2004. Pharmacology of cardiac potassium channels. *Cardiovasc Res*, 62, 9-33.
- Thomas, N. L. & Williams, A. J. 2012. Pharmacology of ryanodine receptors and  $Ca^{2+}$ -induced  $Ca^{2+}$  release. *Wiley Interdisciplinary Reviews: Membrane Transport and Signaling*, 1, 383-397.
- Thomas, P. & Smart, T. G. 2005. HEK293 cell line: A vehicle for the expression of recombinant proteins. *Journal of Pharmacological and Toxicological Methods*, 51, 187-200.
- Tinker, A., Sutko, J. L., Ruest, L., Deslongchamps, P., Welch, W., Airey, J. A., Gerzon, K., Bidasee, K. R., Besch, H. R., Jr. & Williams, A. J. 1996. Electrophysiological effects of ryanodine derivatives on the sheep cardiac sarcoplasmic reticulum calcium-release channel. *Biophys J*, 70, 2110-9.
- Tristani-Firouzi, M. & Etheridge, S. 2010. Kir 2.1 channelopathies: the Andersen–Tawil syndrome. *Pflügers Archiv - European Journal of Physiology*, 460, 289-294.
- Tse, H.-F., Chan, Y.-C., Siu, C.-W., Lau, Y.-M., Lau, C.-P. & Li, R. A. 2009. Synergistic Effects of Inward Rectifier (IK1) and Pacemaker (If) Currents on the Induction of Bioengineered Cardiac Automaticity. *Journal of Cardiovascular Electrophysiology*, 20, 1048-1054.

- Vaidyanathan, R., Taffet, S. M., Vikstrom, K. L. & Anumonwo, J. M. 2010. Regulation of cardiac inward rectifier potassium current (I(K1)) by synapse-associated protein-97. *J Biol Chem*, 285, 28000-9.
- Van Den Heuvel, N. H., Van Veen, T. A., Lim, B. & Jonsson, M. K. 2014. Lessons from the heart: mirroring electrophysiological characteristics during cardiac development to in vitro differentiation of stem cell derived cardiomyocytes. *J Mol Cell Cardiol*, 67, 12-25.
- Van Veen, A. A., Van Rijen, H. V. & Opthof, T. 2001. Cardiac gap junction channels: modulation of expression and channel properties. *Cardiovasc Res*, 51, 217-29.
- Verkerk, A. O., Veerman, C. C., Zegers, J. G., Mengarelli, I., Bezzina, C. R. & Wilders, R. Patch-Clamp Recording from Human Induced Pluripotent Stem Cell-Derived Cardiomyocytes: Improving Action Potential Characteristics through Dynamic Clamp. LID - E1873 [pii] LID - 10.3390/ijms18091873 [doi].
- Vozzi, C., Dupont, E., Coppens, S. R., Yeh, H.-I. & Severs, N. J. 1999. Chamber-related Differences in Connexin Expression in the Human Heart. *Journal of Molecular and Cellular Cardiology*, 31, 991-1003.
- Walsh, K. B. 2014. Targeting cardiac potassium channels for state-of-the-art drug discovery. *Expert Opin Drug Discov*, 1-13.
- Wang, H., Xi, Y., Zheng, Y., Wang, X. & Cooney, A. J. 2016. Generation of electrophysiologically functional cardiomyocytes from mouse induced pluripotent stem cells. *Stem Cell Research*, 16, 522-530.
- Warren, C. M., Krzesinski, P. R., Campbell, K. S., Moss, R. L. & Greaser, M. L. 2004. Titin isoform changes in rat myocardium during development. *Mechanisms of Development*, 121, 1301-1312.
- Warren, M., Spitzer, K. W., Steadman, B. W., Rees, T. D., Venable, P., Taylor, T., Shibayama, J., Yan, P., Wuskell, J. P., Loew, L. M. & Zaitsev, A. V. 2010. High-precision recording of the action potential in isolated cardiomyocytes using the near-infrared fluorescent dye di-4-ANBDQBS. *American Journal of Physiology - Heart and Circulatory Physiology*, 299, H1271.
- Wokosin, D. L., Loughrey, C. M. & Smith, G. L. 2004. Characterization of a range of fura dyes with two-photon excitation. *Biophys J*, 86, 1726-38.
- Woltjen, K., Michael, I. P., Mohseni, P., Desai, R., Mileikovsky, M., Hamalainen, R., Cowling, R., Wang, W., Liu, P., Gertsenstein, M., Kaji, K., Sung, H.-K. & Nagy, A. 2009. piggyBac transposition reprograms fibroblasts to induced pluripotent stem cells. *Nature*, 458, 766-770.
- Wrzosek, A., Schneider, H., Grueninger, S. & Chiesi, M. 1992. Effect of thapsigargin on cardiac muscle cells. *Cell Calcium*, 13, 281-92.
- Yang, X., Rodriguez, M., Pabon, L., Fischer, K. A., Reinecke, H., Regnier, M., Sniadecki, N. J., Ruohola-Baker, H. & Murry, C. E. 2014. Tri-iodo-L-thyronine promotes the maturation of human cardiomyocytes-derived from induced pluripotent stem cells. *J Mol Cell Cardiol*, 72, 296-304.
- Yu, J., Vodyanik, M. A., Smuga-Otto, K., Antosiewicz-Bourget, J., Frane, J. L., Tian, S., Nie, J., Jonsdottir, G. A., Ruotti, V., Stewart, R., Slukvin, Ii & Thomson, J. A. 2007. Induced pluripotent stem cell lines derived from human somatic cells. *Science*, 318, 1917-20.
- Zhang, J., Wilson, G. F., Soerens, A. G., Koonce, C. H., Yu, J., Palecek, S. P., Thomson, J. A. & Kamp, T. J. 2009. Functional Cardiomyocytes Derived From Human Induced Pluripotent Stem Cells. *Circulation Research*, 104, e30-e41.
- Zhang, X.-H., Wei, H., Šarić, T., Hescheler, J., Cleemann, L. & Morad, M. 2015. Regionally diverse mitochondrial calcium signaling regulates spontaneous pacing in developing cardiomyocytes. *Cell Calcium*, 57, 321-336.
- Zhou, Z. & Lipsius, S. L. 1992. Properties of the pacemaker current (If) in latent pacemaker cells isolated from cat right atrium. *The Journal of Physiology*, 453, 503-523.

Zwi, L., Caspi, O., Arbel, G., Huber, I., Gepstein, A., Park, I. H. & Gepstein, L. 2009. Cardiomyocyte differentiation of human induced pluripotent stem cells. *Circulation*, 120, 1513-23.